1990

Intracellular Calcium And The Regulation Of Growth Hormone Release By Growth Hormone-releasing Factor And Somatostatin In Rat Somatotrophs

Benoit Thierry Lussier

NOTICE

The quality of this microform is heavily dependent upon the quality of the original thesis submitted for microfilming. Every effort has been made to ensure the highest quality of reproduction possible.

If pages are missing, contact the university which granted the degree.

Some pages may have indistinct print especially if the original pages were typed with a poor typewriter ribbon or if the university sent us an inferior photocopy.

Reproduction in full or in part of this microform is governed by the Canadian Copyright Act, R.S.C. 1970, c. C-30, and subsequent amendments.

AVIS

La qualité de cette microforme dépend grandement de la qualité de la thèse soumise au microfilmage. Nous avons tout fait pour assurer une qualité supérieure de reproduction.

S'il manque des pages, veuillez communiquer avec l'université qui a conféré le grade.

La qualité d'impression de certaines pages peut laisser à désirer, surtout si les pages originales ont été dactylographiées à l'aide d'un ruban usé ou si l'université nous a fait parvenir une photocopie de qualité inférieure.

La reproduction, même partielle, de cette microforme est soumise à la Loi canadienne sur le droit d'auteur, SRC 1970, c. C-30, et ses amendements subséquents.

INTRACELLULAR CALCIUM AND THE REGULATION OF GROWTH HORMONE RELEASE BY GROWTH HORMONE-RELEASING FACTOR AND SOMATOSTATIN IN RAT SOMATOTROPHS

by

Benoit T. Lussier

Department of Physiology

Submitted in partial fulfilment
of the requirements for the degree of
Doctor of Philosophy

Faculty of Graduate Studies
The University of Western Ontario
London, Ontario
March 1990

ISBN 0-315-55263-8

ABSTRACT

The release of growth hormone (GH) from the somatotrophs of the anterior pituitary is under the control of two hypothalamic peptides, GH-releasing factor (GRF) and somatostatin (SRIF), which stimulates and inhibits release respectively. The aim of this study was to explore the role of intracellular Ca^{2+} ($[Ca^{2+}]_i$) in the regulation of GH release by GRF and SRIF in acutely dispersed purified rat somatotrophs.

The role of extracellular Ca^{2+} was studied by assessing the effect of Ca^{2+}-free medium and Ca^{2+} antagonists on GRF-induced GH release. The fluorescent dye indo-1 was used to measure $[Ca^{2+}]_i$. Ca^{2+} influx was evaluated by measuring ^{45}Ca uptake.

GRF-stimulated GH release was inhibited in Ca^{2+}-free medium. The Ca^{2+} antagonists nifedipine and diltiazem, inhibited basal, K^+- and GRF-induced GH release. GRF stimulated a triphasic increase in ^{45}Ca uptake. GRF also stimulated a biphasic increase in $[Ca^{2+}]_i$, which was entirely dependent on Ca^{2+} influx. SRIF decreased ^{45}Ca uptake in steady and non-steady states. It also inhibited the steady state GRF-induced increase in ^{45}Ca uptake. SRIF lowered baseline $[Ca^{2+}]_i$ and inhibited the increase in $[Ca^{2+}]_i$ stimulated by GRF. To study the underlying mechanisms involved in the control of $[Ca^{2+}]_i$ by GRF and SRIF, the effect of K^+ depolarization, cAMP analogues and protein kinase C (PKC) activators on Ca^{2+} fluxes and $[Ca^{2+}]_i$ were examined. K^+-dependent depolarization stimulated a nifedipine-sensitive Ca^{2+} influx which was not inhibited by SRIF, and which resulted in an increase in $[Ca^{2+}]_i$. 8-(4-Chlorophenylthio)-cAMP raised $[Ca^{2+}]_i$ by stimulating a nifedipine- and SRIF-sensitive Ca^{2+} influx. The PKC activators 1,2-dioctanoylglycerol and the phorbol 12-myristate 13-acetate raised $[Ca^{2+}]_i$ by stimulating a nifedipine- and SRIF-sensitive Ca^{2+} influx.

The conclusions of this study are a) Ca^{2+} is essential for GRF-induced GH release; b) GRF stimulates Ca^{2+} influx which results in a biphasic increase in $[Ca^{2+}]_i$; c) SRIF lowers $[Ca^{2+}]_i$ by inhibiting Ca^{2+} influx; d) GRF could stimulate Ca^{2+} influx by depolarizing the cell or by increasing cAMP- and PKC-dependent phosphorylation.

To

Jean-Jacques Lussier M.D., Ph.D. (1920-1975)

and

Michel P. Lussier LL.L (1948-1986)

who are not here to share in the accomplishment

ACKNOWLEDGEMENTS

I wish to express my gratitude to Dr. Jacob Kraicer, under whose supervision this work was conducted. His patient guidance, encouragement and his clear and analytical scientific thinking, not to mention his habit of asking "what's the physiological significance of your results", were invaluable.

Many thanks to Drs. D. Olson, J. Rylett, R. Weick and T. Kennedy, the members of my advisory committee, for their judicious criticisms and comments.

Special thanks to Dr. J. Dixon for his guidance in setting up the intracellular Ca^{2+} concentration assay.

I must thank Dr. S. Sims for the many enlightening discussions on ion channel regulation, and for his support and encouragements.

I would like to thank "The Kraicers" , that is those who have worked in Dr. Kraicer's lab, and have contributed to the creation of a most pleasant working environment. Specifically I warmly thank:

Bruce Moor, the head technician, for his graduate student-proof patience, for virtually carrying out every GH and cAMP radioimmunoassay, for catering to my computer programming needs, and most of all for his friendship.

Michelle French, fellow graduate student and lab mate, for her help in carrying out most of the experiments reported in this thesis, for her criticisms and comments, for her encouragements, moral support, and above all her friendship.

Leigh Yardley and Cathy Cleave for their expert technical assistance.

Pat Rose for helping me with the cAMP radioimmunoassays, and Dave Wood for helping me with the intracellular Ca^{2+} concentration experiments.

I wish to extend my thanks to Bruce Arppe for photographing the figures contained in this thesis.

I acknowledge the Medical Research Council of Canada for supporting this project.

Finally, I also wish to acknowledge the generous financial aid from the Ministry of Colleges and Universities of the Province of Ontario, in the form of Ontario Graduate Scholarships and, as well, from the Faculty of Graduate Studies of the University of Western Ontario, in the form of a Special University Scholarship. I also received financial assistance from the Medical Research Council term grant MT-1634.

TABLE OF CONTENTS

LIST OF TABLES

LIST OF FIGURES

ABBREVIATIONS

ACh	acetylcholine
ACTH	adrenocorticotrophic hormone
AMP	adenosine monophosphate
AN	arcuate nucleus
ANOVA	analysis of variance
AP	action potential
ATP	adenosine triphosphate
bis-oxonol	bis(1,3-diethylthiobarbiturate) trimethineoxnol
BSA	bovine serum albumin
$(Bu)_2$cAMP	dibutyryl cAMP
$[Ca^{2+}]$	Ca^{2+} concentration
$[Ca^{2+}]_i$	free intracellular Ca^{2+} concentration
cAMP	adenosine 3',5'-monophosphate
cpt-cAMP	8-(4-chlorophenylthio) cAMP
CRF	corticotropin-releasing factor
cyclic AMP	adenosine 3',5'-monophosphate
DAG	diacylglycerol
diC_8	1,2-dioctanoyl-glycerol
DMRT	Duncan's multiple range test
DRG	dorsal root ganglion
E_{Ca}	equilibrium potential for Ca^{2+}
E_K	equilibrium potential for K^+
E_m	membrane potential
EC_{50}	concentration which produces half-maximal response
EGTA	ethyleneglycol-bis-(β aminoethyl ester)-N,N,N',N'-tetraacetic acid
ER	endoplasmic reticulum
FSH	follicle-stimulating hormone
G_i	pertussis toxin sensitive GTP-binding protein which inhibits andenylate cyclase
G_k	pertussis toxin-sensitive GTP-binding protein which increases K^+ conductance
G_s	cholera toxin sensitive GTP-binding protein which stimulates adenylate cyclase
GABA	γ-aminobutyric acid
GH	growth hormone
GRF	growth hormone-releasing factor
GTP	guanosine triphosphate
GTP-γ-S	guanosine-5'-O-(3'-thiotrisphosphate)
HEPES	N-2-hydroxyethylpiperazine-N'-2-ethanesulfonic acid
hGRF	human growth hormone-releasing factor
hpGRF	human pancreatic growth hormone-releasing factor

IBMX	3-isobutyl-1-methylxanthine
IP	inositol 4-monophosphate
IP_2	inositol 1,4-bisphosphate
IP_3	inositol 1,4,5-trisphosphate
IP_4	inositol 1,3,4,5-tetrakisphosphate
iv	intravenous
K_d	dissociation constant
K_m	substrate concentration which produces half-maximal enzyme activity
$[K^+]$	K^+ concentration
$[K^+]_e$	extracellular K^+ concentration
K(Ca) channel	Ca^{2+}-activated K^+ channel
kDa	kilodalton
LH	luteinizing hormone
M199	medium 199
M199-A	medium 199 containing 0.1 % BSA, 28 mM $NaCO_3$, pH 7.35 - 7.4 at 37 C
M199-AH/RT	medium 199 containing 0.1 % BSA, 20 mM HEPES, pH 7.35 - 7.4 at room temperature
M199-AH/37	medium 199 containing 0.1 % BSA, 20 mM HEPES, pH 7.35 - 7.4 at 37 C
ME	median eminence
MOPS	3-(N-morpholino)propanesulfonic acid
n-BP	n-butylphthalate
NMG	N-methyl-d-glucamine chloride
OAG	1,2-oleoylacetylglycerol
PCA	perchloric acid
PDB	phorbol dibutyrate
PGE_2	prostaglandin E_2
PI	phosphatidylinositol
PIP	phosphatidylinositol 4-phosphate
PIP_2	phosphatidylinositol 4,5-bisphosphate
PKA	cAMP-dependent protein kinase
PKC	protein kinase C
PLC	phospholipase C
PMA	phorbol 12-myristate 13-acetate
POA	preoptic area
PRL	prolactin
pS	picosiemen
rGRF	rat growth hormone-releasing factor
RHPA	reverse haemolytic plaque assay
RIA	radioimmunoassay
ROCC	receptor-operated Ca^{2+} channel
SMOCC	second messenger-operated Ca^{2+} channel
SR	sarcoplasmic reticulum
SRIF	somatostatin (14 amino acid peptide)
SRIF-28	somatostatin (28 amino acid peptide)

TBA	tetrabutylammonium
TRH	thyrotropin-releasing hormone
TSH	thyroid-stimulating hormone
TTX	tetrodotoxin
VIP	vasoactive intestinal peptide
V_{max}	initial maximum velocity of enzymatic reaction
VMN	ventromedial nucleus
VSCC	voltage-sensitive Ca^{2+} channel
ω-CgTx	ω-conotoxin
4α-PDD	4α-phorbol-12,13 didecanoate
5-HT	serotonin
5K	5 times normal extracellular K^+ concentration (29 - 30 mM)
8Br-cAMP	8-bromo cAMP

CHAPTER 1

INTRODUCTION

The release of growth hormone (GH) from the somatotrophs of the anterior pituitary is under the control of two hypothalamic peptides, growth hormone-releasing factor (GRF) and somatostatin (SRIF). The former stimulates GH release while the later inhibits release.

When the project reported in this thesis was undertaken in January 1985, the structure of GRF had been published only 2 years previously. GRF was known to stimulate GH release from the rat somatotrophs (1) and to stimulate GH mRNA production in rat pituitary cells (2). GRF had been shown to increase cAMP accumulation in somatotrophs (1). There were reports that GRF required extracellular Ca^{2+} to stimulate GH release from mixed pituitary cells (2,3). Somatostatin had been found to inhibit GRF-stimulated GH release. These observations fitted well with the model that Kraicer et al. (4) proposed for the control of GH release.

Originally the aim of Kraicer et al. (5,6) was to establish that adenosine 3',5'-monophosphate (cyclic AMP or cAMP) was a second messenger for the putative GRF. To study the role of cAMP in the control of GH release, it was necessary to use a homogeneous population of somatotrophs. Since the anterior pituitary is a heterogenous gland made up of five or more functional cell types - corticotrophs, which secrete adrenocorticotrophic hormone (ACTH), one or two types of gonadotrophs which secrete follicle-stimulating hormone (FSH) and luteinizing hormone (LH), lactotrophs which secrete prolactin (PRL), thyrotrophs which secrete thyroid-stimulating hormone (TSH) and somatotrophs which secrete GH - changes in cAMP accumulation in mixed anterior pituitary cells could not be localized to a specific cell type.

Using density gradient centrifugation it is possible to obtain a population of purified rat somatotrophs (7). Therefore any change in cellular cAMP associated with a change in GH release could be localized to somatotrophs.

Early experiments using purified rat somatotrophs showed that increasing intracellular cAMP resulted in an increase in GH release (5). When cAMP accumulation was increased endogenously by treating somatotrophs with prostaglandin E_2 (PGE_2), GH release was increased (5,6). If the cells were treated with phosphodiesterase inhibitors such as 3-isobutyl-1-methylxanthine (IBMX) or theophylline, cAMP accumulation and GH release were increased (5,6). Membrane permeable analogues of cAMP, such as dibutyryl cAMP ($(Bu)_2$cAMP), enhanced GH release (5). The working model, derived from these experimental results, proposed that GH release is controlled by cAMP.

When these experiments were repeated in the absence of extracellular Ca^{2+}, GH release could not be stimulated by any manoeuvres which raised cAMP (5,8). Experiments were carried out to determine whether increasing free intracellular Ca^{2+} concentration ($[Ca^{2+}]_i$) could stimulate GH release without increasing cAMP. Two approaches were used to increase $[Ca^{2+}]_i$: either the cells were incubated in high K^+ medium which depolarizes the membrane and opens voltage sensitive Ca^{2+} channels, or the cells were incubated with the Ca^{2+} ionophore A23187. Both treatments stimulated GH release without increasing cAMP accumulation (4).

As a result of these experimental findings the central event in the working model, for the control of GH release, shifted from an increase in cAMP to an increase in $[Ca^{2+}]_i$ (4). Thus in the early 1980's the accepted model was as follows (Figure 1): GRF binds to a receptor in the plasma membrane, stimulates adenylate cyclase, and increases cAMP accumulation. The increase in cAMP leads to an increase in cAMP-dependent protein kinase (PKA) activity. It was proposed that PKA was involved in the mobilisation of Ca^{2+} from an intracellular store to the

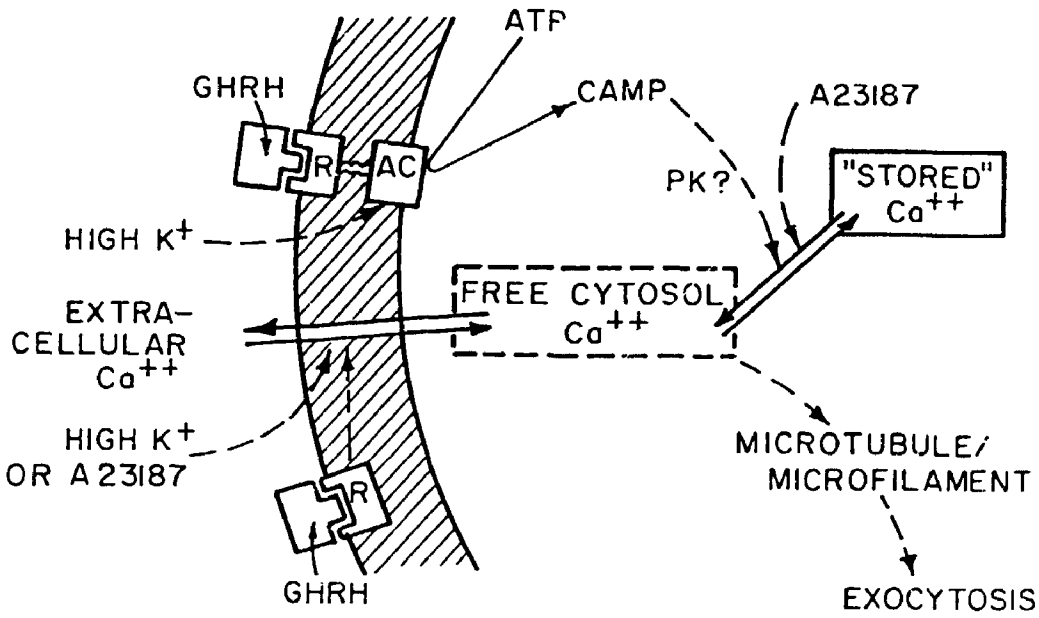

Figure 1. Model depicting the central role of Ca^{2+} in the release of GH from somatotrophs. R: Receptor for GHRH (GRF); AC: adenylate cyclase; PK: cAMP dependent protein kinase (from reference (4)).

cytosol. The model also allowed for GRF-receptor complex-stimulated Ca^{2+} influx. Mobilization and influx of Ca^{2+} leads to an increase in $[Ca^{2+}]_i$. This increase then stimulates exocytosis. This model implied that an increase in cytosolic Ca^{2+} was essential for GH release and allowed for the possibility that Ca^{2+}, as well as cAMP, was a second messenger for the still putative GRF.

SRIF inhibits GH release whether stimulated by increasing cAMP, or increasing $[Ca^{2+}]_i$ (4,8,9). Furthermore, SRIF abolishes GRF-induced GH release while decreasing cAMP accumulation by less than 25 % (1). The modest decrease in cAMP is insufficient to account for complete inhibition of GH release. This observation suggests that SRIF acts via a cAMP-independent pathway to inhibit GH release. Could this be a Ca^{2+}-dependent pathway ?

The studies reported in this thesis were undertaken to explore systematically the role of intracellular Ca^{2+} in the regulation of GH release by GRF and SRIF in rat somatotrophs. The model proposed by Kraicer et al. (4) was used as a starting point. The answers to the following questions were sought:

1. Is Ca^{2+} a second messenger for GRF ?
2. Does GRF increase $[Ca^{2+}]_i$ by stimulating influx and/or mobilization of stored Ca^{2+} ?
3. Does SRIF interfere with the Ca^{2+} status of the cell ?
4. What are the intracellular messengers which lead to the GRF-stimulated increase in $[Ca^{2+}]_i$?

In general, studies of the intracellular action of GRF and SRIF have been carried out either on mixed pituitary cell populations or on a variety of pituitary tumour cell lines which secrete GH or respond to SRIF. The study of intracellular messenger systems using heterogeneous cell populations does not allow for the localization of changes in intracellular metabolites to the cell type of interest. The most widely used cell lines are the rat GH_3 and

GH_4C_1 and the mouse AtT-20 cell lines. The GH_3 cells secrete GH and PRL in response to thyrotropin-releasing hormone (TRH) while GRF has no effect on GH release (10,11). GH_4C_1 cells also secrete GH and PRL. However TRH stimulates PRL release while it inhibits GH secretion (12). Vasoactive intestinal peptide (VIP) stimulates cAMP accumulation in these cells (13). AtT-20 cells secrete ACTH in response to corticotropin-releasing factor (CRF) or VIP (14). SRIF inhibits hormone secretion from all three clonal cell types (15). Tumour cell lines are useful for biochemical and electrophysiological studies of the effects of GRF and SRIF. However, by virtue of the lack of response to GRF, they are of limited value for the study of the cellular physiology of GRF- and SRIF-regulated GH release from somatotrophs. Therefore the studies described in this thesis were carried out on purified somatotrophs. Thus any change in intracellular metabolites, such as cAMP, $[Ca^{2+}]_i$ or Ca^{2+} fluxes, due to the effects of GRF or SRIF can be localised to the somatotrophs. There is also a conceptual reason for using somatotrophs: they are the "natural" target for GRF and SRIF, and GRF and SRIF are the physiological stimulator and inhibitor of GH release.

CHAPTER 2

LITERATURE REVIEW

2.1 Introduction.

In vivo, the pulsatile release of GH from somatotrophs of the anterior pituitary is under the control of two hypothalamic peptides - GRF which stimulates release, and SRIF which inhibits release. This chapter reviews the evidence that GH release is controlled by hypothalamic activity via releasing and inhibiting factors which are secreted into the hypophysial portal system. The significance of the combined effect of SRIF and GRF in controlling pulsatile GH release will also be reviewed. Then the intracellular mechanism of action of both GRF and SRIF in the somatotrophs will be reviewed. Finally free intracellular Ca^{2+} concentration and its regulation will be reviewed within the general context of intracellular Ca^{2+} homeostasis and stimulus-secretion coupling.

2.2. Hypothalamic Control of GH Release: GRF and SRIF.

2.2.1 An Historical Perspective.

It has been known since 1912, through the work of Ascher, in Germany, and Cushing, in the United States, that the removal of the pituitary gland results in, among other things, growth retardation in immature animals (16). In 1921, Evans and Long (17) demonstrated that injections of bovine pituitary extracts to rats resulted in substantial increases in growth. It was not until the mid 1940's that Evans' and Wilhelmi's groups isolated a crystalline protein from hypophysial tissue, which when injected into hypophysectomized rats, produced an increase

in growth without causing the effects of other known pituitary hormones (16). Thus it was established that the somatotrophic function of the pituitary gland was due to secretion of a protein hormone, GH.

The description of the hypophysial portal system by Popa and Felding in 1930 (18) and the lack of extensive innervation of the anterior pituitary, prompted Green and Harris (19), in 1947, to suggest that the hypothalamic control of pituitary function was dependent on a neurohormonal mechanism. This mechanism involves the liberation of hypothalamic factors or hormones into the capillaries of the primary plexus of the portal system in the median eminence (ME). The portal vessels carry the factors down the pituitary stock and into the sinusoids of the gland. There these factors either stimulate or inhibit hormone release from pituitary cells.

Several groups sought to determine whether the Harris model was applicable to control of GH release, and set out to isolate and characterize growth hormone-releasing factor (GRF), the then putative hypothalamic factor involved in the stimulation of GH secretion. In 1962, Franz, Haselbach and Libert (20) reported that prolonged treatment with a acetic acid extract of porcine hypothalamus, stimulated growth in immature female rats. They also reported that the potency of rat pituitary extracts to stimulate growth in hypophysectomized rats, when monitored by the tibial bioassay, was enhanced by prior incubation of the pituitary with the hypothalamic extract. The validity of the tibial test used by Franz et al. was questioned by Deubin and Meites (21) who, two years later, using a standardized tibial bioassay for GH determination, reported that HCl extracts of rat hypothalami stimulated pituitary GH release in vitro. The in vivo effectiveness of such extracts was demonstrated by Pecile et al. (22) and Krulich et al. (23), in 1965, when they reported that the intravenous injection of ovine or rat median eminence extracts resulted in GH depletion of the pituitary gland within 15 min.

The development of a sensitive radioimmunoassay (RIA) for GH in the mid 1960's allowed for the determination of plasma GH concentration (16). It was then possible to study the effect of hypothalamic extracts on plasma GH levels. The intravenous injection of porcine hypothalamic extracts into monkeys, or of bovine hypothalamic extracts into sheep was reported to increase the plasma immunoreactive GH concentration (16,24). Furthermore GH-releasing activity was detected in hypophysial portal blood of rats (25). Intrapituitary administration of a partially purified ovine hypothalamic extract produced a rise in plasma GH concentration in rats (26). It was becoming clear that the Harris neurohormonal model was applicable to the control of GH release.

At the same time as several laboratories were trying to isolate GRF, other groups were investigating which nuclei of the hypothalamus were involved in the control of GH secretion. In the 1960's, Reichlin reported that electrolytic lesions of the arcuate nucleus (AN) and of the ventromedial nucleus (VMN) caused growth retardation in rats (27) and that lesions of the median eminence resulted in a decrease in the GH content of rat pituitary glands (28). Frohman (29) demonstrated that VMN lesions decreased pituitary GH content and decreased the plasma concentration of GH. Hypothalamic lesions also abolished pulsatile GH release (30). Electrical stimulation of these areas resulted in an increase in plasma GH concentration (31,32). These two observations suggested the existence of GH stimulatory centres in the hypothalamus.

Therefore, before 1982, when the structure of GRF was finally elucidated, there was good evidence that hypothalamic GRF existed, and that it was transported to the pituitary by the hypophysial portal system. The lesion and stimulation experiments suggested that the VMN and the AN were stimulatory hypothalamic centres for GH release. These experiments also suggested that GRF would be found in the VMN and the AN of the hypothalamus.

While attempting to purify GRF by gel filtration, Krulich et al. (33) isolated a fraction of ovine hypothalamic extract which inhibited basal GH release from rat pituitary glands in vitro. This was the first evidence for an inhibitory hypothalamic factor involved in GH release. Rice and Critchlow (34), while investigating structures of the central nervous system (CNS) responsible for the stress-induced decrease in GH secretion in rats, found that the ablation of the preoptic area (POA) prevented the stress-dependent drop in plasma GH concentration. Electrolytic lesions of the POA resulted in an increase in the frequency of plasma GH bursts (35), while electrical stimulation of the area reduced GH release (36).

Therefore before 1973, when the structure of the inhibitory factor, or somatotropin-release inhibiting factor (SRIF), was discovered, there was evidence that SRIF existed. The lesion and electrical experiments suggested that the POA was an inhibitory hypothalamic centre for GH release. These experiments also suggested that SRIF would be found in the POA.

2.2.2 GRF.

2.2.2.1 Structure of GRF. In 1982, the structure of human GRF was reported independently by Guillemin's group (37) and Vale's group (38), both from the Salk Institute. Each group took advantage of a different patient with the ectopic GH-releasing factor syndrome. Both of these patients had tumours of pancreatic islets and showed signs of acromegaly with high circulating GH levels (37,38). Guillemin et al. (37) extracted 3 peptides from their tumour which stimulated GH release from cultured pituitary cells; GRF(1-37)-OH, GRF(1-40)-OH and GRF(1-44)-NH_2. The longest peptide was the most potent in stimulating GH release in their assay system while the 40 amino acid peptide was the most abundant. Rivier et al. (38), from Vale's group, identified a single 40 amino acid peptide, GRF(1-40)-OH, in their tumour, which stimulated GH release from cultured rat pituitary cells. The amino acid sequence of the Rivier peptide is identical to that of the Guillemin peptide except for the last 4 amino acids (Fig. 2). These peptides are

HUMAN

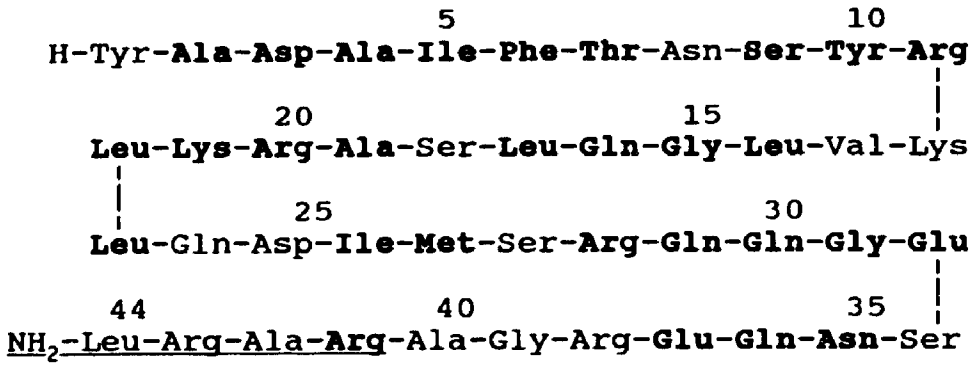

RAT

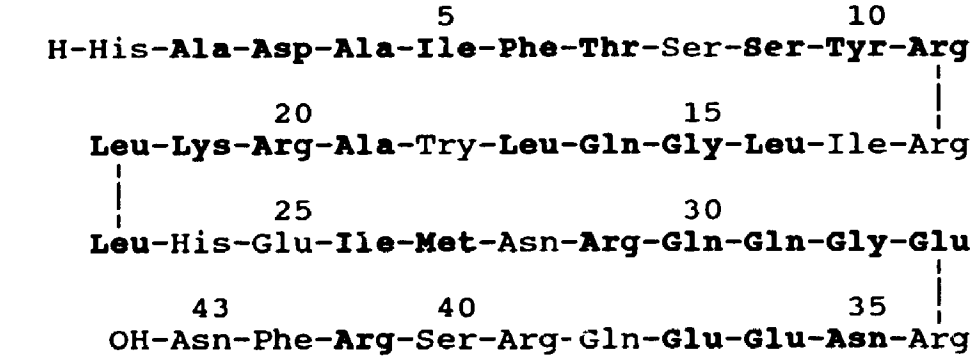

Figure 2. **Amino acid sequences of human and rat GRF.** The first 40 amino acids of hGRF are identical for both forms. The difference between the two forms of hGRF is indicated by the underlined region. Bold amino acids are common to both rat and human GRF.

known as human pancreatic GRF's (hpGRF) and belong to the secretin-glucagon peptide family (37,38). Synthetic hpGRF's were as potent as the extracted peptides in stimulating GH release (37,38).

In the following year Spiess et al. (39) reported the structure and synthesis of rat hypothalamic GRF (rGRF). The peptide is 43 amino acids long and shows 67% homology with hpGRF (Figure 2). This peptide was the first hypothalamic GRF to be identified. By 1984, Ling et al. (40), using human hypothalamic stalk-median eminence collected from cadavers, identified and sequenced GRF(1-40)-OH and GRF(1-44)-NH_2, thus showing that hpGRF's were identical to human hypothalamic GRF's (hGRF).

2.2.2.2 Action of GRF. GRF stimulates GH hormone release in a concentration dependent manner from mixed rat pituitary cells in static incubation (3,37-39,41-44) and in perifusion (41,45-47) as well as from purified rat somatotrophs (1,48-50). Intravenous (iv) injection of GRF to either sodium pentobarbital anesthetized rats or conscious free moving normal and VMN and AN lesioned rats causes a transient increases in plasma GH concentration in a dose dependent fashion (37,51-53). Continuous infusion of large doses of GRF (500 ng/min) produced a transient increase in plasma GH concentration, while small doses (20 ng/ml) produced a sustained moderated increase (51). GH is the only pituitary hormone whose release is stimulated by GRF. Indeed, GRF treatment of cultured mixed rat pituitary cells or iv injections of GRF to rats, stimulates GH but not LH, FSH, TSH, ACTH or PRL secretion (41,51).

2.2.2.3 Localization of GRF in the hypothalamus. The hypothalamic lesion and stimulation experiments suggested that GRF would be located in the AN and VMN. Immunohistochemical studies of human, simian and rat hypothalami reveal that GRF is found in nerve terminals surrounding the capillaries of the hypophysial portal system in the median eminence (54-57). The most prominent cluster of reactive cell bodies is found in the AN while specific GRF

immunoreactivity is also found in cell bodies of the VMN (54-56). Hypothalamic fibres containing GRF outside the median eminence appear to originate from the VMN and project to an area surrounding the third ventricle (56). These studies support the role of GRF as the endogenous GH-releasing agent, and suggest that the stimulatory action of the AN and VMN is related to the release of GRF. The existence of fibres projecting to non-median eminence structures suggests that GRF may also act as a neurotransmitter or neuromodulator.

2.2.2.4 Control of GRF Release. Little is known of the neuronal pathways involved in the regulation of GRF secretion. What is known is mostly derived from passive immunization studies. Catecholamine-, opioid- and γ-aminobutyric acid (GABA)-stimulated GH release is abolished, in rats, by passive immunization with anti-GRF serum (58-60). These results suggest that neurons from other neural structures may project to the AN and VMN and play a role in the control of GRF release.

Short-loop negative feed back of GH secretion by GH has been known for over 30 years (36,61,62). Kraicer et al. (46) have recently demonstrated that an inhibitory effect of an increase in circulating GH does not occur at the level of the pituitary. Katakami et al. (63) reported that the GRF content of hypothalami from hypophysectomized rats (no circulating GH) was lower than that of control hypothalami. They also found that basal and high K^+-induced GRF release from hypothalamic fragments from the hypophysectomized rat was lower than release by fragments from control rats. The authors conclude that GH has a stimulatory feed back effect on GRF synthesis. However, they point out that their data could be interpreted as indicating an increase in GRF release in the absence of GH. Though it is unclear how GH affects GRF containing cells of the hypothalamus, GH does affect GRF release. (see also 2.2.3.4)

2.2.3. SRIF

2.2.3.1 Structure of SRIF. In 1973, Guillemin and his group (64) reported the structure of SRIF (Figure 3), a cyclic 14 amino acid peptide isolated from ovine hypothalami, which inhibitedbasal GH release by rat pituitary cells in culture and lowered plasma GH concentration in anesthetized and conscious rats (65). Furthermore native and synthetic SRIF's were found to be equipotent. In 1980, several groups reported the isolation of a 28 amino acid form of hypothalamic SRIF (SRIF-28) (66-68). The biological activity of SRIF-28 is reported to be equal if not greater than that of SRIF (69,70). It is not clear whether SRIF-28 is a precursor for SRIF or an end product. The precursor/product relationship has been demonstrated in some tissues but not in others (71). The 14 amino acid peptide is the predominant species in rat brain (71,72).

2.2.3.2 Action of SRIF. SRIF (both 14 ar 28) is found outside the CNS, notably in the D-cells of the islet of Langerhans, the stomach, the duodenum and the ileum (72). The action of peripheral SRIF on gastrointestinal function and on islet hormone secretion has been extensively reviewed (73-78). Only the action of SRIF on pituitary hormone secretion will be considered in this review.

SRIF inhibits basal GH release from mixed rat pituitary cells in static incubation, and from purified rat somatotrophs in perifusion (64,79). The post-SRIF GH rebound seen in vivo is also seen with rat pituitary cells or somatotrophs in perifusion (45,79,80). SRIF inhibits GH release from acutely dispersed or cultured rat pituitary cells as well as from purified rat somatotrophs, stimulated by adenosine 3',5'-monophosphate (cAMP) analogues, phosphodiesterase inhibitors, prostaglandin E_2 (5), K^+ depolarization (4,9), and protein kinase C activators (48). GRF-stimulated GH release from pituitary cells or somatotrophs is also inhibited in both static incubation and perifusion by SRIF (1,3,42,43,45,80).

SRIF-14

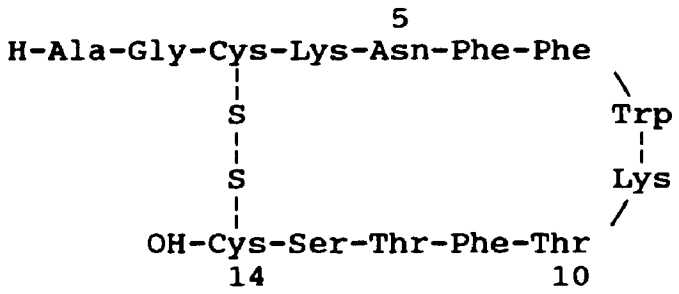

SRIF-28

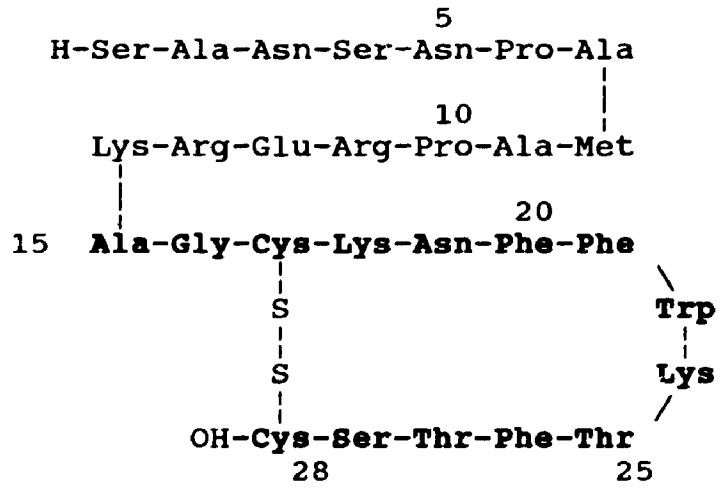

Figure 3. **Amino acid sequence of SRIF-14 and SRIF-28.** SRIF-28(15-28) is identical to SRIF-14.

In vivo, SRIF lowers plasma GH concentration, and prolonged treatment with protamine zinc subcutaneous depot injection reduces the rate of weight gain in young male rats (65). SRIF also inhibits the increase in plasma GH concentration stimulated by several neurotransmitters, drugs, hormones, hypothalamic stimulation and other stimuli (81,82). SRIF also inhibits spontaneous GH secretory bursts (83) as well as GRF-induced increases in plasma GH in vivo (84). Paradoxically, SRIF will stimulate GH secretion by its rebound effect, or "off response". A SRIF infusion rapidly decreases plasma GH concentration; when the infusion is stopped, a large rapid and transient increase in plasma GH concentration occurs (36,81,82,85).

SRIF is also reported to inhibit basal and thyrotropin-releasing hormone (TRH)-stimulated TSH release from rat pituitary cells in culture (82,86). In man, SRIF inhibits the TRH-induced increase in plasma TSH and lowers plasma TSH in hypothyroid patients (81,82). In rats, the administration of anti-SRIF serum results in an increase in both plasma GH and TSH levels, suggesting that SRIF tonically inhibits the release of both pituitary hormones (62).

2.2.3.3 Localization of SRIF in the hypothalamus. Hypothalamic lesion and electrical stimulation experiments suggest that SRIF containing structures would be found in the preoptic area of the hypothalamus. Immunohistochemical studies have shown that the largest concentration of cell bodies containing SRIF is found in the periventricular and preoptic areas (87-89). More specifically the cell bodies are found in the anterior periventricular nucleus, the suprachiasmatic nucleus and the parvocellular component of the paraventricular nucleus (90,91). Cells from these regions have axons that project mostly to the median eminence (92), but also to the AN and the VMN, as well as to extrahypothalamic regions (91). The projection of SRIF neurons to the AN and VMN suggests that SRIF may be involved in the control of GRF release.

2.2.3.4 Control of SRIF release from the hypothalamus. Several in vivo and in vitro approaches have been used to study the control of SRIF secretion from the hypothalamus

(93-95). Each has its advantages and disadvantages, but the data provided by these different techniques generate a consistent picture (96). Dopamine and norepinephrine stimulate release while serotonin (5-HT) and GABA inhibit release. Acetylcholine (ACh) has been reported to increase SRIF levels in portal blood, but is also reported to have either no effect or to stimulate SRIF release from dispersed hypothalamic cells (93).

Of great interest is the possible role of SRIF in GH feedback regulation. As mentioned above, GH inhibits the release of GRF, thus inhibiting the stimulation of its own release. GH inhibits its own release by also stimulating SRIF release from the hypothalamus. GH depletion by hypophysectomy results in decreased SRIF content of the median eminence which is restored by GH replacement (97-99). A direct effect of GH on the hypothalamus is suggested by reports that GH stimulates SRIF release from hypothalamic fragments in vitro (100,101). This action of GH is further supported by the observation that intraventricular adminstration of GH results in an increase in SRIF in portal blood (102). Therefore it is now accepted that both SRIF and GRF are involved in GH short-loop feedback (83).

Insulin-like growth factor I (IGF-1 or somatomedin C), produced by the liver under GH control, inhibits GRF-stimulated GH release from pituitary cells (103). IGF-1 also stimulates SRIF release from hypothalamic fragments in vitro (94,104). These observation suggest that IGF-1 is involved in the long-loop feedback regulation of GH release and that its action on the hypothalamus consists in stimulating SRIF release.

2.2.4 The Interrelation of GRF and SRIF in the Generation of GH Secretory Bursts.

Since the development of the first GH RIA, in the 1960's, it has been known that plasma GH concentration is not constant, but is pulsatile (52,53,85,105-108). The release of GH is episodic and occurs in bursts (85,105-107). Between secretory bursts, or pulses, plasma GH is nearly undetectable. The secretion of GH follows an ultradian rhythm, such that secretory

bursts occur at more or less constant intervals (36,106,107). As previously mentioned, lesion of the VMN results in the suppression of this pulsatile GH secretion (30). This suggested that the pulsatile release of GH is under the control of GRF. This view is supported by the report from Tannenbaum et al. (53) which showed that pulsatile GH release could be restored by iv GRF injections in VMN-AN lesioned rats. Interestingly the second of three identical injections produced a smaller GH response than the other two. They also demonstrated that SRIF could decrease the GH response to the first GRF injection. This led them to suggest that endogenous SRIF levels were high during the second injection. Tannenbaum and Ling (52) reported that if GRF is injected into normal rats during a spontaneous GH secretory burst, plasma GH increased further. However if the injection was given during a GH trough the response was practically non-existent. If the rats were passively immunized with SRIF antiserum, GRF injection during the trough period resulted in a large GH secretory burst. It was concluded that SRIF and GRF secretion from the hypothalamus is phasic, with alternating periods of low and high rates of secretion. It was proposed that SRIF and GRF secretion would be out of phase, such that portal GRF concentration would be highest when that of SRIF would be lowest and vice versa (52). GH secretion from the pituitary would then occur only during GRF peaks. The measurement of SRIF and GRF in portal blood confirmed the Tannenbaum model. Plotsky and Vale (109) found that GRF secretion is episodic, with peak concentration occurring just before the expected GH secretory burst. When the GRF concentration was high the SRIF concentration was moderately reduced.

Using the in vitro model of perifused rat pars distalis cells, Kraicer et al. (80) have shown that SRIF prevents GRF-induced GH release, and that SRIF withdrawal in the presence of GRF results in a GH secretory burst much larger than the typical SRIF rebound. The size of the burst was dependent on the concentration of GRF prior to withdrawal (45). They also found that removing SRIF for only 1 min during a continuous perifusion with GRF resulted in a short GH secretory burst (45). These result suggest that, in vivo, the timing of a GH

secretory burst is dependent on the decrease of portal SRIF concentration and not on the episodic increase in GRF release. The magnitude of the burst, however is dependent on the GRF concentration prior to, and during the low SRIF period (45).

2.2.5 Summary

The release of GH from the somatotrophs of the anterior pituitary is under the combined control of two hypothalamic factors, GRF and SRIF. GRF stimulates release while SRIF inhibits both basal and GRF-induced release. GRF is a 40 to 44 amino acid peptide found in neurons of the ventromedial and arcuate nuclei and secreted into the hypophysial portal system in the median eminence. The cell bodies of the neurons which release SRIF, a 14 amino acid cyclic peptide, into the portal system are located in the preoptic area of the hypothalamus. The control of GRF and SRIF release is probably dependent on input from higher neural centres as well as by circulating levels of GH and IGF-1. The episodic release of GH, in vivo, is due to the phasic release of SRIF and GRF. The timing of a GH secretory burst is dependent on a drop in portal SRIF concentration while the magnitude of the burst is dependent on GRF concentration.

2.3 Mechanism of Action of GRF and SRIF in Somatotrophs.

In the previous section the effect of GRF and SRIF on GH release was reviewed. In this section the intracellular mechanism of action of GRF and SRIF associated with the regulation of GH release will be reviewed. Receptors, and how they modulate cellular metabolism, as well as changes in intracellular metabolites and membrane potential will be considered.

2.3.1 GRF

2.3.1.1 GRF Receptor. GRF binds to specific receptors on the pituitary cell membrane (110-115). GRF binding to mixed anterior rat pituitary cells has a K_d of $4.1x10^{-11}$ M while the binding affinity for isolated rat pituitary cell membranes is lower with a K_d of $1.9x10^{-10}$ M (113,114). The EC_{50} for hpGRF-induced GH release from bovine pituitary cells is one order of magnitude lower than the EC_{50} for hpGRF displacement of radiolabelled hpGRF from bovine GRF receptors (115). Since there is only one class of receptors, as determined by competition binding stuies (113,115), this result suggested that only 10% of GRF receptors need to be occupied for maximal effect. Covalent crosslinking of radiolabelled GRF to rat and bovine pituitary cell membranes has revealed membrane-associated GRF-binding proteins of 26 kDa and 75 kDa (111,112). The number of receptors present on the surface of the cell can be regulated by glucocorticoids (113); this correlates well with the observation that glucocorticoids enhance the responsiveness of pituitary cells to GRF (43). GRF may down regulate its own receptor. Indeed pituitary cell membranes from rats infused with GRF for 24 h have lower GRF specific binding than membranes from saline infused rats (116). Studies using cultured rat pituitary cells have shown that the reversible decrease in specific binding increases with exposure time, and that it is GRF concentration-dependent (117).

2.3.1.2 cAMP is a second messenger for GRF. The binding of GRF to its receptor is the starting point for the cAMP second messenger cascade. The binding of a hormone to its receptor allows the interaction of the receptor complex with a GTP-binding protein (G_s) and the binding of GTP. The activated G_s then can interact with the membrane bound enzyme, adenylate cyclase, which catalyses the conversion of ATP to cAMP. cAMP then interacts with cAMP-dependent protein kinase (PKA) and facilitates the cleaving of the catalytic subunit. This subunit then catalyses the phosphorylation of protein substrates. Cyclic AMP is broken down to AMP by phosphodiesterase.

Sutherland (118) proposed that if a hormone uses cAMP as a second messenger, then 4 criteria have to be met. For GRF these would be: 1) GRF will stimulate adenylate cyclase activity in somatotrophs; 2) GRF will increase cAMP accumulation prior to, or concurrent with, an increase in GH release from somatotrophs; 3) Phosphodiesterase inhibitors will potentiate GRF-stimulated GH release from somatotrophs; and 4) Membrane permeable cAMP analogues will stimulate GH release from somatotrophs.

GRF fulfils all the criteria. GRF has been shown to stimulate adenylate cyclase in rat, human and bovine pituitary cells membranes (119-122). Recently Narayanan et al. (123) demonstrated that rat GRF stimulates adenylate cyclase in a rat somatotroph membrane preparation in a concentration dependent fashion, and that this effect is dependent on GTP. The effect of GRF on cAMP release or accumulation by pituitary cells in vitro was established soon after the discovery of its structure (3,42,44). Sheppard et al. (1) showed that hpGRF raised cAMP accumulation in rat somatotrophs prior to a detectable increase in GH release. Stimulation of GH release from pituitary cells and purified somatotrophs by cAMP analogues has been known for some time (5). The phosphodiesterase inhibitors IBMX and theophylline stimulate GH release by raising cAMP accumulation (6,124). Concentrations of GRF which neither increase cAMP accumulation nor GH release, can stimulate both when rat somatotrophs are treated with IBMX at an ineffective concentration (1). Thus phosphodiesterase inhibitors potentiate the effect of GRF.

2.3.1.3 Ca^{2+} is essential for GRF action. The essential requirement for extracellular Ca^{2+} for the action of GRF was reported shortly after the structure was announced (2,3,44). Bilezikjian and Vale (3) showed that GRF-stimulated GH release from rat pituitary cell cultures was decreased in a concentration dependent fashion by the Ca^{2+} antagonist verapamil and by Co^{2+} and Cd^{2+}. A report from the same group also showed that chelating extracellular Ca^{2+} with ethyleneglycol-bis-(β-aminoethyl ether)-N,N,N',N'-tetraacetic acid (EGTA) dramatically

decreased the GRF-induced GH release from cultured pituitary cells. These results suggest that GRF stimulates Ca^{2+} influx. GRF also causes $[Ca^{2+}]_i$ to increase in rat pituitary cells (125,126) and rat somatotrophs (50,127). This effect is inhibited by either Ca^{2+} antagonists or Ca^{2+}-free medium (50,125,126). Thus GRF presumably increases $[Ca^{2+}]_i$ by stimulating Ca^{2+} influx. Increasing cAMP accumulation by either activating adenylate cyclase with forskolin, or cAMP analogues, raises $[Ca^{2+}]_i$ in rat pituitary tumour cells (15,128). This suggests that the effect of GRF on $[Ca^{2+}]_i$ may be cAMP-dependent.

2.3.1.4 Phosphoinositide cycle and Protein Kinase C (PKC). The phosphoinositide cycle and PKC intracellular signalling systems may play a role in GRF-induced GH release. The cycle consists of the phosphorylation and dephosphorylation of inositol and its incorporation into membrane phospholipids (Figure 4) (129). Phosphorylated inositol combines with diacylglycerol (DAG) to form the membrane phospholipid phosphatidylinositol (PI), which is phosphorylated stepwise to give phosphatidylinositol-4-monophosphate (PIP) and phosphatidylinositol-4,5-bisphosphate (PIP_2). The membrane bound G-protein-dependent enzyme phosphlipase C (PLC) hydrolyses PIP_2 producing DAG and inositol 1,4,5-trisphosphate (IP_3). Hydrophilic IP_3, which is found in the cytosol, is stepwise dephosphorylated to inositol 1,4-bisphosphate (IP_2), inositol 1-monophosphate (IP) and finally back to inositol. IP_3 can be further phosphorylated to inositol 1,3,4,5-tetrakisphosphate (IP_4). In certain cell types, IP_3 and IP_4 stimulate the mobilization of stored Ca^{2+} and Ca^{2+} influx (129-131). DAG binds to Ca^{2+}- and phospholipid-dependent protein kinase C (PKC) and increases the affinity of the enzyme for Ca^{2+}. This increased affinity results in an increase in PKC activity and a translocation of the enzyme from the cytosol to the membrane at resting $[Ca^{2+}]_i$ (130,132,133). The binding of hormones to their receptors increases PLC activity via the action of a G-protein, thus increasing the turnover rate of the phosphoinositide cycle (130,134,135). Consequently the concentration of DAG in the membrane and IP_3 in the cytosol increases. This leads to an increase in protein phosphorylation and $[Ca^{2+}]_i$.

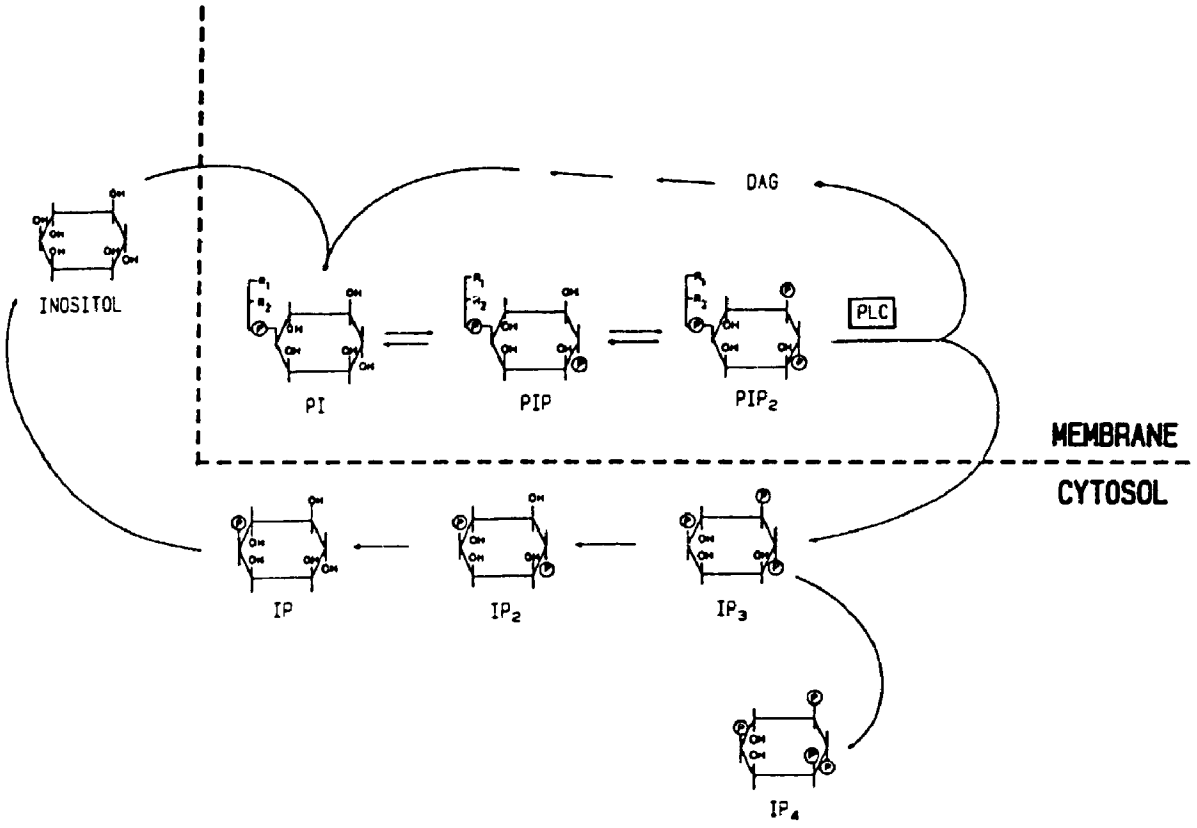

Figure 4. **The phosphoinositide cycle.** PI: phosphatidylinositol; PIP: phosphatidylinositol-4-monophosphate; PIP_2: phosphadylinositol-4,5-bisphosphate; IP: inositol 1-mono-phosphate; IP_2: inositol 1,4-bisphosphate; IP_3: inositol 1,4,5-trisphosphate; IP_4: inositol 1,3,4,5-tetrakisphosphate; DAG, diacylglyceraol; PLC, phospholipase C.

There are conflicting reports as to whether GRF stimulates the phosphoinositide cycle. Canonico et al. (136) reported that GRF increased ^{32}P incorporation into phosphatidylinositol in cultured rat pituitary cells. On the other hand Escobar et al. (137) were unable to detect changes in the accumulation of [^{3}H]-inositol phosphate in GRF-treated cultured rat pituitary cells.

The involvement of PKC in GRF action is suggested by the observation that agents which stimulate PKC, such as phorbol esters and diacylglycerol analogues, stimulate GH release from anterior pituitary cells and purified somatotrophs (2,48,138-145). However, French et al. (48) recently demonstrated that though activation of PKC with phorbol esters and DAG analogues stimulates GH release from purified somatotrophs, PKC activity is not essential for GRF-induced GH release. They also reported that both phorbol ester and DAG analogues significantly increase cAMP accumulation in somatotrophs. Therefore whether the phosphoinositide cycle and PKC are involved in the mechanism of action of GRF in somatotrophs is still unclear.

2.3.1.5 GRF causes membrane depolarization. Kato et al. (125) have shown, using the voltage sensitive dye bis-(1,3-diethylthiobarbiturate) trimethineoxonol (bis-oxonol), that GRF causes a Na^{+}-dependent depolarization of rat pituitary cells. The same group previously reported that extracellular Na^{+} was essential for GRF-induced GH release from rat pituitary cells (146). However, GRF-induced GH release is insensitive to the voltage-sensitive Na^{+} channel blocker tetrodotoxin (TTX) (147,148). Interestingly $(Bu)_2$cAMP-stimulated GH release was also found to be Na^{+}-dependent (146). Thus Kato et al. proposed that GRF depolarizes pituitary cells by activating TTX-insensitive Na^{+} channels via cAMP (125,146).

2.3.2 SRIF

SRIF receptors have been identified in brain, exocrine pancreas, adrenal cortex, anterior pituitary, and in several tumour cell lines and they are neither functionally nor structurally homogenous (149). Therefore this review will deal with pituitary SRIF receptors and mechanisms of action of SRIF in pituitary cells. Most of the information we have on the mechanism of action of SRIF in pituitary cells is derived from experiments carried out with pituitary tumour cell lines. Interestingly the first SRIF receptor was identified in GH secreting GH_4C_1 rat pituitary tumour cells (12). Another cell line, which is used in the study of the action of SRIF, is the murine ACTH secreting AtT-20 pituitary tumour, which also has SRIF receptors (150,151). It should be noted that these cells are different from normal pituitary cells in many ways (see Chapter 1), and that pathways and mechanisms which are present in these cells may not be present in the somatotrophs.

2.3.2.1 Pituitary SRIF receptor. Studies using radiolabelled SRIF analogues have revealed that rat pituitary cells have specific SRIF receptors (152-155). The reported K_d for SRIF binding is in the range of $1.1x10^{-9}$ to $0.16x10^{-9}$ M. Cross-linking experiments show that pituitary cells contain a 200 kDa binding protein (149), while photoaffinity labelling experiments reveal a 88 kDa SRIF binding protein (156). Ca^{2+} potentiates specific binding of SRIF to pancreatic acinar cells as well as to brain membranes at concentrations lower than 0.1 mM, while higher concentrations inhibit binding (157). However this Ca^{2+} sensitivity is absent in pituitary receptors (158). Two classes of SRIF receptors with different affinities have been reported in the rat brain, but the pituitary has only high affinity receptors (159,160). The pituitary SRIF receptor has a greater affinity for SRIF-28 than for SRIF (161), as would be expected given the reported higher biological activity of SRIF-28 (70). In AtT-20 cells, down-regulation of the receptor, as indicated by a decrease in SRIF binding capacity, occurs after prolonged exposure to SRIF or SRIF-28 (162).

2.3.2.2 SRIF receptor is coupled to a G-protein. To study the role of G-proteins in the inhibitory action of SRIF on GH release, it is necessary to bypass the G-protein-dependent signal transduction pathways associated with GRF-dependent activation of adenylate cyclase or the activation of phospholipase C which then results in the activation of PKC. Boyd et al. (163) have done this by stimulating GH release from ovine anterior pituitary cells by stimulating adenylate cyclase directly with forskolin, and stimulating PKC directly with phorbol esters. The inhibitory action of SRIF on forskolin- and phorbol ester-stimulated GH release from ovine pituitary cells is completely abolished by pertussis toxin (163). Pertussis toxin is known to reduce the inhibitory effect of G_i, the GTP-binding protein which inhibits adenylate cyclase (164). SRIF does not reduce cAMP accumulation in ovine pituitary cells stimulated with either forskolin or phorbol esters (163). This suggested that SRIF acts via G_i and that the G-protein would act at a site other than adenylate cyclase. The role of G-proteins in the intracellular mechanism of action SRIF will be reviewed in more detail below in the context of the effect of SRIF on cAMP accumulation, Ca^{2+} conductance, membrane potential and $[Ca^{2+}]_i$.

2.3.2.3 cAMP accumulation. Cyclic AMP accumulation by rat pituitaries or by rat somatotrophs stimulated with GRF is modestly reduced by SRIF, while the augmented release of GH is abolished (1-3,42). Direct enzyme activity measurements in isolated membranes, from rat anterior pituitary cells or GH_3 cells, indicated that SRIF decreased adenylate cyclase activity (119-121,165-166). In GH_4C_1 pituitary tumour cells, pertussis toxin blocks the SRIF inhibition of both VIP-stimulated cAMP accumulation and adenylate cyclase activity, suggesting that SRIF acts on adenylate cyclase via G_i (13). However, Narayanan et al. (123) found that SRIF had no effect on adenylate cyclase from purified rat somatotrophs. In this preparation GRF-stimulated GH release is completely abolished by SRIF while cAMP accumulation is decreased by less than 25%. The mechanism by which cAMP is reduced is not clear, however activation of phosphodiesterase is probably not involved (167). The modest drop in cAMP accumulation

may not be biologically significant since SRIF totally inhibits GH release from pituitary cells and somatotrophs treated with cAMP analogues (5,6,9,168-170).

2.3.2.4 SRIF causes membrane hyperpolarization. Israel et al. (171) using intracellular recording techniques showed that SRIF hyperpolarizes purified rat somatotrophs. More recently, using bis-oxonol, SRIF has been shown to repolarize or hyperpolarize rat pituitary cells depolarized by GRF (125). To study the mechanism which underlies SRIF-dependent hyperpolarization, Koch et al. (128) studied the effect of SRIF on E_m using bis-oxonol and altering extracellular concentrations of Na^+, Cl^-, Ca^{2+} and K^+. They found that only increasing extracellular K^+ concentration prevented the hyperpolarizing or repolarizing effects of SRIF. Furthermore the K^+ channel blocker tetrabutylammonium (TBA) also prevented the repolarizing and hyperpolarizing effects (172). The authors proposed that SRIF hyperpolarizes the cell by increasing K^+ conductance (128,172). The hyperpolarization effect of SRIF is inhibited by pertussis toxin, indicating that the change in K^+ conductance is mediated via G_i (173).

2.3.2.5 SRIF decreases Ca^{2+} conductance. Patch clamp, in the whole-cell configuration, allows for the measurement of ion currents across the membrane of small cells. Whole-cell voltage clamp revealed that SRIF blocks depolarization-induced Ca^{2+} currents in several types of neuronal cells (174-176). Luini et al. reported that SRIF had a similar action on Ca^{2+} currents in mouse pituitary AtT-20 cells (14,177). They found that for a given depolarization, SRIF reversibly decreased the resulting maximal Ca^{2+} current. SRIF also increased the time to reach maximum Ca^{2+} current. These effects were independent of cAMP (14). The action of SRIF was not reversible if the cells were depolarized in the presence of guanosine-5'-O-(3'-thiotrisphosphate) (GTP-γ-S: a non-hydrolysable analogue of GTP), but was abolished by pertussis toxin (177). This suggests that SRIF-dependent changes in Ca^{2+} conductance are mediated by G_i-Ca^{2+} channel interactions.

2.3.2.6 SRIF lowers $[Ca^{2+}]_i$. SRIF decreases basal $[Ca^{2+}]_i$ in mouse pituitary AtT-20 (14,177), rat pituitary GH_3 (178) and GH_4C_1 (13,128,172) cells, as well as in rat pituitary cells (125) and somatotrophs (50,179,180). In GH_4C_1 and AtT-20 cells the drop in $[Ca^{2+}]_i$ is abolished by pertussis toxin (13,177). This suggests that G_i is involved in the decrease of $[Ca^{2+}]_i$. G_i may act directly on Ca^{2+} channels to decrease Ca^{2+} influx, or indirectly by increasing K^+ conductance to lower E_m. SRIF also inhibits stimulated increases in $[Ca^{2+}]_i$. Treating rat somatotrophs with low concentrations of the Ca^{2+} ionophore bromo-A23187 results in an increase in $[Ca^{2+}]_i$ which is inhibited by SRIF (181). The increase in $[Ca^{2+}]_i$ induced by elevated cAMP accumulation, brought about by either stimulating adenylate cyclase with forskolin, or by treatment with cAMP analogues, is inhibited by SRIF in rat pituitary tumour cells (15,128). Similar increases in $[Ca^{2+}]_i$ stimulated by CRF in AtT-20 cells (15,182) and by GRF in rat pituitary cells (125) or somatotrophs (50) are also inhibited by SRIF. Since SRIF does not inhibit rat somatotroph adenylate cyclase, the decrease in GRF-stimulated increase in $[Ca^{2+}]_i$ can be attributed to hyperpolarization and decreased Ca^{2+} conductance.

2.3.3 Summary.

GRF stimulates GH release from somatotrophs by interacting with its receptor on the surface of the cell. The receptor interacts with G_s and stimulates adenylate cyclase. This results in an increase in cAMP accumulation which leads to the activation of PKA. The PKA is at the beginning of a cascade which ends with the release of GH. However GRF-induced GH release also requires extracellular Ca^{2+}. cAMP or PKA may cause a Na^+-dependent depolarization which would stimulate Ca^{2+} influx leading to an increase in $[Ca^{2+}]_i$ and GH release.

SRIF inhibits GH release from the somatotrophs by interacting with its receptor on the surface of the cell. The receptor interacts with a pertussis toxin-sensitive G-protein. This G-

protein most probably does not interact with rat somatotroph adenylate cyclase. However it may be involved in the increase in K^+ conductance, which leads to hyperpolarization. It may also be involved in the reduction of Ca^{2+} conductance. Both these effects may be responsible for the SRIF-dependent lowering of $[Ca^{2+}]_i$, which is believed to be responsible for the inhibition of GH release.

2.4 Stimulus-secretion Coupling and Intracellular Ca^{2+}.

2.4.1 The Douglas Model for Stimulus-secretion Coupling.

In the early 1960's, Douglas and co-workers, while investigating the mechanism by which acetylcholine (ACh) stimulates catecholamine release from adrenal chromaffin cells, coined the term "stimulus-secretion coupling" (183). By this they referred to all the events occurring in a cell exposed to a secretagogue, which lead to the release of a secretory product by exocytosis. They had found that chromaffin cells released catecholamine abundantly when perfused with ACh. This effect was abolished when Ca^{2+} was removed from the perfusion medium, and returned when Ca^{2+} was added back to the medium (183). When Douglas and his group studied the effect of ACh on chromaffin cell membrane potential, they found that ACh caused depolarization but never generated action potentials. The ACh-dependent depolarization was dependent primarily on Na^+. However, when Na^+ was removed from the medium, ACh still depolarized the membrane and stimulated catecholamine release. This depolarization was attributed to Ca^{2+} influx (183). From these experiments Douglas proposed the following scheme for stimulus-secretion coupling: ACh interaction with its plasma membrane receptor leads to an altered membrane chemistry, which in turn increases the membrane permeability to Na^+ and Ca^{2+}, which leads to depolarization (without action potentials). The entry of Ca^{2+} leads to catecholamine release by exocytosis. This scheme has been extended to other neurosecretory, neuronal, exocrine and endocrine cells (183-185).

2.4.2 Intracellular Ca^{2+} Homeostasis.

For Ca^{2+} to act as a signal for the onset of secretion, as suggested by the Douglas model, $[Ca^{2+}]_i$ has to undergo rapid and large fluctuations (186). The most efficient way to achieve this is by maintaining $[Ca^{2+}]_i$ as low as possible, such that a small addition of Ca^{2+} to the cytosol results in a large increase in $[Ca^{2+}]_i$. Ca^{2+} is a signalling agent not only for secretion but for a large number of functions, including the regulation of metabolic pathways, the synthesis of hormones, muscle and nonmuscle motility and several other membrane linked processes (186,187). Most Ca^{2+} regulated processes require the reversible binding of Ca^{2+} to an enzyme. The average K_m for Ca^{2+} of such enzymes is in the 0.1 to 1 μM range. Thus $[Ca^{2+}]_i$ is maintained in this range. The extracellular Ca^{2+} concentration, on the other hand, is approximately 1.2 mM. Therefore there exists a 10,000 fold concentration gradient for Ca^{2+} across the cell membrane. The significance of this gradient is that a small change in plasma membrane permeability leads to a Ca^{2+} influx which results in a rapid and massive increase in $[Ca^{2+}]_i$.

The total Ca^{2+} concentration in cells is much higher than the free Ca^{2+} concentration. Indeed erythrocytes contain 20 μM Ca^{2+}, axons 200-400 μM, brain cells 1.5 mM, liver cells 1.6 mM and heart cells 4 mM (186). The free Ca^{2+} corresponds to less than 0.1% of the total intracellular Ca^{2+}. The bulk of cellular Ca^{2+} is bound to membranes and to Ca^{2+}-binding proteins, and sequestered in mitochondria, endoplasmic reticulum (ER) and calciosomes. The calciosome, found in nonmuscle cells, is an intracellular organelle containing the Ca^{2+}-binding protein calsequestrin, which has properties similar to those of the sarcoplasmic reticulum (SR) of muscle (188).

Several structures in the cell are involved in Ca^{2+} homeostasis (186,189,190). The plasma and organelle membranes, as well as soluble proteins, bind Ca^{2+}. The plasma membrane contains Na^+/Ca^{2+} exchangers and Ca^{2+}-ATPases which extrude Ca^{2+} from the cell,

as well as Ca^{2+} channels which allow Ca^{2+} to enter the cell. The mitochondria have Ca^{2+}-uniporters, which transport Ca^{2+} from the cytosol to the mitochondrial matrix, as well as Na^+/Ca^{2+} exchangers which extrude Ca^{2+} into the cytosol. The ER/calciosomes have Ca^{2+}-ATPases which pump Ca^{2+} into their lumens, as well as IP_3-regulated Ca^{2+} channels which allow the release of stored Ca^{2+} into the cytosol. In the sections that follow, these Ca^{2+} handling systems and their role in Ca^{2+} homeostasis and the generation of a Ca^{2+} signal will be reviewed.

2.4.2.1 Bound Ca^{2+}. Over 99.9% of cellular Ca^{2+} is in the bound form or precipitated as calcium phosphates in the mitochondria. A sizable fraction of total cellular Ca^{2+} is bound with high affinity to membrane phospholipids (186,191). The soluble cytosolic Ca^{2+}-binding protein, calmodulin (CaM), may be important in buffering free Ca^{2+}. However it should be remembered that the primary function of CaM is Ca^{2+}-dependent regulation of enzyme activity, and not Ca^{2+} buffering. Cellular CaM concentration varies from 2 μM in muscle to 30 μM in brain, and with a K_d of about 1 μM, in the presence of 1 mM Mg^{2+}, it can buffer from 8 to 120 μM Ca^{2+} (186).

2.4.2.2 Na^+/Ca^{2+} Exchangers. There are two Na^+/Ca^{2+} exchangers in the cell. The first is found in the plasma membrane, and the second is found in the mitochondrial membrane (186,187,189,190). The former is important in lowering $[Ca^{2+}]_i$, while the latter may be important in raising $[Ca^{2+}]_i$.

The plasma membrane Na^+/Ca^{2+} exchanger was first characterized in heart muscle and giant squid axon (192-194). The driving force for this carrier is the Na^+ concentration gradient across the cell membrane, which is maintained by the action of Na^+/K^+-ATPase. This system is electrogenic, as it transfers 3 Na^+ into the cell while it extrudes 1 Ca^{2+} from the cytosol (186). Its affinity for Ca^{2+} is relatively low with a K_m of 1 - 20 μM (187). Therefore this system may not be significant in the maintenance of $[Ca^{2+}]_i$ in the 100 nM range. However

the Ca^{2+} affinity of the exchanger can be increased to a functional level, by PKA-dependent phosphorylation in heart muscle (195).

The mitochondrial Na^+/Ca^{2+} exchanger is electroneutral, in that it transfers 1 Ca^{2+} from the mitochondrial matrix to the cytosol, while 2 Na^+ are transferred to the matrix (186,187). The function of this system, and the mitochondria in general, in the control of cytosol Ca^{2+} appears to be minor (187). It is believed that the exchanger's primary function is the regulation of mitochondrial matrix Ca^{2+} concentration (186,187,189,190).

2.4.2.3 Mitochondrial Ca^{2+}-uniporter. The mitochondria obtain Ca^{2+} from the cytosol via a Ca^{2+}-uniporter. The driving force for this Ca^{2+} uptake is the electrical gradient generated by the pumping of H^+ out of the matrix by the respiratory electron chain. This results in a membrane potential across the inner mitochondrial membrane of 150 to 180 mV negative inside (189). The rate of Ca^{2+} uptake is regulated by $[Ca^{2+}]_i$ (189). Under normal physiological conditions the mitochondria do not contain large amounts of Ca^{2+} (1-5 nmol/mg mitochondrial protein), however isolated mitochondria, or mitochondria from injured cells can accumulate very large quantities of Ca^{2+} due to the formation of Ca phosphate precipitates.

2.4.2.4 Ca-ATPase. There are two Ca-ATPases or Ca^{2+} pumps in cells, one in the plasma membrane and the other in ER/calciosome membrane (186,188-190). Plasma membrane Ca-ATPase was first described in erythrocytes (196). The Ca^{2+} pump is a single 138 kDa protein with Mg^{2+}-dependent ATPase activity, which transports Ca^{2+} out of the cell with a 1:1 stoichiometry to hydrolysed ATP (187,197). The plasma membrane pump is electroneutral since it exchanges 2 H^+ for each Ca^{2+} extruded from the cell (198,199). The pump has a high affinity for Ca^{2+} with a K_m of approximately 1 μM, which allows it to extrude Ca^{2+} at physiological resting $[Ca^{2+}]_i$ (186,187). The rate of pumping is dependent on $[Ca^{2+}]_i$. The affinity of the enzyme for Ca^{2+} is allosterically increased by Ca^{2+}-calmodulin (Ca-CaM) (200,201). The activity

of the pump is also controlled by cAMP-dependent phosphorylation (200,202). Recently it has been shown that PKC-dependent phosphorylation increases the maximal pumping rate (V_{max}) (201,203).

Most of what is known about ER/calciosome Ca-ATPase is based on experiments carried out on SR Ca-ATPase. However, it is assumed that their properties are similar. The SR pump is a single 100 kDa protein (204). It is a Mg^{2+}-dependent ATPase which transports Ca^{2+} into the ER with a 2:1 stoichiometry to hydrolysed ATP (186,187). The ATPase has a high affinity for Ca^{2+} with a K_m varying from 0.1 to 1 μM (186,187).

The hysteretic character of plasma membrane Ca-ATPase activation by Ca-CaM may play a significant role in the control of $[Ca^{2+}]_i$. In other words, Ca-ATPase, once stimulated by Ca-CaM, will pump Ca^{2+} out of the cell at a high rate even when $[Ca^{2+}]_i$ has returned to basal levels (205,206). This allows for a high exchange rate of Ca^{2+} across the plasma membrane without raising the overall cytosol Ca^{2+} concentration (207).

2.4.2.5 Voltage-sensitive Ca^{2+} channels. Ion channels have been classified as voltage-sensitive or receptor-operated. Examples of the former are the Na^+ and K^+ channels of axons, while the ACh receptor of the motor end plate is an example of the latter. Plasma membrane Ca^{2+} channels have also been classified into these categories: voltage-sensitive Ca^{2+} channels (VSCC) and the receptor-operated Ca^{2+} channels (ROCC) (147,208). The ROCC's have been further classified into true ROCC, such as the glutamate or N-methyl-D-aspartic acid (NMDA)-gated channel in neurons (209), and second messenger-operated Ca^{2+} channel (SMOCC), such as the IP_3-regulated Ca^{2+} channels in lymphocytes and mast cells (210,211). In this section characteristics of VSCC's will be reviewed, while in the next section the properties of SMOCC's, which are also found in organelle membranes, will be reviewed.

Three functional types of VSCC's (T, N, and L) have been characterized using patch clamp either in the whole-cell or cell attached configurations (212-214). They are classified according to electrical, kinetic, and pharmacological criteria, and tissue distribution. Electrical characteristics include membrane potentials at which they activate and the conductance of individual channels. Kinetic characteristics include the rate at which Ca^{2+} currents decrease during sustained depolarization (rate of inactivation), and the rate at which Ca^{2+} currents return to zero after a return to resting potential (rate of deactivation). Pharmacological characteristics include inhibition of Ca^{2+} currents by inorganic, Cd^{2+} and Ni^{2+}, and organic, dihydropyridines and ω-conotoxin (ω-CgTX), Ca^{2+} antagonists.

The T type VSCC's, or transient channels, are found in various cell types including rat pituitary cells (213,215). They are responsible for transient Ca^{2+} currents. They activate at E_m's more positive than -70 mV (213,216) and produce a maximal inward current at an E_m of -20 mV (212,217). The conductance of a single T type channel is 8 pS (measured with 90-110 mM $BaCl_2$) (213,216,218). The rate of inactivation is rapid (time constant: τ = 20-50 ms). Deactivation of the channel, measured in GH_3 cells, is slow (219). These channels are sensitive to Ni^{2+} , but not to Cd^{2+}, ω-CgTX or dihydropyridine blockade (213).

The N type VSCC's, or neural channels, are found only in neuronal cells. They activate at E_m more positive than -30 mV (213,216) and produce a maximal inward current at E_m of +20 mV (212,217). The conductance of a single N type channel is 13 pS ($BaCl_2$) (213,216,218). The rate of inactivation is moderate (τ = 50-80 ms). This channel is sensitive to Cd^{2+} and ω-CgTX, but not to Ni^{2+} or dihydropyridine blockade (213).

The L type VSCC's, or the long-lasting channels, are found in various cell types including rat pituitary cells (213,215). They are responsible for sustained Ca^{2+} currents. They activate at E_m more positive than -10 mV (213,216) and produce a maximal inward current at

E_m of +10 mV (212,217). The conductance of a single L type channel is 25 pS ($BaCl_2$). The rate of inactivation is very slow (τ > 500 ms) (213,216,218). The deactivation of the L channel, as evaluated in GH_3 cells, is fast (219). These channels are sensitive to Cd^{2+}, ω-CgTX and dihydropyridine, but not to Ni^{2+} blockade (213).

The L type VSCC's can be modulated by several second messenger systems. Neurotransmitters and hormones have been shown to alter Ca^{2+} current in a variety of tissues (220). These effects are, in many cases, mediated by second messengers such as G-proteins, cAMP, and PKC. G-proteins have been reported to either increase or decrease evoked Ca^{2+} currents in several systems (177,220,221). The effect of cAMP on cardiac muscle Ca^{2+} currents is well established (222-225). Phosphorylation of Ca^{2+} channels in vitro by PKA has been reported (226). The voltage sensitivity of the GH_3 cell L type channel is dependent on phosphorylation by PKA (227). PKC activators such as phorbol esters and diacylglycerol analogues, are reported to either increase or decrease Ca^{2+} currents in several cell types (220,228-231). These results have been interpreted as demonstrating PKC-dependent modulation of Ca^{2+} channels. Channel phosphorylation or G-protein interaction with a channel alters the voltage sensitivity, or probability of opening of the channel, but does not change conductance of the channel (220).

In summary VSCC's are classified into three categories, T, N, and L, which differ in their conductance, activation potential and sensitivity to Ca^{2+} antagonists. The voltage sensitivity of L type channels can be modulated by G-proteins and either PKA- or PKC-dependent phosphorylation. The significance of Ca^{2+} channels in the regulation of $[Ca^{2+}]_i$, is that they allow for triggered increases in $[Ca^{2+}]_i$. Indeed either neurotransmitters or hormones, via their second messengers or their effect on E_m, may modulate Ca^{2+} influx through VSCC's.

2.4.2.6 Inositol phosphate-regulated SMOCC's and Ca^{2+} mobilization. SMOCC's in the ER/calciosome membrane are involved in the mobilization of Ca^{2+} stores. IP_3 was first demonstrated to stimulate the liberation of stored Ca^{2+} from ER in permeabilized pancreatic acinar cells (232). Interestingly IP_3 stimulates the mobilization of about 30-50% of non-mitochondrial stored Ca^{2+} (129). The remainder can, however, be mobilized by Ca^{2+} ionophores. IP_3 binds to microsomal membranes with high affinity and specificity (129,130). Recently a 260 kDa protein has been purified which is believed to be the IP_3 receptor (233). Immunocytochemical studies, using an antibody to the 260 kDa protein, has revealed that the receptor is localised on parts of the ER (234). The IP_3 receptor and the IP_3-sensitive Ca^{2+} channel are believed to be the same molecule (129,130). The conductance of the SR channels is about 10 pS (235). The binding of 3 IP_3 molecules is required for channel opening (236).

As mentioned above, IP_3 is reported to stimulate Ca^{2+} influx across the plasma membrane in lymphocytes and mast cells. The influx is believed to be through IP_3 gated channels. Putney (237) has proposed a capacitive model as an alternative for Ca^{2+} influx in non-excitable cells. In this model the ER is filled with Ca^{2+} from the extracellular milieu by an as yet unknown route. The binding of IP_3 to the ER Ca^{2+} channel causes the emptying of the ER into the cytosol. Extracellular Ca^{2+} then flows through the ER into the cytosol. IP_4 is reported to raise $[Ca^{2+}]_i$ only if IP_3 is present (129). This increase is in part dependent on extracellular Ca^{2+}. Berridge and Irvine (129) have suggested that IP_4 controls the transfer of Ca^{2+} between intracellular pools, such that Ca^{2+} could be transferred from a vesicle which is filled from the extracellular fluid, but devoid of IP_3-gated channel, to a vesicle which has such channels.

2.4.2.7 Summary. In this section the different mechanisms involved in the regulation of $[Ca^{2+}]_i$ at a level 10,000 times lower than extracellular fluid were reviewed. The bulk of cellular Ca^{2+} is either bound to membranes or sequester by organelles. Ca^{2+} enters the cell through Ca^{2+}

channels which are either voltage-sensitive or receptor-operated. Ca^{2+} is removed from the cytosol by plasma membrane and ER/calciosome Ca-ATPases. The mitochondrial Ca^{2+}-uniporter and the plasma membrane Na^+/Ca^{2+} exchanger may also remove Ca^{2+} from the cytosol, but to a much lesser extent. Organelle stored Ca^{2+} can enter the cytosol via the mitochondrial Na^+/Ca^{2+} exchanger or IP_3-gated ER/calciosome Ca^{2+} channel. The combined action of all these systems maintains $[Ca^{2+}]_i$ in the 0.1 to 1 μM range.

The general scheme outlined above is constructed from experimental evidence from different tissues and different experimental preparations. Though all the regulatory processes have been described individually, they may not all be found in all cell types. For example the three types of Ca^{2+} channels are not always found together in the same cell. Though Ca-ATPase is ubiquitous, only the erythrocyte ATPase has been shown conclusively to be regulated by PKC. Finally the intracellular binding sites for IP_3 and for IP_4 have only been reported in a limited number of cell types.

2.4.3 The Intracellular Ca^{2+} Signal.

2.4.3.1 Three Criteria for Ca^{2+} as an Intracellular second messenger. The stimulation-secretion coupling model proposed by Douglas gave a central role to Ca^{2+}. Indeed, as mentioned above, he suggested that an increase in $[Ca^{2+}]_i$ is necessary for hormone release. One can establish 3 criteria which would have to be met before Ca^{2+} could be accepted as a second messenger for hormone- or neurotransmitter-stimulated secretion. The criteria are similar to those proposed by Sutherland for the establishment of cAMP as a second messenger, and are based on what is known about $[Ca^{2+}]_i$ regulation (see above).

1. Any agent which raises $[Ca^{2+}]_i$ must result in secretion even in the absence of stimulating hormone or neurotransmitter.

2. Any agent which prevents $[Ca^{2+}]_i$ from increasing must prevent hormone- or neurotransmitter-stimulated secretion.

3. A stimulating hormone or neurotransmitter must cause an increase in $[Ca^{2+}]_i$ which should precede or be concurrent with the onset of secretion.

2.4.3.2 Experimental approach to the study of Ca^{2+} signalling. Several experimental approaches have been used to study the role of Ca^{2+} in the control of secretion. The most straightforward way to determine if a secretagogue stimulates Ca^{2+} influx is to assess the effect of removing extracellular Ca^{2+} on hormone release (183). However this approach cannot take into account the possible leaching out of essential intracellular Ca^{2+} stores during prolonged exposure to low extracellular Ca^{2+}. This limitation can be overcome by monitoring the effect of Ca^{2+} antagonists on secretagogue-induced hormone release (238). The antagonists used are of two types, either multivalent cations such as Mg^{2+}, Co^{2+}, Mn^{2+}, Cd^{2+}, Ni^{2+} and La^{3+}, or organic compounds such as phenylalkylamines (verapamil), benzothiazepines (diltiazem) and dihydropyridines (nifedipine). The advantage of the organic antagonist is that they are relatively specific for Ca^{2+} channels, and as mentioned above, dihydropyridines are specific for L type channels.

Another approach to the study of the role of Ca^{2+} in stimulus-secretion coupling is to measure Ca^{2+} fluxes across the plasma membrane with ^{45}Ca. These experiments yield information on the flux of Ca^{2+} across the membrane, and how it is altered by secretagogues (239,240).

The essential measurement for the study of Ca^{2+} as a second messenger is the determination of $[Ca^{2+}]_i$. Until 1980 $[Ca^{2+}]_i$ was measured with intracellularly injected photoproteins, such as aequorin, metallochromic indicators, such as arsenazo III, (241,242) or

with Ca^{2+}-sensitive electrodes (243). These techniques require impalement of the cell, a procedure which is not readily applicable to small cells. In 1980 Tsien and his group (244) developed a Ca^{2+}-sensitive fluorescent dye, quin2. The tetrakisacetoxymethyl ester of quin2 (quin2/AM) is lipophilic, and therefore can diffuse freely across the cell membrane (245,246). Intracellular non-specific esterases remove the AM groups producing hydrophilic quin2 which becomes trapped in the cell. In the presence of free ionized calcium quin2 fluoresces in a concentration dependent manner (247). One major disadvantage of quin2 is, that at intracellular concentrations needed for $[Ca^{2+}]_i$ measurements, it acts as a Ca^{2+} buffer (245,248,249). Two more dyes, fura-2 and indo-1, have been developed which have lower Ca^{2+} affinities and higher fluorescent yield (250) (see Appendix). Quin2, indo-1, and especially fura-2 fluorescence measurement, have become the methods of choice for the determination of $[Ca^{2+}]_i$ in a wide variety of cells (248,249,251).

2.4.3.3 Biphasic $[Ca^{2+}]_i$ signals. The $[Ca^{2+}]_i$ changes induced by peptide secretagogues in pituitary cells, as measured with Ca^{2+} sensitive fluorescent dyes, are generally biphasic. The first phase is a rapid increase which reaches a peak and then drops rapidly either to a plateau higher than baseline, or to baseline, and then increases to a new plateau. Such responses are seen with TRH in GH_3 cells (252,253) and rat lactotrophs (254), and with GnRH in rat gonadotrophs (255-257). In all case, if the cells are incubated in Ca^{2+}-free medium and challenged with the peptide, the first phase is retained while the second is abolished (252,254,257,258). If the cells are incubated in the presence of Ca^{2+} antagonists (verapamil or dihydropyridines) the second phase is also inhibited (252,253,256). This has been interpreted as indicating that the second phase is due to an influx of Ca^{2+} through a L type VSCC, while the first phase is due to mobilization of Ca^{2+} stores. GnRH (259-261) and TRH (262,263) are reported to increase the phosphoinositide cycle turnover and increase IP_3 levels in gonadotrophs and GH_4C_1 cells respectively. IP_3 stimulates stored Ca^{2+} mobilization in gonadotrophs (255) as well as in GH cells (264). This suggests that GnRH and TRH could

stimulate IP_3-dependent Ca^{2+} release from the ER/calciosome. In these cells the hormone-induced change in $[Ca^{2+}]_i$ is the result of the coordination of two process: mobilization of stored intracellular Ca^{2+} by IP_3, followed by an influx of Ca^{2+} from the extracellular milieu.

2.4.4 Exocytosis.

Although not directly relevant to this thesis, the actual mechanism of exocytosis is currently an area of extensive investigation. Some highlights will be reviewed below.

The last event in stimulus-secretion coupling is the release of the secretory product by exocytosis. Exocytosis has been divided into 2 categories: constitutive and regulated (265). Constitutive, or continuous exocytosis seems not to be under specific control. Regulated exocytosis, as its name indicates, is controlled by the action of second messengers (265,266). There are 4 steps to exocytosis: 1) the adhesion of intracellular vesicles or secretory granules to the plasma membrane, 2) the fusion of vesicular and plasma membranes resulting in the formation of a pore, 3) the widening of the pore and 4) discharge of the contents of the vesicle into the extracellular space with the incorporation of the vesicular membrane into the cellular membrane (267).

Exocytosis can be measured by quantifying the amount of secretory product released into the extracellular space or by measuring the increase in membrane surface area resulting from the fusion of secretory vesicle to the plasma membrane (266,268). The surface area of the plasma membrane is proportional to the electrical capacitance of the membrane. Thus during exocytosis, as the membrane surface increases, the electrical capacitance of the membrane also increases. Changes in the cell capacitance can be measured using patch clamp in the whole-cell configuration, with the added ability of controlling the intracellular environment (268-270).

The intracellular mechanisms of exocytosis are unknown. Some characteristics of the process are known, but how they relate to the four steps still remains to be determined. The involvement of Ca^{2+} in regulated exocytosis is suggested by the observations that exocytosis does not occur when extracellular Ca^{2+} is removed, that it is stimulated in permeabilized cells by increasing Ca^{2+} concentration and that, in intact cells, it is accompanied by an increase in $[Ca^{2+}]_i$ (183,265,266). The increased $[Ca^{2+}]_i$ is only one step in the exocytotic pathway. Indeed botulinum toxin inhibition of ACh-stimulated catecholamine release from adrenal chromaffin cells is not reversed by increasing $[Ca^{2+}]_i$. This suggests the existence of at least one step downstream from the Ca^{2+} signal (266).

Calmodulin and other Ca^{2+}-binding proteins may be involved in the action of Ca^{2+} in stimulating exocytosis (265). Exocytosis requires Mg-ATP at concentrations in the mM range. ATP does not affect the Ca^{2+} affinity of the process, but increases the extent of secretion in permeabilized chromaffin cells (266). Diacylglycerol and phorbol esters have also been shown to enhance exocytosis by either increasing the Ca^{2+} sensitivity of the process or by increasing the extent of exocytosis (the amount of secretory product released) without changing the Ca^{2+} sensitivity (266). The involvement of PKC has been confirmed in permeabilized chromaffin cells. Down regulation of PKC by prolonged exposure to phorbol esters, or inhibition of PKC by sphingosine results in a inhibition of Ca^{2+} induced secretion (271).

GTP-binding proteins may be involved in exocytosis. In mast cells, when $[Ca^{2+}]_i$ is kept constant with high levels of EGTA, intracellular administration of GTP-γ-S stimulates exocytosis, as monitored by changes in membrane capacitance (269). This observation suggests the existence of a Ca^{2+}-independent exocytotic pathway in permeabilized cells (265,268,269). This effect of GTP analogues on Ca^{2+}-independent exocytosis has been reported for several cell types (265). GTP analogues have also been shown to enhance Ca^{2+}-dependent exocytosis (265). The response to GTP-analogues in permeabilized cells can be interpreted in three ways,

1) activation of G-protein results in the formation of DAG which stimulates PKC-dependent exocytosis, 2) the G-protein acts to transduce the Ca^{2+} signal and 3) a G-protein-dependent pathway exists which is independent from the Ca^{2+}-dependent system (265).

It is possible to suggest a scheme based on the observations listed above. The binding of a secretagogue to its receptor would result in the G-protein-dependent activation of PLC which would result in the production of IP_3 and DAG. IP_3 would mobilize stored Ca^{2+} which would bind CaM and PKC. DAG would increase the affinity of PKC for Ca^{2+}, and increase the phosphorylation of protein substrates. This phosphorylation is, of course ATP-dependent, and necessary for exocytosis. To date, a specific protein whose phosphorylation would be uniquely associated with exocytosis has not been reported. G-proteins may have functions other than the activation of PLC and several models have been proposed where G-proteins would be involved in the adhesion and/or fusion of secretory granule and plasma membranes (265).

2.4.5 Summary.

According to the stimulus-secretion coupling model, the binding of a secretagogue to its receptor results in a Ca^{2+}-dependent exocytosis. The $[Ca^{2+}]_i$, which is maintained between 100 and 300 nM by the action of a CaM-, PKA-, and PKC-regulated Ca^{2+}-ATPase, increases. The increase is due to the opening of voltage-sensitive Ca^{2+} channels whose opening probability is modulated by PKA- and PKC-dependent phosphorylation or by G-proteins. Alternatively, in some cells, the increase in $[Ca^{2+}]_i$ is dependent on the IP_3-stimulated mobilization of stored Ca^{2+} from the ER or calciosomes. The increase in $[Ca^{2+}]_i$ results in an increase in PKC activity, which is believed to play a key role in the process of exocytosis. The function of the PKC-phosphorylated protein may, in some unknown way, interact with G proteins to stimulate exocytosis.

2.5 The Project.

In this chapter the regulation of GH release from somatotrophs of the anterior pituitary has been reviewed. GRF, a 44 amino acid hypothalamic peptide synthesised in the arcuate and ventromedial nuclei and released into the hypophysial portal system, stimulates GH release. SRIF, a 14 amino acid hypothalamic peptide synthesised by cells of the preoptic area and released into the hypophysial portal system, inhibits GH release. The combined effect of these peptide results in the ultradian pulsatile release of GH in vivo. GRF-stimulated GH release is dependent on an increase in cAMP accumulation and a rise in $[Ca^{2+}]_i$ in somatotrophs. The abolition of GRF-stimulated GH release from rat somatotrophs is not due to an inhibition of adenylate cyclase activity, but could be due to a decrease in $[Ca^{2+}]_i$. The role of Ca^{2+} in stimulus-secretion coupling was also reviewed in this chapter.

As indicated in Chapter 1 the objective in this thesis was to study systematically the role of intracellular Ca^{2+} in the regulation of GH release from purified rat somatotrophs by GRF and SRIF. The answers to the following questions were sought:

1. Is Ca^{2+} a second messenger for GRF ?

2. Does GRF increase $[Ca^{2+}]_i$ by stimulating influx and/or mobilization of stored Ca^{2+} ?

3. Does SRIF interfere with the Ca^{2+} status of the cell ?
    a. Does SRIF inhibit Ca^{2+} influx ?
    b. Does SRIF decrease the basal and GRF stimulated increase in $[Ca^{2+}]_i$?

4. What are the intracellular messages which lead to the GRF-stimulated increase in $[Ca^{2+}]_i$?

a. Does depolarization stimulate Ca^{2+} influx which leads to an increase in $[Ca^{2+}]_i$?

b. Do cAMP-dependent processes stimulate Ca^{2+} influx which lead to an increase in $[Ca^{2+}]_i$?

c. Does PKC stimulate Ca^{2+} influx which leads to an increase in $[Ca^{2+}]_i$?

Several experimental approaches were used to answer these questions. The role of extracellular Ca^{2+} was studied by monitoring the effect of Ca^{2+}-free medium and Ca^{2+} antagonists on GRF-induced GH release. The fluorescent dye indo-1 was used to measure $[Ca^{2+}]_i$. Ca^{2+} influx was evaluated by measuring ^{45}Ca uptake and/or combining $[Ca^{2+}]_i$ measurements with incubation in Ca^{2+}-free medium and treatment with Ca^{2+} antagonists.

CHAPTER 3

MATERIALS AND METHODS

3.1 Somatotroph Purification.

3.1.1 Cell dispersion.

Adult male Sprague-Dawley rats (Charles River, St-Constant, Quebec; Crl:CD(SD)BR) weighing 175 - 200 g on arrival were maintained in a temperature-controlled (25 ± 1 C) sound-proofed room (lights on for 14 h) for at least two weeks before being placed in single cages on the afternoon preceding each experiment. Twenty to thirty rats were killed by decapitation within 20 sec of removal from the rat room between 08:00 - 09:00 h. The nervosa-intermedias were discarded and the partes distales were minced and dissociated at 37 C for 2 - 2.5 h in Minimum Essential Medium (Eagle's; 330-1650, Grand Island Biological Co., Grand Island, NY) containing 0.1% bovine serum albumin (BSA: Bovine Albumin Powder, Cohn fraction V; Armour Pharmaceutical Co, Chicago, IL; dialysed as described in reference (272) and lyophilized), 0.1% trypsin (0152-13-1; 1:250, Difco Laboratories, Detroit, MI) and 28.5 mM $NaHCO_3$, brought to pH 7.35 - 7.40 with moistened 95% O_2 - 5% CO_2. The dispersed cells ($2x10^6$ - $4x10^6$/rat) were centrifuged (500 x g for 10 min at room temperature) and resuspended in medium 199 (M199; 400-1200; Grand Island Biological Co., Grand Island, NY) containing 0.1% BSA and 28 mM $NaHCO_3$ brought to pH 7.35 - 7.40 with moistened 95% O_2 - 5% CO_2 at 37 C (M199-A) for experiments involving incubation in Ca^{2+}-free medium, treatment with Ca^{2+} antagonists, and ^{45}Ca loading. For experiments involving the measurement of intracellular Ca^{2+} concentration, cells were resuspended in M199 (1:10 dilution of M199 (10x) 330-1181; Grand Island Biological Co., Grand Island, NY) containing 0.1 % BSA and 20 mM N-2-hydroxyethylpiperazine-N'-2-

ethanesulfonic acid (HEPES) titrated to pH 7.35 - 7.40 with NaOH at room temperature (M199-AH/RT).

3.1.2 Density gradients.

The production of a cell population enriched in somatotrophs was accomplished by a two-stage discontinuous density gradient centrifugation. Dialysed BSA density gradients, as previously described (6,272), were used for purifying cells for ^{45}Ca uptake studies. Percoll density gradients were used to purify somatotrophs for studies of intracellular calcium concentration. A brief description of the latter procedure follows. A stock solution of Percoll (17-0891-01; Pharmacia LKB, Uppsala, Sweden) in M199 containing 20 mM HEPES (pH 7.35 - 7.40 at room temperature) was prepared by diluting 1 part M199 (10x) - 200 mM HEPES (pH 6.8) to 9 parts Percoll. Three density solutions were prepared by diluting stock Percoll with M199 - 20 mM HEPES (pH 7.35 - 7.40 at room temperature) as follows: 1.086 g/ml = 67.7% (v/v); 1.076 g/ml = 58.8% and 1.069 g/ml = 53.7%. The densities of the solutions were measured by weighing a known volume of solution dispensed with an Eppendorf repeater pipette using a previously calibrated Eppendorf Combitip. Densities were adjusted when necessary. Two discontinuous gradients were prepared: the first made of a top 3 ml layer of cell suspension, a middle 2.5 ml layer of 53.7% Percoll (1.069 g/ml) and a bottom 2.5 ml layer of 67.7% Percoll (1.086 g/ml). The different layers were added top to bottom to siliconized 15 ml "COREX" glass test tubes (8441; Corning Glass Works, Corning, NY) using a syringe fitted with tubing. The second gradient was made of a top layer of cell suspension, a middle layer of 58.8% Percoll (1.076 g/ml) and a bottom layer of 67.7% Percoll (1.086 g/ml).

No more than $3x10^7$ cells, resuspended in 3 ml of M199-AH/RT, were layered onto one gradient. The first gradient was centrifuged at 2,000 x g for 30 min at room temperature. All cells collected from the middle layer of the first gradient were washed in 10 ml of M199-AH/RT, centrifuged (500 x g for 10 min), resuspended in 3 ml of M199-AH/RT, layered on a single

second gradient in siliconized 15 ml COREX glass test tube, and centrifuged at 2,000 x g for 30 min at room temperature. Cells removed from the middle layer of the second gradient were washed in 10 ml of M199-AH/RT, centrifuged (500 x g for 10 min), resuspended in 10 ml of M199-AH/37 (pH 7.35 - 7.40 at 37 C) and allowed to equilibrate for 30 min at 37 C in a siliconized Erlenmeyer flask in a Dubnoff incubator-shaker before the cells were loaded with dye. Histological examination of the purified somatotrophs (6) revealed a routine purity of over 94%. These cells were 93 - 95% viable when evaluated by the trypan blue exclusion test. The final number of cells corresponded to 15 - 20% of the total initial yield.

3.2 Static Incubation of Purified Somatotrophs.

3.2.1 Static Incubation in Ca^{2+}-free Medium.

Somatotrophs were purified on BSA gradients using Ca^{2+}-free buffers (8). After the second gradient centrifugation, the cells were resuspended in phosphosaline buffer, divided into equal volumes, centrifuged (500 x g for 10 min), and then resuspended in either M199-A or low Ca^{2+} M199-A (low Ca^{2+}). Both media were prepared from a supply of M199 (formula no. 78-0047, Grand Island Biological, Grand Island, NY) free of Hanks' salts. M199 A was prepared by adding BSA (0.1%) and Hank's salts, and low Ca^{2+} was prepared by adding Hanks' salts without $CaCl_2$ and BSA (8). The cells were allowed to equilibrate for 30 min at 37 C in a siliconized Erlenmeyer flask in a Dubnoff incubator-shaker, gassed with moistened 95% O_2 - 5% CO_2. The media were removed after centrifugation (500 x g for 10 min at room temperature) and the cells were resuspended in M199-A or low Ca^{2+} respectively. Cells were then transferred to Teflon beakers and incubated for 10 min at 37 C in the incubator-shaker, gassed with moistened 95% O_2 - 5% CO_2 before the addition of 2 ng/ml hpGRF (synthetic hpGRF-(1-40)-OH, gift from Dr. J. Rivier and W. W. Vale) or vehicle. Each experimental group consisted of four beakers. Samples were removed 2, 4, 8, and 16 min after addition and transferred to siliconized Pyrex test tubes. An aliquot was quickly taken and centrifuged for 15 sec to recover

supernatant for the determination of GH release into the medium, while the rest was flash-frozen (without centrifugation) and stored at -80 C for cAMP determination.

3.2.2 Static Incubation with Ca^{2+} Antagonists.

Somatotrophs were purified on normal BSA gradients. After the second gradient centrifugation, cells were resuspended in M199-A and allowed to equilibrate for 30 min at 37 C in a siliconized Erlenmeyer flask in a Dubnoff incubator-shaker, gassed with moistened 95% O_2 - 5% CO_2. The medium was removed after centrifugation (500 x g for 10 min at room temperature) and the cells were resuspended in M199-A and transferred to Teflon beakers in the incubator-shaker, and gassed with moistened 95% O_2 - 5% CO_2 for 10 min before the addition of Ca^{2+} antagonists. Secretagogues were added 10 min later. Each experimental group consisted of four beakers. Samples were taken at designated times and processed as above for GH release and cAMP accumulation determination.

In the high K^+ studies, the incubation medium was prepared from a supply of M199 (formula no. 78-0047) free of Hanks' salts. Normal M199-A was prepared by adding Hank's salts, giving a final [K^+] of 5.8 mM. High K^+ was prepared by increasing the [K^+] by a factor of 5 and reducing the [Na^+] to maintain isotonicity, so that a final [K^+] of 29 mM was obtained (8).

3.2.3 Static Incubation with cAMP Analogues.

Somatotrophs were purified on Percoll gradients. After equilibrating for 30 min at 37 C, somatotrophs were centrifuged (500 x g for 10 min) and resuspended in M199-AH/37, and incubated in Teflon beakers in a Dubnoff incubator-shaker at 37 C. Either 10^{-4} or 10^{-3} M dibutyryl ($(Bu)_2$cAMP) or 10^{-5}, 10^{-4} or 10^{-3} M chlorophenylthio-cAMP (cpt-cAMP) was added to the medium. Each experimental group consisted of four beakers. Cell aliquots (including medium) were removed from every beaker after 4, 12 and 32 min. The aliquots were quickly

centrifuged for 15 sec, and a sample of the supernatant was frozen and stored for later GH release determination.

3.3 ^{45}Ca Uptake

3.3.1 ^{45}Ca Loading for Time Course Studies.

After equilibrating for 30 min at 37 C, somatotrophs, purified on BSA gradients, were ntrifuged (500 x g for 10 min) and resuspended in M199-A at a concentration of no less than 250,000 cells/ml and incubated in Teflon beakers in a Dubnoff incubator-shaker at 37 C, gassed with moistened 95% O_2 - 5% CO_2. At the appropriate time [U-^{3}H]-mannitol (NET-101; New England Nuclear, Dorval, Quebec, Canada) and [^{45}Ca]-$CaCl_2$ (NEZ-013; New England Nuclear, Dorval, Quebec, Canada) were added to the incubation beakers to give a final concentration of ^{45}Ca and of ^{3}H of 3 - 5 μCi/ml and 9 - 15 μCi/ml respectively (^{3}H/^{45}Ca ratio = 3). The final Ca^{2+} concentration was 1.2 mM, thus giving a medium Ca^{2+} specific activity of 2.5 - 4.2 Ci/mole.

3.3.2 ^{45}Ca Loading for Single Time Point Studies.

After equilibrating for 30 min at 37 C, somatotrophs, purified on BSA gradients, were centrifuged (500 x g for 10 min) and resuspended in M199-A at a concentration of $0.75x10^6$ - $4.2x10^6$ cells/ml and incubated in 2 ml polystyrene beakers in a Dubnoff incubator-shaker at 37 C, gassed with moistened 95% O_2 - 5% CO_2. At the appropriate time [U-^{3}H]-mannitol and [^{45}Ca]-$CaCl_2$ were added to the incubation beakers to give a final concentration of ^{45}Ca and of ^{3}H of 5 μCi/ml and 15 μCi/ml respectively (^{3}H/^{45}Ca ratio = 3). The final Ca^{2+} concentration was 1.2 mM, thus giving a medium Ca^{2+} specific activity of 4.2 Ci/mole.

3.3.3 n-Butylphthalate "Sandwich".

At predetermined times after the addition of tracer to the incubation medium, 200 µl aliquots (cells plus medium) were drawn from the incubation beakers , and the cells were separated from the radioactive medium by centrifugation through n-butylphthalate (n-BP: D-30; Fisher Scientific Company, Fair Lawn, NJ) into perchloric acid (PCA). The technique was a modification of the silicone oil sandwich method described by Finkelstein and Adelberg (273) where the silicone oil was replaced by n-BP. The cell sample was transferred to a Beckman 400 µl conical polyethylene Microfuge tube (314326; Beckman Instruments Inc., Fullerton, CA) containing a 5 mm thick layer of n-BP (specific gravity 1.049) on top of 50 µl of 18% PCA acid (w/v - specific gravity 1.10 - 9652; J.T. Baker Chemical Co., Phillipsburg, NJ). The tube was immediately centrifuged at maximum speed (9,390 x g) in a Beckman Microfuge B (Beckman Instruments Inc., Spinco division, Palo Alto, CA) for 45 sec. In preliminary experiments, where the PCA was replaced by 0.6 M sucrose (specific gravity 1.10), it was established that a 5 mm layer of n-BP was the thinnest stable layer which allowed maximal cell recovery. Centrifugation for 45 sec removed virtually all (98%) the cells from the medium and allowed for a 77 ± 11% (± SEM; n=5) recovery of the extractable GH in the cell pellet. This calculated recovery was obtained by comparing the amount of GH extracted with 0.01 N NaOH from cell pellets centrifuged through the n-BP sandwich and cell pellets centrifuged through medium.

After centrifugation, an aliquot of the supernatant was removed for later GH determination. Then the tube was frozen, and kept at -80 C overnight. The next day the frozen tubes were cut through the n-BP layer with a single edged razor blade. The conical tips, containing frozen PCA and precipitated protein, were transferred to liquid scintillation vials containing 1 ml of distilled water. Ten ml of Beckman Ready-Solv HP/b liquid scintillation cocktail (158727; Beckman Instruments Inc., Galway, Ireland) were added to the vials and the ^{3}H and ^{45}Ca content of the tips was determined by liquid scintillation counting using a LKB

1217 Betarack liquid scintillation counter (Wallac Oy, Turku, Finland). ^{3}H and ^{45}Ca dpm were calculated using a double label program with ^{3}H and ^{45}Ca quench curves.

3.3.4 Determination of ^{45}Ca Net Uptake.

^{3}H-mannitol was used as an extracellular space marker. The medium $^{3}H/^{45}Ca$ ratio, R, was determined for each experiment. To calculate the net ^{45}Ca uptake the ^{3}H equivalent in ^{45}Ca counts for each sample (sample ^{3}H dpm / R) was subtracted from the raw ^{45}Ca count. The data were expressed as corrected ^{45}Ca dpm/1000 cells.

3.3.5 General experimental protocol for ^{45}Ca uptake measurements.

Radioactive Ca uptake experiments were carried out either under steady or non-steady state conditions. Steady state exists when the rate of GH secretion is constant. When the rate of GH secretion is changing cells are in non-steady state. For steady state experiments, GRF or SRIF was added to the incubation beakers 10 min before adding the ^{45}Ca. Studies of the pattern of GH release from mixed pituitary cells in perifusion (45,79) show that after 10 min of continuous GRF or SRIF exposure the rate of GH release is relatively constant. For steady state experiments the ^{45}Ca content of somatotrophs was determined 7.5, 15, 30, 45, 60, 75, 90, 105, 120, 135, 150 and 180 min after tracer addition. For non-steady state experiments, where an increase in either Ca^{2+} influx or Ca^{2+} efflux is expected, cells were loaded with ^{45}Ca for 90 min. The secretagogues were added to the incubation medium as the cells approached tracer equilibrium. The ^{45}Ca content of somatotrophs was determined after 70 and 89 min of loading and 0.25, 0.5, 1, 2, 4, 8, 16, and 32 min after the addition of secretagogue. For non-steady state experiments with SRIF, where a decrease in Ca^{2+} influx was expected, SRIF was added either 15 min or 6 min after tracer addition. In time course studies, cellular ^{45}Ca content was measured in 2 samples before the addition of SRIF, either 5 and 10 min or 2 and 4 min after tracer addition, and 4, 8, 16, 32, 64, and 96 min after SRIF addition. For all experiments there

were 4 incubation beakers per treatment group, and every beaker was sampled at each time point. Each experiment was carried out at least twice.

3.4 Intracellular Ca^{2+} Concentration Measurements.

3.4.1 Indo-1 loading.

After equilibrating for 30 min at 37 C, somatotrophs, purified on Percoll gradients, were centrifuged (500 x g for 10 min) and resuspended in 10 ml M199-AH/37 to which 10 μl of 1 mM indo-1/AM (pentaacetoxymethyl ester of indo-1, I-1203, Molecular Probes, Inc., Eugene, OR) in dimethyl sulfoxide (DMSO: 9224; J.T. Baker Chemical Co., Phillipsburg, NJ) to give a final concentration of 1 μM. The cells were incubated for 30 min at 37 C, then centrifuged (500 x g for 10 min) and resuspended in M199-AH/RT to yield a cell density of $2.5x10^6$ cells/ml. Half million cell aliquots were transferred to 1.5 ml microcentrifuge tubes containing 1 ml of M199-AH/RT. The cells were kept in suspension at room temperature until fluorescence measurements were made. The cells were incubated at room temperature for at least 45 min after the end of the loading to allow for the complete hydrolysis of indo-1/AM.

3.4.2 Fluorescence measurements.

Just before fluorescence measurement individual cell aliquots were centrifuged for 3 sec in a Beckman Microfuge E (Beckman Instruments Inc., Spinco division, Palo Alto, CA) run at half power, resuspended in 100 μl of simplified medium (135 mM NaCl, 6 mM KCl, 1.2 mM $CaCl_2$, 1 mM $MgCl_2$, 2.8 mM dextrose and 20 mM HEPES titrated to pH 7.37 with NaOH at 37 C), and transferred to plastic fluorometric cuvettes (H116; Hughes and Hughes, Romford, Essex, England) containing 2 ml of simplified medium.

Fluorescence measurements of indo-1 loaded cells were obtained with a Perkin-Elmer LS-5 spectrofluorimeter (Perkin-Elmer Ltd., Beaconsfield, Buckinghamshire, England). The

content of the cuvette was thermostatically controlled at 37 C and was continuously mixed by a magnetic microstirrer. The excitation wavelength was 329 nm and the emission wavelength was 405 nm. Excitation and emission slit widths were 5 nm and 10 or 20 nm respectively.

Calibration of the fluorescence vs intracellular free Ca^{2+} concentration ($[Ca^{2+}]_i$) was done using the ionomycin and Mn^{2+} technique (274). The divalent cation that penetrates the cells via the ionophore quenches the fluorescence of the dye. $[Ca^{2+}]_i$ for a given fluorescence, F, was calculated as (250):

$$[Ca^{2+}]_i = K_d (F - F_o) / (F_{sat} - F) \qquad [1]$$

where K_d is the dissociation constant for the indo-1/Ca complex and is equal to 250 nM at 37 C (250), F_{sat} is the fluorescence of the saturated dye, obtained in Ca^{2+} containing media (1.2 mM) in the presence of 10^{-5} M ionomycin, and F_o is the fluorescence of the dye in the absence of Ca^{2+}. F_o was calculated as follows (275):

$$F_o = 1/12 (F_{sat} - F_{auto}) + F_{auto} \qquad [2]$$

where F_{auto} is the autofluorescence, determined after the addition of 2 mM $MnCl_2$ and corrected for the Mn^{2+}-dependent fluorescence of ionomycin, and 12 is the ratio of F_{sat} over F_o.

3.4.3 General experimental protocol for $[Ca^{2+}]_i$ measurements.

All experiments were repeated at least three times. The responsiveness of each cell preparation was ascertained by challenging the cells with 10^{-9} M rat GRF (rGRF). The result of this challenge is shown in the top panel of the relevant figures. Other panels in a figure show results from the same cell preparation. A standard protocol was used when studying $[Ca^{2+}]_i$ in Ca^{2+}-containing medium, and another when studying $[Ca^{2+}]_i$ in Ca^{2+}-free medium.

In normal Ca^{2+}-containing medium (1.2 mM), baseline fluorescence was recorded for 2 min, then vehicles for secretagogues and/or inhibitors (usually 10 µl) were added in sequence as controls. Two min after the addition of the last vehicle, secretagogues and/or inhibitors were added in sequence to the cuvette. The response to the first addition was followed for 2 min while that to the last addition was followed for 5 min. For calibration purposes, 10^{-5} M ionomycin (free acid: 407950; Calbiochem, Bering Diagnostic, La Jolla, CA) then 2 mM $MnCl_2$ were added to the cuvette. A second addition of ionomycin was needed to evaluate the Mn^{2+}-dependent fluorescence of the ionophore. When using K^+ as secretagogue, vehicle was not added. In Ca^{2+}-free medium (simplified medium without $CaCl_2$), baseline fluorescence was recorded for 15 sec, then 0.5 mM EGTA (10 µl) was added to the cuvette. The secretagogue was then added 10 sec later. The response was followed for 5 min and then 10 µM ionomycin was added, and the response followed for 3 min. Calibration was achieved by adding 1.7 mM $CaCl_2$ followed by 2 mM $MnCl_2$ and the second ionomycin addition.

3.5 Intracellular Indo-1 Concentration Measurement.

The apparent intracellular concentration of indo-1 ($[indo\text{-}1]_i$) was evaluated for every cell sample. A standard curve of F_{sat} against [indo-1] (pentasodium salt - 402095; Calbiochem, Bering Diagnostic, La Jolla, CA - dissolved in 115 mM KCl, 20 mM NaCl, 1 mM $MgCl_2$, 1.2 mM $CaCl_2$, and 10 mM 3-(N-morpholino)propanesulfonic acid (MOPS) titrated to pH 7.05 with KOH at 37 C) was used to calculated $[indo\text{-}1]_i$ as follows:

$$[indo\text{-}1]_i = C \times V / (n \times cv) \qquad [3]$$

where C is the concentration of indo-1 in the cuvette as given by the standard curve, V is the volume of the cuvette, n is the total number of cells in the cuvette and cv is the average cell volume (1.77 pl assuming a sphere with a diameter of 15 µm).

3.6 Purified Somatotroph Perifusion.

Perifusions of somatotrophs were carried out to determine whether intracellular indo-1 and simplified medium affected the ability of cells to secrete GH. The response of purified somatotrophs to graded concentrations of rGRF perifused with M199-AH/37, and of purified somatotrophs loaded with indo-1 and perifused with simplified medium were studied using a two column perifusion system (9,48). Somatotrophs were purified by Percoll density gradients. Half the cells were then incubated in M199-AH/37 containing 10 μM indo-1/AM for 30 min at 37 C, while the other half was incubated in M199-AH/37 for 30 min at 37 C. Half a million indo-1 loaded cells were transferred to one column and perifused with simplified medium, while half a million control cells were transferred to the other column and perifused with M199-AH/37. The media flow rate in both columns was 1 ml/min. A stock solution of rGRF was diluted with M199-AH/37 or with simplified medium immediately before use. One min fractions were collected and frozen for later GH determination.

3.7 Growth Hormone Release Measurements.

Growth hormone content of media from both perifusions and static incubations was measured in triplicate by the double antibody radioimmunoassay (RIA) using reagents provided by the NIDDK National Hormone and Pituitary Program, University of Maryland School of Medicine. Samples from each experiment were measured within one assay, with an intra-assay coefficient of variation of less than 5%. A single label RIA program was used to calculate the GH content of each assay tube using a linear regression line of logit (B/B_0) versus log concentration of rat GH standards. The results were expressed as ng per fraction, for perifusion, or as ng per 1000 cells, for static incubation, of the NIDDK Rat Growth Hormone GH-RP-1 or GH-RP-2 Standards. The lowest detectable GH concentration was 0.5 and 0.1 ng/assay

tube for GH-RP-1 and GH-RP-2 respectively. The mid range concentration was 2 and 0.5 ng/assay tube for GH-RP-1 and GH-RP-2 respectively.

3.8 cAMP Accumulation Measurements.

Cyclic AMP was extracted and assayed as previously described (1,6) using the New England Nuclear (Boston, MA) RIA kits, and results are expressed as femtomoles per 1000 cells (fmol/1000 cells). Samples from each experiment were measured within one assay, with an intra-assay coefficient of variation of less than 10%. The lowest detectable concentration and the mid range concentration were 10 and 60 fmol/assay tube respectively.

3.9 Secretagogues and Inhibitors.

rGRF (8068; Peninsula Laboratories, Inc., Belmont, CA) was dissolved in a diluent containing 0.1% heat treated BSA[1], 0.01 N acetic acid and 0.1 mM ascorbic acid and, 1 μg/10 μl aliquots were stored at -80 C. Aliquots were diluted in appropriate media immediately before use. SRIF (S-9129; Sigma Chemical Company, St. Louis, MO) was dissolved in M199-A or simplified medium immediately before use. Nifedipine (N-7634; Sigma Chemical Company, St. Louis, MO) was dissolved in DMSO and kept in the dark until it was diluted 1:47 with M199-A or simplified medium immediately before addition. Diltiazem (D-2521; Sigma Chemical Company, St. Louis, MO) was dissolved in simplified medium. 8-(4-Chlorophenylthio)-cAMP (cpt-cAMP: C-7396; Sigma Chemical Company, St. Louis, MO) was dissolved in M199-A or simplified medium at a concentration of 2 mg/ml. Dibutyryl cAMP ($(Bu)_2$cAMP: D-0627; Sigma Chemical Company, St. Louis, MO) was dissolved in M199-AH/37 or M199-A. Prostaglandin E_2 (PGE_2: 468904; Upjohn, Kalamazoo, MI) was dissolved in redistilled ethanol

---

[1] 200 g/l BSA was dissolved in phospho-saline (50 mM Na_2HPO_4, 150 mM NaCl) and heated to 56 C for 2 h, dialyzed as described in reference (272) and lyophilised.

and diluted 1:134 with simplified medium before addition. Phorbol 12-myristate 13-acetate (PMA: P-8139; Sigma Chemical Company, St. Louis, MO) was dissolved in DMSO and diluted 1:76.5 with simplified medium before use. 1,2-Dioctanoyl-rac-glycerol (diC$_8$: D-1270; Sigma Chemical Company, St. Louis, MO) was dissolved in redistilled ethanol, diluted 1:14.7 with simplified medium and sonicated. The Ca^{2+} ionophore A23187 (C-7522; Sigma Chemical Company, St. Louis, MO) was dissolved in DMSO and was diluted in M199-A to give a final DMSO concentration of 0.013% (v/v).

3.10 Statistical Analysis.

The data are expressed as a mean ± standard error of the mean (SEM). Error bars in figures represent SEM. Where error bars are not present, unless otherwise stated, they were too small to plot. Student t-tests or one way analysis of variance (ANOVA) followed by Duncan's multiple range test (DMRT) were used to compare mean cAMP accumulation, GH release and ^{45}Ca uptake between control and treated groups at each time point. Mean baseline, nadir, peak or plateau $[Ca^{2+}]_i$ were compared by two way ANOVA followed by DMRT. Differences were considered significant for $P < 0.05$. When data were expressed as a mean of means, weighted means were calculated using individual SEM as the weighting factor (276). Sigmoid curves were generated by fitting a four-parameter logistic equation to the data from concentration-response studies using the computer software package "GraphPad" (ISI Software). The program also estimated the value of IC_{50}'s and EC_{50}'s based on the actual or extrapolated maximum and minimum plateaux.

CHAPTER 4

RESULTS

4.1 Ca^{2+} and GRF

4.1.1 GRF-stimulated GH Release in Ca^{2+}-free Medium

To study the extracellular Ca^{2+} requirement for GRF-stimulated GH release, somatotrophs were incubated in low Ca^{2+} medium and challenged with GRF (Figure 5). A concentration of hpGRF (2 ng/ml) was chosen that routinely produced a small, but consistent increase in GH release (1). Basal GH release in low Ca^{2+} medium was not consistently different from that seen in M199-A. hpGRF induced a significant increase in GH release by 8 min, which increased progressively with time. However hpGRF failed to stimulate the release of GH in low Ca^{2+} medium.

Basal cAMP levels were not consistently different in cells incubated in low Ca^{2+} medium and M199-A. hpGRF, when added to cells in M199-A, induced an immediate (within 2 min) and significant increase in cAMP accumulation which increased, with time, to reach 6 times the control level by 16 min. When hpGRF was added to cells in low Ca^{2+} medium, there was a massive and dramatic increase in cAMP, significantly greater than the response seen with hpGRF in M199-A at all times, with levels reaching 28 to 37 times control by 16 min.

4.1.2 GH Release and Ca^{2+} Antagonists.

4.1.2.1 Effect of diltiazem and nifedipine on basal GH release and cAMP accumulation. GH release and cAMP accumulation were examined with concentrations of diltiazem from 10^{-10} to 10^{-6} M (Figure 6) and concentrations of nifedipine from 10^{-9} to 10^{-6} M (Figure 7). Diltiazem

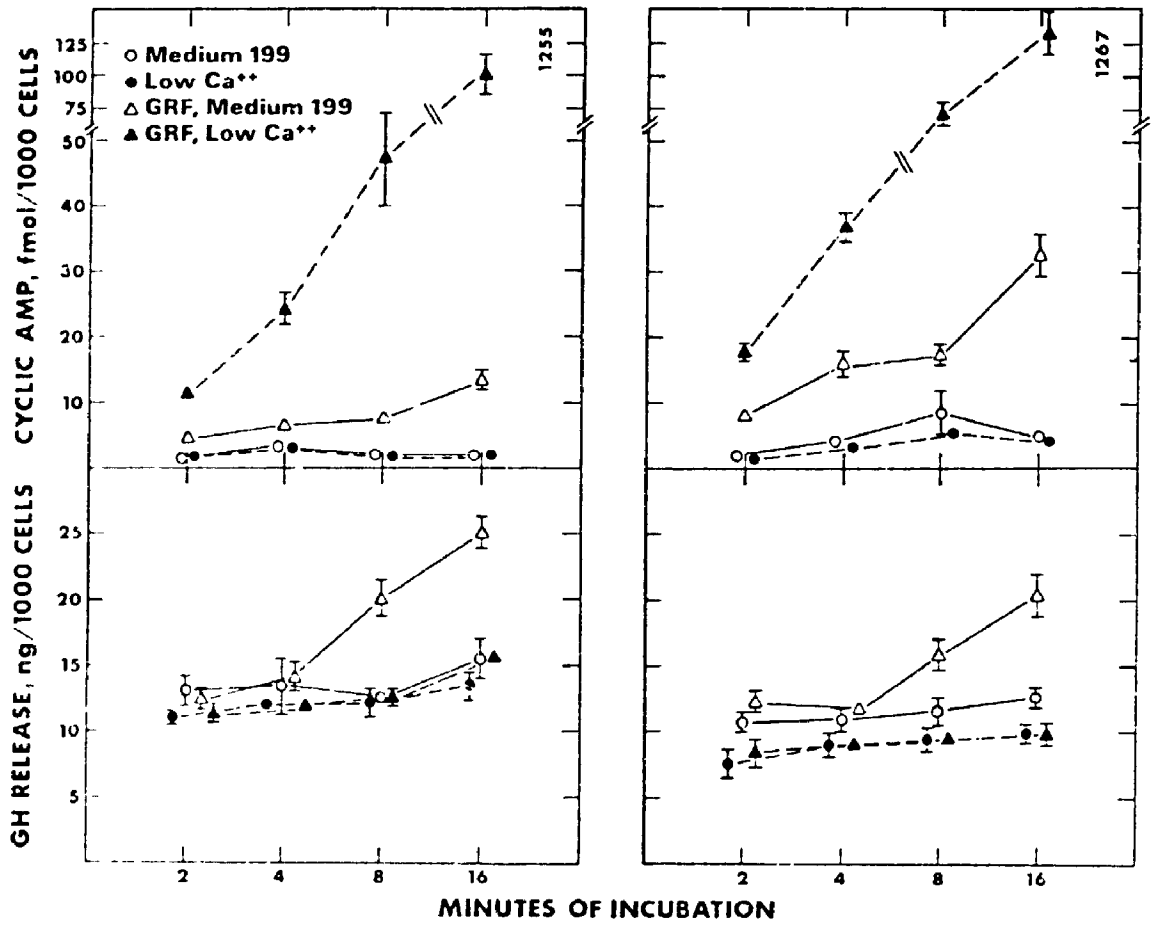

Figure 5. **The effect of 2 ng/ml hpGRF on cyclic AMP accumulation and growth hormone (GH) release by rat somatotrophs in two separate experiments.** GH is expressed as ng of rat GH (RP-1) per 1000 cells. Data points are means of four separate determinations. The error bars are SEM. Where bars do not appear, the SEM was too small to plot.

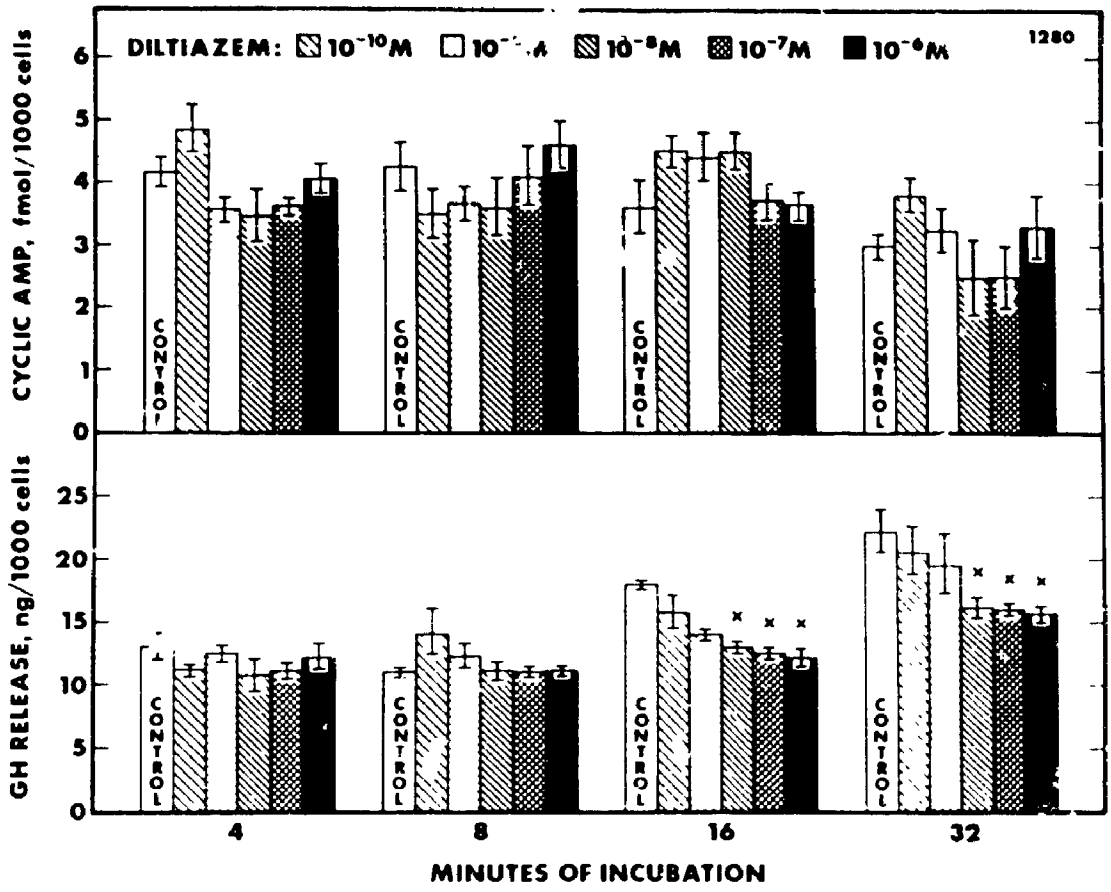

Figure 6. **The effect of diltiazem on basal cyclic AMP accumulation and growth hormone (GH) release by rat somatotrophs.** GH is expressed as ng of rat GH (RP-1) per 1000 cells. Each column represents a mean of four determinations. The error bars are SEM. Values significantly different from control are indicated by "x" ($p<0.05$).

produced a consistent concentration-related decrease in basal GH release by 16 min, which was significant with 10^{-8} M and higher concentrations (Figure 6). There was no consistent or significant change in cAMP accumulation. Nifedipine produced a concentration-related decrease in GH release by 32 min, which was significant at 10^{-7} and 10^{-6} M (Figure 7). Again, there was no consistent change in cAMP accumulation.

4.1.2.2 Effect of diltiazem and nifedipine on high K^+-induced GH release and cAMP accumulation. The K^+ concentration of M199-A is 5.8 mM while that of high K^+ medium is 5 times greater (29 mM). The effect of diltiazem on high K^+-induced GH release and cAMP accumulation over an extended concentration range (Figure 8; 10^{-10},10^{-8}, and 10^{-6} M) was first examined, and then a narrower range (Figure 9; 10^{-8}, 10^{-7}, and 10^{-6} M), was also examined. There were no consistent changes in cAMP accumulation. High K^+ induced a significant increase in GH release by 4 min, which was blocked by diltiazem at 10^{-6} and 10^{-7} M, but not at lower concentration.

The effect of nifedipine on high K^+-induced GH release and cAMP accumulation (Figure 10: 10^{-8}, 10^{-7}, 10^{-6} M; and Figure 11: 10^{-10}, 10^{-9}, 10^{-8} M) was similarly examined. There was again no consistent change in cAMP accumulation. High K^+ induced a significant increase in GH release by 4 min, which was blocked by nifedipine at 10^{-6}, 10^{-7}, and 10^{-8} M at 4, 8, and 16 min but not at 32 min.

4.1.2.3 Effect of diltiazem and nifedipine on GRF-induced GH release and cAMP accumulation. In the first series of experiments the effect of diltiazem from 10^{-9} to 10^{-5} M (Figure 12 and 13), and nifedipine from 10^{-9} to 10^{-6} M (Figure 14), on the increase in GH release and cAMP accumulation induced by rGRF (10^{-10} M) was examined. In the diltiazem study rGRF induced a twofold increase in GH release by 32 min, preceded by a marked and progressive increase in cAMP accumulation by 8 min (Figures 12 and 13) Diltiazem at

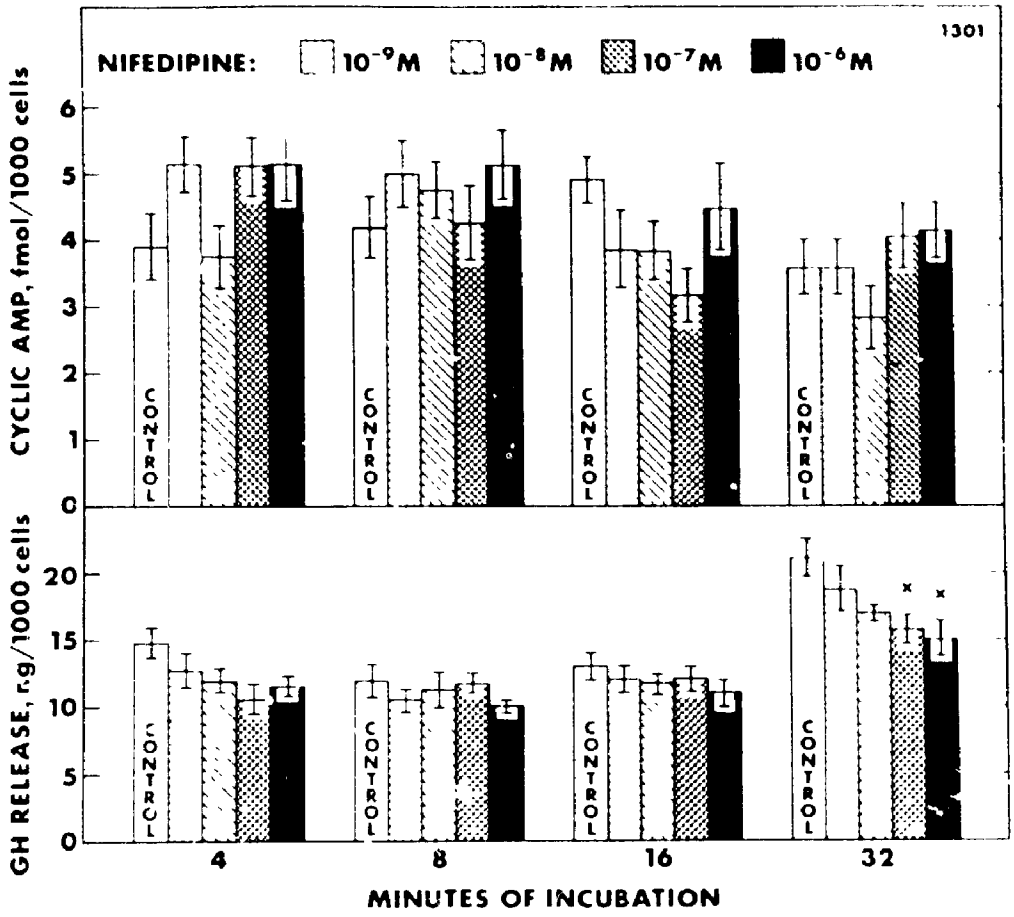

Figure 7. **The effect of nifedipine on basal cyclic AMP accumulation and growth hormone (GH) release by rat somatotrophs.** GH is expressed as ng of rat GH (RP-1) per 1000 cells. Each column represents a mean of four determinations. The error bars are SEM. Values significantly different from control are indicated by "x" ($p<0.05$).

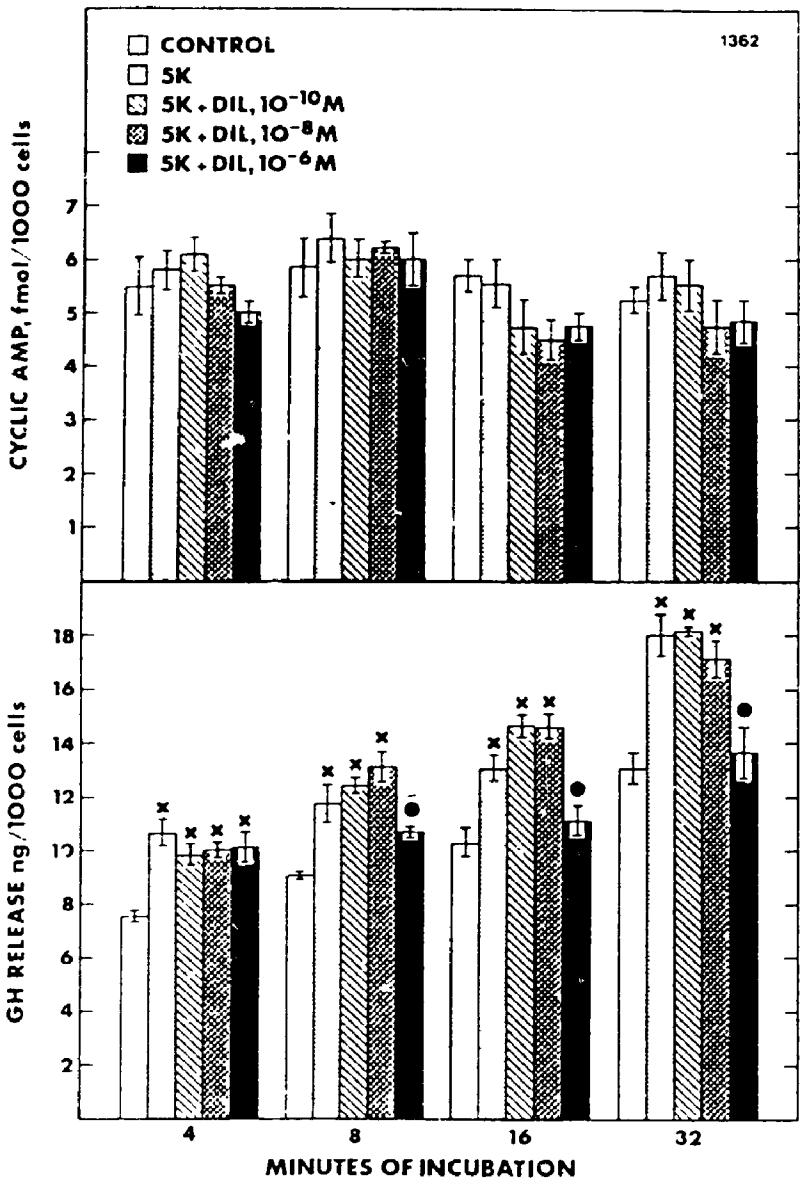

Figure 8. **The effect of 29 mM K^+ (5 times physiological concentration, 5K) and 29 mM K^+ with 10^{-10} to 10^{-6} M diltiazem (DIL) on cyclic AMP accumulation and growth hormone (GH) release by rat somatotrophs.** GH is expressed as ng of rat GH (RP-1) per 1000 cells. Each column represents a mean of four determinations. The error bars are SEM. Values significantly different from control are indicated by "x" ($p<0.05$), while values significantly different from 5K are indicated by "●" ($p<0.05$).

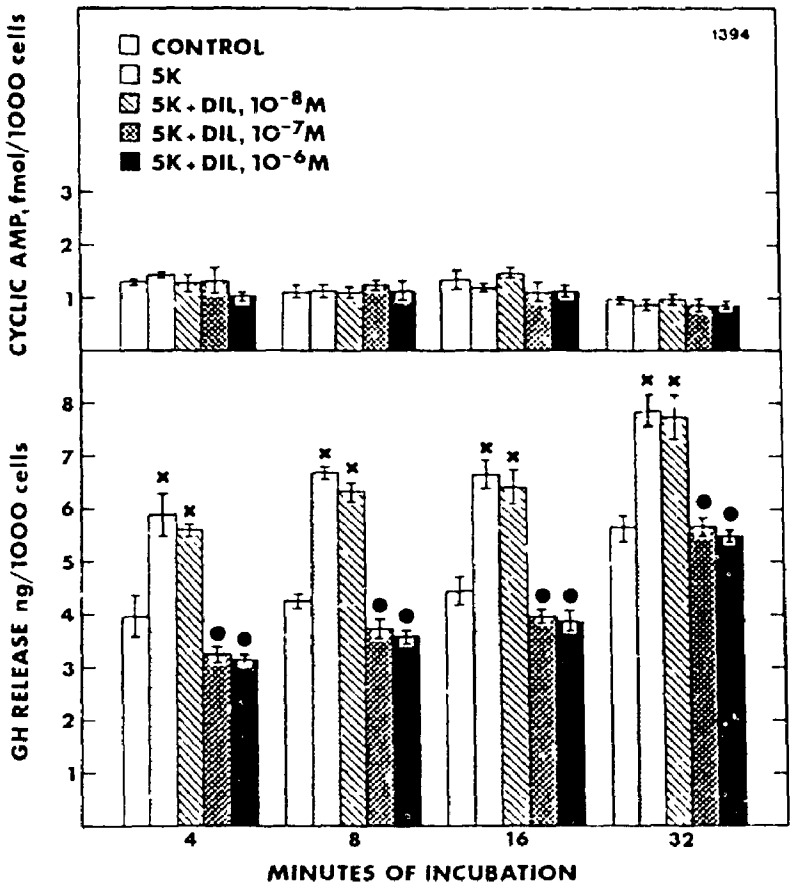

Figure 9. **The effect of 29 mM K^+ (5 times physiological concentration, 5K) and 29 mM K^+ with 10^{-8} to 10^{-6} M diltiazem (DIL) on cyclic AMP accumulation and growth hormone (GH) release by rat somatotrophs.** GH is expressed as ng of rat GH (RP-2) per 1000 cells. Each column represents a mean of four determinations. The error bars are SEM. Values significantly different from control are indicated by "x" ($p<0.05$), while values significantly different from 5K are indicated by "•" ($p<0.05$).

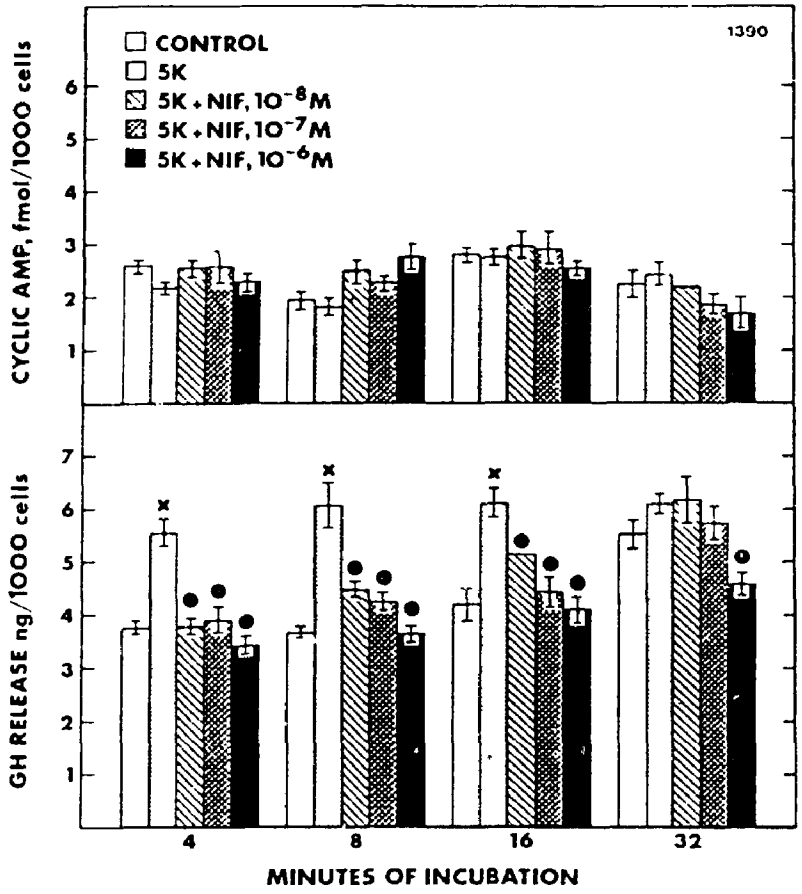

Figure 10. **The effect of 29 mM K^+ (5 times physiological concentration, 5K) and 29 mM K^+ with 10^{-8} to 10^{-6} M nifedipine (NIF) on cyclic AMP accumulation and growth hormone (GH) release by rat somatotrophs.** GH is expressed as ng of rat GH (RP-2) per 1000 cells. Each column represents a mean of four determinations. The error bars are SEM. Values significantly different from control are indicated by "x" ($p<0.05$), while values significantly different from 5K are indicated by "●" ($p<0.05$)

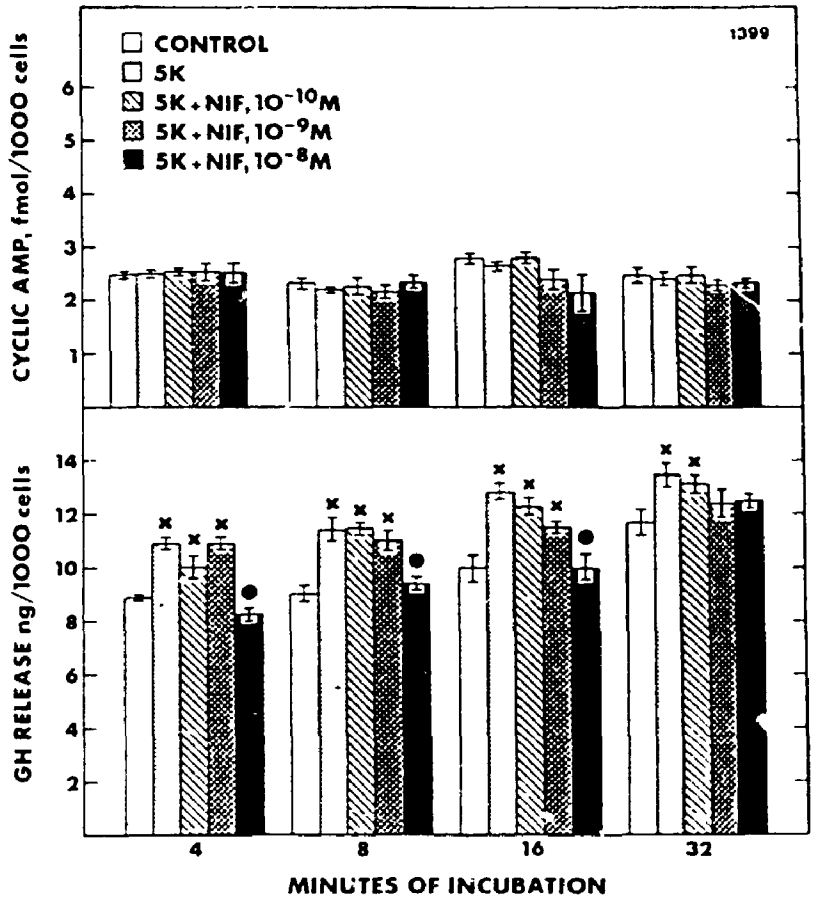

Figure 11. **The effect of 29 mM K^+ (5 times physiological concentration, 5K) and 29 mM K^+ with 10^{-16} to 10^{-8} M nifedipine (NIF) on cyclic AMP accumulation and growth hormone (GH) release by rat somatotrophs.** GH is expressed as ng of rat GH (RP-2) per 1000 cells. Each column represents a mean of four determinations. The error bars are SEM. Values significantly different from control are indicated by "x" ($p<0.05$), while values significantly different from 5K are indicated by "●" ($p<0.05$).

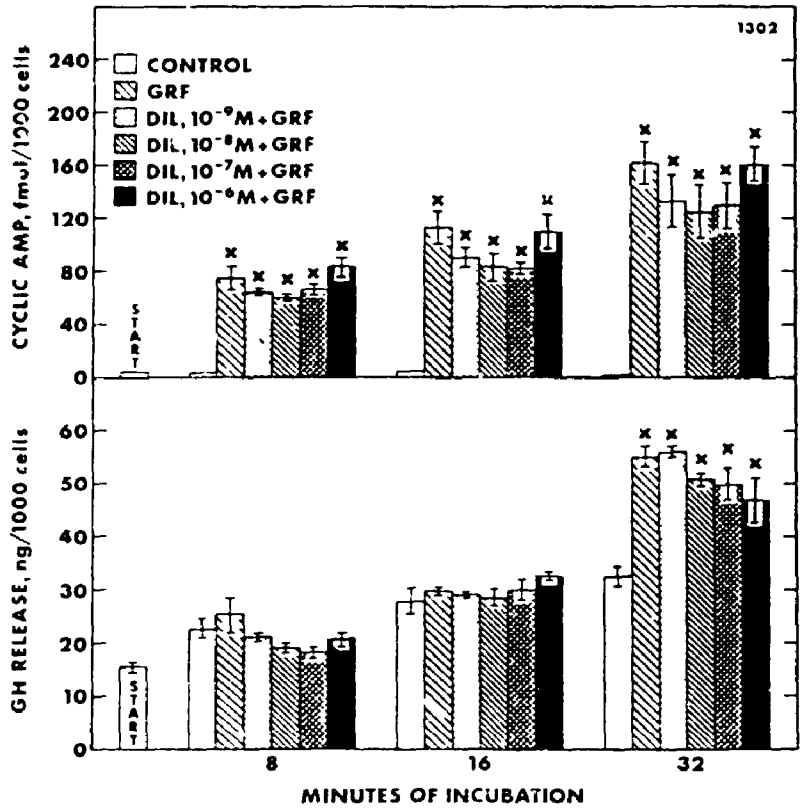

Figure 12. **The effect of 10^{-9} to 10^{-6} M diltiazem (DIL) on 10^{-10} M rGRF-induced cyclic AMP accumulation and growth hormone (GH) release by rat somatotrophs.** "START" samples were taken 5 min prior to diltiazem addition. GH is expressed as ng of rat GH (RP-1) per 1000 cells. Each column represents a mean of four determinations. The error bars are SEM. Where bars do not appear, the SEM was too small to plot. Values significantly different from control are indicated by "x" ($p<0.05$).

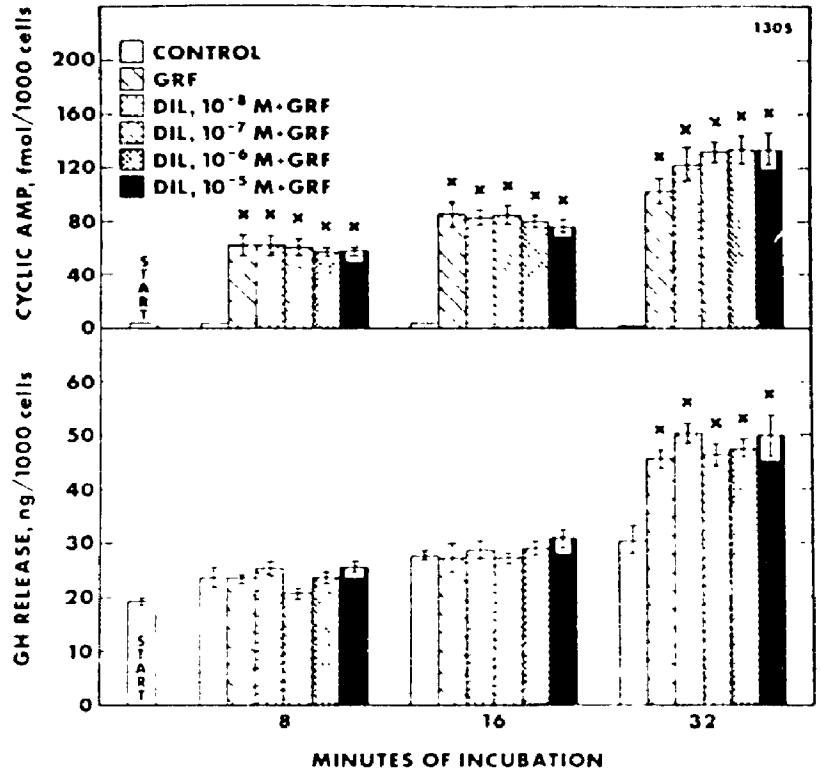

Figure 13. **The effect of 10^{-8} to 10^{-5} M diltiazem (DIL) on 10^{-10} M rGRF-induced cyclic AMP accumulation and growth hormone (GH) release by rat somatotrophs.** "START" samples were taken 5 min prior to diltiazem addition. GH is expressed as ng of rat GH (RP-1) per 1000 cells. Each column represents a mean of four determinations. The error bars are SEM. Where the bars do not appear, the SEM was too small to plot. Values significantly different from control are indicated by "x" ($p<0.05$)

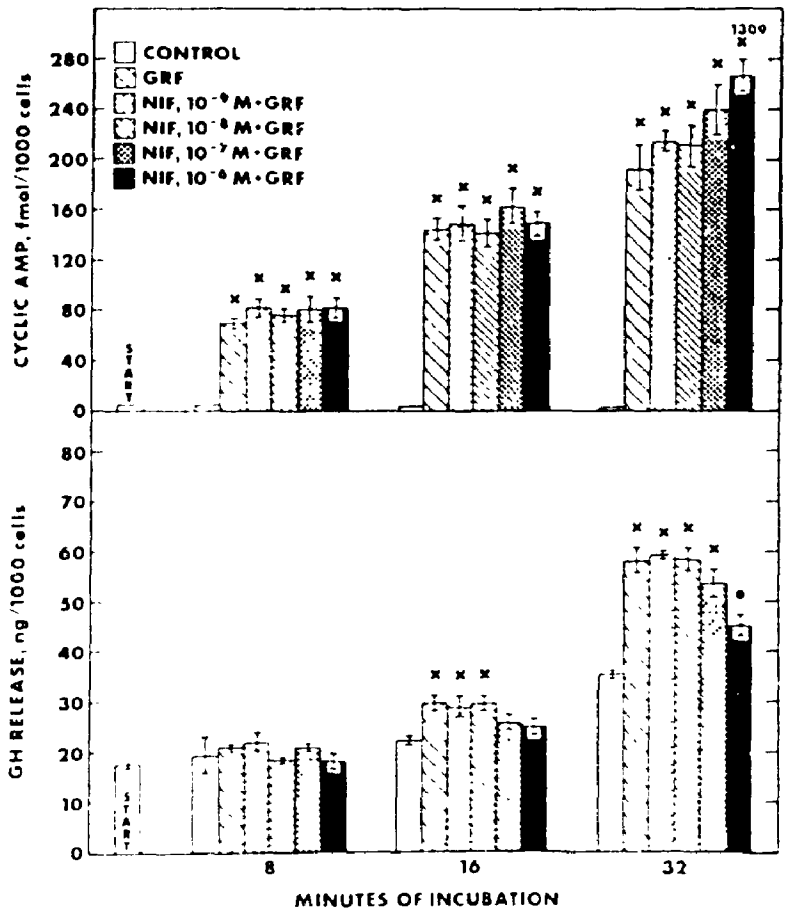

Figure 14. **The effect of 10^{-9} to 10^{-6} M nifedipine (Nif) on 10^{-10} M rGRF-induced cyclic AMP accumulation and growth hormone (GH) release by rat somatotrophs.** "START" samples were taken 5 min prior to nifedipine addition. GH is expressed as ng of rat GH (RP-1) per 1000 cells. Each column represents a mean of four determinations. The error bars are SEM. Where bars do not appear, the SEM was too small to plot. Values significantly different from control are indicated by "x" ($p<0.05$), while values significantly different from GRF are indicated by "●" ($p<0.05$).

concentrations up to 10^{-5} M did not significantly alter this rGRF-induced increase in GH release or cAMP accumulation (Figure 13). In the nifedipine studies, rGRF again induced a significant increase in GH release by 16 min preceded by a marked increase in cAMP accumulation by 8 min (Figure 14). Nifedipine at 10^{-6} M (but not at lower concentrations) did significantly reduce, but not abolish, the rGRF-induced release of GH. Nifedipine did not significantly alter the cAMP response, but at the highest concentration tested (10^{-6} M), nifedipine did consistently increase cAMP accumulation at 32 min (Figure 14).

In a second series, the effects of higher concentrations of diltiazem (Figure 15) and nifedipine (Figure 16) on rGRF-induced GH release and cAMP accumulation was examined in more detail. rGRF again elicited a significant increase in GH release by 16 - 32 min. Diltiazem at 10^{-5} and 10^{-4} M consistently reduced basal GH release in a concentration-related manner (Figure 15). Diltiazem at 10^{-4} M, but not 10^{-5} M, significantly reduced, but did not abolish, the rGRF-induced increase in GH release. Diltiazem did not alter basal cAMP accumulation but at 10^{-4} M, did significantly increase the cAMP response to rGRF at all four times.

In the second series nifedipine at 10^{-6} and 10^{-5} M consistently lowered basal GH release in a concentration-dependent manner (Figure 16). This reduction in basal release was significant at 32 min. In this experiment nifedipine at 10^{-6} M, as well as at 10^{-5} M, completely blocked the rGRF-induced increase in GH release. Nifedipine did not alter basal cAMP accumulation, but at both concentrations did significantly increase the cAMP response to rGRF at 32 min.

4.1.3 GRF and ^{45}Ca uptake.

4.1.3.1 Steady state experiments. ^{45}Ca was introduced into the incubation medium 10 min after exposing the cells to 10^{-9} M GRF. GRF lead to a significant increase in GH secretion

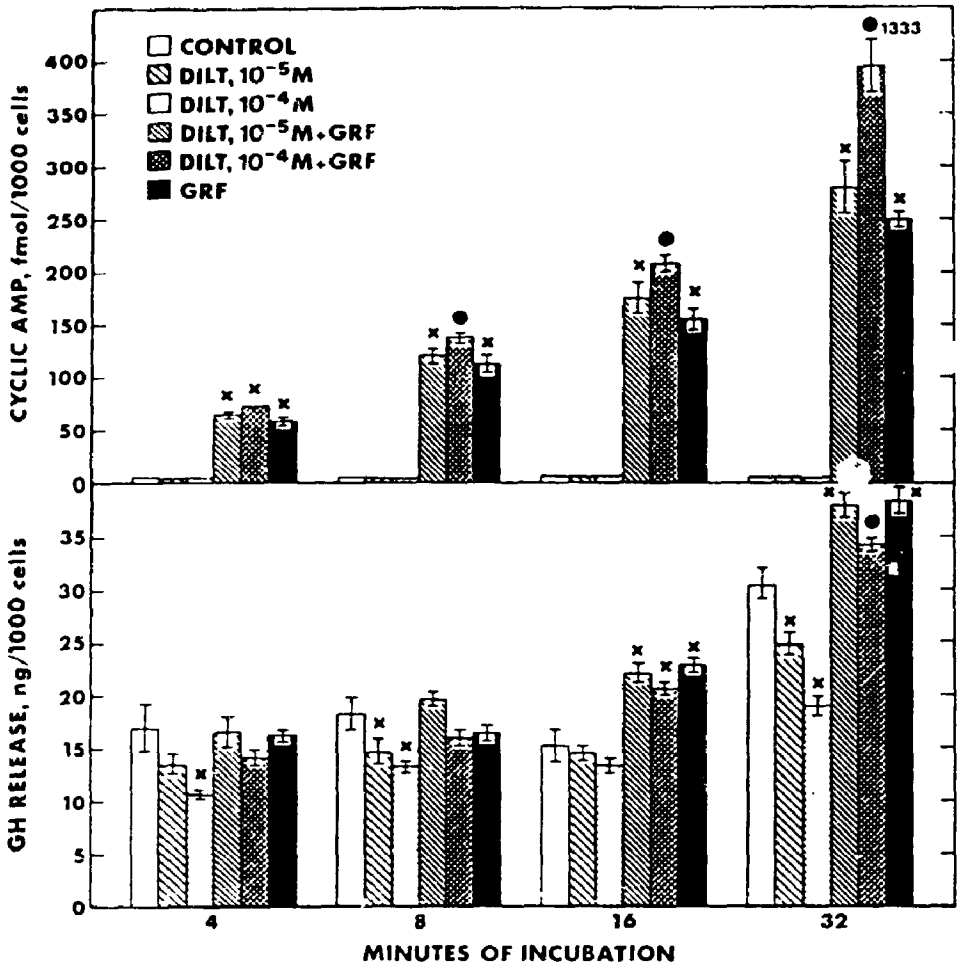

Figure 15. **The effect of 10^{-5} to 10^{-4} M diltiazem (DILT) on basal and 10^{-10} M rGRF-induced cyclic AMP accumulation and growth hormone (GH) release by rat somatotrophs.** GH is expressed as ng of rat GH (RP-1) per 1000 cells. Each column represents a mean of four determinations. The error bars are SEM. Where bars do not appear, the SEM was too small to plot. Values significantly different from control are indicated by "x" ($p<0.05$), while values significantly different from GRF are indicated by "●" ($p<0.05$).

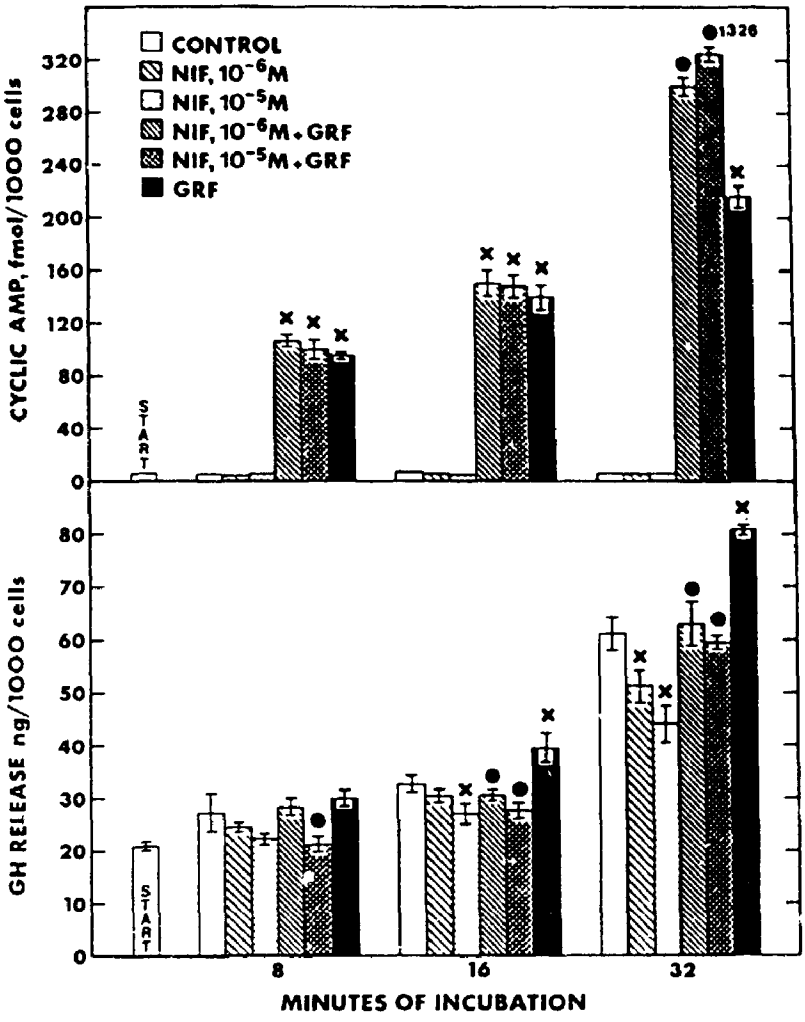

Figure 16. **The effect of 10^{-6} to 10^{-5} M nifedipine (NIF) on basal and 10^{-10} M rGRF-induced cyclic AMP accumulation and growth hormone (GH) release by rat somatotrophs.** "START" samples were taken 5 min prior to the addition of nifedipine. GH is expressed as ng of rat GH (RP-1) per 1000 cells. Each column represents a mean of four determinations. The error bars are SEM. Where bars do not appear, the SEM was too small to plot. Values significantly different from control are indicated by "x" ($p<0.05$), while values significantly different from GRF are indicated by "●" ($p<0.05$).

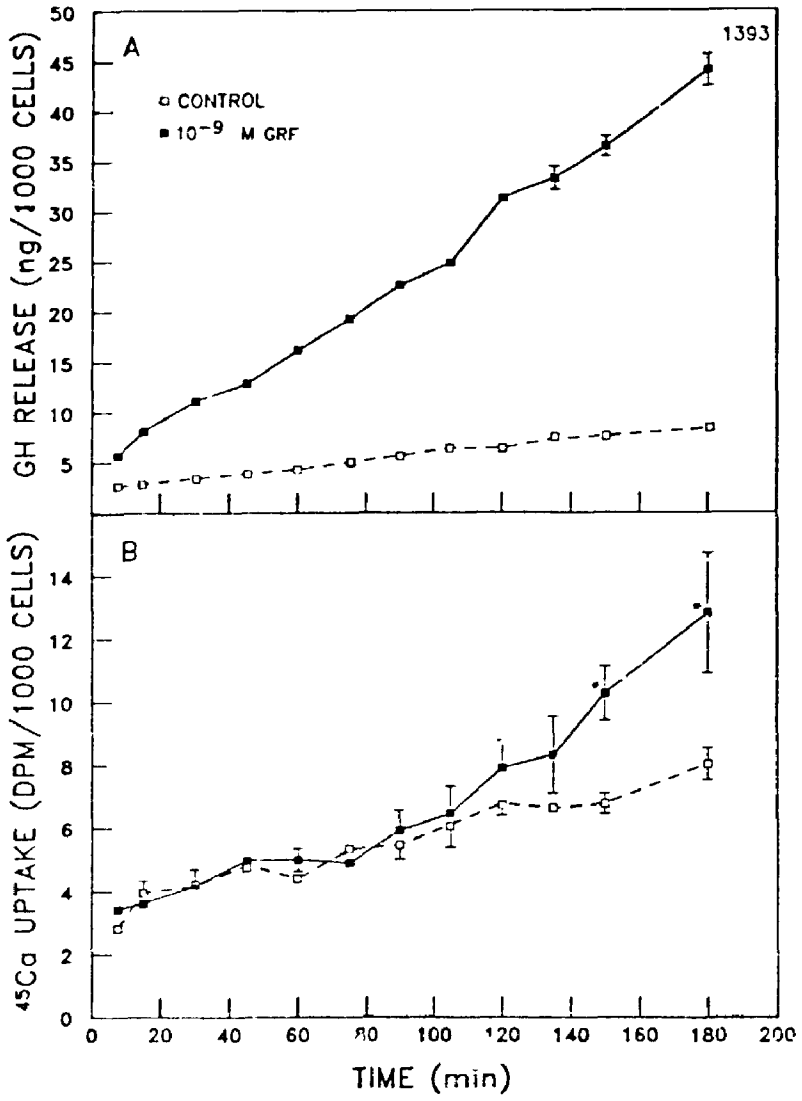

Figure 17. Time course of the effect of 10^{-9} M rGRF on growth hormone (GH) release and steady state ^{45}Ca uptake by rat somatotrophs. Time 0 min corresponds to the addition of [^{45}Ca]-$CaCl_2$ to the incubation medium. GRF was added 10 min prior to the tracer. **A.** GH is expressed as ng of rat GH (RP-2) per 1000 cells. **B.** ^{45}Ca uptake is expressed as corrected ^{45}Ca dpm/1000 cells. Each data point represents a mean of three or four determinations. The error bars are SE. Where bars do not appear, the SEM was too small to plot. Values significantly different from control are indicated by *** ($p<0.05$).

(Figure 17, panel A). In all experiments GRF significantly increased ^{45}Ca uptake after 180 min of tracer loading (Figure 17, panel B). In two of three experiments significant increases were also seen at 120 min and 150 min. Since ^{45}Ca loading never approached tracer equilibrium and the sample variation was high, it was not possible to calculate either the Ca^{2+} net flux across the plasma membrane or the Ca^{2+} pool size. Therefore we could not determine if the increase in ^{45}Ca uptake was the result of an increase in the rate of Ca^{2+} exchange or an increase in the total amount of calcium in the cell (see section 5.1.1.1).

4.1.3.2 Non-steady state experiment - A23187. To test whether the oil sandwich technique was sensitive enough to detect changes in Ca^{2+} influx under non-steady state conditions, we challenged somatotrophs with the calcium ionophore A23187. The cells were loaded with ^{45}Ca for 90 min and then challenged with the ionophore. A23187 at a concentration of 10^{-6} M caused a large increase in ^{45}Ca uptake (208 ± 32% and 154 ± 47% in 2 separate experiments; n=4) (Figure 18). The ^{45}Ca uptake into A23187 treated cells was significantly greater than control within 2 min of addition of the ionophore.

4.1.3.3 Non-steady state experiment - GRF. Once it was established that the method for measuring ^{45}Ca uptake could detect rapid changes in Ca^{2+} influx in non-steady state, the effect of GRF in non-steady state was studied. Somatotrophs were loaded with ^{45}Ca for 90 min and then challenged with 10^{-9} M GRF. This resulted in a marked increase in GH release (Figure 19, panel A) indicating that the treated cells were no longer in steady state. When ^{45}Ca uptake for the GRF group is expressed as a percentage of the uptake for the control group at each time point, a consistent triphasic pattern became apparent (Figure 19, panel B). The first phase consisted of a transient increase in ^{45}Ca uptake peaking at 30 sec. The second phase consisted of a second transient increase peaking at 2 min. The third phase consisted of a sustained increase starting after 16 min. However, GRF treatment did not result in a statistically significant increase in ^{45}Ca uptake at any time point in any given experiment. When the

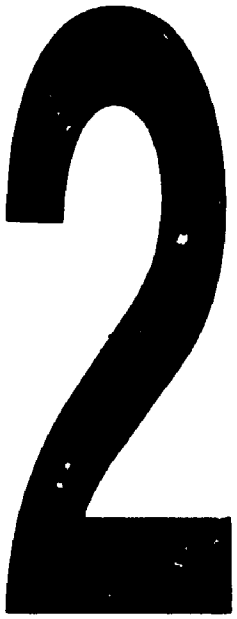

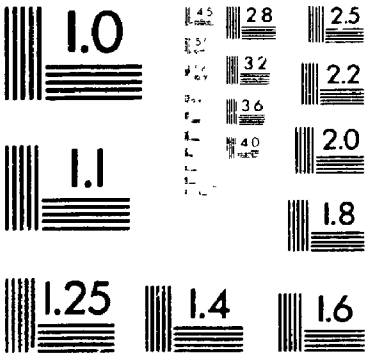
1.0
1.1
1.25
1.4
1.6
1.8
2.0
2.2
2.5
2.8
3.2
3.6
4.0


MicroD

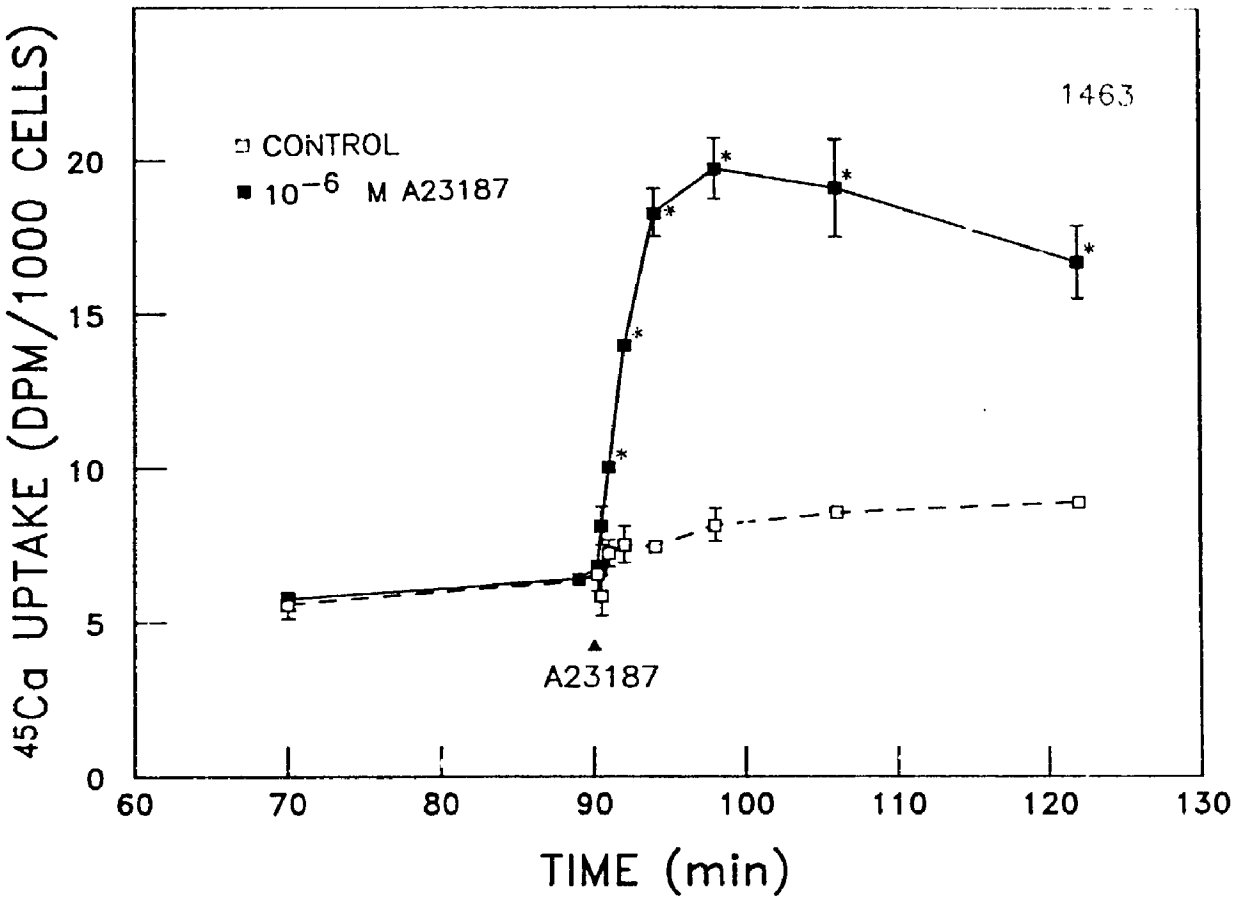

Figure 18. Time course of the effect of 10^{-6} M A23187 on non-steady state ^{45}Ca uptake by rat somatotrophs. Time 0 min corresponds to the addition of [^{45}Ca]-$CaCl_2$ to the incubation medium. The arrow head indicates the addition of A23187 to the incubation medium. ^{45}Ca uptake is expressed as corrected ^{45}Ca dpm/1000 cells. Each data point represents a mean of three or four determinations. The error bars are SEM. Where bars do not appear, the SEM was too small to plot. Values significantly different from control are indicated by "*" ($p<0.05$).

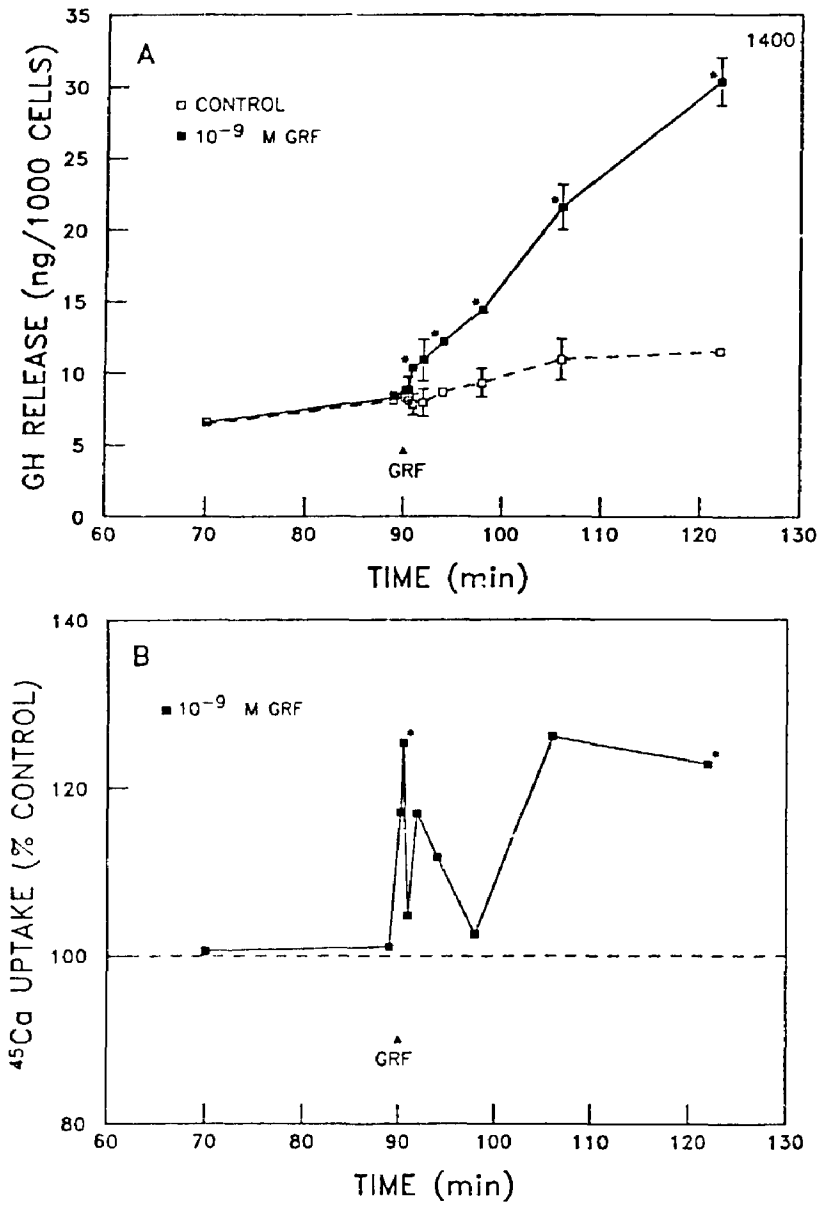

Figure 19. **Time course of the effect of 10^{-9} M rGRF on growth hormone (GH) release and non-steady state ^{45}Ca uptake in rat somatotrophs.** Time 0 min corresponds to the addition of [^{45}Ca]-$CaCl_2$ to the incubation medium. The arrow head indicates the addition of GRF to the incubation medium. **A.** GH is expressed as ng of rat GH (RP-2) per 1000 cells. Each data point represents a mean of three or four determinations for a single experiment. The error bars are SEM. Where bars do not appear, the SEM was too small to plot. **B.** The GRF-induced triphasic ^{45}Ca uptake response. ^{45}Ca uptake in the GRF-treated group is expressed as the % of the of uptake in the control group at each time point. Each data point represents a weighted mean of four separate experiments. SEM are not shown for clarity. Values significantly different from control are indicated by "*" ($p<0.05$).

average of the means for 4 experiments was calculated, the 25 ± 7% (n=4) increase in the first peak, and the 22 ± 4% (n=4) increase in the sustained, elevated uptake at 32 min, were significantly different from control while the 17 ± 8% (n=4) increase in the second peak, though consistent, failed to reach statistical significance.

4.1.4 GRF and $[Ca^{2+}]_i$.

4.1.4.1 Indo-1 intracellular concentration. The loading procedure that was used resulted in an intracellular concentration of indo-1 of 92 ± 2 μM (weighted mean ± SEM of 49 loadings - 363 observations).

4.1.4.2 GH release from indo-1 loaded somatotrophs. This study was carried out to ensure that indo-1 loaded purified somatotrophs, incubated in the simplified medium used in the $[Ca^{2+}]_i$ studies, retain their responsiveness to GRF. The cells were challenged with 10^{-12} M rGRF for 20 min, followed by 30 min of medium, followed by a second 20 min of 10^{-10} M rGRF, followed by 30 min of medium (Figure 20). The GH response of somatotrophs perifused in the usual manner with M199-AH was identical to the indo-1 loaded somatotrophs perifused with simplified medium at both GRF concentrations. GRF caused an immediate (within 1 min) increase in GH release. The low concentration caused a sustained 5 - 8% increase in GH release, while 10^{-10} M GRF resulted in a 14 to 16-fold response. GH secretion peaked within 3 - 5 min and then fell slowly, while GRF was maintained. When the GRF was removed, GH secretion fell quickly to the previous unstimulated level.

4.1.4.3 Baseline $[Ca^{2+}]_i$. The mean baseline $[Ca^{2+}]_i$ for unstimulated somatotrophs incubated in medium containing 1.2 mM $CaCl_2$ was 269 ± 3 nM (weighted mean ± SEM of 45 experiments - 361 observations).

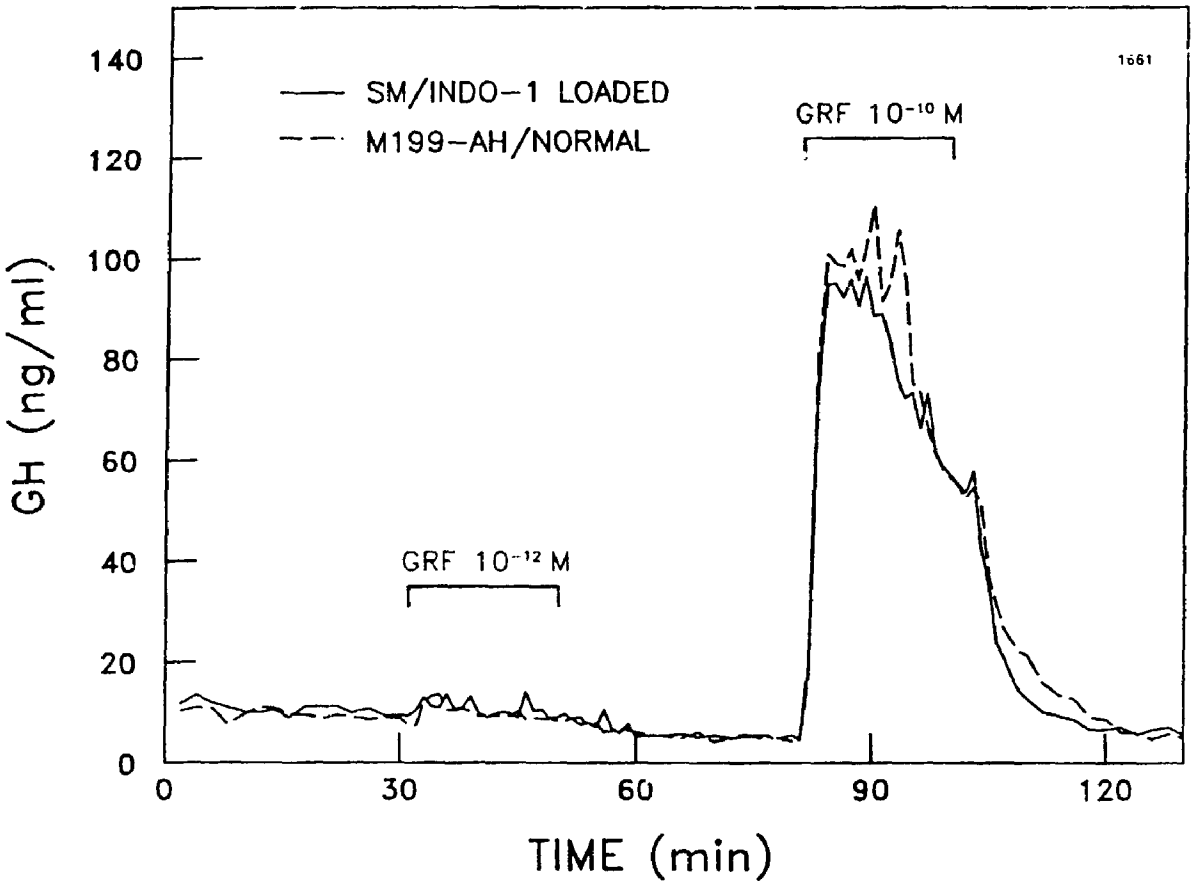

Figure 20. Growth hormone (GH) response to 20-min periods of perifusion with 10^{-12} M and 10^{-10} M rGRF by normal and indo-1-loaded rat somatotrophs. Normal somatotrophs were perifused with M199-AH, while indo-1-loaded somatotrophs were perifused with special medium (SM). GH is expressed as ng of rat GH (RP-2) per ml of perifusate per one min fraction.

4.1.4.4 GRF and $[Ca^{2+}]_i$. The vehicle for GRF had no effect on $[Ca^{2+}]_i$ (Figure 21). GRF caused a biphasic response. The first phase consisted of a rapid increase in $[Ca^{2+}]_i$ peaking approximately 30 sec after the addition of GRF. The second phase consisted of a sustained elevated $[Ca^{2+}]_i$, or plateau, maintained for at least 5 min. Both the peak and the plateau $[Ca^{2+}]_i$ were dependent on GRF concentration (Figure 22). The EC_{50} for peak and plateau, evaluated by fitting a four-parameter logistic equation to the concentration response data, were $2x10^{-10}$ M and $7x10^{-10}$ M respectively.

4.1.4.5 GRF and $[Ca^{2+}]_i$ in Ca^{2+}-free medium. To explore whether the GRF induced increase in $[Ca^{2+}]_i$ was due to an influx of Ca^{2+} or to a redistribution of intracellular stored Ca^{2+}, we carried out a set of experiments in Ca^{2+}-free medium. The apparent baseline $[Ca^{2+}]_i$ in simplified medium without $CaCl_2$, measured 15 sec after the start of the recording period, was 162 ± 4 nM (n=17), which was significantly lower than that for cells tested in 1.2 mM Ca^{2+} media (299 ± 13 nM, n=9) in the same experiment. Contaminating traces of Ca^{2+} (50 - 80 μM) in the Ca^{2+}-free simplified medium were then chelated by adding 0.5 mM EGTA 15 sec after the start of the recording (Figure 23, panel B). The addition of EGTA resulted in an instantaneous decrease in fluorescence. This indicated the presence of extracellular indo-1, which had leaked out of the cells and fluoresced in the presence of contaminating Ca^{2+}. The $[Ca^{2+}]_i$ in Ca^{2+}-free medium containing EGTA, measured 10 sec after the addition of EGTA, was 138 ± 2 nM (n=15). Ionomycin was added to liberate membrane bound stored Ca^{2+}. The large response indicates that stored Ca^{2+} was present in these cells.

When GRF was added 10 sec after the addition of EGTA, so as to minimize the possible leaching out of Ca^{2+} from stores by the chelator, no response to GRF was detected (Figure 23, panel C). Again the addition of ionomycin revealed large Ca^{2+} stores.

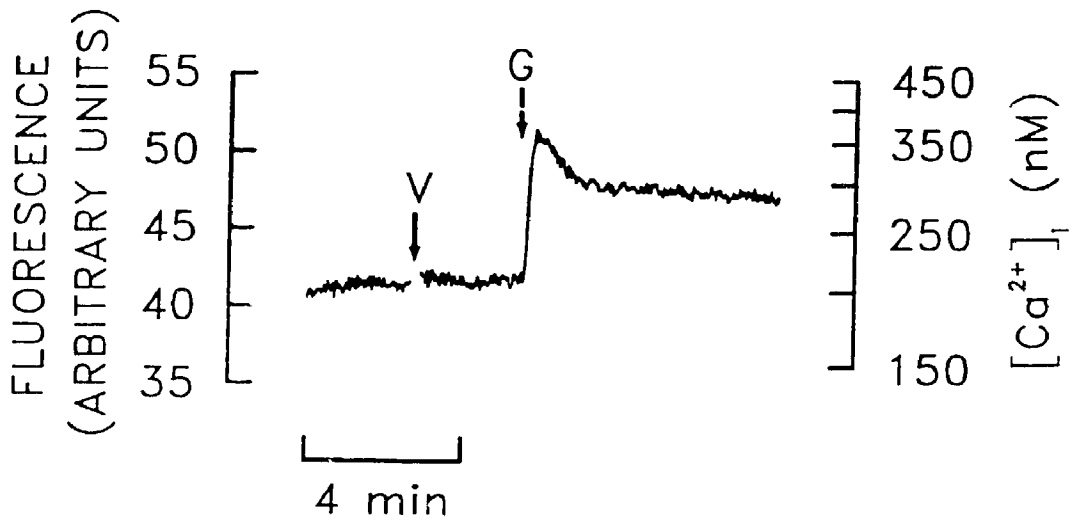

Figure 21. Intracellular Ca^{2+} concentration ($[Ca^{2+}]_i$) response to 10^{-9} M rGRF in rat somatotrophs. $[Ca^{2+}]_i$ was measured in 1.2 mM $CaCl_2$ containing medium at 37 C and pH 7.35-7.4 with the fluorescent dye indo-1 with excitation and emission wavelengths of 329 nm and 405 nm respectively. Arrows indicate additions to the incubation medium. V: vehicle for GRF; G: 10^{-9} M rGRF.

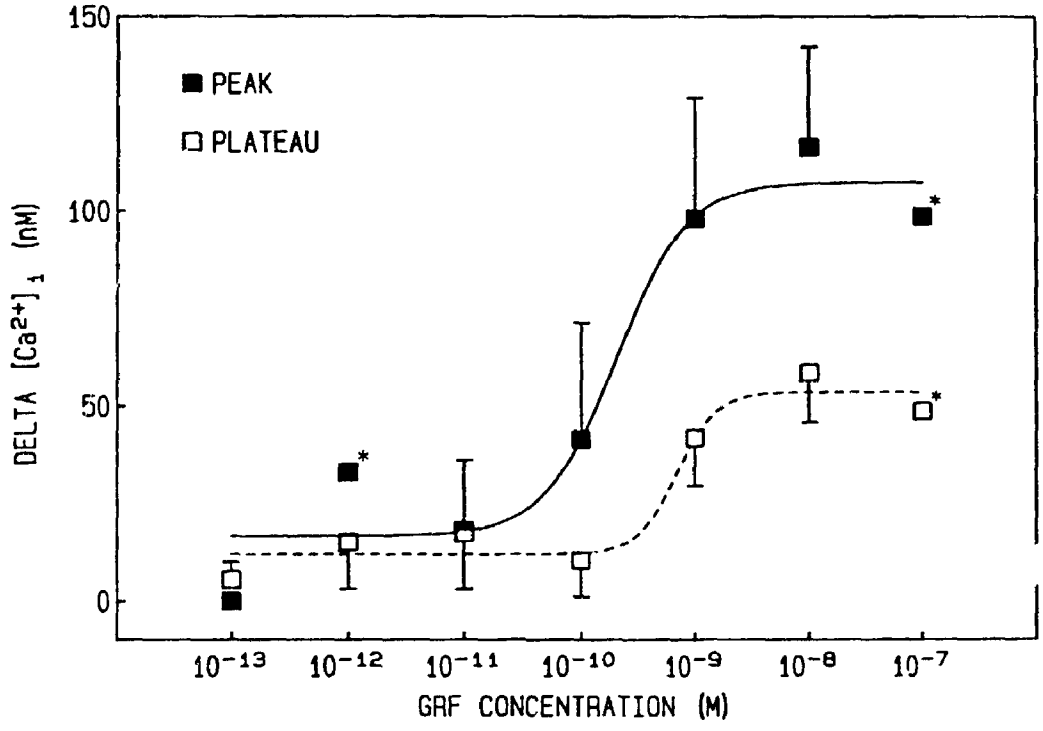

Figure 22. Concentration response curve for rGRF-induced peak and plateau $[Ca^{2+}]_i$ in rat somatotrophs. The response is expressed as the difference (delta) between baseline and peak or plateau $[Ca^{2+}]_i$ measured in 1.2 mM $CaCl_2$ containing medium at 37 C and pH 7.35-7.4 with the fluorescent dye indo-1 with excitation and emission wavelengths of 329 nm and 405 nm respectively. Data points represent a mean of 4 determinations. The error bars are SEM. "*" denotes data points where only two determinations were carried out.

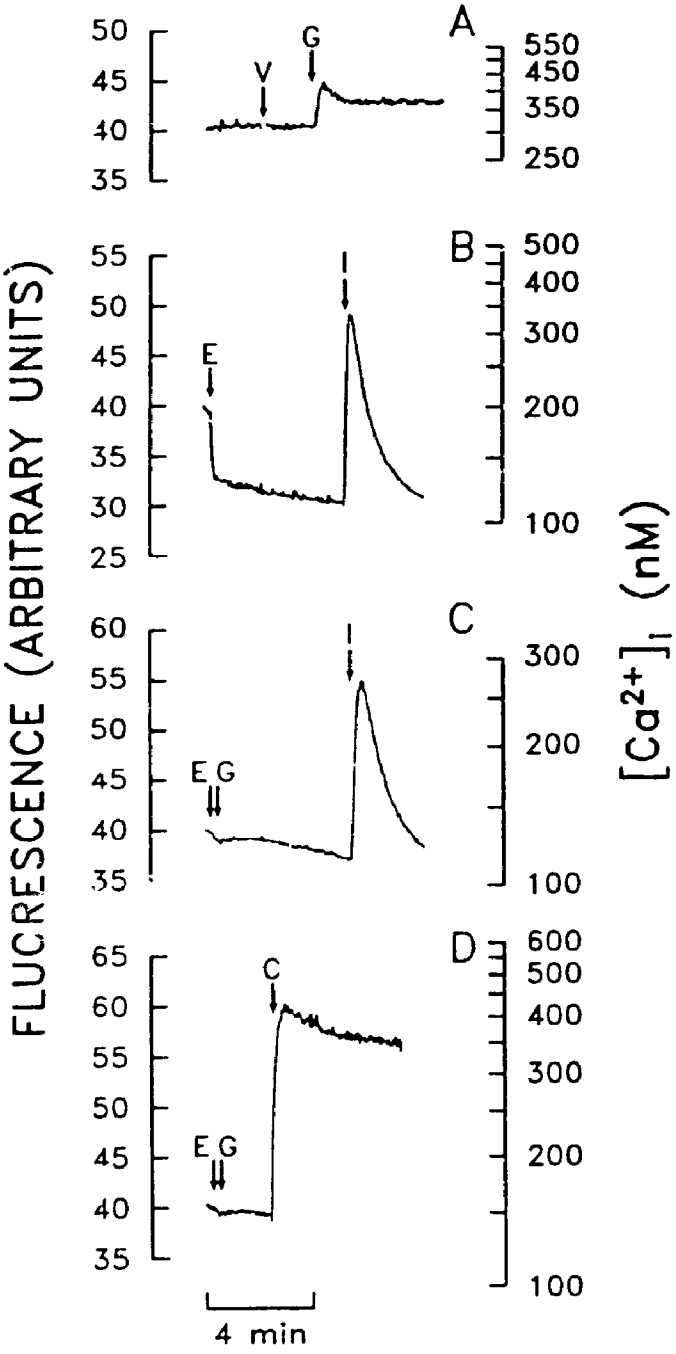

Figure 23. **The effect of removing extracellular Ca^{2+} on GRF-induced changes in $[Ca^{2+}]_i$ in rat somatotrophs.** $[Ca^{2+}]_i$ was measured at 37 C and pH 7.35-7.4 with the fluorescent dye indo-1 with excitation and emission wavelengths of 329 nm and 405 nm respectively. **A.** 10^{-9} M rGRF control in 1.2 mM $CaCl_2$ containing medium. **B.** The effect of adding 0.5 mM EGTA to Ca^{2+}-free medium on $[Ca^{2+}]_i$. **C.** The effect of 10^{-9} M rGRF in Ca^{2+}-free medium with 0.5 mM EGTA. **D.** The effect of adding 1.2 mM $CaCl_2$ to Ca^{2+}-free medium containing 0.5 mM EGTA, after challenging cells with 10^{-9} M rGRF. Arrows indicate additions to the incubation medium. V: vehicle for GRF; G: 10^{-9} M rGRF; E: 0.5 mM EGTA; I: 10^{-5} M ionomycin; C: 1.2 mM $CaCl_2$.

To investigate the possibility that EGTA itself may interfere with Ca^{2+} influx or processes stimulating influx, Ca^{2+} was added back to the cuvette to give a final extracellular Ca^{2+} concentration of 1.2 mM before adding ionomycin (Figure 23, panel D). The maximum $[Ca^{2+}]_i$ was comparable to the plateau concentration seen with GRF in 1.2 mM Ca^{2+} medium without EGTA. Therefore EGTA itself did not prevent the increase in $[Ca^{2+}]_i$. Interestingly, when Ca^{2+} was added back, a biphasic response was sometimes seen.

4.1.4.6 Ca^{2+} antagonists; baseline and GRF-induced increase in $[Ca^{2+}]_i$. The effect of 10^{-8} M to 10^{-4} M of the Ca^{2+} antagonist diltiazem was tested on both baseline $[Ca^{2+}]_i$ and GRF-induced changes. The vehicle for diltiazem had no effect. At concentrations greater than 10^{-6} M, baseline $[Ca^{2+}]_i$ was decreased in a concentration dependent fashion (Figure 24 and 25, panel A). The maximal effect on $[Ca^{2+}]_i$ of each concentration was apparent within 2 min as indicated by a stable nadir below baseline. The EC_{50} of diltiazem for the nadir was found to be approximately $1.6x10^{-5}$ M when a four-parameter logistic equation was fitted to the data to obtain an extrapolated lower plateau (Figures 24 and 25, panel A). The cells were then challenged with 10^{-9} M GRF 2 min into the diltiazem treatment. The GRF response was inhibited, but not abolished, in a concentration dependent fashion, with an IC_{50} of $5x10^{-7}$ (Figure 25, panel B). Even at the highest concentration of diltiazem tested (10^{-4} M) the GRF response was not completely abolished. However $[Ca^{2+}]_i$ did not rise above the pre-antagonist baseline (Figure 24).

A similar experiment was carried out using the Ca^{2+} antagonist nifedipine (Figure 24). The vehicle for nifedipine had no effect. At concentrations greater than 10^{-9} M, baseline $[Ca^{2+}]_i$ was decreased in a concentration dependent fashion, reaching a stable nadir within 2 min, with an EC_{50} of approximately 10^{-7} M as given by a four parameter logistic equation (Figures 24 and 26, panel A). The cells were then challenged with 10^{-9} M GRF 2 min into the nifedipine treatment The GRF response was inhibited, but not abolished, in a concentration

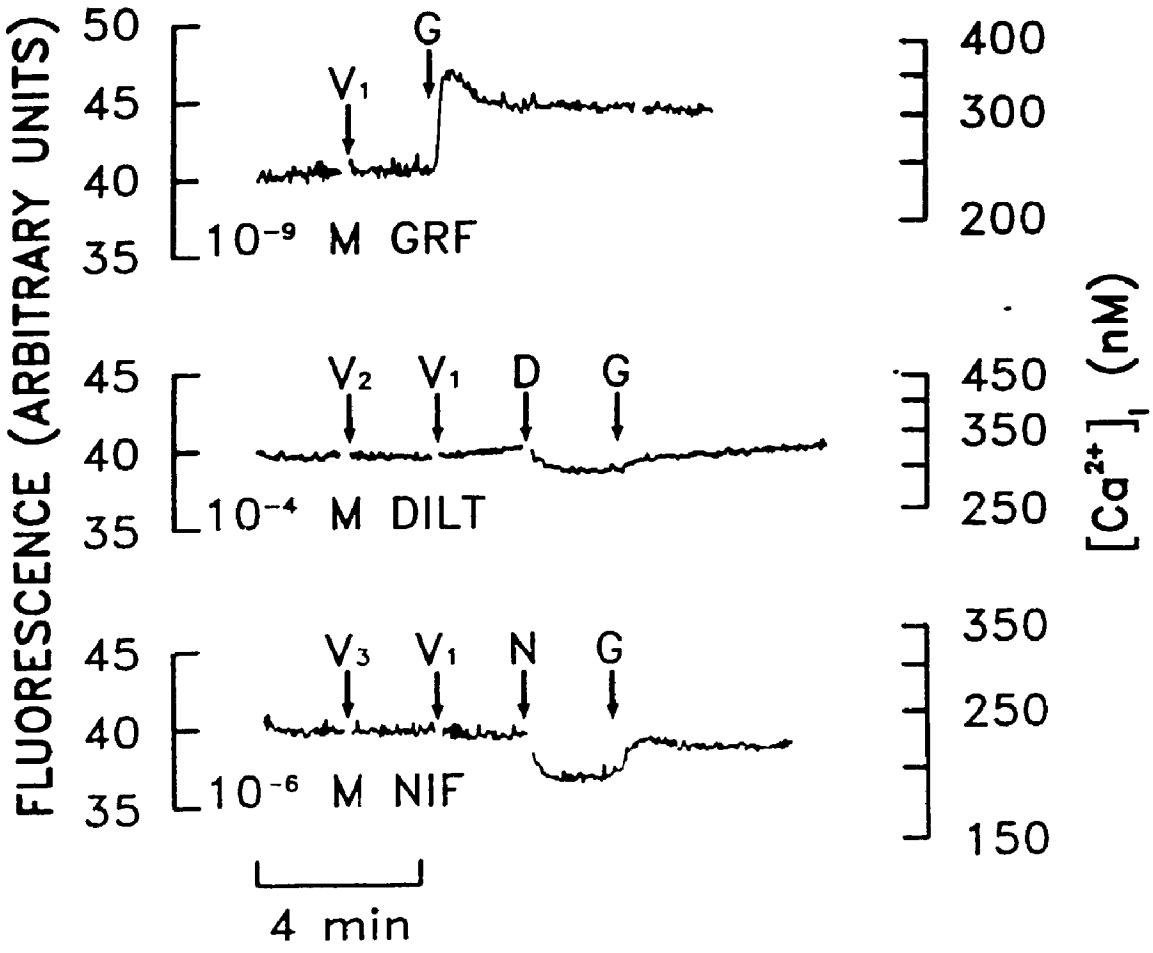

Figure 24. **Diltiazem (DILT)- and nifedipine (NIF)-dependent inhibition of GRF-induced $[Ca^{2+}]_i$ response in rat somatotrophs.** $[Ca^{2+}]_i$ was measured in 1.2 mM $CaCl_2$ containing medium at 37 C and pH 7.35-7.4 with the fluorescent dye indo-1 with excitation and emission wavelengths of 329 nm and 405 nm respectively. Arrows indicate additions to the incubation medium. V_1: vehicle for GRF; V_2: diltiazem vehicle; V_3: vehicle for nifedipine; G: 10^{-9} M rGRF; D: 10^{-4} M diltiazem; N: 10^{-6} M nifedipine.

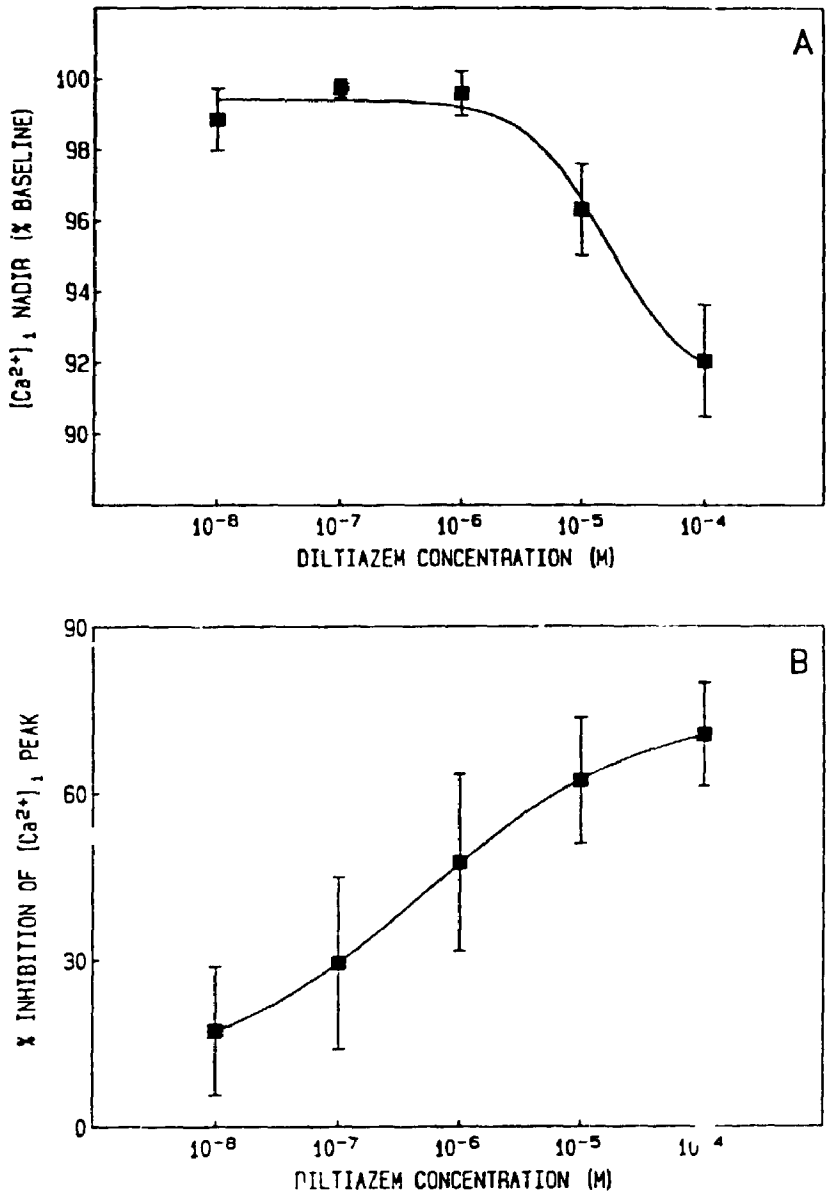

Figure 25. **Concentration response for diltiazem-dependent $[Ca^{2+}]_i$ nadir and diltiazem-dependent inhibition of GRF-induced $[Ca^{2+}]_i$ response in rat somatotrophs.** $[Ca^{2+}]_i$ was measured in 1.2 mM $CaCl_2$ containing medium at 37 C and pH 7.35-7.4 with the fluorescent dye indo-1 with excitation and emission wavelengths of 329 nm and 405 nm respectively. **A.** Concentration response of diltiazem-dependent $[Ca^{2+}]_i$ nadir. The nadir is expressed as % baseline $[Ca^{2+}]_i$ measured before addition of diltiazem. **B.** Concentration response for diltiazem-dependent inhibition of the 10^{-9} M rGRF $[Ca^{2+}]_i$ response. The % inhibition was calculated as the % decrease of the 10^{-9} M rGRF-dependent peak $[Ca^{2+}]_i$ in the presence of diltiazem. Data points represent a mean of 4 determinations. The error bars are SEM.

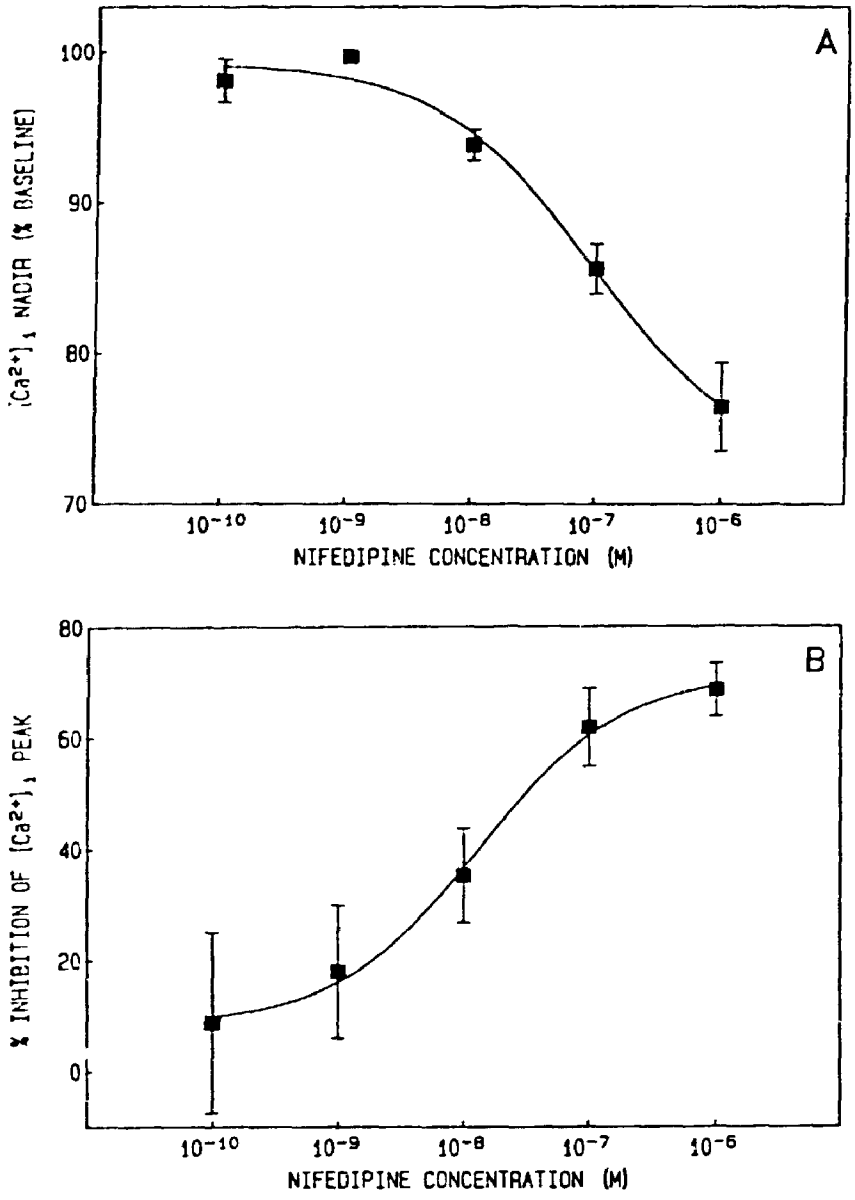

Figure 26. **Concentration response for nifedipine-dependent nadir $[Ca^{2+}]_i$ and nifedipine-dependent inhibition of GRF-induced $[Ca^{2+}]_i$ response in rat somatotrophs.** $[Ca^{2+}]_i$ was measured in 1.2 mM $CaCl_2$ containing medium at 37 C and pH 7.35-7.4 with the fluorescent dye indo-1 with excitation and emission wavelengths of 329 nm and 405 nm respectively. **A.** Concentration response of nifedipine-dependent $[Ca^{2+}]_i$ nadir. The nadir is expressed as % baseline $[Ca^{2+}]_i$ measured before addition of diltiazem. **B.** Concentration response for nifedipine-dependent inhibition of the 10^{-9} M rGRF $[Ca^{2+}]_i$ response. The % inhibition was calculated as the % decrease of the 10^{-9} M rGRF-dependent peak $[Ca^{2+}]_i$ in the presence of nifedipine. Data points represent a mean of 4 determinations. The error bars are SEM. Where bars do not appear, the SEM was too small to plot.

dependent fashion, with an IC_{50} of $1.3x10^{-8}$ M (Figure 26, panel B). Again, even at the highest concentration of nifedipine tested (10^{-6} M) the GRF response was not completely abolished. However $[Ca^{2+}]_i$ did not rise above the pre-antagonist baseline (Figure 24).

To determine whether the plateau phase of the GRF response, once initiated, is due to a sustained Ca^{2+} influx, somatotrophs were treated with nifedipine once the GRF response was initiated. Cells were challenged with 10^{-9} M GRF, and the response was followed for 2 min. At this point 10^{-6} M nifedipine was added (Figure 27, panel C). GRF produced the typical biphasic response. Nifedipine rapidly (within 1 min) decreased the plateau $[Ca^{2+}]_i$ to a nadir well below the baseline. $[Ca^{2+}]_i$ then increased slightly but stabilized well below baseline.

4.2 Ca^{2+} and SRIF

4.2.1 SRIF and ^{45}Ca Uptake.

4.2.1.1 Steady state experiment - Time course. Figure 28, panel A shows the effect of 10^{-9} M SRIF on steady state GH release from the purified somatotrophs in one of three replicate experiments. At late time points, 135 min and 180 min, cumulative GH released with SRIF was significantly reduced. SRIF also significantly lowered the overall rate of GH secretion, calculated as the slope of the least square linear regression line of GH release verses time, in 2 of 3 experiments. Therefore SRIF steady state is different from the control steady state. Figure 28, panel B shows the ^{45}Ca uptake for the control and 10^{-9} M SRIF treated groups in the same representative experiment. No consistent pattern was seen, however, SRIF significantly lowered ^{45}Ca uptake by 43 ± 14% to 23 ± 9% (n=4) in individual experiments. These decreases were not always observed, but when detectable, they were seen only after 90 min of ^{45}Ca loading.

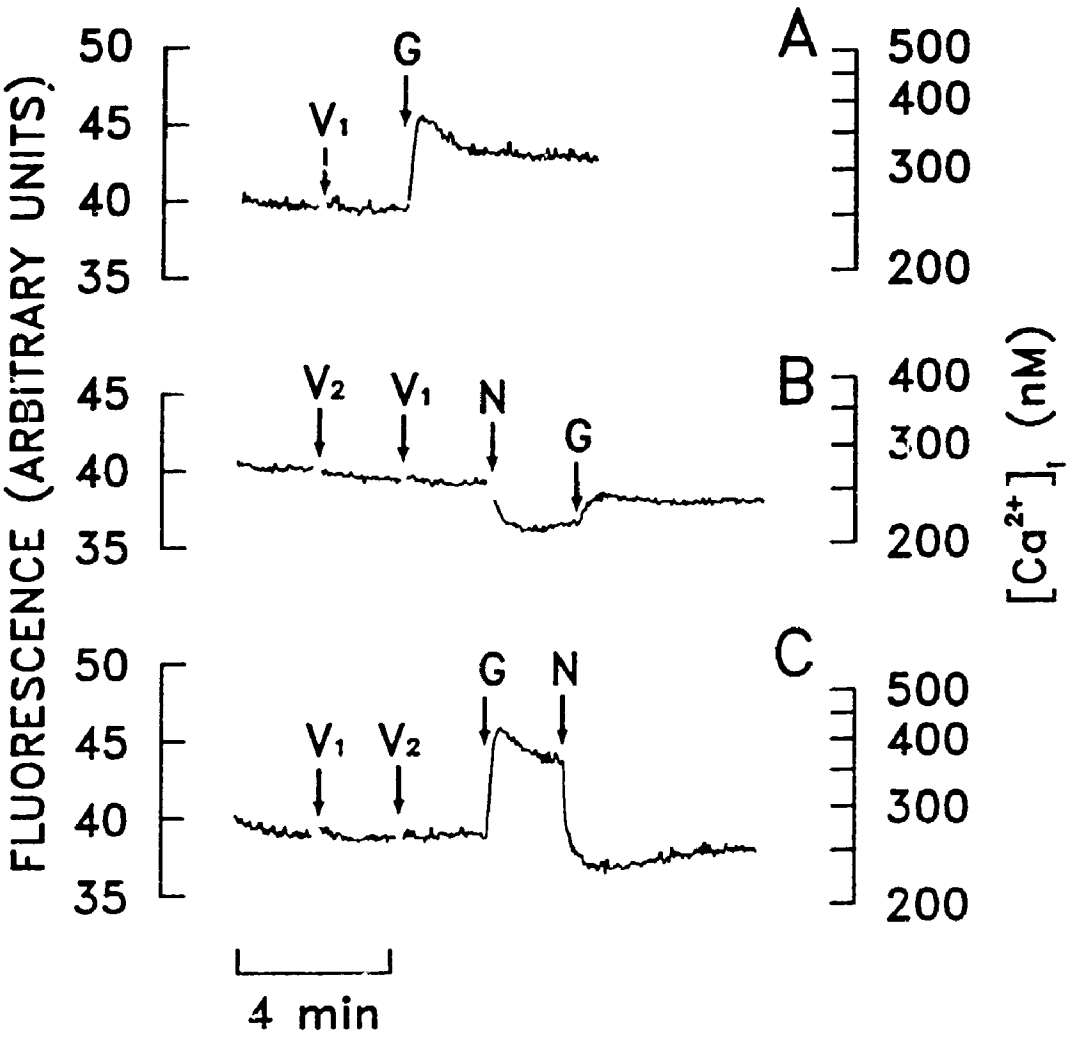

Figure 27. **The effect of 10^{-6} M nifedipine on the second phase of the 10^{-9} M rGRF induced $[Ca^{2+}]_i$ response.** $[Ca^{2+}]_i$ was measured in 1.2 mM $CaCl_2$ containing medium at 37 C and pH 7.35-7.4 with the fluorescent dye indo-1 with excitation and emission wavelengths of 329 nm and 405 nm respectively. **A.** 10^{-9} M rGRF control. **B.** The effect of 10^{-6} M nifedipine on the onset of the 10^{-9} M rGRF response. **C.** The effect of 10^{-6} M nifedipine on the second phase of the 10^{-9} M rGRF response. Arrows indicate additions to the incubation medium. V_1: vehicle for GRF; V_2: vehicle for nifedipine; G: 10^{-9} M rGRF; N: 10^{-6} M nifedipine.

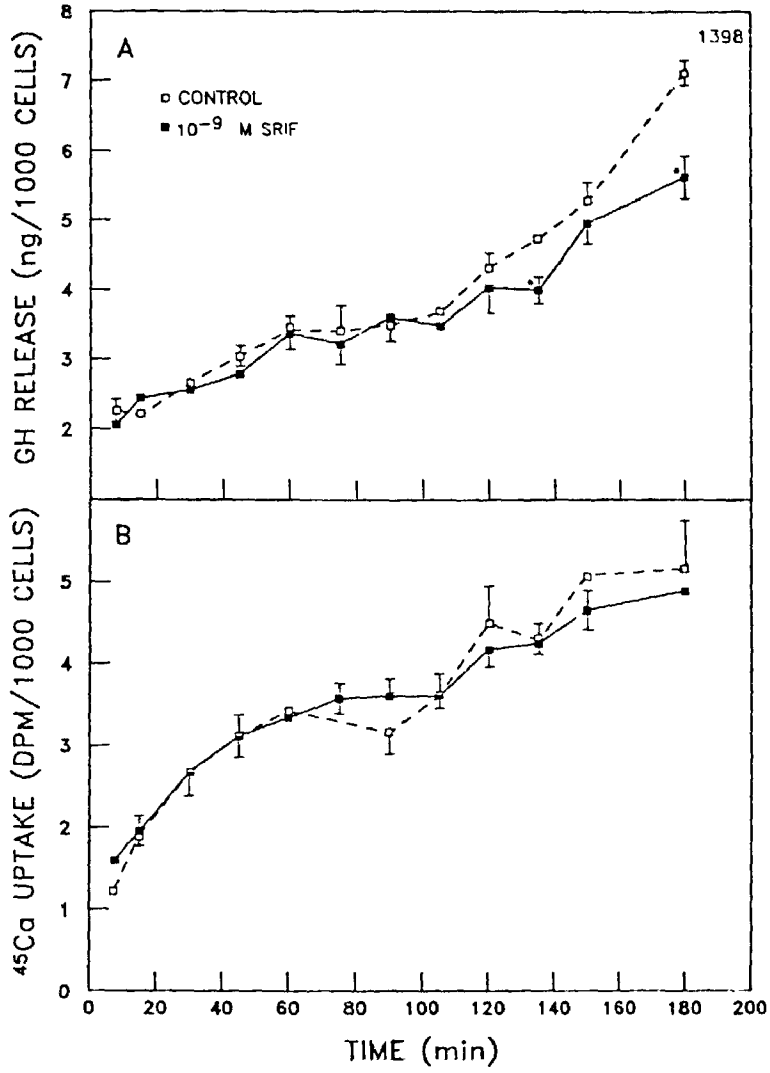

Figure 28. Time course of the effect of 10^{-9} M SRIF on growth hormone (GH) release and steady state ^{45}Ca uptake by rat somatotrophs. Time 0 min corresponds to the addition of [^{45}Ca]-$CaCl_2$ to the incubation medium. SRIF was added to the incubation medium 10 min prior to tracer addition. **A.** GH is expressed as ng of rat GH (RP-2) per 1000 cells. **B.** ^{45}Ca uptake is expressed as corrected ^{45}Ca dpm/1000 cells. Each data point represents a mean of three or four determinations. The error bars are SEM. Where bars do not appear, the SEM was too small to plot. Values significantly different from control are indicated by *** ($p<0.05$).

4.2.1.2 Steady state experiments - Single time point. A steady state single time point determination of ^{45}Ca uptake was then carried out. The rational for the single time point determination was that it would increase the amount of tissue per sample, and therefore theoretically reduce sample variability. Somatotrophs were incubated with 10^{-9} M SRIF for 10 min before ^{45}Ca was added to the incubation medium. A single sample was taken from each incubation beaker 90 min after addition of ^{45}Ca. SRIF consistently decreased uptake by 0.8 ± 0.4 and 1.0 ± .7 dpm/1000 cells (n=4) in two separate experiments (Figure 29). The decrease in the first experiment (10 ± 5%, n=4; Figure 29) was significant while the decrease in the second (12 ± 8%, n=4) did not reach significance. There were no significant changes in GH release.

4.2.1.3 Steady state experiments - Single time point - SRIF and GRF. Figure 30 shows the ^{45}Ca uptake and GH release by purified somatotrophs in steady state. Cells were treated with 10^{-7} M SRIF for 10 min. Then, in the continuing presence of SRIF, GRF was added to give a final concentration of 10^{-9} M. Ten min latter ^{45}Ca was added. The cells were sampled after 150 min of ^{45}Ca loading. GRF caused the expected 2.5 - 3 fold increase in GH release. SRIF decreased basal release by 21 ± 5% and 18 ± 4% (n=4) in two separate experiments (significant in one experiment) and completely abolished the GRF-induced GH release. GRF caused a significant 7 ± 4% and 26 ± 7% (n=4) increase in ^{45}Ca uptake in two separate experiments. SRIF decreased basal uptake by 17 ± 5% (n=4 in both experiments) and completely abolished the GRF-induced uptake of ^{45}Ca lowering the uptake to below the basal level.

4.2.1.4 Non-steady state experiments - Time course. Non-steady state experiments were carried out to test whether SRIF can quickly decrease Ca^{2+} influx in non-stimulated somatotrophs. SRIF was added to the incubation medium 6 or 15 min after adding ^{45}Ca. Figure 31 shows the results of such an experiment when 10^{-9} M SRIF was added 15 min after

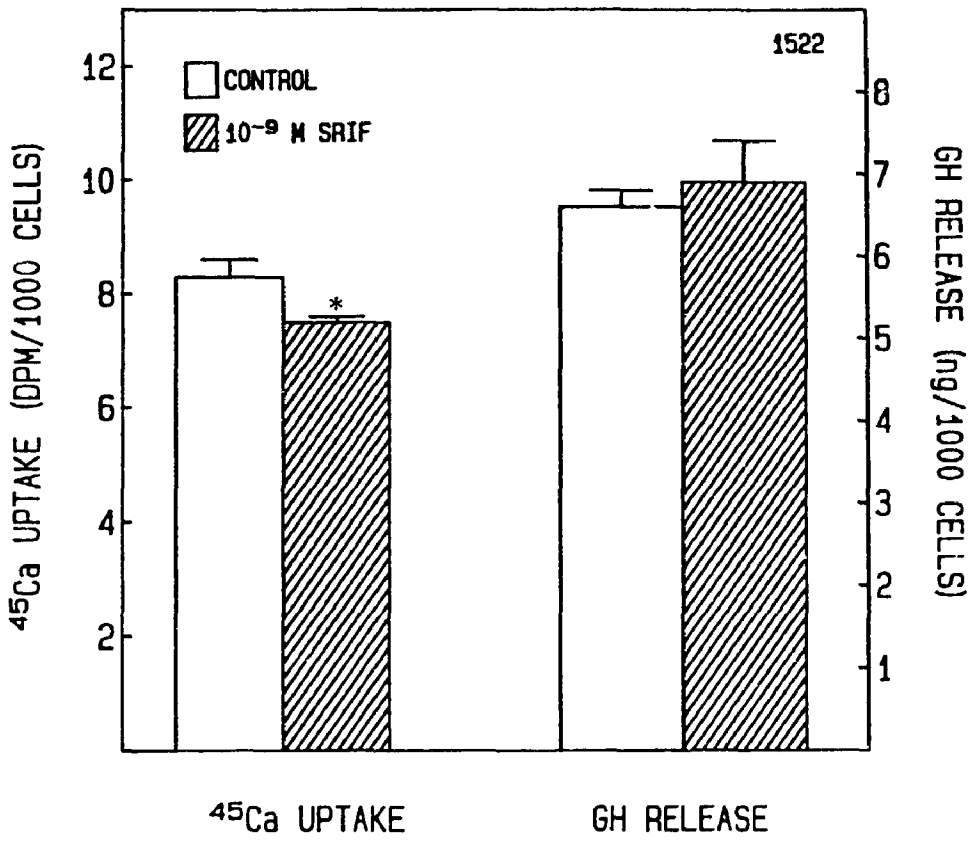

Figure 29. **The effect of 10^{-9} M SRIF on steady state ^{45}Ca uptake and growth hormone (GH) release by rat somatotrophs after 90 min of ^{45}Ca loading.** GRF was added to the incubation medium 10 min prior to the addition of [^{45}Ca]-$CaCl_2$. ^{45}Ca uptake is expressed as corrected ^{45}Ca dpm/1000 cells. GH is expressed as ng of rat GH (RP-2) per 1000 cells. Each data point represents a mean of four determinations. The error bars are SEM. Values significantly different from control are indicated by "*" ($p<0.05$).

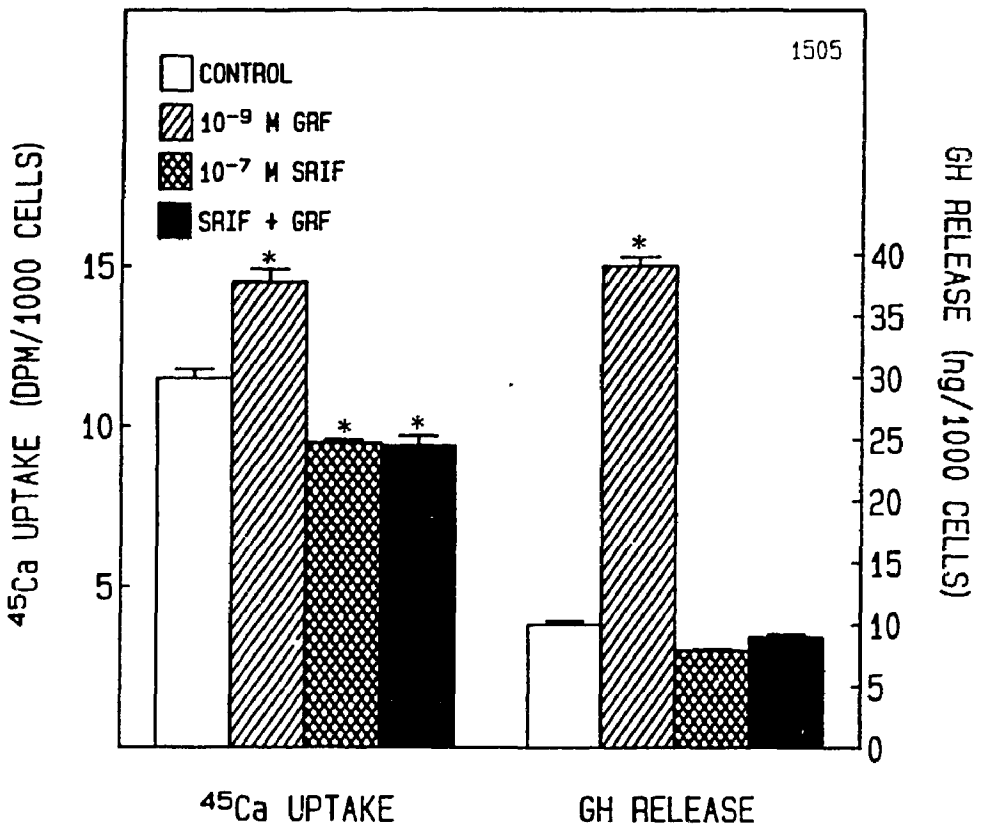

Figure 30. **The effect of 10^{-7} M SRIF and 10^{-9} M rGRF on steady state ^{45}Ca uptake and growth hormone (GH) release by rat somatotrophs after 150 min of ^{45}Ca loading.** SRIF and GRF were added to the incubation medium 20 min and 10 min prior to the addition of [^{45}Ca]-$CaCl_2$ respectively. ^{45}Ca uptake is expressed as corrected ^{45}Ca dpm/1000 cells. GH is expressed as ng of rat GH (RP-2) per 1000 cells. Each data point represents a mean of four determinations. The error bars are SEM. Where bars do not appear, the SEM was too small to plot. Values significantly different from control are indicated by "*" ($p<0.05$).

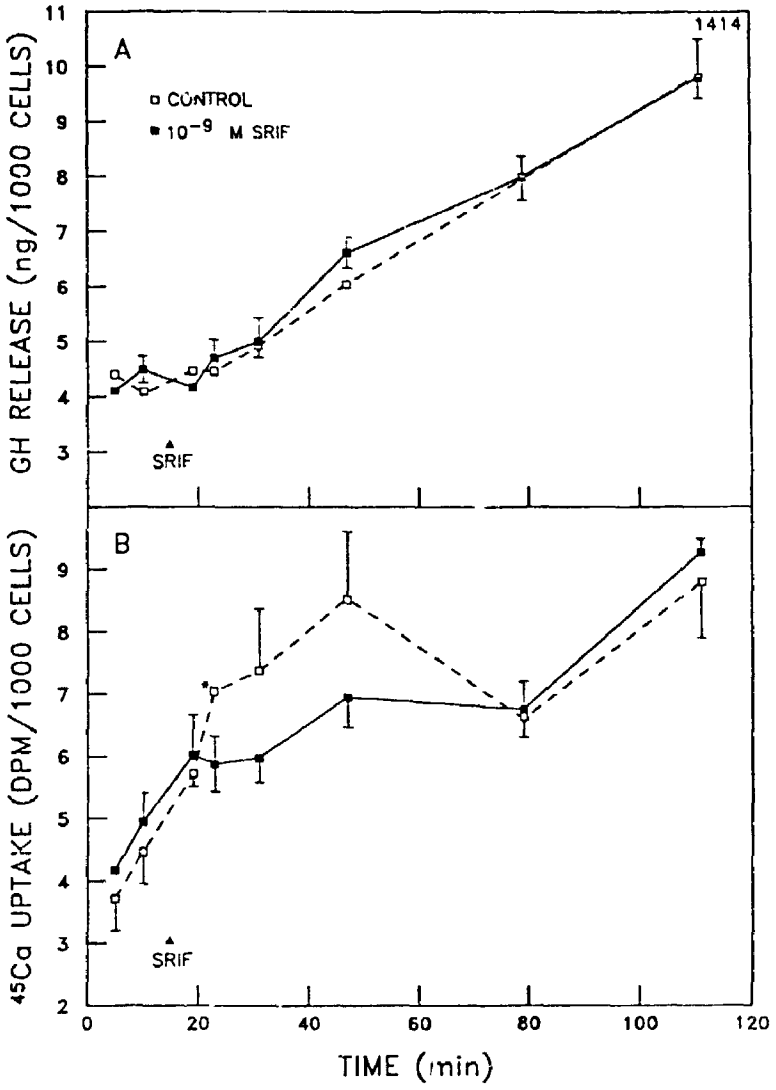

Figure 31. **Time course of the effect of 10^{-9} M SRIF on growth hormone (GH) release and non-steady state ^{45}Ca uptake in rat somatotrophs.** Time 0 min corresponds to the addition of [^{45}Ca]-$CaCl_2$ to the incubation medium. Arrow heads indicate the addition of SRIF to the incubation medium. **A.** GH is expressed as ng of rat GH (RP-2) per 1000 cells. **B.** ^{45}Ca uptake is expressed as corrected ^{45}Ca dpm/1000 cells. Each data point represents a mean of three or four determinations for a single experiment. The error bars are SEM. Where bars do not appear, the SEM was too small to plot. Values significantly different from control are indicated by "*" ($p<0.05$).

the tracer. The SRIF treatment did not significantly decrease GH release (Figure 31, panel A). However, SRIF caused a "break" in the uptake curve. Eight min after addition of SRIF, uptake was significantly lower than control (Figure 31, panel B). The two uptake curves were identical by 64 min after addition. When SRIF was increased to 10^{-7} M, the "break" in the ^{45}Ca uptake was more pronounced (not shown).

4.2.1.5 Non-steady state experiments - Single time point. Single time point experiments were then carried out to clarify the possible inhibition of basal (in the absence of a secretagogue) Ca^{2+} influx by SRIF at the lower concentration. SRIF (10^{-9} M) was added 6 min after the tracer. Cells were sampled for ^{45}Ca content 8 min after SRIF addition. There were no significant differences in either GH release or ^{45}Ca uptake (Figure 32).

4.2.1.6 Non-steady state experiments - Single time point - SRIF and A23187. Single time point experiments were carried out to determine if SRIF could decrease ^{45}Ca uptake in somatotrophs treated with 10^{-6} M A23187 (Figure 33). Cells were loaded with ^{45}Ca for 80 min before adding 10^{-7} M SRIF. Ten min later the cells were challenged with 10^{-6} M A23187 and cells were sampled for ^{45}Ca content 8 min after ionophore addition. SRIF by itself inhibited basal release of GH. A23187 did not stimulate GH release, however, it prevented the SRIF-dependent inhibition of GH release. The lack of effect on A23187 on GH release in static incubation is not unexpected since the ionophore produces a transient increase in GH release (9). If the amount of GH in the incubation medium is high at the time A23187 is added, the subsequent increase in total GH in the medium may be insignificant. Nevertheless A23187 more than doubled ^{45}Ca uptake. SRIF had no effect on A23187-induced ^{45}Ca uptake. However the ^{45}Ca uptake by cells treated with SRIF alone was significantly lower than before SRIF treatment.

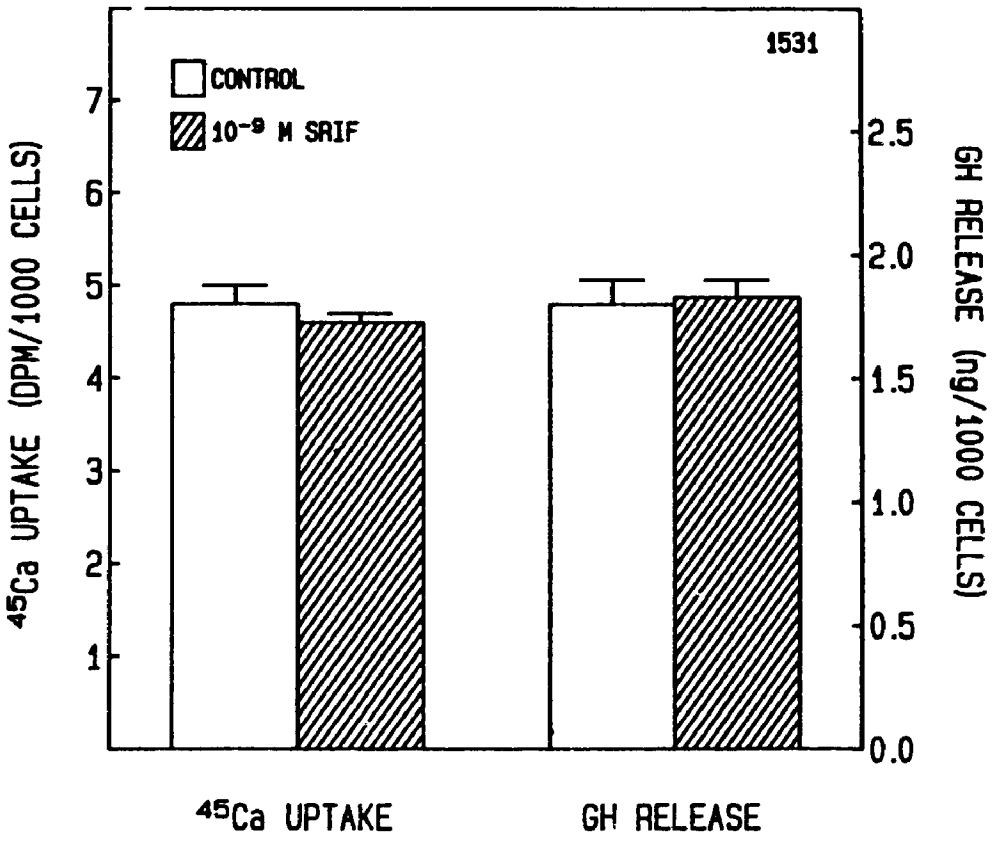

Figure 32. **The effect of 10^{-9} M SRIF on non-steady state ^{45}Ca uptake and growth hormone (GH) release by rat somatotrophs after 8 min of exposure.** SRIF was added to the incubation medium 6 min after the addition of [^{45}Ca]-$CaCl_2$. The single samples were taken 8 min after SRIF addition. ^{45}Ca uptake is expressed as corrected ^{45}Ca dpm/1000 cells. GH is expressed as ng of rat GH (RP-2) per 1000 cells. Each data point represents a mean of four determinations. The error bars are SEM.

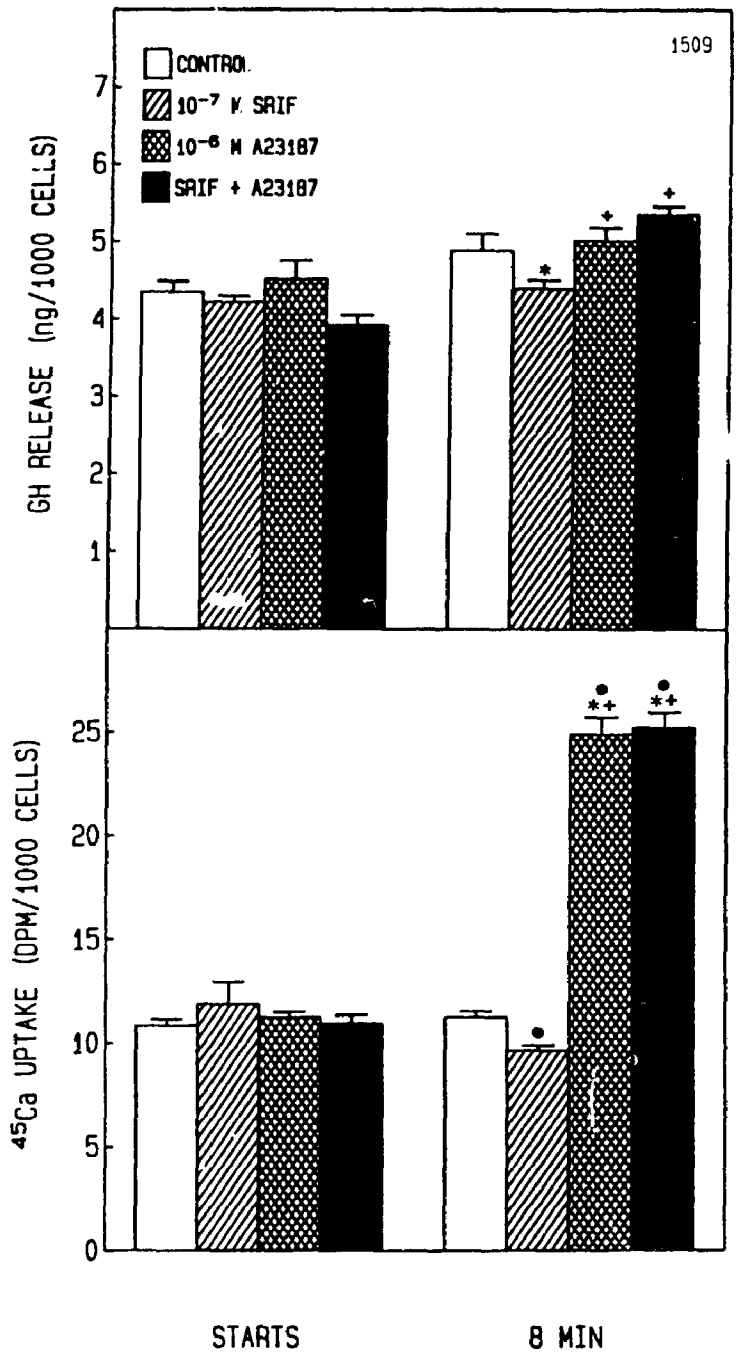

Figure 33. **The effect of 10^{-7} M SRIF and 10^{-6} M A23187 on non-steady state ^{45}Ca uptake and growth hormone (GH) release from rat somatotrophs after 8 min of exposure to A23187.** "STARTS" samples were taken after 72 min of ^{45}Ca loading. SRIF and A23187 were added to the incubation medium after 80 min and 90 min of ^{45}Ca loading respectively. The second sample was taken 8 min after A23187 addition. ^{45}Ca uptake is expressed as corrected ^{45}Ca dpm/1000 cells. GH is expressed as ng of rat GH (RP-2) per 1000 cells. Each data point represents a mean of four determinations. The error bars are SEM. Values significantly different from control are indicated by "*" ($p<0.05$), values significantly different from SRIF are indicated by "+" ($p<0.05$) and ^{45}Ca uptake values significantly different from "STARTS" are indicated by "●" ($p<0.05$).

4.2.2 SRIF and $[Ca^{2+}]_i$.

4.2.2.1 Baseline $[Ca^{2+}]_i$. SRIF decreased $[Ca^{2+}]_i$ in a concentration dependent fashion (Figures 34 and 35) between 10^{-6} M and 10^{-14} M with an EC_{50} of 1.2×10^{-10}, estimated from a four-parameter logistic equation fitted to the data. The drop in $[Ca^{2+}]_i$ was detectable within 5 sec of the addition of SRIF, and its maximal effect, as indicated by a nadir, was apparent in about 45 sec. $[Ca^{2+}]_i$ then tended to drift upwards, but this was not always seen, and never reached the pre-SRIF baseline (Figure 34).

4.2.2.2 SRIF and GRF-Induced Increase in $[Ca^{2+}]_i$. To test whether SRIF could prevent the GRF induced response, somatotrophs were treated for 2 min with SRIF (10^{-10} M, 10^{-9} M and 10^{-8} M), and then GRF (10^{-9} M) was introduced in the continued presence of SRIF (Figure 36). The low concentrations of SRIF (10^{-10} M and 10^{-9} M) decreased baseline $[Ca^{2+}]_i$ by 6 ± 3% and 12 ± 1% (n=3) respectively, and inhibited the peak phase but not the plateau phase of the GRF response. A higher concentration of SRIF, 10^{-8} M, decreased baseline $[Ca^{2+}]_i$ by 16.1 ± 0.4% (n=3), and prevented both the peak and plateau phases of the GRF response. GRF did cause $[Ca^{2+}]_i$ to increase slightly, but the maximum was well below the pre-SRIF baseline level.

To further study the interaction between SRIF and GRF, we tested the effect of SRIF (10^{-10} M, 10^{-9} M and 10^{-8} M) on the GRF response after it had been initiated. Cells were challenged with 10^{-9} M GRF, and the response followed. Two min after the addition of GRF, SRIF was added (Figure 37). GRF, in all cases, produced the typical biphasic response. The low concentration of SRIF (10^{-10} M) had no significant effect on the GRF-induced plateau (Figure 37, panel B). SRIF at 10^{-9} M and 10^{-8} M reduced plateau $[Ca^{2+}]_i$ by 19 ± 2% and 27 ± 4% (n=3) respectively. After reaching a nadir, the $[Ca^{2+}]_i$ slowly increased. With 10^{-9} M SRIF, the $[Ca^{2+}]_i$ tended to return to the plateau level, while with 10^{-8} M, it stabilized at the pre-GRF baseline level.

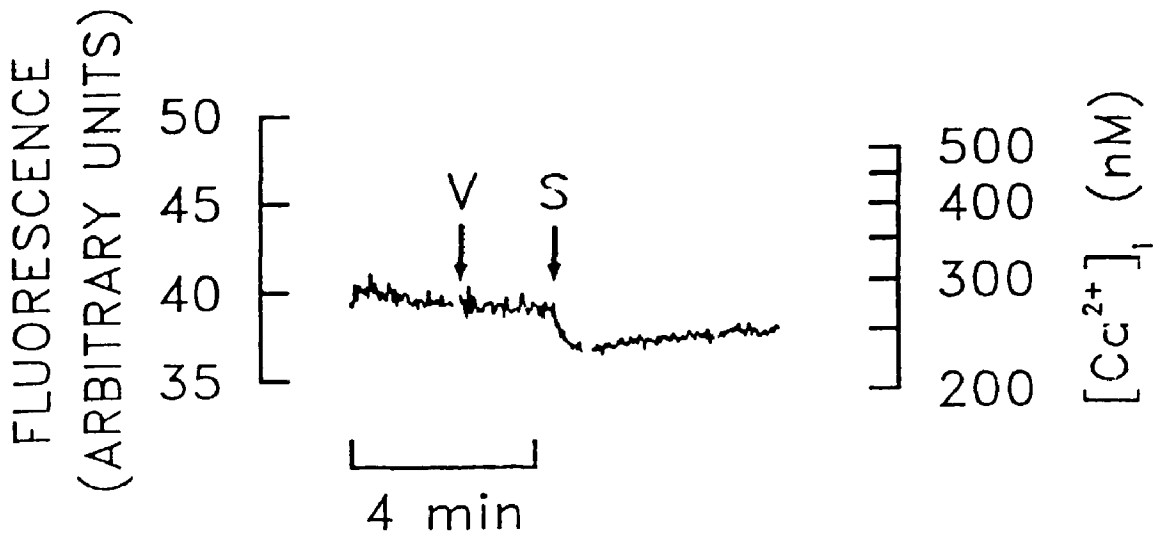

Figure 34. Intracellular Ca^{2+} concentration ($[Ca^{2+}]_i$) response to 10^{-8} M SRIF in rat somatotrophs. $[Ca^{2+}]_i$ was measured in 1.2 mM $CaCl_2$ containing medium at 37 C and pH 7.35-7.4 with the fluorescent dye indo-1 with excitation and emission wavelengths of 329 nm and 405 nm respectively. Arrows indicate additions to the incubation medium. V: vehicle for SRIF; S: 10^{-8} M SRIF.

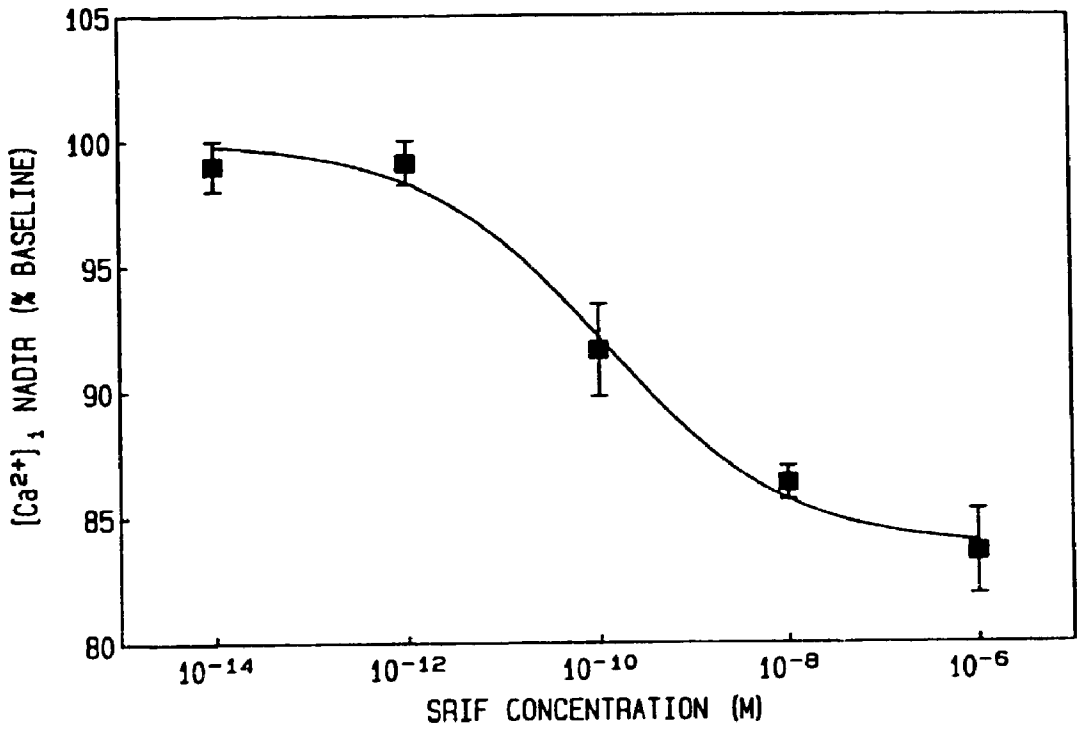

Figure 35. **Concentration response for SRIF-dependent $[Ca^{2+}]_i$ nadir in rat somatotrophs.** $[Ca^{2+}]_i$ was measured in 1.2 mM $CaCl_2$ containing medium at 37 C and pH 7.35-7.4 with the fluorescent dye indo-1 with excitation and emission wavelengths of 329 nm and 405 nm respectively. $[Ca^{2+}]_i$ nadir is expressed as % baseline $[Ca^{2+}]_i$ measured before addition of SRIF. Data points represent a mean of 3 determinations. The error bars are SEM.

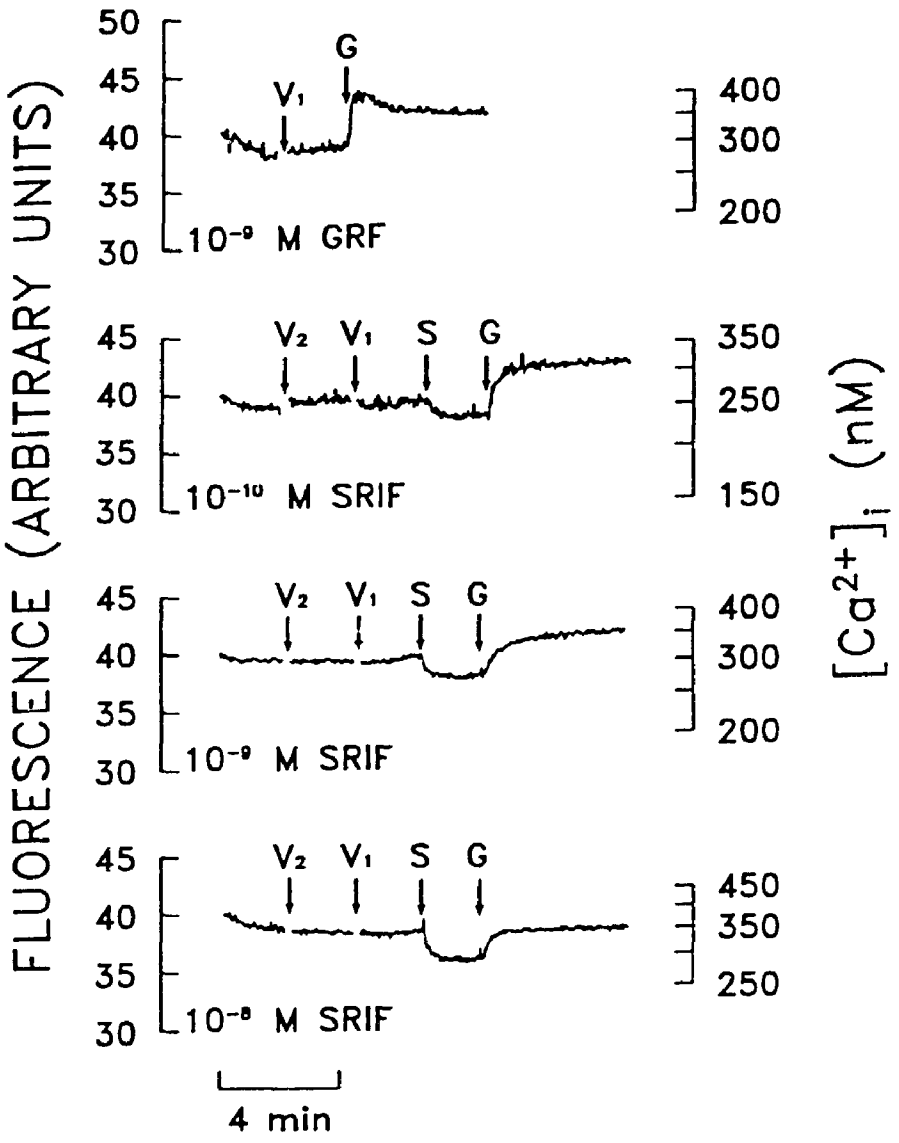

Figure 36. Inhibition of the 10^{-9} M GRF-dependent $[Ca^{2+}]_i$ biphasic response in rat somatotrophs. $[Ca^{2+}]_i$ was measured in 1.2 mM $CaCl_2$ containing medium at 37 C and pH 7.35-7.4 with the fluorescent dye indo-1 with excitation and emission wavelengths of 329 nm and 405 nm respectively. Arrows indicate additions to the incubation medium. V_1: vehicle for GRF; V_2: vehicle for SRIF; G: 10^{-9} M rGRF; S: SRIF.

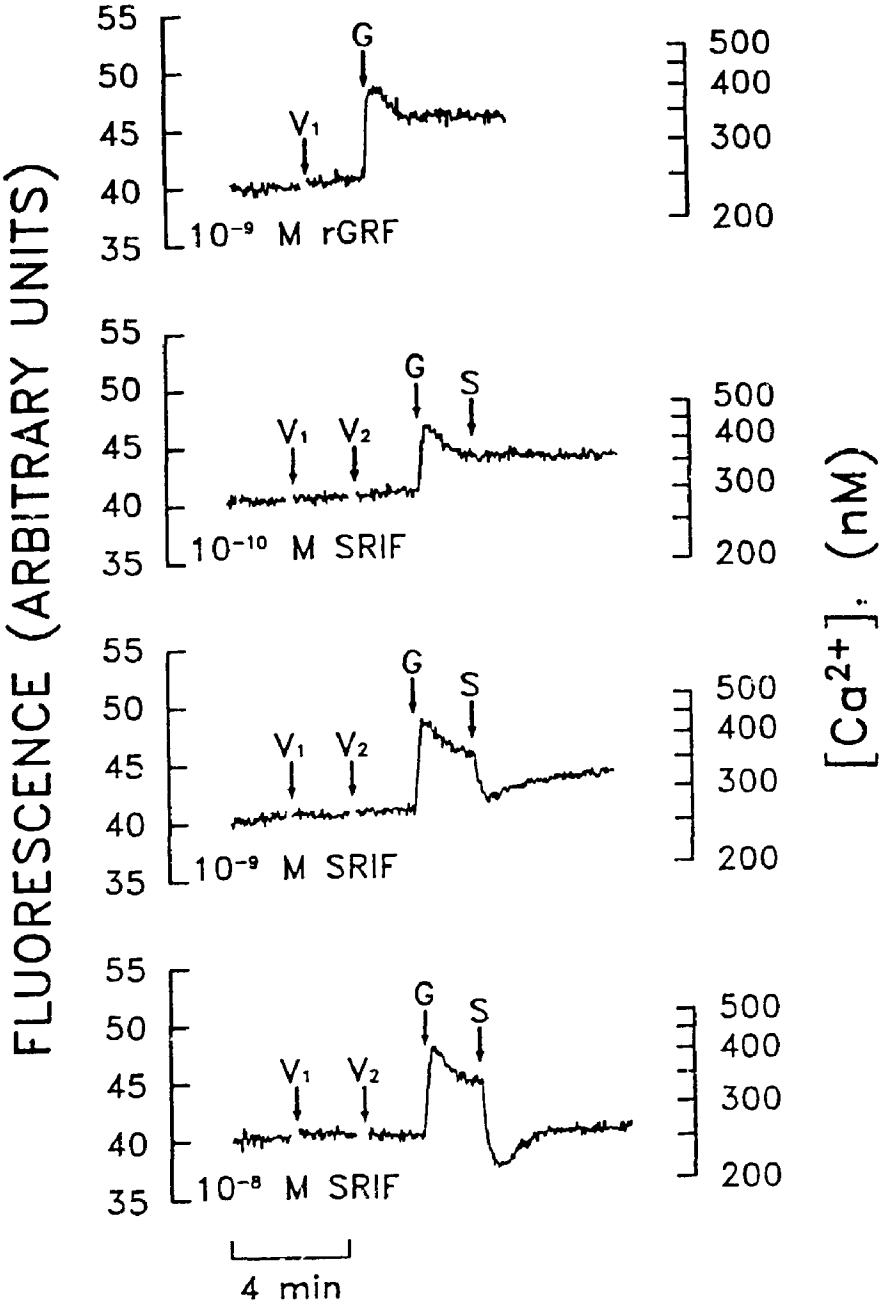

Figure 37. Inhibition of the second phase of the 10^{-9} M GRF-dependent $[Ca^{2+}]_i$ biphasic response in rat somatotrophs. $[Ca^{2+}]_i$ was measured in 1.2 mM $CaCl_2$ containing medium at 37 C and pH 7.35-7.4 with the fluorescent dye indo-1 with excitation and emission wavelengths of 329 nm and 405 nm respectively. Arrows indicate additions to the incubation medium. V_1: vehicle for GRF; V_2: vehicle for SRIF; G: 10^{-9} M rGRF; S: SRIF.

4.3 Ca^{2+} and Intracellular Second Messengers

4.3.1 High K^+ Depolarization.

4.3.1.1 ^{45}Ca Uptake. Non-steady state experiments - Time course. To test whether K^+ depolarization stimulates Ca^{2+} influx, a ^{45}Ca uptake experiment in non-steady state was carried out. Figure 38 shows the effect of increasing extracellular K^+ concentration 5 fold (from 5.8 to 29 mM) on both GH release and ^{45}Ca uptake. High K^+ stimulated the immediate release of GH (Figure 38, panel A). In replicate experiments the K^+ group released more GH than the control group at all time points. High K^+ also stimulated ^{45}Ca uptake (Figure 38, panel B). ^{45}Ca uptake by the K^+ treated group was higher than that for the control group at all time points. Significant increases were detectable, in one experiment, after 1 min, and in a second experiment, at later time points only.

Non-steady state experiments - Single time point. Figure 39 shows the result of a single time point experiment. Somatotrophs were loaded with ^{45}Ca for 80 min before 10^{-7} M SRIF was added to the incubation medium. Ten min later the cells were challenged with 29 mM K^+. A first "Starts" sample was taken 3 min before adding SRIF and a second sample was then taken 8 min after adding SRIF. High K^+ caused a significant increase in GH release (Figure 39). GH release was significantly increased by 20 to 21%. When SRIF was present, the K^+-induced GH release was completely blocked. Increasing the K^+ concentration of the incubation medium to 29 mM, in two experiments, led to a significant 26% and 62% increase in ^{45}Ca uptake. The K^+-induced increase in uptake was not affected by SRIF (Figure 39).

4.3.1.2 Intracellular $[Ca^{2+}]$. The effect of high K^+ on $[Ca^{2+}]_i$ is shown in Figure 40. The extracellular K^+ concentration was rapidly changed from 6 mM to 30 mM (5 fold increase) by adding 4 M KCl to the cuvette. This also increased the osmolality of the medium by 48 mOsM. Therefore an equivalent volume of 4 M N-methyl-d-glucamine chloride (NMG) was used as a

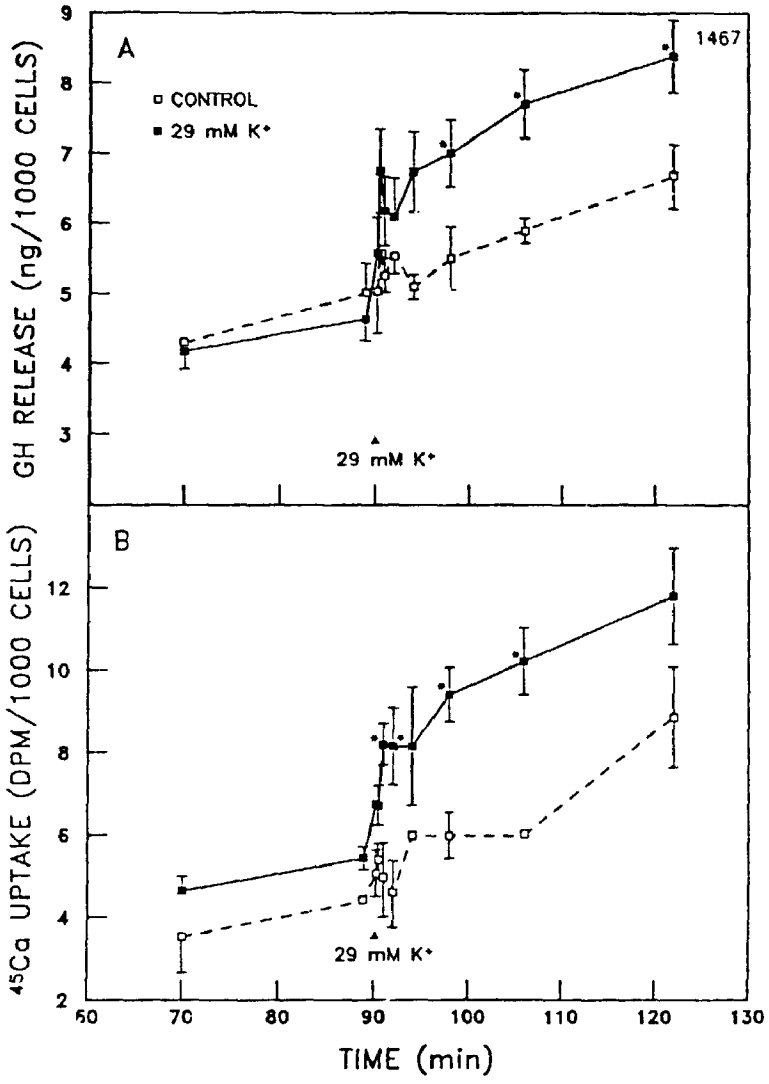

Figure 38. Time course of the effect of 29 mM K^+ on growth hormone (GH) release and non-steady state ^{45}Ca uptake by rat somatotrophs. Time 0 min corresponds to the addition of [^{45}Ca]-$CaCl_2$ to the incubation medium. The arrow head indicates the addition of 29 mM K^+ to the incubation medium. **A.** GH is expressed as ng of rat GH (RP-2) per 1000 cells. **B.** ^{45}Ca uptake is expressed as corrected ^{45}Ca dpm/1000 cells. Each data point represents a mean of three or four determinations. The error bars are SEM. Where bars do not appear, the SEM was too small to plot. Values significantly different from control are indicated by "*" ($p<0.05$).

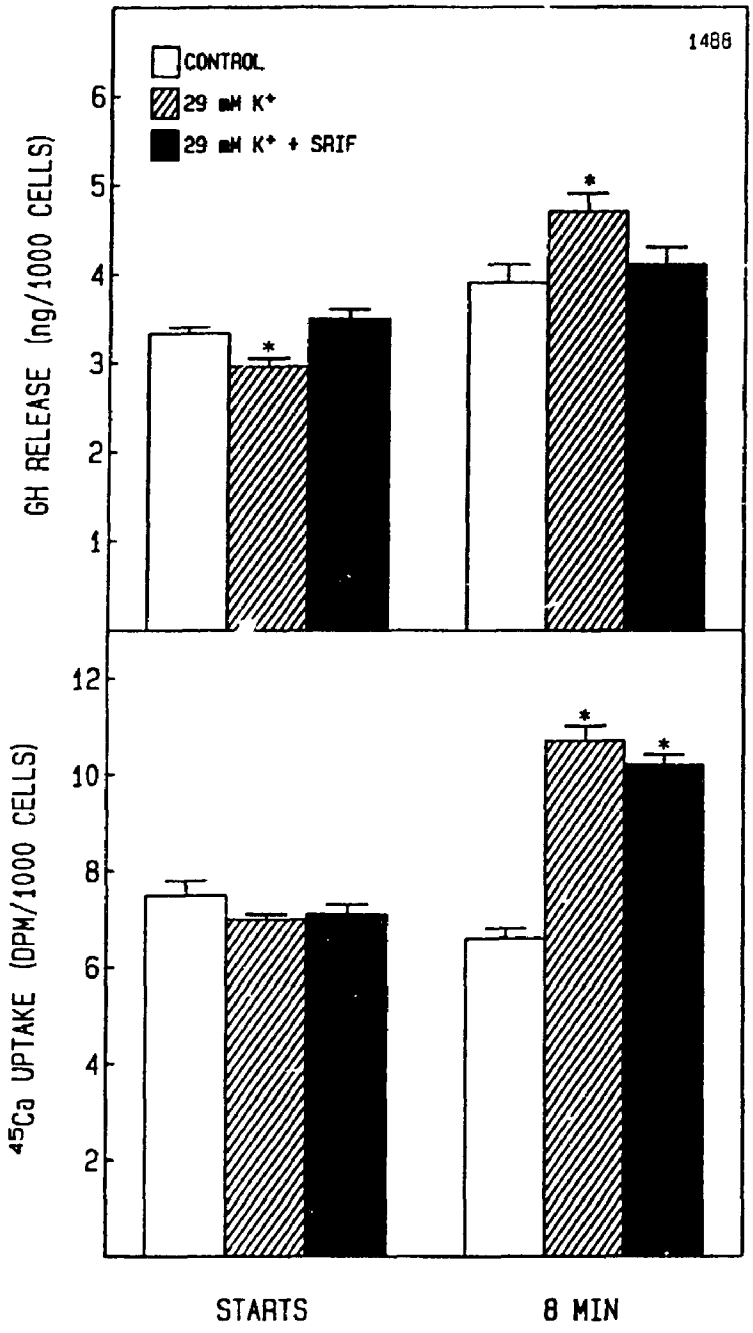

Figure 39. **The effect of 29 mM K^+ and 10^{-7} M SRIF on non-steady state ^{45}Ca uptake and growth hormone (GH) release from rat somatotrophs after 8 min of exposure to 29 mM K^+.** "STARTS" samples were taken after 72 min of ^{45}Ca loading. SRIF and K^+ were added to the incubation medium after 80 min and 90 min of ^{45}Ca loading respectively. The second sample was taken 8 min after K^+ addition. ^{45}Ca uptake is expressed as corrected ^{45}Ca dpm/1000 cells. GH is expressed as ng of rat GH (RP-2) per 1000 cells. Each data point represents a mean of four determinations. The error bars are SEM. Values significantly different from control are indicated by "*" ($p<0.05$).

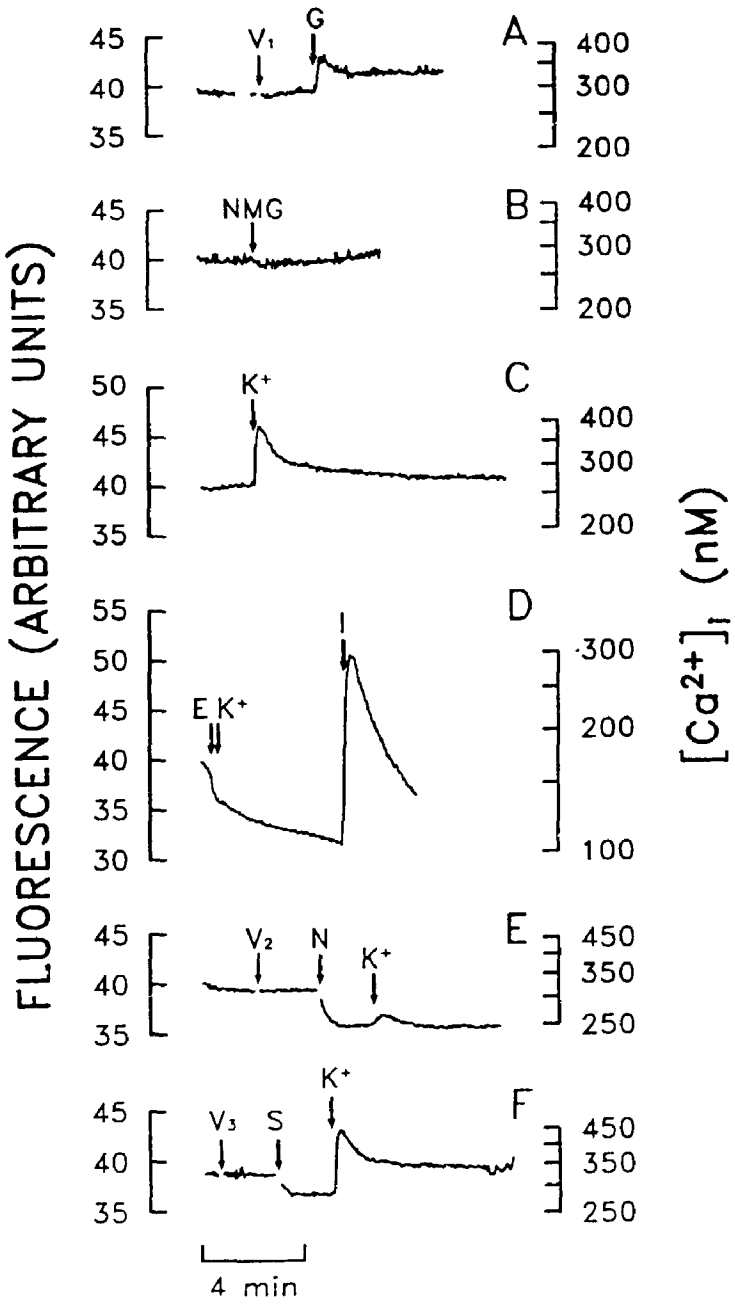

Figure 40. **The effect of Ca^{2+}-free medium, 10^{-6} M nifedipine and 10^{-9} M SRIF on the 30 mM K^+-induced increase in $[Ca^{2+}]_i$ in rat somatotrophs.** $[Ca^{2+}]_i$ was measured in 1.2 mM $CaCl_2$ containing medium at 37 C and pH 7.35-7.4 with the fluorescent dye indo-1 with excitation and emission wavelengths of 329 nm and 405 nm respectively. **A.** 10^{-9} M rGRF control. **B.** 24 mM N-methyl-d-glucamine chloride osmotic control. **C.** 30 mM K^+ control. **D.** The effect of Ca^{2+}-free medium containing 0.5 mM EGTA on the 30 mM K^+-induced increase in $[Ca^{2+}]_i$. **E.** The effect of 10^{-6} M nifedipine on the 30 mM K^+-induced increase in $[Ca^{2+}]_i$. **F.** The effect of 10^{-9} M SRIF on the 30 mM K^+-induced increase in $[Ca^{2+}]_i$. Arrows indicate additions to the incubation medium. V_1: vehicle for GRF; V_2: vehicle for nifedipine; V_3: vehicle for SRIF; G: 10^{-9} M rGRF; NMG: 24 mM N-methyl-d-glucamine chloride; K^+: 30 mM K^+; E: 0.5 mM EGTA; I: 10^{-5} M ionomycin; N: 10^{-6} M nifedipine; S: 10^{-9} M SRIF.

control. The NMG did not alter the $[Ca^{2+}]_i$ (Figure 40, panel B). 30 mM K^+ induced an immediate and transient 40 ± 8% (n=4) increase in $[Ca^{2+}]_i$ reaching a peak at 16 ± 1 sec (n=16) (Figure 40, panel C). The $[Ca^{2+}]_i$ then dropped, initially rapidly then gradually, reaching the baseline level within 10 min. The rise time for the high K^+-induced response was about half that observed with GRF. High K^+ had no detectable effect on $[Ca^{2+}]_i$ when the cells were incubated in Ca^{2+}-free medium containing 0.5 mM EGTA. The presence of organelle bound Ca^{2+} was confirmed by the large transient increase in $[Ca^{2+}]_i$ when 10^{-5} M ionomycin was added to the cell suspension (Figure 40, panel D).

When somatotrophs were incubated with 10^{-6} M nifedipine, baseline $[Ca^{2+}]_i$ decreased by 18 ± 3% (n=4). After 2 min of treatment with nifedipine, K^+ was added. High K^+ caused only a small and transient increase in $[Ca^{2+}]_i$, with a peak value well below the pre-nifedipine baseline (Figure 40, panel E).

SRIF, as expected, decreased baseline $[Ca^{2+}]_i$ by 15 ± 1% (n=4) when applied at a concentration of 10^{-9} M. Adding K^+ 2 min after SRIF, transiently increased $[Ca^{2+}]_i$ to a peak level 31 ± 5% (n=4) greater than the pre-SRIF baseline (Figure 40, panel F). The increase was not significantly different from the 40 ± 8% increase observed with high K^+ in the absence of SRIF. As with high K^+ alone, $[Ca^{2+}]_i$ then decreased, first rapidly, then gradually to the pre-SRIF baseline. Increasing the concentration of SRIF to 10^{-7} did not inhibit the response to 30 mM K^+ (not shown).

4.3.2 Cyclic AMP.

4.3.2.1 $(Bu)_2$cAMP and ^{45}Ca uptake. Non-steady state experiments - time course. The effect of $(Bu)_2$cAMP on ^{45}Ca uptake and GH release in non-steady state was investigated (Figure 41). Cells were loaded with ^{45}Ca for 90 min before being challenged with 5 mM $(Bu)_2$cAMP. $(Bu)_2$cAMP consistently elevated GH release (Figure 41, panel A). In two experiments, GH

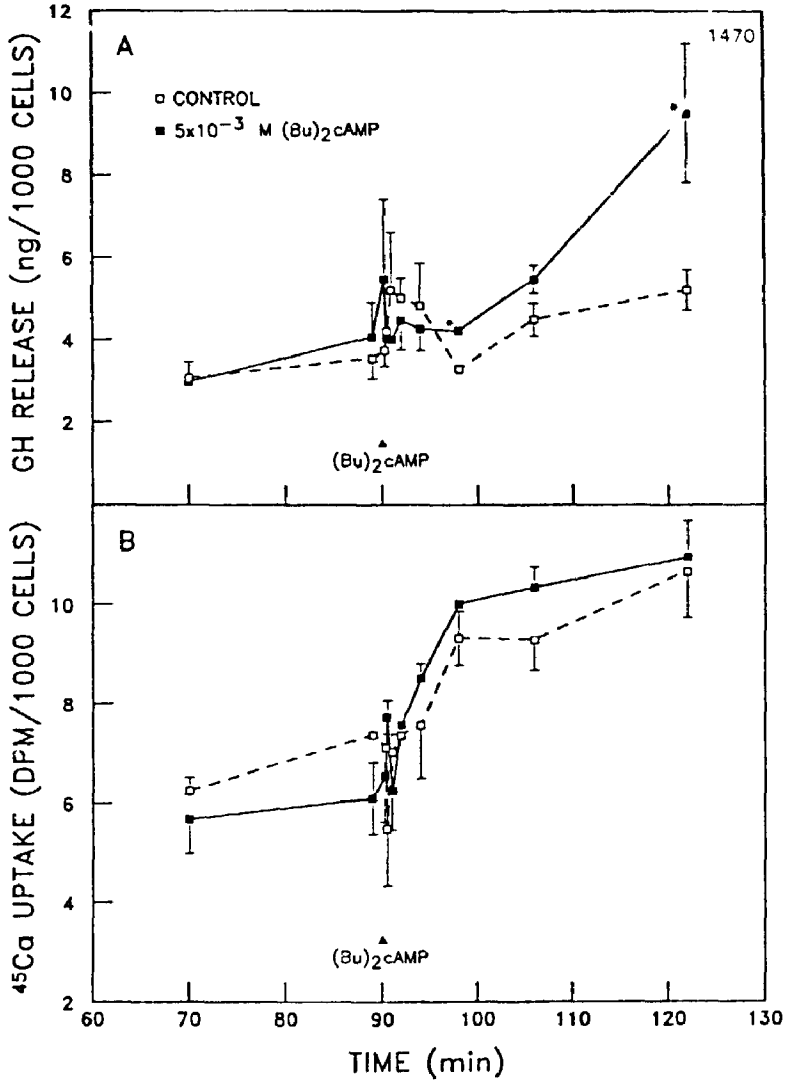

Figure 41. Time course of the effect of $5x10^{-3}$ M $(Bu)_2$cAMP on growth hormone (GH) release and non-steady state ^{45}Ca uptake by rat somatotrophs. Time 0 min corresponds to the addition of [^{45}Ca]-$CaCl_2$ to the incubation medium. The arrow head indicates the addition of $(Bu)_2$cAMP to the incubation medium. **A.** GH is expressed as ng of rat GH (RP-2) per 1000 cells. **B.** ^{45}Ca uptake is expressed as corrected ^{45}Ca dpm/1000 cells. Each data point represents a mean of three or four determinations for a single experiment. The error bars are SEM. Where bars do not appear, the SEM was too small to plot. Values significantly different from control are indicated by "*" ($p<0.05$).

release was significantly increased by 32%, 27% and 73% after 2 min, 8 min and 32 min respectively. $(Bu)_2$cAMP had no consistent or significant effect on ^{45}Ca uptake at any time point (Figure 41, panel B).

Non-steady state experiment - single time point. In an attempt to decrease sample variability, a single time point experiment was carried out to study the effects of $(Bu)_2$cAMP and SRIF on ^{45}Ca uptake (Figure 42). Somatotrophs were loaded with ^{45}Ca for 80 min before 10^{-7} M SRIF was added to the incubation medium. Ten min later the cells were challenge with 5 mM $(Bu)_2$cAMP. "Starts" samples were taken 3 min before SRIF addition. A second sample was taken after 8 min of $(Bu)_2$cAMP exposure. SRIF did not alter basal GH release. $(Bu)_2$cAMP significantly increased GH release by 15%, and SRIF blocked this increase (Figure 42). SRIF decreased ^{45}Ca uptake consistently but not significantly. $(Bu)_2$cAMP had no effect on ^{45}Ca uptake, and did not prevent the consistent SRIF-dependent decrease in uptake (Figure 42).

4.3.2.2 cpt-cAMP and $[Ca^{2+}]_i$. To ascertain whether cAMP alters $[Ca^{2+}]_i$, we tested the effect of the non-fluorescent cAMP analogue cpt-cAMP and PGE_2 on $[Ca^{2+}]_i$. Cpt-cAMP is water soluble and membrane permeable and, as $(Bu)_2$cAMP, it stimulates GH release from rat somatotrophs in a concentration dependent manner (Table I).

The cpt-cAMP was added in a volume of 50 µl. Addition of this volume resulted in an instantaneous decrease in fluorescence due to a dilution effect. It is for this reason that the $[Ca^{2+}]_i$ scales in Figure 43 are not shown. Appropriate dilution correction factors, however, were applied to fluorescence measurements when calculating $[Ca^{2+}]_i$ in Table II.

Incubation of somatotrophs with 10^{-4} M cpt-cAMP caused $[Ca^{2+}]_i$ to increase (Figure 43, panel B). The response consisted of a slow rise to a plateau 20 ± 4% (n=4) greater than baseline (Table II). The increase in $[Ca^{2+}]_i$ was detectable within 5 sec after the addition, and

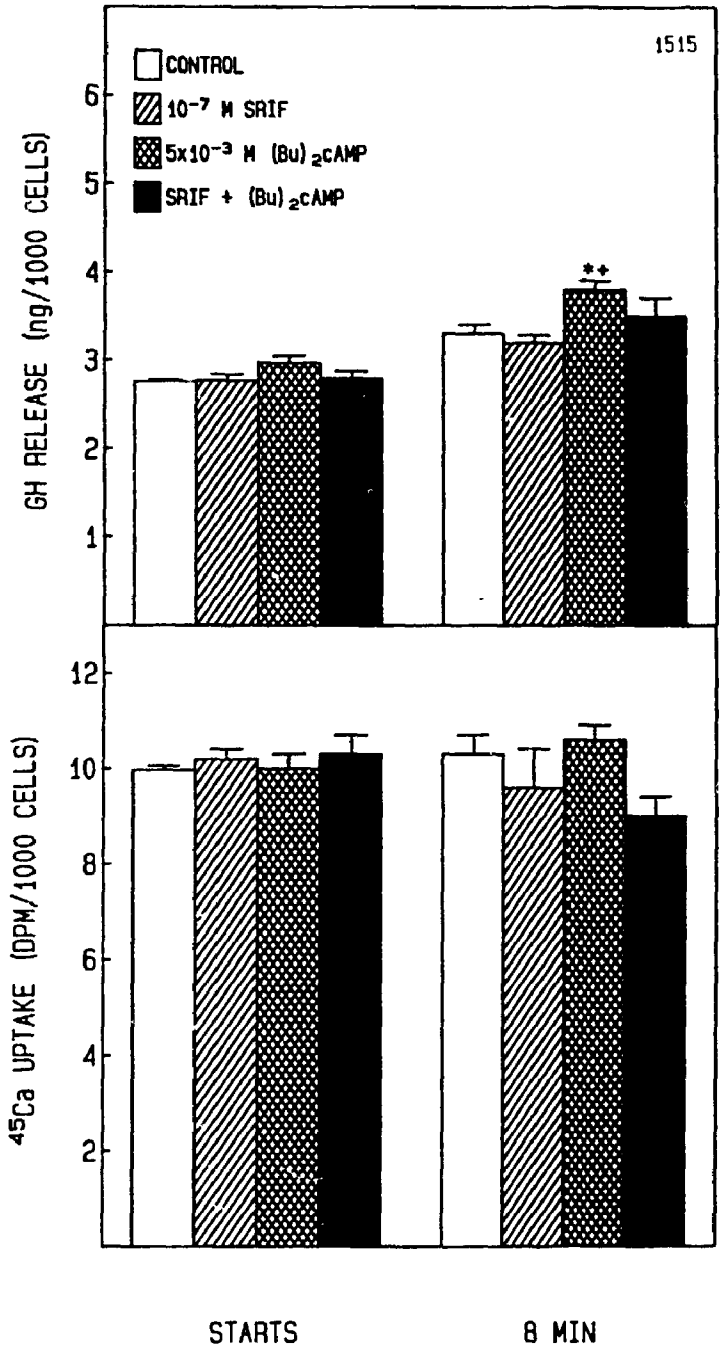

Figure 42. **The effect of $5x10^{-3}$ M $(Bu)_2$cAMP and 10^{-7} M SRIF on non-steady state ^{45}Ca uptake and growth hormone (GH) release from rat somatotrophs after 8 min of exposure to $(Bu)_2$cAMP.** "STARTS" samples were taken after 72 min of ^{45}Ca loading. SRIF and $(Bu)_2$cAMP were added to the incubation medium after 80 min and 90 min of ^{45}Ca loading respectively. The second sample was taken 8 min after $(Bu)_2$cAMP addition. ^{45}Ca uptake is expressed as corrected ^{45}Ca dpm/1000 cells. GH is expressed as ng of rat GH (RP-2) per 1000 cells. Each data point represents a mean of four determinations. The error bars are SEM. Values significantly different from control are indicated by "*" ($p<0.05$).

TABLE I. $(Bu)_2$cAMP- and cpt-cAMP-stimulated GH release (ng/1000 cells) from purified somatotrophs in static incubation.

	4 min		12 min		32 min	
Control	1.64 ± .05[§]		1.77 ± .08		1.82 ± .05	
Concent.	$(Bu)_2$cAMP	cpt-cAMP	$(Bu)_2$cAMP	cpt-cAMP	$(Bu)_2$cAMP	cpt-cAMP
10^{-5} M		1.68 ± .05		1.61 ± .06		1.93 ± .02
10^{-4} M	1.69 ± .01	1.89 ± .11[*]	1.76 ± .07	2.38 ± .07[@]	2.45 ± .12[*]	3.39 ± .07[@]
10^{-3} M	1.82 ± .06	2.23 ± .03[@]	2.20 ± .06[*]	3.29 ± .05[@]	4.07 ± .10[*]	5.21 ± .04[@]

[§] Data expressed as mean ± SEM of 4 observations.
[*] $p < 0.05$ vs Control.
[@] $p < 0.05$ vs Control and $p < 0.05$ $(Bu)_2$cAMP vs cpt-cAMP for each concentration.

TABLE II. Calculated $[Ca^{2+}]_i$ (nM) for cpt-cAMP experiments.

	10^{-9} M rGRF	10^{-4} M cpt-cAMP			
		Control	Ca^{2+}-Free	Nifedipine (10^{-6} M)	SRIF (10^{-9} M)
Baseline	244 ± 10[§]	229 ± 7	134 ± 9	245 ± 6	226 ± 5
EGTA-1[a]			128 ± 8		
EGTA-2[b]			117 ± 10		
Nadir				214 ± 7	209 ± 4
Plateau-1[c]				216 ± 7	211 ± 3
Peak	323 ± 10		300 ± 43[*]		
Plateau-2[d]	289 ± 9	279 ± 11	150 ± 19[*]	240 ± 7	235 ± 9
n	7	8	3	4	4

[§] Data expressed as mean ± SEM of 4 observations.
[*] Response to 10^{-6} M ionomycin.
[a] $[Ca^{2+}]_i$ 5 sec after adding 0.5 mM EGTA.
[b] $[Ca^{2+}]_i$ at the time of cpt-cAMP addition.
[c] $[Ca^{2+}]_i$ in the presence of either nifedipine or SRIF at the time of cpt-cAMP addition.
[d] $[Ca^{2+}]_i$ at the end of the observation period.

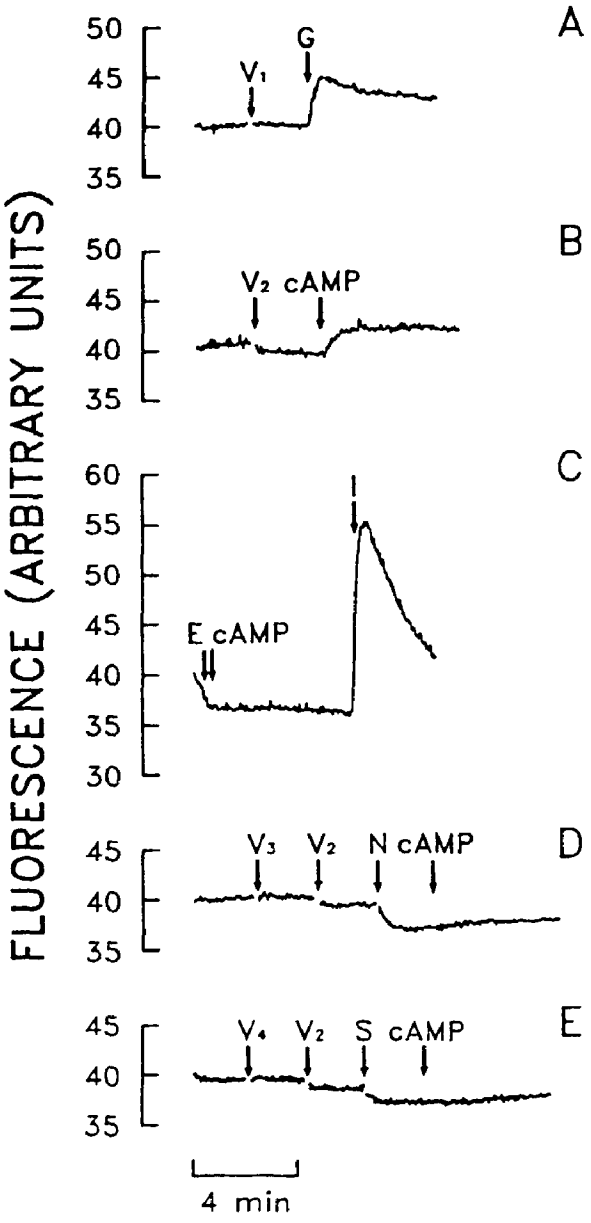

Figure 43. **The effect of Ca^{2+}-free medium, 10^{-6} M nifedipine and 10^{-9} M SRIF on the cpt-cAMP-induced increase in $[Ca^{2+}]_i$ in rat somatotrophs.** $[Ca^{2+}]_i$ was measured in 1.2 mM $CaCl_2$ containing medium at 37 C and pH 7.35-7.4 with the fluorescent dye indo-1 with excitation and emission wavelengths of 329 nm and 405 nm respectively. **A.** 10^{-9} M rGRF control. **B.** 10^{-4} M cpt-cAMP control. **C.** The effect of Ca^{2+}-free medium containing 0.5 mM EGTA on the 10^{-4} M cpt-cAMP-induced increase in $[Ca^{2+}]_i$. **D.** The effect of 10^{-6} M nifedipine on the 10^{-4} M cpt-cAMP-induced increase in $[Ca^{2+}]_i$. **E.** The effect of 10^{-9} M SRIF on the 10^{-4} M cpt-cAMP-induced increase in $[Ca^{2+}]_i$. Arrows indicate additions to the incubation medium. V_1: vehicle for GRF; V_2: vehicle for cpt-cAMP; V_3: vehicle for nifedipine; V_4: vehicle for SRIF; G: 10^{-9} M rGRF; cAMP: 10^{-4} M cpt-cAMP; E: 0.5 mM EGTA; I: 10^{-5} M ionomycin; N: 10^{-6} M nifedipine; S: 10^{-9} M SRIF.

the maximum concentration was seen 135 ± 11 sec (n=9) later. Once the maximum was reached, $[Ca^{2+}]_i$ remained constant at this elevated level until the end of the 5 min observation period.

The response to cpt-cAMP was abolished when cells were incubated in Ca^{2+} free medium containing 0.5 mM EGTA (Figure 43, panel C). Organelle Ca^{2+} stores were not depleted as indicated by the large transient increase in $[Ca^{2+}]_i$ caused by 10^{-5} M ionomycin.

Nifedipine (10^{-6} M) decreased baseline $[Ca^{2+}]_i$ by 12 ± 1% (n=4) (Table II), and reduced, but did not totally abolish, the response to cpt-cAMP (Figure 43, panel D). $[Ca^{2+}]_i$ remained below the pre-nifedipine baseline (Table II).

SRIF (10^{-9} M) lowered baseline $[Ca^{2+}]_i$ by 7 ± 1% (n=4) and inhibited, but did not totally abolish, the response to cpt-cAMP (Figure 43, panel E). The maximal $[Ca^{2+}]_i$ after 5 min was always less than the maximum observed with cpt-cAMP alone, but higher than pre-SRIF baseline.

4.3.2.3 PGE_2 and $[Ca^{2+}]_i$. PGE_2 (10^{-6} M) caused $[Ca^{2+}]_i$ to increase by 21 ± 4% (n=4) (Figure 44, panel B). The response was biphasic. The first phase consisted of a rapid increase in $[Ca^{2+}]_i$ peaking 28 ± 2 sec (n=9) after addition. The second phase consisted of a $[Ca^{2+}]_i$ plateau at a level lower than the peak value, but higher than the pre-PGE_2 baseline. The vehicle for PGE_2 had no effect.

Removing Ca^{2+} from the incubation medium and adding 0.5 mM EGTA abolished the PGE_2 induced increase in $[Ca^{2+}]_i$ (Figure 44, panel C). Intracellular Ca^{2+} stores were not depleted as shown by the large $[Ca^{2+}]_i$ response to 10^{-5} M ionomycin.

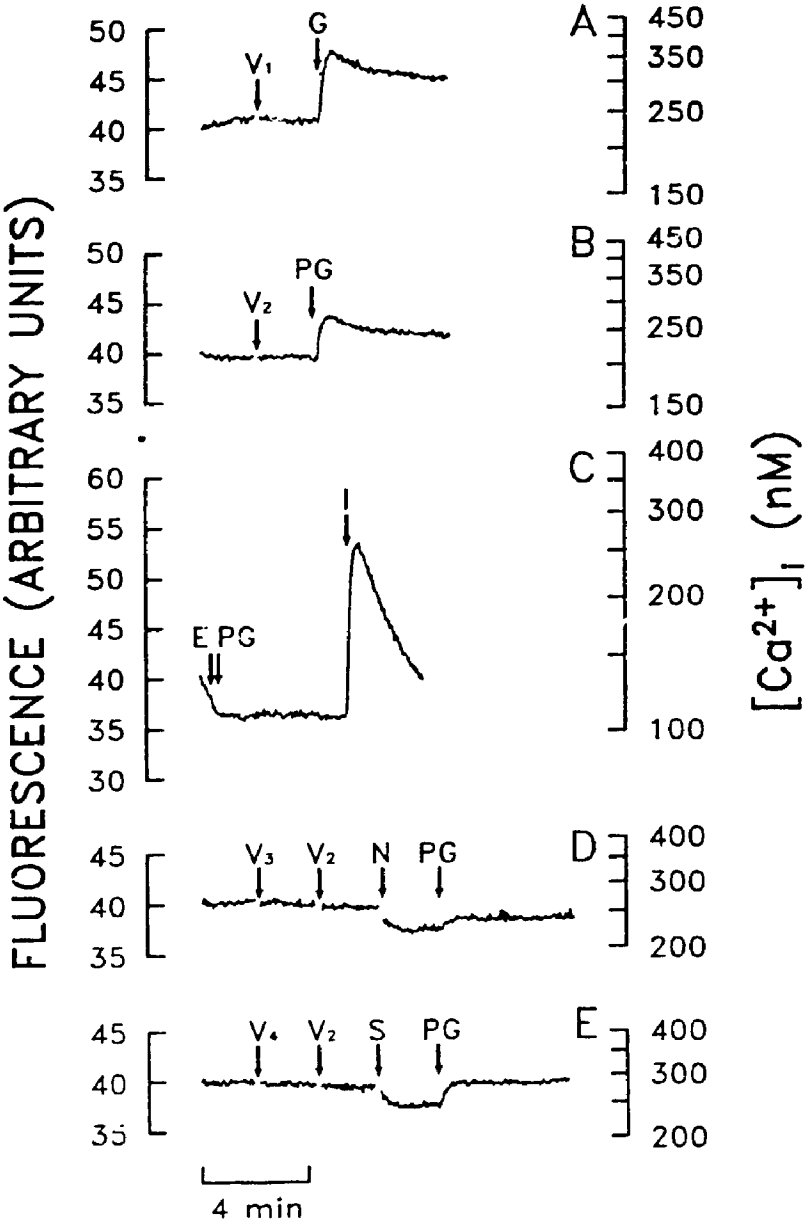

Figure 44. **The effect of Ca^{2+}-free medium, 10^{-6} M nifedipine and 10^{-9} M SRIF on the PGE_2-induced increase in $[Ca^{2+}]_i$ in rat somatotrophs.** $[Ca^{2+}]_i$ was measured in 1.2 mM $CaCl_2$ containing medium at 37 C and pH 7.35-7.4 with the fluorescent dye indo-1 with excitation and emission wavelengths of 329 nm and 405 nm respectively. **A.** 10^{-9} M rGRF control. **B.** 10^{-6} M PGE_2 control. **C.** The effect of Ca^{2+}-free medium containing 0.5 mM EGTA on the 10^{-6} M PGE_2-induced increase in $[Ca^{2+}]_i$. **D.** The effect of 10^{-6} M nifedipine on the 10^{-6} M PGE_2-induced increase in $[Ca^{2+}]_i$. **E.** The effect of 10^{-9} M SRIF on the 10^{-6} M PGE_2-induced increase in $[Ca^{2+}]_i$. Arrows indicate additions to the incubation medium. V_1: vehicle for GRF; V_2: vehicle for PGE_2; V_3: vehicle for nifedipine; V_4: vehicle for SRIF; G: 10^{-9} M rGRF; PG: 10^{-6} M PGE_2; E: 0.5 mM EGTA; I: 10^{-5} M ionomycin; N: 10^{-6} M nifedipine; S: 10^{-9} M SRIF.

Nifedipine (10^{-6} M) decreased baseline $[Ca^{2+}]_i$ by 18 ± 2% (n=4). The response to PGE_2 was significantly inhibited, but not totally abolished; $[Ca^{2+}]_i$ remained far below the pre-nifedipine baseline (Figure 44, panel D).

SRIF (10^{-9} M) lowered baseline $[Ca^{2+}]_i$ by 11 ± 3% (n=4) and inhibited, but did not abolish the response to PGE_2 (Figure 44, panel E). The maximal $[Ca^{2+}]_i$ remained lower than the pre-SRIF baseline.

4.3.3 Protein Kinase C.

4.3.3.1 PMA and $[Ca^{2+}]_i$. PMA (10^{-8} M) caused a transient 24 ± 4% (n=6) increase in $[Ca^{2+}]_i$ (Figure 45, panel B). The increase was detectable within 5 sec and peaked 54 ± 5 sec (n=9) later. $[Ca^{2+}]_i$ then quickly dropped to or below the baseline concentration, 217 ± 23 sec (n=8) after the addition. The vehicle for PMA had no effect.

Removing Ca^{2+} from the incubation medium and adding 0.5 mM EGTA abolished the PMA-induced increase in $[Ca^{2+}]_i$ (Figure 45, panel C). Intracellular Ca^{2+} stores were not depleted, as shown by the large $[Ca^{2+}]_i$ response to 10^{-5} M ionomycin.

Nifedipine (10^{-6} M) decreased baseline $[Ca^{2+}]_i$ by 20 ± 2% (n=5). The response to PMA was markedly inhibited, but not totally abolished; $[Ca^{2+}]_i$ remained far below the pre-nifedipine baseline (Figure 45, panel D).

SRIF (10^{-9} M) lowered baseline $[Ca^{2+}]_i$ by 10 ± 3% (n=6) and reduced but did not totally abolish the response to PMA. Increasing SRIF to 10^{-7} M further reduced the response to PMA, and $[Ca^{2+}]_i$ remained lower than the pre-SRIF baseline (Figure 45, panel E).

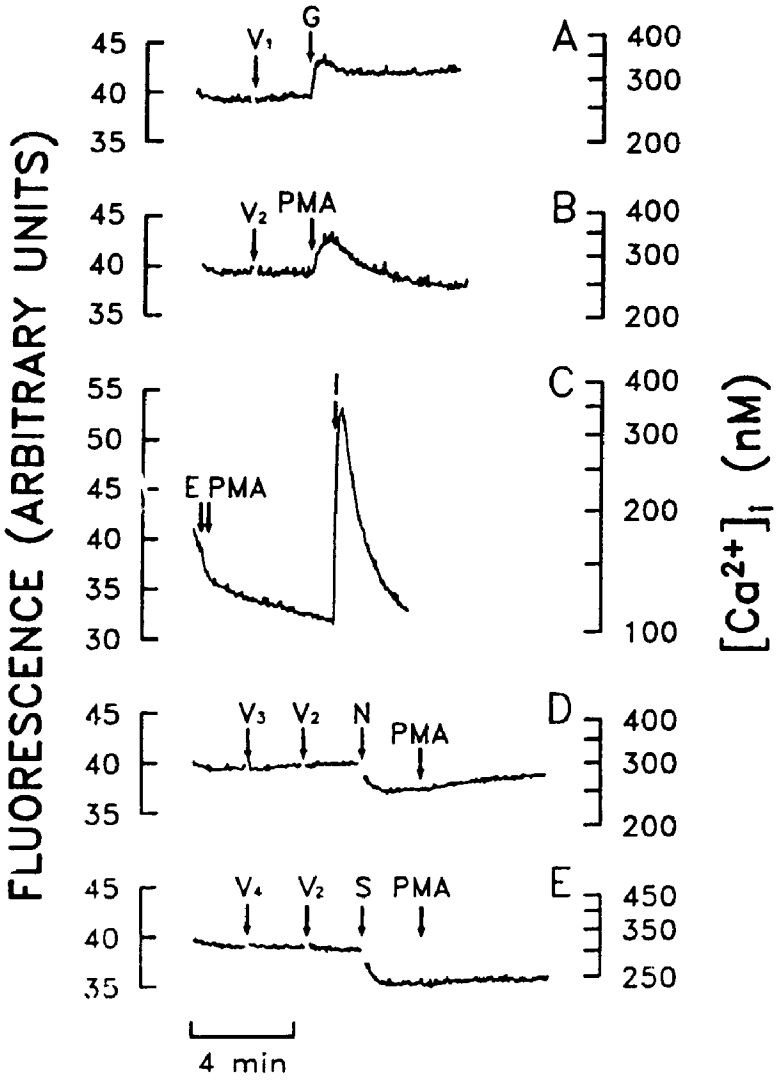

Figure 45. **The effect of Ca^{2+}-free medium, 10^{-6} M nifedipine and 10^{-7} M SRIF on the PMA-induced increase in $[Ca^{2+}]_i$ in rat somatotrophs.** $[Ca^{2+}]_i$ was measured in 1.2 mM $CaCl_2$ containing medium at 37 C and pH 7.35-7.4 with the fluorescent dye indo-1 with excitation and emission wavelengths of 329 nm and 405 nm respectively. **A.** 10^{-9} M rGRF control. **B.** 10^{-8} M PMA control. **C.** The effect of Ca^{2+}-free medium containing 0.5 mM EGTA on the 10^{-8} M PMA-induced increase in $[Ca^{2+}]_i$. **D.** The effect of 10^{-6} M nifedipine on the 10^{-8} M PMA-induced increase in $[Ca^{2+}]_i$. **E.** The effect of 10^{-7} M SRIF on the 10^{-8} M PMA-induced increase in $[Ca^{2+}]_i$. Arrows indicate additions to the incubation medium. V_1: vehicle for GRF; V_2: vehicle for PMA; V_3: vehicle for nifedipine; V_4: vehicle for SRIF; G: 10^{-9} M rGRF; PMA: 10^{-8} M PMA; E: 0.5 mM EGTA; I: 10^{-5} M ionomycin; N: 10^{-6} M nifedipine; S: 10^{-7} M SRIF.

4.3.3.2 diC_8 and $[Ca^{2+}]_i$. The addition of diC_8 ($3x10^{-5}$ M) caused a transient 33 ± 6% (n=3) increase in $[Ca^{2+}]_i$ (Figure 46, panel B). The increase was detectable within 5 sec and peaked 27 ± 4 sec (n=7) later. The $[Ca^{2+}]_i$ then quickly dropped reaching the baseline concentration 73 ± 13 sec (n=7) after the addition, and dropping further below baseline The vehicle for diC_8 had no effect.

Removing Ca^{2+} from the incubation medium and adding 0.5 mM EGTA abolished the diC_8-induced increase in $[Ca^{2+}]_i$ (Figure 46, panel C). Intracellular stores were not depleted, as shown by the large $[Ca^{2+}]_i$ response to ionomycin (10^{-5} M).

Nifedipine (10^{-6} M) decreased baseline $[Ca^{2+}]_i$ by 22 ± 4% (n=3). The response to diC_8 was markedly inhibited, but not abolished; $[Ca^{2+}]_i$ remained far below the pre-nifedipine baseline (Figure 46, panel D).

SRIF (10^{-9} M) lowered baseline $[Ca^{2+}]_i$ by 19 ± 2% (n=3) and reduced, but did not abolish, the response to diC_8 (Figure 46, panel E). $[Ca^{2+}]_i$ remained lower than the pre-SRIF baseline.

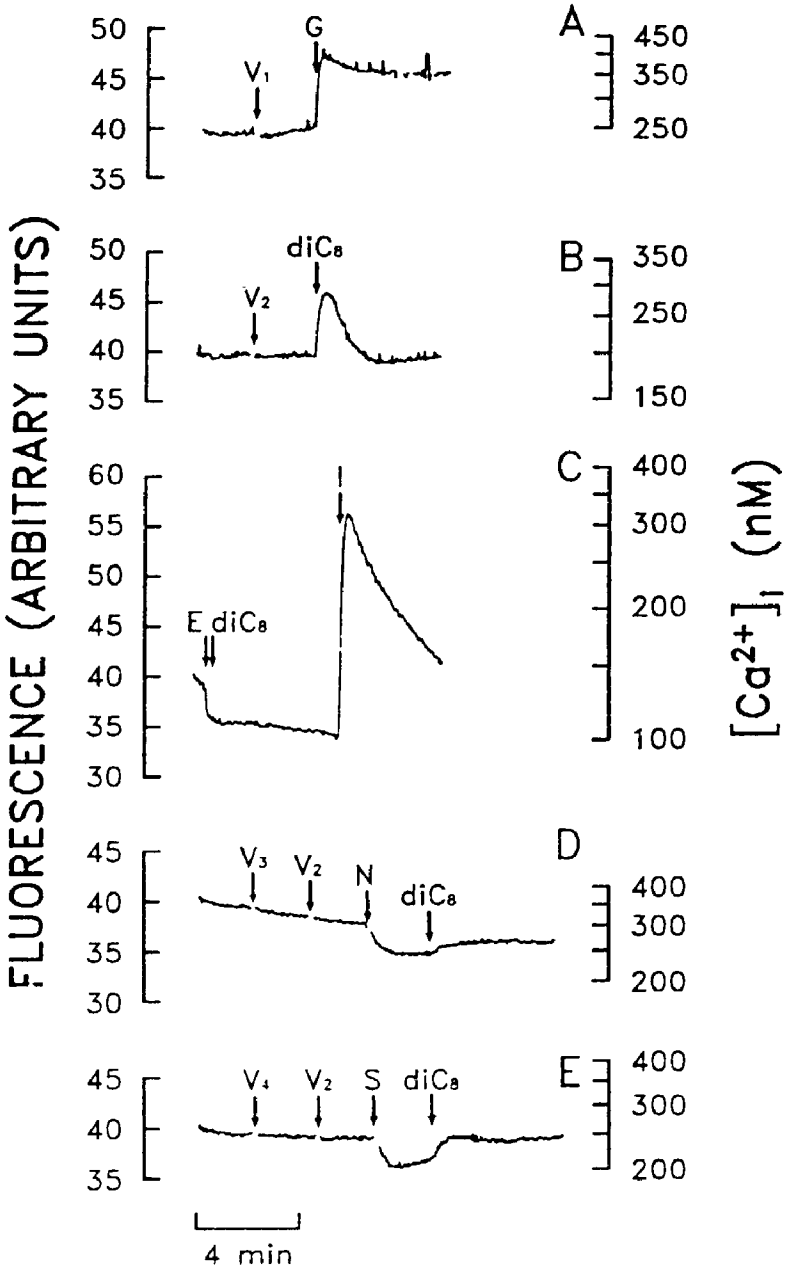

Figure 46. **The effect of Ca^{2+}-free medium, 10^{-6} M nifedipine and 10^{-9} M SRIF on the diC_8-induced increase in $[Ca^{2+}]_i$ in rat somatotrophs.** $[Ca^{2+}]_i$ was measured in 1.2 mM $CaCl_2$ containing medium at 37 C and pH 7.35-7.4 with the fluorescent dye indo-1 with excitation and emission wavelengths of 329 nm and 405 nm respectively. **A.** 10^{-9} M rGRF control. **B.** $3x10^{-5}$ M diC_8 control. **C.** The effect of Ca^{2+}-free medium containing 0.5 mM EGTA on the $3x10^{-5}$ M diC_8-induced increase in $[Ca^{2+}]_i$. **D.** The effect of 10^{-6} M nifedipine on the $3x10^{-5}$ M diC_8-induced increase in $[Ca^{2+}]_i$. **E.** The effect of 10^{-9} M SRIF on the $3x10^{-5}$ M diC_8-induced increase in $[Ca^{2+}]_i$. Arrows indicate additions to the incubation medium. V_1: vehicle for GRF; V_2: vehicle for diC_8; V_3: vehicle for nifedipine; V_4: vehicle for SRIF; G: 10^{-9} M rGRF; diC_8: $3x10^{-5}$ M diC_8; E: 0.5 mM EGTA; I: 10^{-5} M ionomycin; N: 10^{-6} M nifedipine; S: 10^{-9} M SRIF.

CHAPTER 5

Ca^{2+} IS A SECOND MESSENGER FOR GRF

5.1 Three Criteria for Ca^{2+} as a Second Messenger.

The calcium ion (Ca^{2+}) has an essential role in the model for stimulus-secretion coupling as proposed by Douglas (183). According to this model an increase in the free intracellular Ca^{2+} concentration ($[Ca^{2+}]_i$) is required for secretion to occur. A neurotransmitter or hormone stimulates secretion by increasing $[Ca^{2+}]_i$ in some way. Since the increase in $[Ca^{2+}]_i$ acts as a messenger between the hormone-receptor interaction and the exocytotic process, one refers to Ca^{2+} as an intracellular second messenger for the neurotransmitter or hormone.

Adenosine 3',5'-monophosphate (cyclic AMP or cAMP) fulfills the Sutherland criteria (118) as an intracellular second messenger for GRF (1,5,119-123,165-166,277). However, extracellular Ca^{2+} is required for cAMP to stimulate GH release in somatotrophs (5,8). This observation suggests that Ca^{2+} is also a second messenger for GRF in somatotrophs , and that Ca^{2+} acts beyond, or independently of, cAMP (4).

Before Ca^{2+} can be accepted as a true second messenger for GRF in somatotrophs, it has to meet at least three criteria, analogous to Sutherland's criteria for cAMP (118). They are the following:

1. Any agent that increases $[Ca^{2+}]_i$ will stimulate GH release even in the absence of GRF.
2. Any agent that prevents an increase in $[Ca^{2+}]_i$ will prevent GRF-induced GH release.
3. GRF will cause an increase in $[Ca^{2+}]_i$ which precedes or is concurrent with GH release.

5.1.1 Technical Considerations.

The strategy in this thesis was to assess the role of Ca^{2+} in GH release, using essentially three experimental approaches; a) the measurement of GH release (and cAMP accumulation) under conditions which would alter Ca^{2+} availability to the somatotroph, b) the actual measurement of altered Ca^{2+} fluxes with altered GH secretion and c) the measurement of $[Ca^{2+}]_i$ with altered GH secretion.

5.1.1.1 ^{45}Ca Uptake experiments. The studies of Ca^{2+} fluxes were carried out by measuring ^{45}Ca uptake by somatotrophs. Uptake experiments were carried out under one of two sets of conditions: steady state and non-steady state. The first condition exists when Ca^{2+} influx equals efflux. When steady state is perturbed, that is, when Ca^{2+} influx is no longer equal to efflux, the system is said to be in non-steady state. Under ideal conditions, data from steady state time course experiments can be used to calculate Ca^{2+} exchange rates across the plasma membrane, and the size of the intracellular Ca^{2+} pools (239,240,278). By comparing uptake in different steady states (i.e. in the presence or absence of hormone), it is possible to determine whether a hormone alters the Ca^{2+} kinetics (exchange rates and pool sizes) of the cell (239,240). Non-steady state time course experiments yield information on how fast a hormone acts and whether it stimulates or inhibits Ca^{2+} fluxes (240).

GH release was used as an index for Ca^{2+} steady state. It was assumed that changes in GH release reflect changes in $[Ca^{2+}]_i$. If GH release was constant, then $[Ca^{2+}]_i$ would be constant and Ca^{2+} influx and efflux would have to be equal. The rate of GH release from somatotrophs challenged with GRF or SRIF in perifusion is relatively constant after about 10 min

of exposure (45,79,80,279). Therefore, in steady state uptake experiments, somatotrophs were allowed to equilibrate for 10 min after the addition of GRF or SRIF, before adding radiolabelled tracer to the incubation medium.

Kinetic parameters for Ca^{2+} fluxes can be calculated from steady state data using 3-compartment mathematical models (240,278). The data fit the models if the uptake vs time curve is described by a double exponential equation. Uchikawa and Borle (278) published solutions which allow the calculation of the Ca^{2+} exchange rates between compartments, the unidirectional rate constants and the compartment sizes from the parameters of the double exponential equation.

When double exponential curves were fitted to the present data, the error of the estimates of the regression parameters was so high that meaningful kinetic parameters could not be calculated. The poor fit of the data to the model was due to the high variability in the sample both between and within time points. The high variability was due to the paucity of tissue per sample. The problem of high sample variability plagued the non-steady state experiments as well. Indeed the changes in uptake that were seen were approximately 20-25%, while the overall variability of the ^{45}Ca uptake measurement, using 50,000 cells per sample, was 15-20%.

The silicone oil sandwich technique for separating cells from radioactive medium (273), from which the n-BP sandwich technique was derived, requires samples containing approximately 4 mg of protein (280). This amount of protein corresponds to about $7x10^6$ cells per sample (15 μg protein per 100,000 cells). The somatotroph purification technique used for these experiments yielded a maximum of $8x10^6$ to $9x10^6$ cells for a 30 rat preparation. It is obvious that it was prohibitive, in a 12 point time course experiment, to increase the amount of tissue per sample to the optimal level. To overcome the problem of insufficient tissue, a two

stage experimental approach was adopted. The overall strategy was to carry out either steady state or non-steady state time course experiments using a number of time points, and then, in a second experiment to "zoom in" on single critical times, thus increasing cell numbers per sample. This decreased sample variability in the second experiment by allowing an increase in the number of cells per sample. Using a purified somatotroph preparation from 30 rats it was possible to increase the number of cells per sample by a factor of 2 to 10. The advantage of the two stage approach over a single time point alone is that the single time point measurement is not an isolated observation, since it can be interpreted in the light of the time course experiments.

5.1.1.2 The measurement of $[Ca^{2+}]_i$. To determine if GRF causes $[Ca^{2+}]_i$ to increase, it was necessary to measure the intracellular concentration of free Ca^{2+}. The trapped Ca^{2+} sensitive fluorescent dye technique was used. It was found that of the three fluorescent dyes, quin2, fura-2 and indo-1, the third was best suited for measuring $[Ca^{2+}]_i$ changes in somatotrophs in suspension (see Appendix). Changes in fluorescence measured by this technique reflect the average $[Ca^{2+}]_i$, and not changes at the single cell level (281). Therefore results must be interpreted with the knowledge that they reflect what is happening in the **majority** of cells at any given time.

Another approach in studying the effect of GH secretagogues on Ca^{2+} flux was to measure changes in $[Ca^{2+}]_i$, while preventing Ca^{2+} influx with Ca^{2+}-free medium, or with the Ca^{2+} antagonists nifedipine or diltiazem. The variability in $[Ca^{2+}]_i$ measurements is related to the stability of the spectrofluorimeter's light source and photomultiplier as well as whether $[Ca^{2+}]_i$ is saturating for the dye. The Ca^{2+} concentrations measured in this study were well within the limits of reliable measurements (see Appendix). Results from $[Ca^{2+}]_i$ measurement experiments are more reliable than data from ^{45}Ca uptake experiments which are at, if not below, the lower limit of the assay due to the small amount of tissue per sample. For this

reason conclusions about Ca^{2+} fluxes based on $[Ca^{2+}]_i$ measurements were given more weight than those from uptake experiments.

5.1.1.3 The prevention of Ca^{2+} influx. Two strategies were used to prevent Ca^{2+} influx. The first was to incubate the cells in a "no added" Ca^{2+} medium, with or without the Ca^{2+}-chelator, EGTA. The conventional interpretation using this approach, is that if secretagogues no longer stimulate hormone release, then this can be interpreted as indicating that Ca^{2+} influx is required for release. However this interpretation may be flawed, since incubating cells in "no added" Ca^{2+} medium with or without EGTA may prevent release, not by blocking Ca^{2+} influx, but by leaching out an essential intracellular Ca^{2+} pool. In order to minimize this possibility, secretagogues were tested within 10 sec after the addition of EGTA.

The second strategy used to prevent Ca^{2+} influx employed the Ca^{2+} antagonists, nifedipine and diltiazem. These are discussed more fully below.

In summary, two very different techniques were used to block Ca^{2+} influx into the somatotrophs - "no added" Ca^{2+}, with or without Ca^{2+} chelator in the incubation medium, and Ca^{2+} antagonists. Obtaining similar results with these two very different methods, would strengthen conclusions concerning the role of Ca^{2+} influx in the release process.

Testing for the three criteria for Ca^{2+} as an intracellular second messenger for GRF was carried out by combining all the approaches mentioned above.

5.1.2 The 1st Criterion: Raising $[Ca^{2+}]_i$ Stimulates GH Release.

Two approaches were used to raise $[Ca^{2+}]_i$ without affecting cAMP accumulation. The first consisted of exposing somatotrophs to depolarizing concentrations of K^+. This technique raises $[Ca^{2+}]_i$ (Figure 40) by stimulating Ca^{2+} influx (Figures 38 and 40) presumably through

voltage sensitive Ca^{2+} channels (Figures 8 - 11). The second approach consisted of treating cells with divalent cation ionophores such as A23187. When an ionophore interacts with a cell membrane, Ca^{2+} can flow into the cell down its electrochemical gradient (Figure 18). An ionophore-dependent increase in Ca^{2+} influx also results in an increase in $[Ca^{2+}]_i$ ((181) and unpublished observation). Experiments carried out by Kraicer et al. (4) showed that when somatotrophs were exposed to A23187 or to high extracellular $[K^+]$ in static incubation GH release was increased while cAMP accumulation was unchanged. When somatotrophs were perifused with media containing either A23187 or depolarizing concentrations of K^+, GH release was transiently stimulated within minutes ((9) and Figures 8 - 11, 38 and 39).

In the current studies it has been demonstrated that agents such as cpt-cAMP, PGE_2, PMA and diC_8, which raise cAMP accumulation and stimulate protein kinases, also raise $[Ca^{2+}]_i$ by stimulating Ca^{2+} influx (Figure 43-46). All these agents are GH secretagogues but are ineffective in Ca^{2+}-free medium ((5,8), and unpublished observations). These results suggest that any agent which raises $[Ca^{2+}]_i$ stimulates GH release.

From these experiments it is concluded that increasing $[Ca^{2+}]_i$ stimulates GH release in the absence of GRF. Therefore the first criterion for Ca^{2+} as a second messenger is met.

5.1.3 The 2nd Criterion: Preventing an increase in $[Ca^{2+}]_i$ prevents GRF-induced GH Release.

In these studies two strategies were used to prevent an $[Ca^{2+}]_i$ increase during GRF-induced GH release. The first consisted of incubating somatotrophs in medium with no added Ca^{2+} (4,8). The second consisted of treating cells with organic Ca^{2+} channel blockers (Ca^{2+} antagonists). Both of these procedures decrease baseline $[Ca^{2+}]_i$ and prevent secretagogue-induced increases in $[Ca^{2+}]_i$ (Figs 23, 24, 43-46).

5.1.3.1 Low extracellular Ca^{2+}. Medium 199 prepared without $CaCl_2$ has a Ca^{2+} concentration no greater than 85 μM (8). When cells were challenged with GRF in low Ca^{2+} medium, GH release was inhibited, and cAMP accumulation was increased 28-37 fold (Figure 5). The higher than normal cAMP accumulation seen with low Ca^{2+} medium has been reported for GH secretagogues that raise cAMP (i.e. IBMX and PGE_2) (8). The increase is attributable to the Ca^{2+} sensitivity of adenylate cyclase and not to an inhibition of phosphodiesterase ((123) and unpublished observations). The essential requirement for extracellular Ca^{2+} for GRF action has been reported for mixed pituitary cell populations (2,3,44). The large increase in cAMP accumulation conclusively shows that the inhibition of GRF-induced GH release in low Ca^{2+} medium is not due to a decrease in adenylate cyclase activity or a decrease in cAMP accumulation. This result is consistent with the reports that $(Bu)_2$cAMP-, IBMX- or PGE_2-induced GH release from somatotrophs is inhibited in low Ca^{2+} medium (5,8). These results suggest that the action of elevated $[Ca^{2+}]_i$ in GRF-stimulated GH release, occurs at a step or steps after cAMP.

Since the procedure used to purify somatotrophs (see Chapter 3) for the low Ca^{2+} medium experiments involved prolonged exposure of cells to low extracellular Ca^{2+} concentration, it cannot be excluded that this treatment leaches out Ca^{2+} from an essential intracellular pool, rather than simply preventing influx. However it is unambiguous that Ca^{2+} is essential for GRF-induced GH release.

5.1.3.2 Ca^{2+} antagonists. In the second approach, two Ca^{2+} antagonists were used to prevent Ca^{2+} influx; the dihydropyridine nifedipine and the benzothiazepine diltiazem. In the first series (Figures 6 and 8) both Ca^{2+} antagonists produced a concentration-related decrease in basal GH release, and a decrease in $[Ca^{2+}]_i$ (Figures 25 panel A, and 26 panel A) presumably secondary to a decreased Ca^{2+} influx. Cyclic AMP levels were, as expected, unaltered over the concentration range used.

High K^+ studies were then carried out (Figures 8-11) to confirm that Ca^{2+} antagonists were effective. Sustained high K^+ lead to an instantaneous increase in Ca^{2+} influx (Figures 38 and 39), with a subsequent rapid, but transient burst of GH release, reaching a peak within 2 min and then falling rapidly to baseline levels (9). As would be predicted, diltiazem at concentrations greater than 10^{-7} M blocked the augmented release of GH induced by high K^+, as did nifedipine at concentrations greater than 10^{-8} M. As expected, high K^+ did not cause a consistent change in cAMP accumulation. Of interest, the blocking effect of nifedipine was more obvious at earlier times (4, 8, and 16 min) than at 32 min. This is most likely due to the transient nature of the GH response to high K^+ (9). These data are consistent with previous studies (282,283) reporting that phenylalkylamine Ca^{2+} channel antagonists (verapamil and D600) also block high K^+-induced GH release from the adenohypophysis. We conclude that both diltiazem and nifedipine are effective in blocking the high K^+-induced Ca^{2+} influx into somatotrophs and that nifedipine is more potent by an order of magnitude.

In the next series, we examined the effect of the two antagonists on GRF-induced GH release and cAMP accumulation. A concentration of GRF (10^{-10} M) was chosen to produce a small, consistent, significant, and reproducible increase in GH release, which is preceded by an increase in cAMP accumulation (1). Diltiazem was first tested over a large range of concentrations (Figures 12, 13, and 15). Only at 10^{-4} M was it effective in significantly reducing (but not totally blocking) GRF-induced GH release (Figure 15). Nifedipine was also tested over a large range of concentrations (Figures 14 and 16). Nifedipine was effective in blocking the GRF-induced release of GH at a concentration of 10^{-6} M (Figures 14 and 16). In each case where the antagonist was effective, the GRF-induced increase in cAMP accumulation was further augmented. We attribute this to an increase in adenylate cyclase activity resulting from the decrease in $[Ca^{2+}]_i$ (123). The observation that there is no reduction in the magnitude of the GRF-induced increase in cAMP further reinforces our previous conclusion (4,8,9) that Ca^{2+} is required at a step or steps after cAMP.

The results of the GRF studies are more difficult to interpret than the results of the high K^+ series, since much higher concentrations of antagonists (2- to 3-orders of magnitude) were required to decrease or abolish GRF-induced GH release. The concentration of diltiazem (10^{-4} M) and of nifedipine (10^{-5} M) required to inhibit GRF-induced GH release are very high. One can not exclude the possibility that the inhibition of GH release is non-specific, or due to an intracellular site of action for the antagonists (284,285). However, similar observations have been reported for the effect of nisoldipine (a dihydropyridine) on K^+- and TRH-induced release of prolactin from GH_4C_1 cells (286).

Several factors may account for the higher concentrations of Ca^{2+} antagonists required to block GRF- versus K^+-induced GH release. Cells may possess both voltage-sensitive Ca^{2+} channels (VSCC), which would open when the membrane is depolarized by high K^+, and receptor-operated Ca^{2+} channels (ROCC), which would open when GRF binds to its receptor (147,208). Antagonists may be more effective in blocking Ca^{2+} entry through VSCC's than through ROCC's (287,288).

Multiple classes of VSCC's have been demonstrated in clonal pituitary cells (227,289,290), showing kinetic and pharmacological differences. Both rapidly and slowly inactivating Ca^{2+} currents exist (corresponding to the T and L type of McClesky et al. (216)), with only the slowly inactivating (L type) current blocked by dihydropyridines, where blockade occurred with very slow onset (290). Moreover, the function of the dihydropyridine-sensitive class of Ca^{2+} channels requires that they be phosphorylated by cAMP-dependent protein kinase (PKA) to be active (227). Thus, we would predict that the blockers used in our study exert their action by blocking calcium entry through slowly inactivating L type VSCC's.

The differential effects of nifedipine on the blockade of high K^+- versus GRF-induced release of GH might be explained by the different way in which K^+ and GRF cause

depolarization. Elevation of K^+ likely causes **persistent** depolarization of cells (since the membrane potential should be shifted to the new equilibrium potential for K^+ of about -37 mV). This depolarization may result in transient activation of T, and sustained activation of L channels. On the other hand, GRF may act to induce bursts of action potentials, with both T and L channels contributing to Ca^{2+} influx for the duration of GRF stimulation, thereby leading to persistent entry of Ca^{2+} and sustained GH release. The continued entry of Ca^{2+} through T channels may provide for a dihydropyridine-insensitive pathway for secretion. Yet another property of dihydropyridine may contribute to the differences seen. Cohen and McCarthy (290) provided evidence that the **onset** of the nimodipine blockade of the Ca^{2+} current is very slow, and thus, should have little effect on stimulus-secretion coupling in normally functioning pituitary cells. It is not yet known if action potentials do indeed underlie the response of normal somatotrophs to GRF.

Interestingly the concentration-dependent effect of diltiazem on basal GH release was different from its effect on baseline $[Ca^{2+}]_i$. Indeed concentrations of the antagonist as low as 10^{-8} M maximally decreased basal GH release, whereas concentrations as high as 10^{-5} and 10^{-4} M were required to moderately decrease baseline $[Ca^{2+}]_i$. On the other hand the concentration-dependent effect of nifedipine on both basal GH release and baseline $[Ca^{2+}]_i$ was similar. Both diltiazem and nifedipine inhibited the GRF-induced increase in $[Ca^{2+}]_i$ in a concentration-dependent manner (Figures 24, 25 and 26). The concentration-dependent inhibition of GRF-induced GH release and $[Ca^{2+}]_i$ increase by nifedipine were similar. However the concentration-dependent inhibition of these two responses by diltiazem was different. While only very high concentrations of diltiazem (10^{-4} M) reduced the GRF-induced GH release, the GRF-dependent increase in $[Ca^{2+}]_i$ was sensitive to the whole range of concentrations tested (Figure 25, panel B).

5.1.3.3 Summary. Preventing $[Ca^{2+}]_i$ from increasing, by blocking Ca^{2+} influx, either by removing extracellular Ca^{2+} or by treating the cells with Ca^{2+} antagonists, prevents GRF-induced GH release. Therefore the second criterion is met. In addition, the Ca^{2+} which is essential for GRF-induced release of GH is most probably from an extracellular source since blocking Ca^{2+} influx blocks GH release.

5.1.4 The 3rd Criterion: GRF causes an increases in $[Ca^{2+}]_i$ which is concurrent with GH release.

To determine if GRF raises $[Ca^{2+}]_i$, the intracellular concentration of free Ca^{2+} was measured using the trapped Ca^{2+}-sensitive fluorescent dye indo-1. The observed baseline $[Ca^{2+}]_i$ of 269 $\pm$ 3 nM in unstimulated somatotrophs is comparable to values reported for rat pituitary tumour cells (GH_4C_1) measured with quin2 (291,292), normal rat pituitary cells (126) and rat somatotrophs in suspension (180) or individual rat somatotrophs (50,179,181,293) measured with fura-2. However this baseline level is about twice as high as that reported for mouse pituitary tumour cells (AtT-20) (14,177), rat pituitary tumour cells (GH_3) (252) measured with quin2 and rat somatotrophs measured with fura-2 (127). The difference in the reported baseline $[Ca^{2+}]_i$ may be related to the proportion of unstimulated cells which secrete GH. Indeed Holl et al. (179) showed that unstimulated rat somatotrophs, identified by reverse haemolytic plaque assay (RHPA), which have a high rate of basal GH secretion, have higher $[Ca^{2+}]_i$ than cells with a low basal rate of hormone release.

GRF caused a biphasic increase $[Ca^{2+}]_i$ (Figure 21). The first phase of the GRF response was a rapid increase in $[Ca^{2+}]_i$, detectable within 5 sec. The second phase was a decrease in $[Ca^{2+}]_i$ to a plateau which was always higher than baseline, and maintained for at least 5 min. The timing of the onset of the GRF-induced increase in $[Ca^{2+}]_i$, when compared to the timing of the GRF-induced increase in GH release, is consistent with the increase in $[Ca^{2+}]_i$ occurring prior to, or concurrent with GH release (Figures 20 and 21).

This ability of GRF to raise $[Ca^{2+}]_i$ in pituitary cells was first reported by Schöfl et al. (126). They used quin2 to measure GRF-induced increases in $[Ca^{2+}]_i$ in a mixed population of acutely dispersed rat pituitary cells, and found that the increase was monophasic. Measurements using fura-2 also yielded similar results (125). A monophasic response to GRF in a mixed cell population was also observed with indo-1 in the current study (see Appendix). The discrepancy between the pattern of the GRF-induced increase in $[Ca^{2+}]_i$ seen with mixed pituitary cells and purified somatotrophs may be related to the amount of light produced in dye loaded somatotrophs responding to GRF. In a mixed cell population, up to 40% of the cells are somatotrophs. Thus only 40% of the cells will increase their $[Ca^{2+}]_i$ when exposed to GRF. If the difference in fluorescence between the peak and the plateau is of the same magnitude as the noise due to the 60% non-responding cells then it would not be possible to detect a biphasic response in a mixed cell population.

Holl et al. (50) found that GRF transiently increased $[Ca^{2+}]_i$ in RHPA identified rat somatotrophs, while Snyder et al. (127) reported that the response consisted of a monophasic increase to a plateau. Snyder's group used the ratio technique for fura-2 measurements, but used a single light source spectrofluorimeter (Perkin Elmer 650-10s). The disadvantage of this approach is a loss in temporal resolution, since the excitation wavelength is changed from 340 nm to 360 nm by manually resetting the monochromator. Therefore it may not be possible to detect the biphasic increase. Holl's group used dual excitation wavelength fluorescent videomicroscopy with digital image analysis to measure $[Ca^{2+}]_i$ with the ratio technique for fura-2. They reported the average $[Ca^{2+}]_i$ for 21 cells. However they indicated that a plateau was observed in individual cells. The relatively small sample size, and the cell to cell variations in fluorescence may explain why the plateau was not apparent when the average response was examined. The data presented in the current study are a better estimate of the **average** response since the sample size was $5x10^5$ cells as opposed to 21.

The maximum increase in $[Ca^{2+}]_i$ of the peak and of the plateau were concentration-dependent with EC_{50}'s of $2x10^{-10}$ M and $7x10^{-10}$ M respectively. The GRF concentration dependence of the $[Ca^{2+}]_i$ response is similar to the concentration dependence of GH released for purified somatotrophs in static incubation with an EC_{50} of about 10^{-10} M (unpublished observation and (1)).

The biphasic response is most probably a real phenomenon, and not an artifact due to the presence of indo-1 in the cells. Two observations support this statement. First, indo-1 loaded somatotrophs perifused with a medium identical to that used in the dye studies (see Chapter 3) had a normal rate of basal GH release, and the response to various concentrations of GRF was the same as the response of control cells (Figure 20). Second, the pattern of GH release during continuous GRF exposure is biphasic, with a peak phase and a plateau phase (Figure 20 and (45,80,279)). It is tempting to attribute the biphasic nature of the GH release pattern to the biphasic change in $[Ca^{2+}]_i$. However simultaneous measurements of both $[Ca^{2+}]_i$ and GH release will have to be carried out to confirm this relationship.

The biphasic nature of the $[Ca^{2+}]_i$ response may suggest that the elevation of $[Ca^{2+}]_i$ is dependent on two sources of Ca^{2+}. Gershengorn and Thaw (252) reported that TRH produced a biphasic $[Ca^{2+}]_i$ response in GH_3 cells. They found that the plateau phase was dependent on extracellular Ca^{2+}, while the peak phase was not Furthermore they found that intracellular Ca^{2+} stores were significantly reduced by TRH treatment. They concluded that the Ca^{2+} pool responsible for the peak was intracellular while the pool responsible for the elevated plateau was extracellular. Similar biphasic responses were observed in GnRH challenged rat gonadotrophs (255,257,294) and TRH challenged rat lactotrophs (254).

Alternatively the biphasic response may be dependent on only extracellular Ca^{2+}. The peak would be due to the initial event which raises $[Ca^{2+}]_i$. The plateau would correspond to

a new steady state where the rate of Ca^{2+} removal from the cytosol is increased in response to the elevated $[Ca^{2+}]_i$ (186,187,189). The source of Ca^{2+} for the GRF response is discussed below (section 5.2)

In summary, GRF causes $[Ca^{2+}]_i$ to increase. The timing of the increase is consistent with at least a concurrent increase in GH release. Consequently the third criterion is met.

5.2 The Source of Ca^{2+} for the GRF $[Ca^{2+}]_i$ Response.

The inhibition of GRF-induced GH release by incubation of somatotrophs in low Ca^{2+} medium and by Ca^{2+} antagonists implies that the essential Ca^{2+} pool for GH release is extracellular. On the other hand the biphasic GRF-induced increase in $[Ca^{2+}]_i$ suggests that an intracellular Ca^{2+} pool may also be involved in GH release. This discrepancy may be explained by a leaching out of an essential intracellular Ca^{2+} pool during prolonged incubation in low Ca^{2+} medium, or to an intracellular site of action for Ca^{2+} antagonists, which would lead to an inhibition of intracellular Ca^{2+} mobilization. Experiments were carried out to determine the contribution of extracellular and intracellular Ca^{2+} to the GRF-induced $[Ca^{2+}]_i$ response in rat somatotrophs.

5.2.1 Extracellular Source.

5.2.1.1 ^{45}Ca Uptake experiments. Uptake of ^{45}Ca was measured to determine if GRF stimulates Ca^{2+} influx. Both steady state and non-steady state experiments were carried out. GH release was used as an index for Ca^{2+} flux steady state.

In steady state time course experiments the rate of GH release from GRF treated cells was constant, and greater than the rate of GH release from control cells (Figure 17). A concentration of GRF which produces a maximal GH release was chosen. Clearly these two

groups correspond to different steady states (Figure 17). Uptake of ^{45}Ca by GRF treated cells was higher than that for control cells. The difference is most noticeable after 120 min of loading. Single time point measurements taken after 150 min of loading confirmed that GRF stimulates ^{45}Ca uptake (Figure 30). The increase in uptake is dependent on either an increase in the Ca^{2+} exchange rate across the membrane or an increase in the size of intracellular Ca^{2+} pools. Both are dependent on an initial increase in Ca^{2+} influx or a decrease in Ca^{2+} efflux.

To determine if GRF stimulates Ca^{2+} influx, non-steady state ^{45}Ca uptake experiments were carried out. Untreated somatotrophs in steady state were loaded with ^{45}Ca, until their radioactive content was approximately constant. The steady state was then perturbed by challenging the cells with GRF, and their ^{45}Ca content was monitored over time and compared to that of unchallenged control cells. An increase in ^{45}Ca uptake indicates a net Ca^{2+} influx, that is, more Ca^{2+} is entering than leaving the cell. A decrease indicates a net Ca^{2+} efflux, that is, more Ca^{2+} is leaving than entering the cell (239,240,280).

In preliminary experiments, to determine whether the n-BP sandwich technique was appropriate for detecting rapid changes in net Ca^{2+} influx, somatotrophs where challenged with the Ca^{2+} ionophore A23187. A23187, in non-steady state experiments resulted in a very large sustained increase in ^{45}Ca uptake detectable within 30 sec. (Figure 18) Similarly, exposing somatotrophs to depolarizing extracellular concentrations of K^+ (29 mM), moderately increased uptake within 30 sec (Figure 38). Therefore the n-BP sandwich method can be used to monitor rapid changes in Ca^{2+} influx.

GRF (10^{-9} M) caused a small (15 - 25%) consistent increase in ^{45}Ca uptake. Surprisingly the response was consistently triphasic - two transient increases and a sustained plateau (Figure 19 panel B). The first increase peaked in 30 sec. Then uptake dropped nearly to baseline within 1 min, only to reach a second peak, somewhat lower than the first, by 2 min.

By 8 min the ^{45}Ca content of the cells was back to near baseline, and by 16 min it plateaued to the level of the first peak. It should be noted that this triphasic response was seen consistently in four independent experiments.

The first phase is due to a rapidly initiated and large increase in Ca^{2+} influx, followed by an even larger increase in efflux. The stimulated efflux removes ^{45}Ca from the cell, along with the unlabelled Ca^{2+}, faster than it enters the cell. Therefore the total amount of ^{45}Ca in the cell drops. The second phase may be due to either a decrease in Ca^{2+} efflux or an increase in influx. A decrease in Ca^{2+} efflux is most probable since Ca-ATPase activity is related to $[Ca^{2+}]_i$, and at the onset of the second phase $[Ca^{2+}]_i$ has presumably been reduced. As the $[Ca^{2+}]_i$ increases due to unchallenged influx (increase in ^{45}Ca content) Ca-ATPase activity increases again, removing more Ca^{2+} than enters the cell (decrease in ^{45}Ca content). The third phase can be explained in the same way as the second.

In summary, steady state experiments show that GRF stimulates ^{45}Ca uptake by somatotrophs for up to 180 min. Non-steady state experiments show that GRF triggers a complex sequence of events involving both influx and efflux, which results in a triphasic response over 32 min.

5.2.1.2 $[Ca^{2+}]_i$ Measurement experiments. If the GRF-induced $[Ca^{2+}]_i$ response is solely dependent on extracellular Ca^{2+}, then blocking influx should abolish the response. Ca^{2+} influx was decreased by either incubating somatotrophs in Ca^{2+}-free medium with 0.5 mM EGTA, or by treating the cells with nifedipine or diltiazem.

Removing Ca^{2+} from the extracellular medium decreased baseline $[Ca^{2+}]_i$ within 2 min. Furthermore, $[Ca^{2+}]_i$ did not increase when cells incubated in Ca^{2+}-free medium were challenged with GRF at a concentration which causes a maximal increase in $[Ca^{2+}]_i$ in normal

medium (Figure 23). Similar results have been reported for mixed rat pituitary cells (126) as well as for RHPA identified somatotrophs (126). When Ca^{2+} was added back to the extracellular medium after GRF, then $[Ca^{2+}]_i$ increased rapidly to a level comparable to the plateau level of the GRF response (Figure 23 panel D). From these results it was concluded that the $[Ca^{2+}]_i$ response is due to influx.

Preventing Ca^{2+} influx by treating somatotrophs with the Ca^{2+} antagonists diltiazem and nifedipine resulted in a concentration dependent decrease in baseline $[Ca^{2+}]_i$ (Figures 24, 25 panel A and 26 panel B). Other Ca^{2+} antagonists and blockers are reported to also decrease baseline $[Ca^{2+}]_i$ in rat somatotrophs (126).

Both diltiazem and nifedipine inhibited the GRF-induced increase in $[Ca^{2+}]_i$ in a concentration-dependent manner (Figures 24-26). The antagonists did not affect the biphasic nature of the response. However, the level of the peak and plateau were reduced. At the highest concentration of either antagonist, GRF caused a small increase in $[Ca^{2+}]_i$ which never exceeded the pre-antagonist baseline. This response can be explained in several ways. Small amounts of Ca^{2+} from an intracellular store may be mobilized (253). Alternatively, and more likely, the antagonist concentration may not be high enough to block all the Ca^{2+} channels (incomplete blockade). T type Ca^{2+} channels, which are insensitive to diltiazem and nifedipine (218), may be present in these cells (213,215).

In summary, the initiation of the GRF-induced $[Ca^{2+}]_i$ response is dependent on an extracellular source of Ca^{2+}. ^{45}Ca uptake experiments show that GRF stimulates Ca^{2+} influx within sec. Measurements of $[Ca^{2+}]_i$ in the absence of extracellular Ca^{2+} or in the presence of Ca^{2+} antagonists indicate that Ca^{2+} influx is responsible for at least the initial increase of $[Ca^{2+}]_i$ induced by GRF.

5.2.2 Intracellular Source.

Blocking Ca^{2+} influx with Ca^{2+} antagonists or by incubation in Ca^{2+}-free medium can yield information on the role of Ca^{2+} stores as well as on Ca^{2+} influx. In Ca^{2+}-free medium, GRF-induced GH release was blocked (Figure 5), and GRF had no effect on $[Ca^{2+}]_i$ (Figure 23). When indo-1 loaded cells incubated in Ca^{2+}-free medium were treated with the divalent cation ionophore ionomycin, a large transient increase in $[Ca^{2+}]_i$ was observed. Ionomycin penetrates both the plasma membrane and organelle membranes. Thus organelle sequestered Ca^{2+} flows into the cytosol, where it can interact with indo-1, and then flows out of the cell. A transient response after ionophore treatment in Ca^{2+}-free medium indicates the presence of intracellular stores (181,295). The ionomycin sensitive Ca^{2+} pool most probably does not represent all the mobilizable stored calcium. Therefore the presence of this Ca^{2+} pool does not exclude the involvement of another rapidly depletable pool in the GRF response.

GRF caused a sub-baseline $[Ca^{2+}]_i$ response when L type Ca^{2+} channels were blocked with nifedipine or diltiazem. As mentioned above this response could be due to the mobilization of a small Ca^{2+} store. Putney's capacitance model (237) for the receptor-regulated Ca^{2+} entry in non-excitable cells, postulates the existence of an intracellular Ca^{2+} pool, which would be filled from the extracellular compartment and would empty into the cytosol. Inositol (1,4,5) trisphosphate (IP_3) dependent emptying of the pool then leads to Ca^{2+} influx. Such a "trigger pool" could explain why the GRF sub-baseline response can be seen with Ca^{2+} antagonists but not in Ca^{2+}-free medium (294). However, GRF does not increase the turnover of the phosphoinositide cycle in somatotrophs (French, personal communication), thus it is unlikely that IP_3-stimulated Ca^{2+} mobilization occurs in these cells.

The sub-baseline response is most probably due to Ca^{2+} influx resulting from an incomplete blockade of L type channels by the antagonists, or to the existence of antagonist-

insensitive T type channels (213,215). The lack of response to GRF in the absence of extracellular Ca^{2+} favours this possibility. Furthermore a sub-baseline response was seen when somatotrophs were stimulated with high K^+ in the presence of nifedipine (Figure 40). Potassium depolarization is believed to increase $[Ca^{2+}]_i$ only by augmenting Ca^{2+} influx through VSCC's. Thus the K^+-induced sub-baseline response, in Ca^{2+} antagonist-treated cells, would have to be due to an incomplete blockade of L type channels or to T type channel-dependent influx.

The fact that the initiation of the $[Ca^{2+}]_i$ response is dependent on Ca^{2+} influx, does not exclude the possibility that the plateau phase might be due to mobilization of Ca^{2+} stores secondary to the increase in $[Ca^{2+}]_i$ (Ca^{2+}-dependent Ca^{2+} mobilization). Nifedipine caused $[Ca^{2+}]_i$ to decrease rapidly to below baseline when added during the GRF plateau phase. The fact that $[Ca^{2+}]_i$ decreased indicates that the plateau is not dependent on Ca^{2+}-activated Ca^{2+} mobilization. If it were, nifedipine would not abolish the plateau, since the majority of Ca^{2+} responsible for the elevated concentration would be from an intracellular source.

In summary, though intracellular Ca^{2+} stores are present in somatotrophs, both phases of the GRF-induced increase in $[Ca^{2+}]_i$ are dependent on influx of extracellular Ca^{2+} alone. The sub-baseline increase in $[Ca^{2+}]_i$ seen in Ca^{2+} antagonist treated, GRF-stimulated cells is probably due to incomplete blockade of VSCC's.

5.3 Biphasic Nature of the GRF-Induced Increase in $[Ca^{2+}]_i$.

Since there is only one source of Ca^{2+}, the biphasic response is due, as mentioned above, to a sequential activation of Ca^{2+} influx and Ca^{2+} removal from the cytosol. GRF, by binding to its receptor, causes Ca^{2+} channels to open, possibly through the action of cAMP, and results in an increase in Ca^{2+} conductance. The increased conductance leads to an influx

of Ca^{2+} down its electrochemical gradient. Consequently $[Ca^{2+}]_i$ increases. Elevated $[Ca^{2+}]_i$ then stimulates regulatory processes which tend to lower $[Ca^{2+}]_i$ by two types of mechanisms. The first reduces influx (i.e. Ca^{2+} channel inactivation). The second increases the removal of Ca^{2+} from the cytosol. These could involve the activation of Ca-ATPases by elevated $[Ca^{2+}]_i$, Ca-calmodulin (Ca-CaM), cAMP-dependent protein kinase or protein kinase C. A new equilibrium between influx and efflux would then be attained, and $[Ca^{2+}]_i$ would reach a plateau.

The existence of the peak is dependent on a difference between the rate of activation of Ca^{2+} influx and the rate of activation of Ca^{2+} removal. In other words it takes longer for the regulatory processes to reach their new maximum rate of Ca^{2+} removal than it does to fully open Ca^{2+} channels. When the maximal rate of Ca^{2+} removal is reached, it has to be greater than the influx, so that $[Ca^{2+}]_i$ can drop.

The first two phases of the ^{45}Ca uptake response to GRF are consistent with the proposed mechanism for the biphasic $[Ca^{2+}]_i$ responses (Figure 19 panel B). The peak $[Ca^{2+}]_i$ occurs at 30 sec during the first ^{45}Ca uptake peak, corresponding to high net Ca^{2+} influx. The decrease in $[Ca^{2+}]_i$ from the peak to the plateau occurs during a period of net efflux, which corresponds to the first trough of the uptake curve seen at 1 min. For the plateau phase of the $[Ca^{2+}]_i$ response to occur, high Ca^{2+} efflux must decrease, such that efflux equals influx. This decrease in efflux leads to the increased ^{45}Ca uptake seen between 1 and 4 min.

5.4 Summary.

The calcium ion is a second messenger for GRF in rat somatotrophs since the three essential criteria are met. Increasing $[Ca^{2+}]_i$ with Ca^{2+} ionophores and depolarizing concentrations of K^+ stimulates GH release. Preventing an increase in $[Ca^{2+}]_i$ by incubating somatotrophs in Ca^{2+}-free medium or with Ca^{2+} antagonists, prevents GRF-induced GH release.

Finally, GRF causes an increase in $[Ca^{2+}]_i$. The only source of Ca^{2+} involved in the GRF-induced increase in $[Ca^{2+}]_i$ is extracellular. The biphasic nature of the response is due to a difference in the rate of activation of Ca^{2+} influx and of Ca^{2+} removal from the cytosol.

CHAPTER 6

SRIF ALTERS THE Ca^{2+} STATUS OF THE SOMATOTROPH

6.1 Introduction.

Somatostatin inhibits basal GH release (79) and abolishes GRF-induced GH release by somatotrophs (1,80,123). GRF stimulation of GH release is preceded by an increase in cAMP accumulation (1). Although GRF-stimulated GH release is abolished by SRIF, cAMP accumulation, in either mixed pituitary cells or in somatotrophs, is only slightly decreased (1,3,42,123). However, Narayanan et al. (123) demonstrated that in a purified somatotroph membrane preparation, basal and GRF-stimulated adenylate cyclase activity is not inhibited by SRIF. The mechanism by which cAMP is reduced is not clear, however activation of phosphodiesterase is probably not involved (167). The modest drop in cAMP probably does not play a significant role in the inhibition of GH release since SRIF totally inhibits GH release from pituitary cells and somatotrophs treated with cAMP analogues (5,6,9,168-170). Thus SRIF would appear to act at a step after or independently of cAMP.

In Chapter 5 it was concluded that Ca^{2+} is an intracellular second messenger for GRF in rat somatotrophs. When GRF binds to its receptor $[Ca^{2+}]_i$ increases due to increased Ca^{2+} influx through L type VSCC's. It would appear that this increase in $[Ca^{2+}]_i$ is essential for GH release. Could SRIF exert its inhibitory effect on GH release by inhibiting Ca^{2+} influx or by otherwise decreasing $[Ca^{2+}]_i$?

In order to investigate the mechanism of action of SRIF in purified rat somatotrophs, experiments were carried out to evaluate the effect of SRIF on Ca^{2+} fluxes and $[Ca^{2+}]_i$.

6.2 SRIF Inhibits ^{45}Ca Uptake In Somatotrophs.

As with the study of the effects of GRF on ^{45}Ca uptake, a two stage experimental approach was used to investigate the effects of SRIF. Both steady and non-steady state experiments were carried out. In a first series of steady state experiments a number of time points of interest were identified. Then in a second series only selected time points were further analyzed, in order to maximize the amount of tissue per sample.

6.2.1 Unstimulated Somatotrophs.

As a first approach to explore the effect of SRIF on unstimulated (in the absence of secretagogue) Ca^{2+} fluxes, steady state time course ^{45}Ca uptake experiments were carried out. Using GH release as an index for Ca^{2+} steady state, somatotrophs were allowed to equilibrate for 10 min before adding ^{45}Ca to the incubation medium. SRIF caused small, detectable and significant decreases in ^{45}Ca uptake, but not consistently in all experiments, even though the rate of GH release was inhibited (Figure 28). The less variable single time measurements were then made in steady state (Figure 29). The sample was taken after 90 min of loading because, in time course experiments, ^{45}Ca uptake in the SRIF treated group was consistently lower than in the control group at this time point. Uptake was significantly lower in the SRIF group. In steady state, a decrease in ^{45}Ca uptake can be due to either a decrease in the exchange rate of Ca^{2+} across the plasma membrane or to a decrease in intracellular Ca^{2+} pools. Both are dependent on either an initial decrease in influx or an increase in efflux.

To investigate whether SRIF decreased Ca^{2+} influx, non-steady state experiments were then carried out. It is clear that the ^{45}Ca content of the cell will not change appreciably, once

isotopic equilibrium is reached (constant ^{45}Ca content), if the influx of Ca^{2+} is decreased. Therefore, when an inhibition of influx is expected, the steady state is perturbed during the initial phase of ^{45}Ca uptake (240) so that a break in the uptake curve would be seen. When a physiological concentration of SRIF (10^{-9} M) was introduced into the incubation medium after 6 to 15 min of loading, such a break was seen (Figure 31), but this was not consistent (Figure 32). At higher concentrations (10^{-7} M) the break was more pronounced and consistently seen. In an attempt to detect a significant decrease in ^{45}Ca uptake caused by 10^{-9} M SRIF, a single time point experiment was then carried out. The sample was taken 8 min after adding SRIF, at a time when the break in the uptake curve was expected. A significant decrease could not be detected. Experiments carried out under similar conditions using clonal pituitary cell lines and mixed rat pituitary cells, showed that SRIF markedly decreased ^{45}Ca uptake after 15 min of exposure, but only at a concentration of 10^{-7} M and higher (296).

At physiological concentrations (10^{-9} M), SRIF was found to affect uptake significantly, but not consistently, when monitored in a time course steady state experiment. Yet it did decrease uptake consistently and significantly in single time point steady state experiments. Conversely, the same concentration of SRIF produced a detectable break in the uptake curve but did not produce a significant decrease in single time point non-steady state experiments. The fact that a significant decrease in uptake was seen in single time point steady state experiments but not in the time course experiments, demonstrates the necessity of increasing the amount of tissue per sample. However, the amount by which the number of cells per sample was increased in single time point non-steady state experiments with 10^{-9} M SRIF was still insufficient to reduce the variability sufficiently to reveal a significant decrease in uptake. However, the SRIF treated group consistently had a lower uptake than control. Therefore, at physiological concentrations, the SRIF-induced decrease in ^{45}Ca uptake, though not statistically significant, is probably biologically relevant.

A break in an uptake curve can be explained either by a decreased influx of Ca^{2+} or an increased efflux, or both. If SRIF stimulates Ca^{2+} efflux, then treatment of somatotrophs with SRIF before increasing Ca^{2+} influx with the Ca^{2+} ionophore A23187, should result in a decrease in uptake. Indeed the net influx (influx - efflux) in SRIF treated cells would then be lower than in control cells, since A23187-dependent influx is not expected to be altered by SRIF. Therefore ^{45}Ca content would be expected to be less in cells treated with A23187 and SRIF than in cells treated with A23187 alone. Clearly this is not the case in non-steady state experiments carried out after 80 min of loading, suggesting that SRIF does not stimulate Ca^{2+} efflux (Figure 33). Comparable SRIF concentrations are reported to decrease the fractional ^{45}Ca efflux from preloaded pituitary cells (297), indicating a lack of **stimulatory** effect of SRIF on efflux (298). Therefore, the decrease in uptake can only be due to a decrease in Ca^{2+} influx. A net efflux (more Ca^{2+} leaving the cell than entering the cell) will occur if SRIF inhibits Ca^{2+} influx without simultaneously decreasing Ca^{2+} efflux. This should result in a decrease in the ^{45}Ca content of the cell. This is precisely what is seen in non-steady state experiments where SRIF is applied when the system is near tracer equilibrium, after 80 min of ^{45}Ca loading. The ^{45}Ca content of the cells after SRIF treatment was significantly lower than before SRIF treatment (Figure 33).

6.2.2 GRF-Stimulated Somatotrophs.

In single time point, steady state experiments high concentrations of SRIF (10^{-7} M) significantly decreased ^{45}Ca uptake when evaluated after 150 min of loading in a single time point experiment (Figure 30). GRF at a concentration that causes both a maximum GH release and $[Ca^{2+}]_i$ increase, significantly increased uptake. When SRIF and GRF were both present, GH release was no different from control, and ^{45}Ca uptake was the same as with SRIF alone. Because of the lack of temporal resolution of this single time point experiment, it is not possible to attribute the SRIF-dependent decrease in uptake to a decrease in Ca^{2+} influx as it is impossible to attribute the GRF-dependent increase to an increase in influx. What is clear,

however, is that GRF does alter the Ca^{2+} status of the somatotroph, by either increasing the exchange rate between cellular and extracellular compartments, or by increasing the size of one or more intracellular compartments. SRIF alone, either reduces the exchange rate, the compartment sizes or both. It also prevents GRF-dependent alterations in the Ca^{2+} status of the cell.

6.3 SRIF Lowers $[Ca^{2+}]_i$.

Once SRIF was shown to inhibit Ca^{2+} influx, it remained to determine its effect on $[Ca^{2+}]_i$. Intracellular free Ca^{2+} concentration is dependent on the balance between Ca^{2+} influx and the rate of Ca^{2+} removal from the cytosol. It was predicted that SRIF-dependent inhibition of influx would result in a decrease in $[Ca^{2+}]_i$. Therefore the effect of SRIF on $[Ca^{2+}]_i$ was measured directly.

6.3.1 SRIF Lowers Baseline $[Ca^{2+}]_i$.

Somatostatin decreased baseline $[Ca^{2+}]_i$ in a concentration-dependent manner (Figures 34 and 35) with an EC_{50} of about 10^{-10} M. A similar response to SRIF has been reported for the ACTH secreting mouse pituitary tumour cell line AtT-20 (14,177), the GH secreting rat pituitary cells line GH_4C_1 (13,128,172) and GH_3 (178), and rat somatotrophs (50,179,180,293). The EC_{50} for SRIF in the current study was 10^{-10} M which is about 36-fold and 20-fold lower than the EC_{50} for AtT-20 (estimated from Figure 2 in reference (14)) and GH_3 cells respectively (178). After reaching a nadir, $[Ca^{2+}]_i$ tended to drift towards baseline when treated with concentrations of SRIF of 10^{-8} M or greater (Figure 34). In AtT-20 cells, with 10^{-7} M SRIF, there was a true return to baseline which occurred within 7 min (14,177). In GH_4C_1 cells, $[Ca^{2+}]_i$ returned to baseline when treated with 10^{-7} M SRIF (128,172). In somatotrophs, with SRIF concentrations greater than 10^{-8} M, the tendency to return to baseline was (293) or was not (180) seen.

Either a decrease in the basal (unstimulated) Ca^{2+} influx without a concurrent decrease in the rate of removal of Ca^{2+} from the cytosol, or an increase in the rate of removal without a concurrent increase in influx, can account for the SRIF-induced drop in $[Ca^{2+}]_i$. Ca^{2+} can be removed from the cytosol by either being pumped out of the cell or into the ER/calciosomes and mitochondria. The fact that ^{45}Ca uptake was reduced by SRIF suggests that the decrease in $[Ca^{2+}]_i$ is not due exclusively to a sequestration, for if this were the case, uptake would not be reduced. As stated above, SRIF does decrease influx. Furthermore the magnitude of the decrease in $[Ca^{2+}]_i$ is similar to the decrease seen with Ca^{2+} antagonists, thus suggesting but by no means proving, that the decrease is primarily due to an inhibition of influx. This is further supported by the reports that SRIF hyperpolarizes clonal pituitary cells (13,128,172,178) and somatotrophs (171), thus causing the closing of VSCC's, and consequently a reduction in Ca^{2+} influx.

6.3.2 SRIF Inhibits the GRF-Induced Increase in $[Ca^{2+}]_i$.

Prior treatment of somatotrophs with SRIF inhibited the GRF-induced $[Ca^{2+}]_i$ increase in a concentration-dependent manner (Figure 36). Surprisingly SRIF did not affect both phases of the GRF response equally. At low concentrations (10^{-10} M), SRIF abolished the GRF-induced peak, but had no effect on the plateau. At higher concentrations the plateau was also inhibited. Finally at the highest concentration tested (10^{-8} M), a small increase in $[Ca^{2+}]_i$ was observed, however it never exceeded the baseline level (sub-baseline response).

In order to determine whether SRIF inhibits the second phase of the GRF $[Ca^{2+}]_i$ response, which is due to a sustained Ca^{2+} influx, SRIF was added to the incubation mixture during the GRF-dependent plateau. SRIF caused a concentration-dependent decrease in $[Ca^{2+}]_i$ (Figure 37). The lowest concentration tested (10^{-10} M) had no effect on the level of the plateau $[Ca^{2+}]_i$. A 10-fold increase in concentration transiently reduced $[Ca^{2+}]_i$. A 100-fold

increase rapidly decreased $[Ca^{2+}]_i$ to below the pre-GRF baseline. After reaching a nadir $[Ca^{2+}]_i$ increased to, and remained at, the baseline level.

Both phases of the GRF-induced $[Ca^{2+}]_i$ increase were dependent on Ca^{2+} influx (see section 5.2.2). Therefore SRIF inhibited this response, by inhibiting Ca^{2+} influx. SRIF could prevent the increase by stimulating removal of Ca^{2+} from the cytosol, but as mentioned above this is unlikely.

Of lesser importance, but of interest, is the observation that even at high concentrations, SRIF did not completely abolish the increase in $[Ca^{2+}]_i$ induced by GRF, though the response never reached baseline. There are two possible explanations for the sub-baseline response. The first is that GRF may cause the mobilization of a small intracellular Ca^{2+} store (see section 5.2.2). The second, and more likely, is that the GRF-induced Ca^{2+} influx may not be completely blocked. The sub-baseline increase in $[Ca^{2+}]_i$, however, does not lead to an increase in GH release. Indeed $2x10^{-9}$ M GRF-induced GH release was reported to be completely abolished by $6x10^{-9}$ M SRIF in static incubation (1). These observations strongly suggest that for GH release to be greater than basal, $[Ca^{2+}]_i$ must increase above baseline. The sub-baseline response may explain why, in perifusion, SRIF decreased basal GH release (79) even at a concentration of 10^{-9} M (45,80) while GH release remained at the basal level during simultaneous exposure to 10^{-10} M GRF and 10^{-9} M SRIF. The drop in baseline $[Ca^{2+}]_i$ seen with SRIF is consistent with the inhibition of basal GH release. The sub-baseline increase in $[Ca^{2+}]_i$ is consistent with the inability of SRIF, in the presence of GRF, to decrease GH release below basal.

6.4 Mechanism of Action of SRIF: Basis for the Differential Effect.

An interesting and unexpected finding in this study is the differential effect of SRIF on the biphasic GRF-induced $[Ca^{2+}]_i$ increase. In Chapter 5 it was established that the GRF-induced increase in $[Ca^{2+}]_i$ was due solely to an influx of extracellular Ca^{2+}. It was also proposed that the biphasic nature of this increase was due to a difference in the rates of activation of Ca^{2+} influx and Ca^{2+} removal from the cytosol. The height of the $[Ca^{2+}]_i$ peak would be dependent on the maximum influx and on the difference in the rates of activation; the greater the influx and the longer the lag between reaching maximum influx and maximum removal rate, the higher the peak.

Maximum influx is dependent on the number of open Ca^{2+} channels. This is dependent on the total number of functional channels and their probability of opening, which is in turn dependent on membrane potential (E_m) (174,229). The rate of activation of Ca^{2+} influx (equivalent to the rate of activation of inward Ca^{2+} current in voltage clamp experiments) is dependent on the activation kinetics of individual Ca^{2+} channels. If the time taken to achieve maximum influx is of the same magnitude as the time taken to achieve the maximum rate of Ca^{2+} removal from the cytosol, the peak would not occur. The existence of the plateau is dependent on the fact that the increase in the rate of removal is secondary to the increase in $[Ca^{2+}]_i$. The height of the plateau is dependent on the final maximum influx, i.e. on number of open channels.

The differential effect could be due to a simple concentration effect of SRIF. If somatotrophs possess two classes of SRIF receptors and two classes of Ca^{2+} channels, then high affinity receptors would be negatively coupled to rapidly activating channels, while low affinity receptors would be negatively coupled to slowly activating channels. However, this is unlikely because pituitary cells have only one class of SRIF receptors (159,160).

Since both peak and plateau are affected by the number of open channels, low concentrations of SRIF, which affect only the peak, must in some way affect the Ca^{2+} influx activation kinetics. SRIF is known to slow down the rate of activation of inward Ca^{2+} currents in spinal cord neurons, sympathetic neurons, neuroblastoma-glioma cells, and AtT-20 cells (14,174-176). Recently Bean (174) has proposed a model for neurotransmitter inhibition of Ca^{2+} currents which could explain the change in activation kinetics seen with SRIF. The model assumes that closed voltage-sensitive Ca^{2+} channels would exist in two states, "willing" to open and "reluctant" to open. Individual channels in each state would have a different voltage dependence for opening. The activation kinetics of Ca^{2+} currents would be dependent on how rapidly equilibrium between the two states occurs, once "willing" channels open. Bean proposed that SRIF would alter the equilibrium between the two closed states such that the proportion of channels in the "reluctant" state would be increased. This new equilibrium implies at least one of the rate constants for the "reluctant"/"willing" conversion would have to change. Decreasing the rate constant for the "reluctant" to "willing" conversion would reduce the speed at which a new equilibrium between "reluctant" and "willing" channels would occur, and increase the proportion of channels in the "reluctant" state. The mechanism by which SRIF would decrease this rate constant is unknown but G-protein interaction is a good candidate (174).

SRIF at high concentrations (10^{-8} M) decreases the GRF-induced plateau $[Ca^{2+}]_i$. Therefore SRIF has to decrease the number of open Ca^{2+} channels. The number of open channels is dependent on the membrane potential. Thus the more negative the E_m, the smaller the number of open channels. SRIF is reported to hyperpolarize pituitary tumour cells by increasing K^+ conductance (128,172,178). Hence the total number of open VSCC's would be decreased. SRIF is also reported to decrease inward Ca^{2+} currents in voltage clamp experiments (14,174-176). This suggests that SRIF can decrease the number of open channels independent of membrane potential. Either the number of functional Ca^{2+} channels is decreased as predicted by the Reuter and Scholz model for the regulation of Ca^{2+}

conductance in cardiac muscle (225), or the overall probability of channel opening at a given E_m is decreased as a result of increasing the proportion of "reluctant" closed channel as predicted by the Bean model (174).

The differential effect of SRIF on the GRF-induced $[Ca^{2+}]_i$ increase can be explained by its effect on the activation kinetics of Ca^{2+} influx and on the number of open Ca^{2+} channels. At low concentrations, SRIF would affect activation kinetics, but only slightly decreasing, if at all, the number of open channels. Thus the peak and not the plateau of the GRF response would be reduced. At higher concentrations, activation kinetics would be further affected and the number of open channels would be significantly decreased, so that both the peak and the plateau are reduced.

6.5 Summary.

SRIF inhibits basal and GRF-dependent steady state ^{45}Ca uptake. The SRIF-dependent decrease in basal non-steady state ^{45}Ca uptake is due to an inhibition of Ca^{2+} influx. SRIF decreases baseline $[Ca^{2+}]_i$ in a concentration dependent manner. It also inhibits the GRF-induced biphasic increase in $[Ca^{2+}]_i$ in a differential fashion. Low concentrations abolish the peak, or first phase, without affecting the plateau, or second phase. At high concentrations, both phases are inhibited such that the GRF response is sub-baseline. The reported ability of SRIF to slow the activation rate of Ca^{2+} currents and to decrease Ca^{2+} conductance may explain the differential effect of SRIF on the GRF-induced $[Ca^{2+}]_i$ increase. Therefore the inhibitory effect of SRIF on GH release would then be dependent on the ability of SRIF to decrease, or at least retard, an increase in $[Ca^{2+}]_i$. This effect of SRIF would be achieved by decreasing Ca^{2+} influx.

CHAPTER 7

INTERACTIONS BETWEEN Ca^{2+} AND OTHER INTRACELLULAR SIGNALLING SYSTEMS

7.1 Introduction.

In Chapter 5 it was established that Ca^{2+} is an intracellular second messenger for GRF in rat somatotrophs, and that it is essential for GH release. GRF-stimulated GH release is dependent on an increase in $[Ca^{2+}]_i$ resulting from an increase in Ca^{2+} influx. Ca^{2+} influx is brought about by the opening of L type VSCC's. The opening of such channels is dependent on a change in membrane potential and/or channel phosphorylation by either cAMP-dependent protein kinase (PKA) and/or protein kinase C (PKC) (223,227,229). The possibility that all three signalling systems may be involved in GRF-dependent increases in Ca^{2+} influx is suggested by the fact that K^+-depolarization, membrane permeable cAMP analogues, PGE_2, and PKC activators all stimulate GH release from rat somatotrophs (4,5,9,48). Furthermore GRF is reported to depolarize pituitary cells (125), increase cAMP accumulation by somatotrophs (1,123) and increase the rate of turnover of the phosphoinositide cycle in pituitary cells (136).

The next series of experiments was carried out to investigate the involvement of other intracellular signalling systems in mediating the GRF-induced increase in Ca^{2+} influx and subsequent increase in $[Ca^{2+}]_i$. The role of membrane depolarization and protein phosphorylation were specifically investigated. The effect of K^+-depolarization, cAMP analogues, PGE_2, and stimulators of PKC on $[Ca^{2+}]_i$ and ^{45}Ca uptake were studied. Particular attention was given to the shape and timing of the $[Ca^{2+}]_i$ response to these GH secretagogues as

compared to the GRF response. The extracellular Ca^{2+} dependence and SRIF sensitivity of these responses were used to evaluate the involvement of these signalling systems in the GRF-induced increase in Ca^{2+} influx and subsequent increase in $[Ca^{2+}]_i$ and GH release.

7.2 Membrane Depolarization.

7.2.1 K^+-Depolarization Increases $[Ca^{2+}]_i$.

Depolarizing somatotrophs by increasing the extracellular K^+ concentration ($[K^+]_e$) from 6 to 30 mM (5K), resulted in a transient increase in $[Ca^{2+}]_i$ with a return to baseline within 10 min (Figure 40, panel C). K^+-depolarization-dependent increases in $[Ca^{2+}]_i$ have previously been reported in mouse (182) and rat (13,128,253,299) pituitary tumour cells, mixed rat pituitary cells (126,257), rat gonadotrophs (256,257), rat lactotrophs (254) and rat somatotrophs (180,181). The response to 15 to 55 mM $[K^+]_e$ in GH_3 cells consisted of an increase in $[Ca^{2+}]_i$ to a sustained plateau (253,299). Varying the $[K^+]_e$ from 9 to 118 mM produced different $[Ca^{2+}]_i$ responses in GH_4C_1 cells, ranging from an initial peak followed by a nadir and then a plateau, at low concentrations, to a rapid rise and a slow decay that did not reach baseline, at high concentrations (13,128). Depolarization of normal pituitary cells and gonadotrophs with 25 to 50 mM K^+ raised $[Ca^{2+}]_i$ to a plateau (257). Two different responses to 50 and 55 mM K^+ respectively have been reported in somatotrophs (180,181). In one study $[Ca^{2+}]_i$ rapidly increased. Then, after reaching a peak, $[Ca^{2+}]_i$ slowly decayed, remaining well above baseline. In the second study $[Ca^{2+}]_i$ increased rapidly and decayed rapidly to reach a plateau above baseline within 8 min. The difference in the shape of the $[Ca^{2+}]_i$ response to K^+-depolarization from cell type to cell type may be related to a different proportion of T and L type VSCC's. Similarly the range of responses seen in GH_4C_1 cells may be due to the presence of both types of channels, since the opening of the T type channels occurs at more negative membrane potentials than the opening of L type channels (216).

It is important to note that the shape of the K^+-induced $[Ca^{2+}]_i$ response is similar to the K^+-induced GH release pattern seen in perifusion (9). When somatotrophs were challenged with 29 mM K^+, GH release rapidly increased to a peak and then returned to basal, even though high K^+ was maintained.

The peak $[Ca^{2+}]_i$ seen in the current study with 30 mM K^+ was comparable to the peak values seen with GRF. However the rise time for K^+-depolarization, at 16 ± 1 sec, was half the rise time for GRF. The shapes of the two responses were also different (Figure 40). In both cases a peak occurred; however, in the GRF response, $[Ca^{2+}]_i$ dropped to a stable elevated plateau, whereas in the K^+-depolarization response, $[Ca^{2+}]_i$ dropped to baseline. The difference in rise time may reflect the existence of an intracellular messenger which would be necessary for GRF-dependent depolarization. Furthermore, the plateau phase of the GRF $[Ca^{2+}]_i$ response may also be dependent on the presence of an intracellular messenger, since depolarisation alone does not support the plateau phase.

7.2.2 K^+ Stimulates Ca^{2+} Influx.

The K^+-induced increase in $[Ca^{2+}]_i$ results from an increase in Ca^{2+} influx. Both time course and single time point non-steady state ^{45}Ca uptake experiments showed that 29 mM K^+ (5K) increased uptake (Figures 38 and 39). In the time course experiment the increase in uptake was detectable within 1 min (Figure 38). The largest difference between control and K^+ treated groups was observed after 8 min. Interestingly the uptake curves for both groups were parallel after 8 min. This suggests that the K^+-induced increase in uptake was transient. The single time point experiments confirmed that ^{45}Ca uptake was greater for the 5K group after 8 min.

Potassium depolarization has been known to increase ^{45}Ca uptake by pituitary cells. In most cases, the initial rate of uptake at the time of depolarization or uptake after more than

20 min of loading under non-steady state conditions have been reported. These protocols are different from those used in this study. However, in all cases the initial rate of uptake for the high K^+ groups was greater than that for the control groups in GH_3 cells (300-302), and normal bovine (283) and rat (303,304) pituitary cells. It was also found, after a longer period of loading, that high K^+ increased uptake in bovine pituitary cells (283), and in rat pituitary glands in vitro (305).

To further investigate the role of depolarization in stimulating Ca^{2+} influx, $[Ca^{2+}]_i$ measurements were carried out in Ca^{2+}-free medium and with nifedipine. In Ca^{2+}-free medium, as expected, 5K did not cause a change in $[Ca^{2+}]_i$, even though intracellular Ca^{2+} stores were present (Figure 40, panel D). The lack of response to high K^+ in Ca^{2+}-free medium has been documented for pituitary cells (126) and for somatotrophs (180,181). This result suggests that the high K^+ response is due primarily to Ca^{2+} influx. In the presence of 10^{-6} M nifedipine the response to 5K was virtually abolished. 5K produced only a small, sub-baseline, transient increase in $[Ca^{2+}]_i$ (Figure 40, panel E). The effect of Ca^{2+} antagonists on high K^+-induced $[Ca^{2+}]_i$ increase has also been reported in GH_3 cells (253), normal pituitary cells (208,306) and somatotrophs (180). The fact that the sub-baseline response was not observed in the absence of extracellular Ca^{2+}, suggests that it was due to an incomplete blockade of L type channels. Indeed the maximal inhibitory concentration of nifedipine for a high K^+-induced $[Ca^{2+}]_i$ increase in rat pituitary cells is reported to be $3x10^{-5}$ M (306). The possibility of a small influx through dihydropyridine-insensitive T type VSCC's cannot be excluded.

These observations confirm that high K^+-stimulated GH release is dependent on Ca^{2+} influx. This conclusion was based on the observation that 5K did not stimulate GH release in Ca^{2+}-free medium (4) or in the presence of Ca^{2+} antagonists (Figures 8-11).

The data from the ^{45}Ca uptake experiments and the $[Ca^{2+}]_i$ measurements in Ca^{2+}-free medium and with nifedipine show that K^+-depolarization stimulates Ca^{2+} influx into rat somatotrophs through L type VSCC's. The decay in $[Ca^{2+}]_i$ following the peak is most probably due to regulatory mechanisms which may include Ca-ATPase activation in response to elevated $[Ca^{2+}]_i$ and slow inactivation of Ca^{2+} channels.

7.2.3 SRIF does not Inhibit K^+-Induced Ca^{2+} Influx.

Though SRIF inhibited 5K-induced GH release (Figure 22 and (9)) it did not inhibit 5K-induced ^{45}Ca uptake in single time point non-steady state experiments (Figure 39) nor did it inhibit the 5K-induced increase in $[Ca^{2+}]_i$ (Figure 40, panel F). This result indicates that the 5K-induced Ca^{2+} influx is not inhibited by SRIF. This lack of effect on $[Ca^{2+}]_i$ has been reported in AtT-20 mouse pituitary tumour cells (182), GH_3 rat pituitary tumour cells (178), normal mixed rat pituitary cells (125) and somatotrophs (181).

The lack of inhibitory effect of SRIF on 5K-induced Ca^{2+} influx supports the suggestion that SRIF hyperpolarizes the somatotrophs by increasing K^+ conductance (128). Indeed SRIF is known to hyperpolarize rat clonal pituitary cells and somatotrophs (128,171,178). The lack of effect of SRIF on high K^+-induced Ca^{2+} influx can easily be explained by this hypothesis. In medium containing a normal $[K^+]$ (5.8 to 6 mM), increasing K^+ conductance leads to hyperpolarization. This occurs because membrane potential (E_m) normally tends toward the equilibrium potential for K^+ (E_K) and because E_K is more negative than the resting E_m at this $[K^+]_e$. The more negative membrane potential causes VSCC's to close, and therefore Ca^{2+} influx is decreased. This is consistent with the SRIF dependent inhibition of ^{45}Ca uptake seen in unstimulated somatotrophs (see section 6.2.1). In medium with a high $[K^+]$ (29 - 30 mM) the cells are depolarized because E_K is now less negative than the resting E_m. If K^+ conductance is then increased, E_m would move closer to E_K and be even less negative than resting E_m. If anything, at high $[K^+]_e$, SRIF would be expected to further depolarize the cell.

If this is indeed the case then SRIF would not cause VSCC's to close, thus Ca^{2+} influx would not be inhibited.

The lack of inhibition of high K^+-induced Ca^{2+} influx by SRIF does not mean that SRIF cannot act by hyperpolarizing the cell. If depolarization were due, for example, to an increase in Na^+ conductance, then an increase in K^+ conductance would tend to repolarize the cell. As the cell returned to resting E_m, VSCC's would close and consequently Ca^{2+} influx would be reduced.

The lack of inhibitory effect of SRIF on the K^+-induced increase in $[Ca^{2+}]_i$ implies that the SRIF inhibition of K^+-induced GH release (4,9) is not due to a decrease in $[Ca^{2+}]_i$. In perifusion studies high concentrations of SRIF ($6x10^{-8}$ M) significantly inhibited, but did not abolish high K^+-induced GH release (9). This incomplete blockade of GH release could be explained by the transient $[Ca^{2+}]_i$ response. However the unattenuated $[Ca^{2+}]_i$ response suggests that SRIF can inhibit GH release in a Ca^{2+}-independent manner. A cAMP-dependent mechanism is unlikely since SRIF does not inhibit adenylate cyclase in these cell (123), and high K^+ does not stimulate cAMP production in rat somatotrophs (4). Furthermore, there is evidence which suggests that SRIF action is dependent on a G-protein which acts at a site other than adenylate cyclase (163). In the light of the proposed role of G-proteins in the regulation of Ca^{2+}-independent exocytosis (265) it is possible that the SRIF receptor-coupled G-protein may inhibit GH release at a step after Ca^{2+}.

7.2.4 GRF and Membrane Depolarization.

The data presented in this study do not yield direct information on an effect of GRF on membrane potential. However, they allow predictions about E_m to be made.

GRF, by increasing Ca^{2+} influx, should cause the cells to depolarize. A 5,000-fold Ca^{2+} concentration gradient exists across the cell membrane (1.2 mM outside; 250 nM inside). This means that the equilibrium potential for Ca^{2+} (E_{Ca}) is +110 to +120 mV. GRF, by stimulating Ca^{2+} influx, in effect increases Ca^{2+} conductance; therefore, it causes E_m to tend towards E_{Ca} and thus becomes less negative than the resting E_m. This depolarization could cause further opening of VSCC's, and raise E_m even more. If the depolarization is rapid and large enough, then Na^+ channels may open and cause the membrane to depolarize even further. If K^+ and Ca^{2+} conductances are increased simultaneously, the membrane potential may not change appreciably since the depolarizing effect of increased Ca^{2+} conductance would be balanced by the hyperpolarizing effect of increased K^+ conductance. This may be the case, since somatotrophs have Ca^{2+}-activated K^+ channels (K(Ca) channel) which would allow for an increase in K^+ conductance as $[Ca^{2+}]_i$ increases (307).

It is unclear whether depolarization has to occur prior to the increase in Ca^{2+} influx in GRF-stimulated somatotrophs. There are two possible sequences of events. Either GRF causes an increase in Na^+ conductance (which results in depolarization), which in turn causes L type VSCC's to open, or GRF causes an increase in Ca^{2+} conductance (which results in depolarization), which in turn causes Na^+ channels to open. Kato and Suzuki (125) recently reported that GRF causes a Na^+-dependent depolarization of normal mixed rat pituitary cells, and that the GRF-induced $[Ca^{2+}]_i$ increase is dependent on extracellular Na^+. The same group (146) also reported that Na^+ in the extracellular medium was necessary for GRF to stimulate GH release from rat pituitary cells. The voltage-sensitive Na^+ channel blocker tetrodotoxin (TTX) was ineffective in blocking GRF-induced GH release from cultured bovine and rat pituitary cells (146,147) suggesting that the increase in Na^+ conductance would be due to a voltage-insensitive channel.

It has been suggested that GRF may stimulate GH release by increasing the frequency of action potentials (AP) in somatotrophs in a way similar to TRH in GH_3 cells (308). Whether somatotrophs spontaneously generate action potentials is controversial. Neither intracellular nor current clamp recordings of membrane potentials have demonstrated spontaneous AP, though evoked AP were observed in rat and bovine somatotrophs (171,309). Intracellular recordings show that GRF increases Ca^{2+}-dependent voltage noise (147). Recently extracellular recordings from cultured rat pituitary cells showed that GRF stimulated rhythmic K^+- and Ca^{2+}-dependent hyperpolarizing currents, presumably involving K(Ca) channels (310). To date this is the only report that suggests that GRF may stimulate Ca^{2+}-dependent AP.

7.2.5 Summary.

The data presented in this section suggest that depolarization can stimulate Ca^{2+} influx. However, the fact that $[Ca^{2+}]_i$ increased transiently and returned to baseline in 5K-treated cells while GRF caused a biphasic response, suggests that depolarization may be only one of several modes of action of GRF.

7.3 Protein Phosphorylation - cAMP Dependent Protein Kinase.

The effect of the activation of PKA on the Ca^{2+} signalling system was studied by treating somatotrophs with membrane permeable analogues of cAMP or by stimulating adenylate cyclase activity via the PGE_2 receptor. The effects of these agents on $[Ca^{2+}]_i$ and ^{45}Ca uptake, and how they were affected by SRIF, Ca^{2+}-free medium and nifedipine, were studied.

7.3.1 cAMP Increases $[Ca^{2+}]_i$.

To study the effect of cAMP analogues on $[Ca^{2+}]_i$ with trapped Ca^{2+}-sensitive dyes, one must use a non-fluorescent compound. The commonly used analogues of cAMP, 8-bromo

cAMP (8Br-cAMP) and $(Bu)_2$cAMP, fluoresce at the wavelengths used to monitor indo-1 Ca^{2+}-dependent fluorescence. It was necessary therefore to find a non-fluorescent analogue. Miller et al. (311) tested the potency of several cAMP analogues and determined that 8-(4-chlorophenylthio) cAMP (cpt-cAMP) was 100 times more potent than cAMP in stimulating hepatic cAMP-dependent protein kinase in vitro. In static incubation 0.1 mM cpt-cAMP did not cause detectable fluorescence, and stimulated GH release to the same extent as 1 mM $(Bu)_2$cAMP (Table I). Therefore 0.1 mM cpt-cAMP was used to investigate the effect of cAMP on $[Ca^{2+}]_i$.

Cpt-cAMP increased $[Ca^{2+}]_i$ to a sustained level above baseline in a monophasic manner (Table II and Figure 43). This is somewhat different from the response found by others using different cell preparations. Koch et al. (128) reported that cpt-cAMP increased $[Ca^{2+}]_i$ in a biphasic manner in GH_4C_1 cells, similar to the response seen with GRF in somatotrophs. Holl et al. (293) have shown, using the ratio method for fura-2, that 8Br-cAMP and $(Bu)_2$cAMP raised $[Ca^{2+}]_i$ in individual somatotrophs. 8Br-cAMP raised $[Ca^{2+}]_i$ to a plateau, which was maintained for 4 min. Then $[Ca^{2+}]_i$ decreased to a lower plateau. $(Bu)_2$cAMP raised $[Ca^{2+}]_i$ to a peak by 30 sec, then it slowly decreased to baseline. In purified somatotrophs, when the $[Ca^{2+}]_i$ response to 8Br-cAMP, determined with indo-1, was corrected for autofluorescence, a biphasic response was seen (unpublished observation). Raising intracellular cAMP in somatotrophs with PGE_2, also raised $[Ca^{2+}]_i$ in a biphasic manner similar to the GRF response (Figure 44). Stimulating adenylate cyclase activity with forskolin is reported to also increase $[Ca^{2+}]_i$ in a biphasic manner in clonal pituitary cells (128) and somatotrophs (293).

The discrepancy between the shape of the response to cpt-cAMP in the current study and the biphasic response observed by others, may be related to the rate of entry of the analogue into the cell. In studies where biphasic responses were seen the analogue concentration was 5 to 50 times greater than that used in this study. Consequently the rate of diffusion across the plasma membrane of these compound would be expected to be greater.

As already mentioned the biphasic nature of the response may be due to a high rate of activation of Ca^{2+} influx (see section 5.3), thus the faster the cAMP analogue would enter the cell the faster it would activate processes leading to an influx of Ca^{2+}. The biphasic response seen with PGE_2 could be due to a rapid activation of Ca^{2+} influx mediated by the PGE_2 receptor-stimulated cAMP cascade. However one cannot exclude the possibility that PGE_2 action, in somatotrophs, may involve pathways other than the cAMP cascade.

The most significant effect of cAMP accumulation on $[Ca^{2+}]_i$, regardless of whether it produces a biphasic response or not, is that it maintained $[Ca^{2+}]_i$ at an elevated plateau for prolonged periods of time. This suggests that the plateau phase of the GRF response may be maintained by sustained PKA activity.

7.3.2 Does cAMP Stimulate Ca^{2+} Influx?

Time course and single time point non-steady state ^{45}Ca uptake experiments indicated that 5 mM $(Bu)_2$cAMP had no effect on Ca^{2+} fluxes in somatotrophs while moderately stimulating GH release (Figures 41 and 42). However when $[Ca^{2+}]_i$ measurements in Ca^{2+}-free medium and with nifedipine were carried out, it was found that both the cpt-cAMP- and PGE_2-stimulated $[Ca^{2+}]_i$ increases were abolished or greatly inhibited (Figures 43 and 44). When cells were incubated in Ca^{2+}-free medium, the presence of Ca^{2+} stores was confirmed, thus the cAMP response is due primarily to influx. In the presence of nifedipine, cpt-cAMP and PGE_2 produced a small sub-baseline $[Ca^{2+}]_i$ response, which can be attributed to an incomplete L type VSCC blockade. These results are consistent with the inhibition of $(Bu)_2$cAMP- and PGE_2-dependent GH release in low Ca^{2+} medium (8).

The ^{45}Ca uptake data and the $[Ca^{2+}]_i$ measurement data appear inconsistent. The question of whether influx does or does not occur arises. The high variability in the ^{45}Ca uptake measurement has been discussed above (see section 5.1.1). The Ca^{2+} concentrations

measured in this study were well within the limits of reliable measurements (see Appendix). Thus results from $[Ca^{2+}]_i$ measurement experiment are more reliable than data from ^{45}Ca uptake experiment which are at, if not below, the lower limit of the assay. Thus it is most probable that an increase i cAMP accumulation brings about an increase in $[Ca^{2+}]_i$ by stimulating Ca^{2+} influx through L type VSCC's.

7.3.3 SRIF Inhibits the cAMP-Dependent Increase in $[Ca^{2+}]_i$.

SRIF inhibited both the cpt-cAMP- and PGE_2-induced increases in $[Ca^{2+}]_i$. In both cases, however, a small sub-baseline response was observed (Figures 43 and 44). This result is consistent with the inhibition of $(Bu)_2$cAMP- and PGE_2-dependent GH release by SRIF (6). In GH_4C_1 cells, SRIF was reported to transiently decrease $[Ca^{2+}]_i$ during the plateau phase of the cpt-cAMP response and of the forskolin response (128). Interestingly pretreatment with 10^{-7} M SRIF did not inhibit the biphasic response to forskolin (128).

Though changes in ^{45}Ca uptake were not significant, 10^{-7} M SRIF did consistently decrease uptake below basal in the presence of 5 mM $(Bu)_2$cAMP in non-steady state single time point experiments (Figure 42). This result suggests that the inhibition of the cpt-cAMP- and PGE_2-induced increase in $[Ca^{2+}]_i$ by SRIF is due to an inhibition in Ca^{2+} influx. If this is indeed the case, the small sub-baseline response seen with SRIF could be due to an incomplete blockade of influx.

These observations are consistent with the previously proposed mechanisms of action of SRIF. The decrease in Ca^{2+} influx could be due to an SRIF-dependent decrease in the number of open VSCC's secondary to either a decrease in the number of functional channels or an increase in the proportion of closed channels in the "reluctant" state. Alternatively SRIF may close VSCC's by hyperpolarizing the cell.

7.3.4 Possible Mechanisms for PKA Stimulation of Ca^{2+} Influx.

There are two possible mechanisms by which PKA could stimulate Ca^{2+} influx. The first is that PKA could phosphorylate Ca^{2+} channels and cause them to open. Armstrong and Eckert (227) have suggested that dihydropyridine-sensitive VSCC's must be phosphorylated by PKA for voltage-dependent opening to occur. Phosphorylation of Ca^{2+} channels is consistent with either the Reuter and Scholz, or the Bean models for the regulation of Ca^{2+} conductance (174,225).

The second possibility is that PKA would cause depolarization of somatotrophs, by increasing Na^+ conductance, which would lead to the opening of VSCC's. Koch et al. (128) have reported that cpt-cAMP as well as forskolin, depolarize GH_4C_1 cells. Kato et al. (146) have shown that $(Bu)_2$cAMP-dependent GH release is inhibited when mixed pituitary cells are perifused with Na^+-free medium (146). Replacing extracellular Na^+ with Li^+, did not inhibit $(Bu)_2$cAMP-stimulated GH release, suggesting that the action of cAMP was dependent on depolarization, rather than Na^+ itself (148). The PKA catalytic subunit is known to phosphorylate purified Na^+ channels from rat brain in vitro (312). Exogenous 8Br-cAMP was also found to cause rat synaptosomal Na^+ channel phosphorylation (313). It is unclear whether channel phosphorylation modulates Na^+ conductance. However cAMP is reported to modulate Na^+ conductance in Helix neurons (314). It is not yet known if this effect is due to phosphorylation or, as reported for sensory receptors, to the direct interaction of cAMP with Na^+ channels (315).

7.3.5 Summary.

The data in this section suggest that cAMP-dependent phosphorylation is capable of initiating and maintaining an increase in $[Ca^{2+}]_i$ in rat somatotrophs. The SRIF sensitive increase in $[Ca^{2+}]_i$ is dependent on Ca^{2+} influx through L type VSCC's. The plateau phase of the GRF $[Ca^{2+}]_i$ response is consistent with a sustained increase in cAMP accumulation.

cAMP could increase influx via PKA-dependent phosphorylation of Ca^{2+} channels, which would then change their voltage-dependence, or via cAMP-dependent increases in Na^{+} conductance, which would lead to depolarization of the cell and cause VSCC's to open.

7.4 Protein Phosphorylation - Protein Kinase C.

The effect of PKC on the Ca^{2+} signalling system was investigated by treating somatotrophs with the phorbol ester PMA and the diacylglycerol analogue diC_8, both PKC activators which stimulate GH release from rat somatotrophs (48). The effects of these agents on $[Ca^{2+}]_i$ and how they were affected by SRIF, Ca^{2+}-free medium and nifedipine were studied.

7.4.1 PKC Activators Transiently Increase $[Ca^{2+}]_i$.

Both PMA and diC_8 caused $[Ca^{2+}]_i$ to increase transiently (Figures 45 and 46). In both cases $[Ca^{2+}]_i$, after reaching a peak, dropped to a level below baseline. DiC_8 produced a faster increase in $[Ca^{2+}]_i$ than did PMA. The difference in rise time may reflect different binding affinities for PKC as well as different membrane permeabilities. The qualitative similarity of the responses to both PKC stimulators suggests that the transient nature of the response and the lowering of $[Ca^{2+}]_i$ below baseline are due to the activation of PKC. The transient $[Ca^{2+}]_i$ response is consistent with the transient increase in GH release produced by both PKC stimulators (48).

Similar effects of phorbol esters on intracellular $[Ca^{2+}]_i$ have been reported for pituitary tumour cell lines (291,292,316,317), mixed rat pituitary cell (318) and somatotrophs (293). The response was transient in all cases, however, $[Ca^{2+}]_i$ did not drop below baseline in all cell types. Diacylgl, ol analogues have also been reported to cause transient increases in $[Ca^{2+}]_i$ in GH_4C_1 cells (291).

7.4.2 PKC Activators Stimulate Ca^{2+} Influx.

Incubating somatotrophs in Ca^{2+}-free medium abolished the $[Ca^{2+}]_i$ response to both PMA and diC_8 (Figures 45 and 46). This is consistent with the observation that the stimulatory effect of PMA is abolished and that of diC_8 is significantly inhibited in low Ca^{2+} medium (unpublished observation). In both cases intracellular Ca^{2+} stores were present. Thus the $[Ca^{2+}]_i$ response is primarily due to influx. Nifedipine also inhibited the response; however both PKC stimulators produced a small sub-baseline response. Again these sub-baseline responses are most probably due to an incomplete blockade of Ca^{2+} channels. The extracellular Ca^{2+} dependence of the transient $[Ca^{2+}]_i$ response has been reported for both phorbol esters and diacylglycerol analogues in GH_4C_1 cells (291,292). These results suggest that the transient PKC-stimulated Ca^{2+} influx is dependent on the opening of dihydropyridine-sensitive L type VSCC's.

This conclusion seems inconsistent with the observation that both phorbol esters and diacylglycerol analogues reduce voltage-dependent Ca^{2+} currents in AtT-20 and GH_3 cells (230,231). Recently it has been suggested that this effect was not dependent on PKC but on the interaction between the stimulators and the outer surface of the plasma membrane (228). Indeed, when 1,2-oleoylacetylglycerol (OAG) was introduced into dorsal root ganglion (DRG) cells, as opposed to the outside of the cells, the inhibition of the Ca^{2+} current was not observed. Inhibitors of PKC activity did not prevent the reduction in Ca^{2+} current. Finally, 4α-phorbol-12,13-didecanoate (4αPDD), a phorbol ester which does not activate PKC, also inhibited the Ca^{2+} current. Although it is possible that the PKC activators used in this study reduced Ca^{2+} current in somatotrophs, they nonetheless stimulated influx via the action of PKC.

7.4.3 SRIF Inhibits the PKC-Dependent Increase in $[Ca^{2+}]_i$.

SRIF inhibits PMA- and diC_8-induced increases in $[Ca^{2+}]_i$ (Figures 28 and 29). In both cases a small sub-baseline response was seen even when a very large co ıcentration of SRIF

was used (10^{-7} M). This observation is consistent with the report that SRIF inhibits both PMA- and diC_8-induced GH release (48). Furthermore SRIF is reported to inhibit the 12,13-phorbol dibutyrate (PDB)-induced transient increase in $[Ca^{2+}]_i$ in somatotrophs when added simultaneously to the incubation medium (293). Since the PKC response is dependent on Ca^{2+} influx through L type VSCC's, the inhibitory effect of SRIF is consistent with a decrease in the number of open Ca^{2+} channels, which could be due to a hyperpolarization secondary to an increase in K^+ conductance, a decrease in the number of functional Ca^{2+} channels, or an increase in the proportion of channels in the closed "reluctant" state.

7.4.4 Possible mechanism of action of PKC-activators.

The transient increase in $[Ca^{2+}]_i$ seen in response to PKC activators is due to an increase in Ca^{2+} influx through L type VSCC's. Most probably this influx is due to phosphorylation of ion channels (229). There are reports which suggest that intracellular administration of PKC into neuronal cells can either increase or decrease Ca^{2+} currents (229). Hence, at present it is uncertain whether PKC phosphorylation stimulates Ca^{2+} channel opening. It is also not known if Ca^{2+} influx could be stimulated by Na^+-dependent depolarization triggered by PKC-dependent phosphorylation. However it is known that PMA and diC_8 can produce a small significant increase in cAMP accumulation in somatotrophs (48). It is most likely that this increase in cAMP is dependent on the action of PKC. The consequence of the increase in cAMP may be stimulation of Ca^{2+} influx. The increase in cAMP accumulation is small compared with the GRF-dependent accumulation. However, if cAMP is compartmentalized, the cAMP concentration and consequently PKA activity, in the vicinity of Ca^{2+} channels, may be high enough for channel phosphorylation, and thus stimulation of influx.

The transient nature of the $[Ca^{2+}]_i$ response to either PMA or diC_8, indicates that Ca^{2+} efflux was greater than influx. With comparable peak concentrations, the return of $[Ca^{2+}]_i$ to baseline with PKC activators was faster than with 5K. In the case of 5K the return to baseline

is believed to be due to activation of Ca-ATPase secondary to the elevation of $[Ca^{2+}]_i$, and to slow inactivation of L type VSCC's. The much greater rate at which $[Ca^{2+}]_i$ is reduced in response to PKC stimulators suggests that Ca^{2+} removal from the cytosol was stimulated to a much greater extent than would be expected from the initial increase in $[Ca^{2+}]_i$ alone. Either a rapid blocking of Ca^{2+} influx or a large increase in the rate of Ca^{2+} removal from the cytosol would account for the dip of $[Ca^{2+}]_i$ below baseline.

As mentioned above, PKC activators can directly reduce Ca^{2+} currents, suggesting that influx could be blocked. The effect of OAG on Ca^{2+} currents was reported to be maximal within 10 sec (228,230). Therefore it is unlikely that this effect of PKC activators is responsible for decrease in $[Ca^{2+}]_i$, since peaks were observed within 54 $\pm$ 5 sec and 27 $\pm$ 4 sec of adding PMA or diC_8 respectively. Alternatively PKC could stimulate the removal of Ca^{2+} from the cytosol. Indeed PKC or phorbol esters are reported to stimulate Ca-ATPase in a Ca^{2+}-sensitive fashion in erythrocyte and vascular smooth muscle plasma membranes (201,203,319). It has been demonstrated, for erythrocyte Ca^{2+} pumps, that the PKC-dependent increase in activity is due to an increase in V_{max} (201). High concentrations of PMA have been shown, in some cases, to further lower already low $[Ca^{2+}]_i$ in GH_4C_1 cells incubated in Ca^{2+}-free medium (292). These reports suggest that PKC also stimulates Ca^{2+} efflux. Therefore the rapid decrease in $[Ca^{2+}]_i$ brought about by PKC activators would be due to the PKC-dependent activation of Ca-ATPase.

The role of PKC in mediating the GRF-induced increase in $[Ca^{2+}]_i$ is unclear, since PKC is not essential for GRF-induced increase in GH release (48). The stimulatory actions of PMA and diC_8 on GH release seen in static incubation and perifusion could be explained by the transient increase in $[Ca^{2+}]_i$. The role of PKC in the GRF response may reside in the stimulation of Ca^{2+} efflux by activation of Ca-ATPase once $[Ca^{2+}]_i$ has increased. An experiment reported by French et al. (48) provides indirect evidence which suggests that this

is indeed the case. In perifusion, the return of GH release to basal levels, after GRF removal, was slower for pituitary cells previously treated with PMA, in order to inactivate PKC, than for control cells (48). In normal somatotrophs, the return to the basal levels is thought to be related to the rate at which $[Ca^{2+}]_i$ returns to baseline, or in other words, to the rate of Ca^{2+} pumping. The differences in the rate at which GH returns to basal levels suggests that Ca-ATPase activity in the PMA-pre-treated cells is reduced. This result is consistent with the stimulatory effect of PKC on Ca-ATPase. Ca^{2+}-dependent activation of PKC (320,321), and not DAG-dependent activation, may be responsible for the increase in the PKC-dependent increase in Ca-ATPase activity during GRF treatment. This hypothesis is reinforced by the observation that GRF does not increase the rate of turnover of the phosphoinositide cycle, a source of DAG (French; personal communication). While PKC may not be involved in the initiation of the GRF $[Ca^{2+}]_i$ response, it may be involved in the plateau phase. The effect of PKC on Ca-ATPase allows for a rapid turning off of GH release, a characteristic which is as important for pulsatile release as is a rapid turning on of secretion.

7.4.5 Summary.

The data in this section suggest that PKC-dependent phosphorylation results in a transient increase in $[Ca^{2+}]_i$ due to an increase in Ca^{2+} influx through L type VSCC's. The increase is inhibited by SRIF. It is unclear whether PKC-dependent phosphorylation activates Ca^{2+} channel directly or indirectly via Na^+-dependent depolarization. The data also suggest that PKC stimulates Ca^{2+} efflux. This effect of PKC is most probably dependent on the stimulation of Ca-ATPase activity.

7.5 Summary.

The possible interactions between $[Ca^{2+}]_i$ and other intracellular signalling systems in the control of GH release by GRF and SRIF were investigated. These intracellular signalling systems include depolarization, cAMP-dependent protein phosphorylation and PKC-dependent protein phosphorylation. Membrane depolarization increases $[Ca^{2+}]_i$ by increasing Ca^{2+} influx through dihydropyridine-sensitive voltage-sensitive Ca^{2+} channels (L type VSCC's). It is unclear whether the GRF-induced depolarization stimulates Ca^{2+} influx or whether it is the result of Ca^{2+} influx. The observation that SRIF does not inhibit the K^+-induced increase in $[Ca^{2+}]_i$ supports the hypothesis that SRIF prevents the GRF-induced increase in $[Ca^{2+}]_i$ by increasing K^+ conductance to hyperpolarize the somatotrophs. Cyclic AMP dependent protein kinase stimulates an increase in $[Ca^{2+}]_i$ by increasing Ca^{2+} influx through L type VSCC's. Most probably the plateau phase of the GRF-induced $[Ca^{2+}]_i$ response is supported by a sustained increase in cAMP accumulation. The cAMP-dependent increase in $[Ca^{2+}]_i$ is sensitive to SRIF. Protein kinase C dependent phosphorylation also stimulates an SRIF-sensitive Ca^{2+} influx through L type VSCC's, leading to a transient increase in $[Ca^{2+}]_i$. It is unclear whether a PKC-induced $[Ca^{2+}]_i$ increase is involved in the mediation of GRF action. However it is possible that PKC-stimulated Ca^{2+} efflux is involved in the GRF response.

CHAPTER 8

THE REGULATION OF $[Ca^{2+}]_i$ BY GRF AND SRIF: A MODEL FOR THE CONTROL OF GH RELEASE

8.1 Introduction.

By way of conclusion, a model for the control of GH release from rat somatotrophs is presented in this chapter. This model proposes that GH release is directly related to $[Ca^{2+}]_i$, and that GRF and SRIF control GH release by regulating $[Ca^{2+}]_i$. The model is based on experimental evidence presented in the body of this thesis and literature cited in the previous chapters. The model attempts to integrate observations concerning Ca^{2+} in a logical order while invoking as few unknown or undocumented processes as possible. It is worth stating that limiting the control of GH release to $[Ca^{2+}]_i$ may be an oversimplification. It is understood that GRF and SRIF may regulate GH release by affecting other intracellular signalling systems. This model does not preclude other "second messengers".

8.2 GH Release is Controlled by $[Ca^{2+}]_i$.

Evidence has been presented which confirms that Ca^{2+} is not only a second messenger for GRF, but that it is essential for stimulated GH release. There is also mounting evidence that Ca^{2+} is not only a trigger for GH release but that $[Ca^{2+}]_i$ sets the rate of GH release. Though Ca^{2+} is essential for GH release, how an increase in $[Ca^{2+}]_i$ stimulates exocytosis is unclear and beyond the scope of this thesis.

First let us review a few observations. The Ca^{2+} ionophore, A23187, stimulates a transient increase in GH release (9) in a concentration dependent manner (4). Calcium ionophores also produce a transient increase in $[Ca^{2+}]_i$ (181). Presumably the concentration dependent effect reflects graded increases in $[Ca^{2+}]_i$. Basal GH release is inhibited by nifedipine and diltiazem in a concentration dependent manner. These same Ca^{2+} antagonists also decrease unstimulated baseline $[Ca^{2+}]_i$ in a concentration dependent manner. Finally GH secretion patterns studied in perifusion are qualitatively similar to the observed changes in $[Ca^{2+}]_i$. Indeed the biphasic $[Ca^{2+}]_i$ response to GRF is reflected in the biphasic GH secretion pattern. 5K produces a transient increase in both $[Ca^{2+}]_i$ and GH release. The increases in $[Ca^{2+}]_i$ induced by cpt-cAMP and PGE_2 are monophasic and biphasic respectively. The GH release patterns for $(Bu)_2$cAMP and PGE_2 are also respectively monophasic and biphasic.

All of the GH secretagogues that have been tested in this study, (GRF, 5K, cpt-cAMP, PGE_2, PMA and diC_8) raise $[Ca^{2+}]_i$ above baseline. All inhibitors of basal GH release tested in this study (nifedipine, diltiazem and SRIF) lower $[Ca^{2+}]_i$ below baseline. All inhibitors of stimulated GH release (Ca^{2+}-free medium, nifedipine, diltiazem and SRIF), with the exception of the effect of SRIF on 5K, prevent $[Ca^{2+}]_i$ from rising above the baseline level. These observations suggest that secretagogues, to be effective, must raise $[Ca^{2+}]_i$ above baseline, while inhibitors of GH release must keep $[Ca^{2+}]_i$ at, or below, baseline.

There is evidence which suggests that $[Ca^{2+}]_i$ fluctuates or oscillates in single unstimulated spontaneously secreting somatotrophs (179). It has been proposed that secretagogues may increase either the frequency or the amplitude of oscillations. To date it is not possible to evaluate dynamic GH release from a single cell; therefore it is not possible to comment if these $[Ca^{2+}]_i$ oscillations are reflected in the GH secretion pattern. However, changing the amplitude or the frequency of these oscillations would result in a change in the average $[Ca^{2+}]_i$ (179,281,322,323). Though the discussion which follows is based on average

responses from cell suspensions, and does not take into account $[Ca^{2+}]_i$ oscillations, it is not inconsistent with the oscillation theory.

8.3 Mechanism for the Regulation of $[Ca^{2+}]_i$ by GRF.

To control GH release, GRF must bind to a specific membrane receptor (110,113-115). A GTP binding protein is associated with this receptor. The G-protein (G_s) is known to stimulate adenylate cyclase (110,123). The increase in adenylate cyclase activity would lead to an accumulation of cAMP which would then stimulate PKA activity.

Active PKA would phosphorylate L type VSCC s which would result in an increase in Ca^{2+} conductance. The phosphorylation could lead to an increase in the number of functional, voltage sensitive, Ca^{2+} channels (225,227). At resting E_m, this in itself may be sufficient to raise Ca^{2+} conductance. Alternatively PKA-dependent phosphorylation, according to the Bean model, could stimulate the conversion of Ca^{2+} channels from the closed "reluctant" to the closed "willing" state. In so doing, the channel voltage sensitivity would be shifted to a more negative range (174). Again this could lead to an increase in Ca^{2+} conductance without prior depolarization. The increased Ca^{2+} conductance would lead to membrane depolarization, which in turn could cause an increase in Na^+ conductance. This would further depolarize the membrane and increase Ca^{2+} conductance even more.

Cyclic AMP could bring about an increase in Na^+ conductance either directly by interacting with TTX-insensitive Na^+ channels or through PKA-dependent phosphorylation of Na^+ channels. The increased Na^+ conductance would lead to depolarization which in turn would stimulate Ca^{2+} influx by causing VSCC's to open.

GRF could also stimulate Ca^{2+} influx without causing VSCC phosphorylation. Recently, cholera toxin-sensitive G-proteins (G_s) have been shown to stimulate Ca^{2+} channels (221). It should be pointed out that Bean (174) favoured G-proteins as regulators for the interconversion between the "willing" and "reluctant" states of the closed VSCC.

The increase in Ca^{2+} influx is the sole mechanism by which $[Ca^{2+}]_i$ is raised in GRF-stimulated somatotrophs. Experiments involving ^{45}Ca uptake and the measurement of $[Ca^{2+}]_i$ in Ca^{2+}-free medium and with Ca^{2+} antagonists, reported in this thesis, all show that GRF stimulates Ca^{2+} influx. Furthermore Ca^{2+} stores, in the somatotrophs, have been shown not to contribute to GRF-dependent increase in $[Ca^{2+}]_i$.

The sequence of events which incorporates all the elements mentioned above is as follows (Figure 47). GRF binds to its receptor and stimulates G_s. G_s, interacting directly with Ca^{2+} channels, shifts their voltage sensitivity to a more negative E_m range, by converting them from the "reluctant" to the "willing" closed state. G_s also stimulates adenylate cyclase which increases cAMP accumulation. The increase in cAMP activates PKA and directly stimulates TTX-insensitive Na^+ channels. Active PKA phosphorylates Ca^{2+} channels making them voltage sensitive. PKA may also phosphorylate Na^+ channels to stimulate them further. The increase in Na^+ conductance leads to depolarization, which causes VSCC's to open. The increased Ca^{2+} conductance leads to a rise in $[Ca^{2+}]_i$ which stimulates exocytosis possibly via a PKC-dependent process.

The increase in $[Ca^{2+}]_i$ also causes an increase in K^+ conductance via Ca^{2+}-dependent channels (K(Ca) channels). The increased conductance would tend to repolarize, if not hyperpolarize, the cell (310). GRF decreases outward K^+ current in somatotrophs (307). This suggests that cAMP or PKA may, as in gonadotrophs, inhibit K(Ca) channels (147). K(Ca)

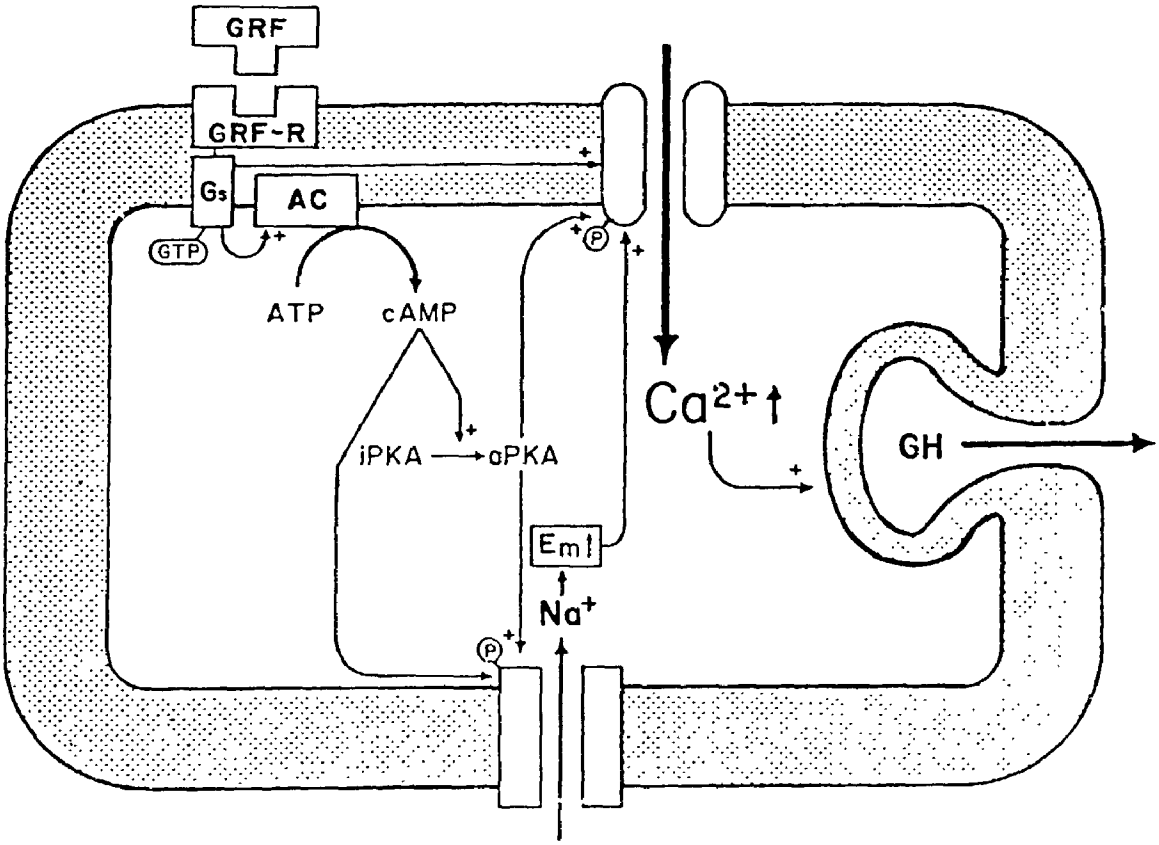

Figure 47. **Model depicting the pathways responsible for the GRF-induced increase in $[Ca^{2+}]_i$ and GH release in rat somatotrophs.** AC: adenylate cyclase; E_m: membrane potential (upward arrow, less negative); G_s: GTP-binding protein G_s; GRF-R: GRF receptor; aPKA: active cAMP-dependent protein kinase; iPKA: inactive cAMP-dependent protein kinase; "+"denotes stimulation; "Ⓟ" denotes channel phosphorylation.

channel activity may explain the lack of full blown action potentials, and the cAMP regulation of the channel may explain the sustained moderate depolarization caused by GRF (125).

8.4 The Biphasic Response: Regulation of $[Ca^{2+}]_i$.

The biphasic nature of the $[Ca^{2+}]_i$ response to GRF is not due to mobilization of stored Ca^{2+}, though stores are present. Both phases of the response are dependent on Ca^{2+} influx. The biphasic nature is due to a difference in the rate of activation of Ca^{2+} influx and the rate of activation of regulatory mechanisms which tend to maintain $[Ca^{2+}]_i$ constant. When influx increases rapidly, $[Ca^{2+}$ increases quickly. In response to this increase, regulatory mechanisms tend to lower $[Ca^{2+}]_i$. If the rates of activation of both processes are of the same order of magnitude, a monophasic increase in $[Ca^{2+}]_i$ occurs. But if the rate of activation of influx is greater than the rate of activation of the regulatory mechanisms, then a biphasic response occurs.

The regulatory mechanisms are of two types, those which decrease Ca^{2+} influx and those which increase Ca^{2+} removal from the cytosol. Those which reduce influx include slow inactivation of Ca^{2+} channels, K(Ca) channel-dependent repolarization, and a decrease in the rate of PKA-dependent phosphorylation (Figure 48). T type Ca^{2+} channels inactivate in approximately 100 msec and L type channels inactivate very slowly and may require minutes to inactivate fully (212,216,218). The high $[Ca^{2+}]_i$ stimulates K(Ca) channels thus causing the membrane potential to become more negative. This decrease in membrane potential would cause VSCC's to close. Adenylate cyclase activity is inhibited by Ca^{2+} (123), thus high $[Ca^{2+}]_i$ would result in a decrease in Na^+ and Ca^{2+} channel phosphorylation. Ca^{2+} channels would close because decreased phosphorylation would render them voltage-insensitive, or shift their voltage sensitivity towards a less negative range of E_m. The decrease in cAMP-dependent

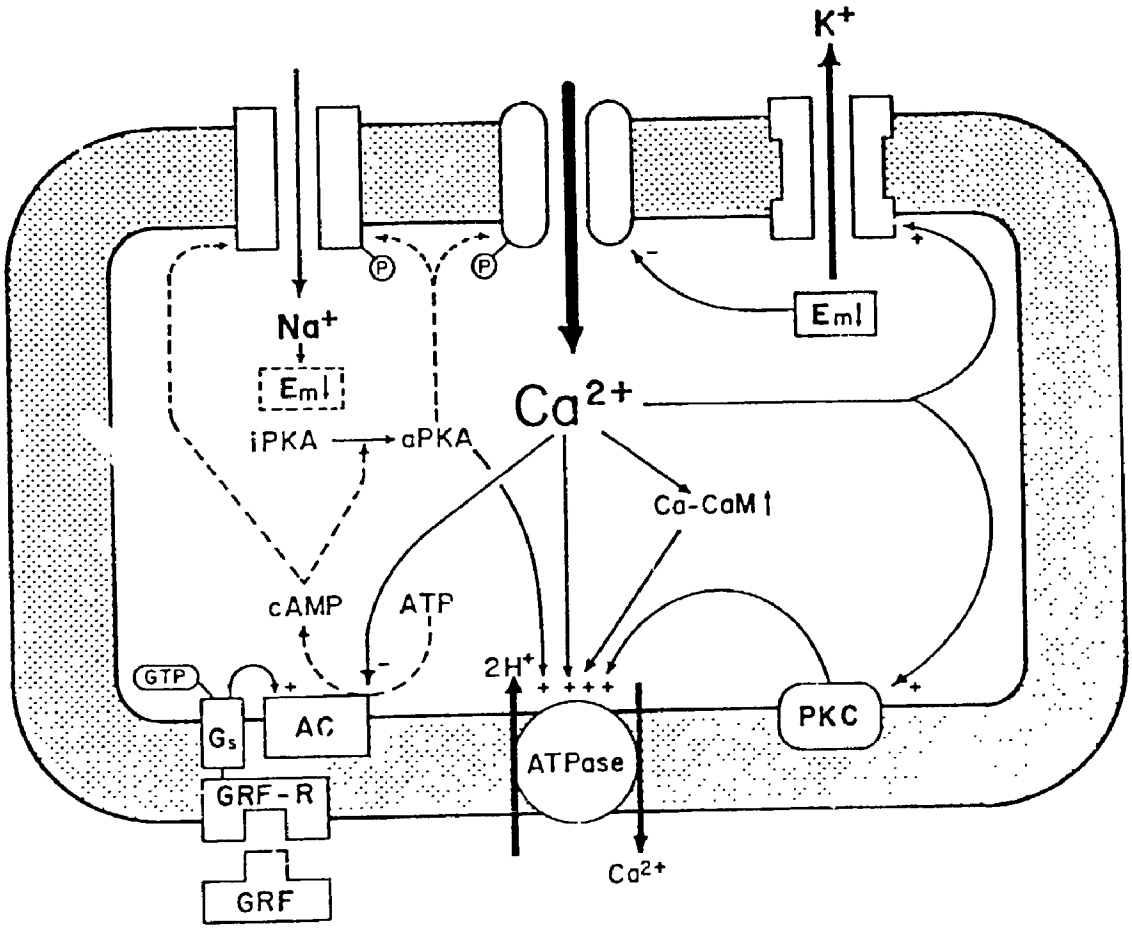

Figure 48. **Model depicting $[Ca^{2+}]_i$ regulatory mechanisms responsible for the biphasic GRF-induced increase in $[Ca^{2+}]_i$ in rat somatotrophs.** AC: adenylate cyclase; Ca-CaM: Ca-calmodulin; E_m: membrane potential (downward arrow, more negative); G_s: GTP-binding protein G_s; GRF-R: GRF receptor; aPKA: active cAMP-dependent protein kinase; iPKA: inactive cAMP-dependent protein kinase; PKC: protein kinase C. "+" denotes stimulation, while "-" denotes inhibition. "Ⓟ" denotes channel phosphorylation. Dashed arrows denote decreased stimulatory effects due to the inhibition of adenylate cyclase by Ca^{2+}.

activation of TTX-insensitive Na^+ channels would lead to a decrease in Na^+ conductance and consequently E_m would become more negative. This would cause more VSCC's to close.

The regulatory mechanisms which remove Ca^{2+} include buffering by soluble Ca^{2+}-binding proteins such as calmodulin (CaM) and pumping of Ca^{2+} into the endoplasmic reticulum or calciosomes and out of the cell by Ca-ATPase (Figure 48). As $[Ca^{2+}]_i$ increases, more and more Ca^{2+} complexes with CaM. By doing so, the concentration of free Ca^{2+} would be buffered. Ca-ATPase activity is under the control of $[Ca^{2+}]_i$, Ca-calmodulin (Ca-CaM), cAMP-dependent phosphorylation and PKC-dependent phosphorylation (187,190,201). As $[Ca^{2+}]_i$ increases, ATPase activity would increase. Though the buffering effect of CaM may be significant, its activation of Ca-ATPase is far more important in $[Ca^{2+}]_i$ regulation. Indeed Ca-CaM increases the K_m for Ca^{2+} of Ca-ATPase (201). Thus not only would the increase in $[Ca^{2+}]_i$ directly stimulate ATPase activity, but by increasing Ca-CaM it would further increase the activity of Ca^{2+} pumps. Since cAMP-dependent phosphorylation also activates Ca-ATPase activity, the signal which stimulates Ca^{2+} influx would also stimulate Ca^{2+} efflux. PKC increases the V_{max} of Ca-ATPase (201). The activity of active, membrane bound, PKC would increase as $[Ca^{2+}]_i$ increases, and bring about an increase in Ca^{2+} pumping.

8.5 Mechanism for the Regulation of $[Ca^{2+}]_i$ by SRIF.

SRIF lowers $[Ca^{2+}]_i$ by decreasing Ca^{2+} influx (Figure 49). SRIF binds to specific membrane receptors and stimulates pertussis toxin-sensitive GTP-binding proteins (G_i) (13,15). The G-protein could interact directly with L type Ca^{2+} channels to alter their voltage sensitivity (174,177). The G-protein may be of the G_k type. G_k is a pertussis toxin-sensitive G-protein which stimulates K^+ channel opening (324-326). The action of G_k would lead to an increase in K^+ conductance which in turn would result in a decrease in E_m to a more negative level. This decrease in E_m would result in the closing of VSCC's.

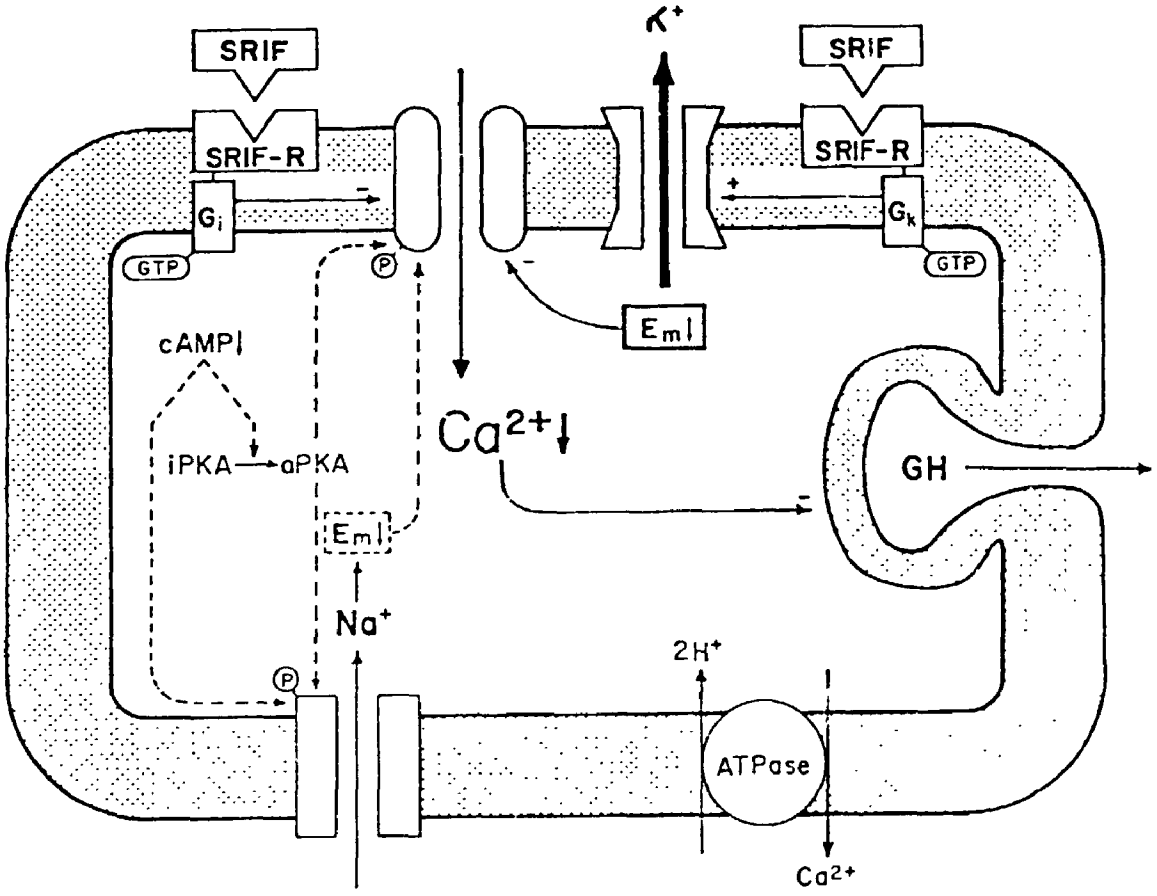

Figure 49. **Model depicting pathways responsible for the SRIF-induced decrease in $[Ca^{2+}]_i$ and inhibition of growth hormone (GH) release in rat somatotrophs.** E_m: membrane potential (downward arrow, more negative); G_i: GTP-binding protein G_i; G_k: GTP-binding protein G_k; aPKA: active cAMP-dependent protein kinase; iPKA: inactive cAMP-dependent protein kinase; PKC: protein kinase C; SRIF-R: SRIF receptor. "+" denotes stimulation, while "-" denotes inhibition. "Ⓟ" denotes channel phosphorylation. Dashed arrows denote decreased stimulatory effects due to the moderate reduction in cAMP accumulation seen in GRF-challenged somatotrophs in the presence of SRIF.

While the inhibitory effect of SRIF on GH release is independent of cAMP, SRIF moderately decreases GRF-induced cAMP accumulation, by an as of yet unknown mechanism. This reduction may not in itself be significant but it may facilitate the SRIF-dependent decrease in $[Ca^{2+}]_i$ in GRF stimulated somatotrophs. This decrease in cAMP would lead to a reduction of Ca^{2+} and Na^+ channel phosphorylation. The resulting decrease in cAMP-dependent activation of TTX-insensitive Na^+ channels would lead to a decrease in Na^+ conductance and to repolarization. The decrease in E_m then would close VSCC's. A decrease in PKA activity would lead to Ca^{2+} channel closure since the resulting decreased phosphorylation would render them voltage-insensitive, or shift their voltage sensitivity towards a less negative range of E_m.

All of these processes probably occur simultaneously. They could all result in a reduction of basal and GRF-stimulated Ca^{2+} influx. and if the rate of Ca^{2+} pumping is not reduced, $[Ca^{2+}]_i$ would decrease. This decrease in $[Ca^{2+}]_i$ would inhibit exocytosis and hence GH release. The possible involvement of several types of G-proteins suggests that either a single SRIF receptor interacts with more than one G-protein or each G-protein is coupled to a specific SRIF receptor (15).

8.6 Future Experimental Testing of the Model.

Many elements of the model remain to be tested in somatotrophs. What follows are outlines of several experimental approaches to test critical points of the model.

One critical point which has to be established is the relationship between the magnitude of $[Ca^{2+}]_i$ and GH release. This should be investigated by simultaneously measuring $[Ca^{2+}]_i$ and GH release. This can be done by perifusing indo-1 or fura-2 loaded somatotrophs in a specially adapted spectrofluorimetric flow-through cuvette, while measuring Ca^{2+}-dependent

fluorescence directly and subsequently assaying GH in the perifusate. The effect of GRF and somatostatin, as well as Ca^{2+}-free medium, Ca^{2+} antagonists, and cAMP analogues on both GH release and $[Ca^{2+}]_i$ would be simultaneously determined.

Another point which should be tested is whether GRF depolarizes somatotrophs. This could be determined by measuring membrane potentials using either classical patch clamp techniques, or the potential-sensitive fluorescent dye bis-oxonol. If, as predicted, GRF depolarizes the cell, then classical electrophysiological approaches should be used to determine which ions are responsible for the depolarization, and the temporal relation between changes in Na^+ and Ca^{2+} conductances. Finally the relationship between an increase in Ca^{2+} conductance and changes in $[Ca^{2+}]_i$ remains to be established. This can be done by simultaneously measuring ion current across the plasma membrane and $[Ca^{2+}]_i$ with fluorescent dyes in the same single cell.

It still remains to be demonstrated that SRIF increases K^+ conductance in somatotrophs. Again classical electrophysiological studies should be carried out to determine whether this is the case. That SRIF inhibits depolarization-induced increases in $[Ca^{2+}]_i$ has not been demonstrated in somatotrophs. The reason why SRIF does not inhibit the increase in $[Ca^{2+}]_i$ stimulated by K^+-dependent depolarization was discussed in chapter 6. To test whether SRIF can inhibit depolarization-induced increases in $[Ca^{2+}]_i$, a similar experiment to the one described in this thesis should be carried out, but using the Na^+ channel activator veratridine, rather than K^+, to depolarize the cells.

The model predicts that the onset of Ca^{2+} influx is dependent on the phosphorylation of L type Ca^{2+} channels by PKA and/or PKC. Before this can be accepted, it would have to be demonstrated that the PKA and/or its catalytic subunits do indeed phosphorylate the dihydropyridine-binding L type Ca^{2+} channel. Once this is established, it will be necessary to

demonstrate that GRF stimulates phosphorylation of dihydropyridine-binding channels in intact somatotrophs.

The involvement of G-proteins in the regulation of either Ca^{2+} and K^+ conductance, and its modulation by GRF and/or SRIF could be investigated using patch-clamp techniques. This would involve carefully combining the use of GTP analogues and pertussis and cholera toxins with protein kinase inhibitors, such that G-protein-dependent effects would not be confounded by channel phosphorylation.

Finally to start investigating the involvement of PKC in the regulation of Ca-ATPase, one should compare the shape of $[Ca^{2+}]_i$ responses to GRF and high K^+ in somatotrophs in which PKC would be inactivated or down regulated by phorbol esters, to that in normal cells. The features of the responses which are sensitive to Ca-ATPase activity, are the biphasic nature of the GRF response and the transient nature of the K^+ response. An increase in the time for $[Ca^{2+}]_i$ to drop from peak to plateau or to baseline in phorbol-treated cells, would indicate the involvement of PKC in the regulation of Ca-ATPase.

8.7 Summary.

The proposed model for the regulation of GH release by GRF and SRIF is based on the apparent relationship between the rate of GH release and $[Ca^{2+}]_i$. The regulation of GH release by GRF and SRIF would involve the regulation of $[Ca^{2+}]_i$. GRF would stimulate GH release by increasing $[Ca^{2+}]_i$. GRF would raise $[Ca^{2+}]_i$ by activating Ca^{2+} influx via cAMP-dependent phosphorylation and G-protein activation of ion channels. The increase in Ca^{2+} influx could be secondary to depolarization. The biphasic nature of GRF-induced increase in $[Ca^{2+}]_i$ would be due to different rates of activation of Ca^{2+} influx and of Ca^{2+} regulatory mechanisms. The regulatory mechanisms would be triggered by the increase in $[Ca^{2+}]_i$ and

would involve inhibition of phosphorylation processes resulting in a decrease in Ca^{2+} influx. The increase in $[Ca^{2+}]_i$ would also stimulate Ca^{2+} pumping.

SRIF would inhibit GH release by decreasing $[Ca^{2+}]_i$. SRIF would lower $[Ca^{2+}]_i$ by decreasing Ca^{2+} conductance by inhibiting Ca^{2+} channels via G-proteins. The SRIF-stimulated interaction between G_k and K^+ channels would lead to hyperpolarization which would result in the closing of Ca^{2+} channels. The moderate SRIF-dependent decrease in cAMP accumulation in GRF-stimulated cells would facilitate the reduction of $[Ca^{2+}]_i$ by decreasing PKA-dependent phosphorylation of VSCC's.

APPENDIX

TRAPPED Ca^{2+} SENSITIVE FLUORESCENT DYES

A.1 Introduction

In 1980 R.Y. Tsien produced a series of chemically engineered Ca^{2+} chelators (244). One of these, quin2, not only binds Ca^{2+} but also fluoresces as it binds Ca^{2+}. The fluorescence of a solution of quin2 is dependent, in a predictable manner, on Ca^{2+} concentration. This chelator, or dye, when introduced into the cytosol of lymphocytes, allowed the measurement of the free intracellular Ca^{2+} concentration (245,247). To introduce the dye into the cell, the acetoxymethyl ester of quin2 (quin2/AM) was used (247). Quin2/AM is membrane permeable and therefore enters the cell. Non-specific intracellular esterases cleave the acetoxymethyl groups off the quin2/AM molecule. Quin2, which is hydrophilic, is then trapped inside the cell. When the cells are exposed to ultraviolet light, quin2 inside the cell fluoresces in the presence of Ca^{2+}.

In 1985 Tsien's group produced two new fluorescent Ca^{2+} chelators, fura-2 and indo-1 (250). The advantage of the new dyes over quin2 is that their affinities for Ca^{2+} are lower (K_d: 224 and 250 nM compared to 115 nM) and their quantum yields are greater (0.49 and 0.56 compared to 0.14 for the dye-Ca complex) (244,250). Another important characteristic of these dyes is the existence of an isobestic point (a wavelength at which the fluorescence is always the same regardless of the $[Ca^{2+}]$) in the excitation spectrum for fura-2 and the emission spectra for indo-1. The fluorescence of the dye in the absence of Ca^{2+} is maximal at a wavelength "a" on one side of this point, while the fluorescence of the dye in the presence of

a saturating concentration of Ca^{2+} is maximal at a wavelength "s" on the other side. The ratio of the fluorescence at both these wavelengths, F_s/F_a, is dependent, in a predictable manner, on Ca^{2+} concentration. The advantage in determining $[Ca^{2+}]_i$ using the fluorescence ratio as opposed to using fluorescence at a single wavelength, is that the measurement is not affected by the amount of dye in the cell or by photobleaching of the dye (249). The ratio technique requires either a spectrofluorometer with two light sources, for fura-2, or with two photodetectors, for indo-1.

In this appendix the three dyes, quin2, fura-2 and indo-1, are characterized in the context of intracellular free Ca^{2+} concentration ($[Ca^{2+}]_i$) measurements in a suspension of acutely dispersed purified rat somatotrophs. Since the spectrofluorimeter used for the study, a Perkin-Elmer LS-5, was equipped with one light source and one photodetector, the focus is on the characteristics which are important for the single excitation-emission wavelength technique.

A.2 Materials and Methods

A.2.1 Solution for Calibration Spectra.

Calcium-magnesium buffers for calibration were made up with a Ca-Mg-EGTA recipes calculated by the Fabiato computer program (327). Serial spectra were obtained form a solution of 20 μM quin2 (tripotassium salt: Q-0501; Sigma Chemical Company, St. Louis, MO), 2 μM fura-2 (pentasodium salt: 34490; Calbiochem, Behring Diagnostic, La Jolla, CA) or 2 μM indo-1 (pentasodium salt: 402095; Calbiochem, Behring Diagnostic, La Jolla, CA) in 115 mM KCl, 20 mM NaCl, 1.252 mM $MgCl_2$, 2.223 mM EGTA and 10 mM MOPS titrated to pH 7.05 with KOH at 37 C (328), to which sequential additions of 87 mM K_2-Ca-EGTA were made. The K_2-Ca-EGTA was prepared from $CaCl_2$, KOH and EGTA using the pH-metric method of Moisescu and

Pusch (329). The pH of the Ca buffer was maintained constant to within 0.005 pH units throughout.

A.2.2 Fluorimetry.

Fluorescence spectra of the dyes and fluorescence measurements of dye loaded cells were obtained with 1 cm disposable plastic fluorometric cuvettes (H116; Hughes and Hughes, Romford, Essex, England) using a Perkin-Elmer LS-5 spectrofluorimeter (Perkin-Elmer Ltd., Beaconsfield, Buckinghamshire, England). The content of the cuvette was kept at 37 C and was continuously mixed by a magnetic microstirrer. Excitation and emission slit widths for spectra were 2.5 nm and 5 nm respectively. For fluorescence measurement of dye loaded cells the excitation and emission slit widths were 5 nm and 10 or 20 nm respectively.

A.2.3 Dye loading of cells.

Acutely dispersed rat pituitary cells (see section 3.1.1) were suspended in 10 ml of M199-AH/37, and allowed to equilibrate for 30 min at 37 C in a siliconized Erlenmeyer flask in a Dubnoff incubator-shaker. The cells were then centrifuged and resuspended in 10 ml of M199-AH/37 to which 10 μl of 10 mM quin2/AM (tetrakisacetoxymethyl ester of quin2: 551828; Calbiochem, Behring Diagnostic, La Jolla, CA), 1 mM fura-2/AM (pentaacetoxymethyl ester of fura-2: 334905; Calbiochem, Behring Diagnostic, La Jolla, CA) or 1 mM indo-1/AM (pentaacetoxymethyl ester of indo-1: I-1203; Molecular Probes, Inc., Eugene, OR) in DMSO were added to give a final concentration of 10 uM, 1 μM and 1 μM respectively. The cells were incubated for 30 min at 37 C, then centrifuged and resuspended in M199-AH/RT. Cell were transferred to 1.5 ml microcentrifuge tubes, and were kept in suspension at room temperature until fluorescence measurements were made. Purified somatotrophs were loaded with indo-1 as described in section 3.4.1.

A.2.4 Fluorescence measurements of dye loaded cells.

Fluorescence measurements of dye loaded cells were carried out as described in section 3.4.2. Calculation of intracellular free Ca^{2+} concentration and of intracellular indo-1 concentration were carried out as described in section 3.4.2 and 3.5. The F_{sat}/F_o ratio in the calculation of F_o was calculated to be 7 and 3 for quin2 and fura-2 respectively, while that for indo-1 was taken to be 12.

A.2.5 Statistical analysis.

Apparent dissociation constants for the dye-Ca complexes were estimated from the negative reciprocal of the slope from the linear regression of the "Scatchard like" plot of fluorescence (328). Linear regression were carried out using the least squares method. Significance of the slope of the regression line was evaluated by either analysis of variance or t-test (330). The comparison of the slope of a regression line with a theoretical value was done using a t-test. An analysis of covariance was used to compare more than two slopes (330).

A.3 Results and Discussion

A.3.1 Quin2

Figure 50 shows one of three sets of excitation and emission spectra for quin2 at different Ca^{2+} concentrations ($[Ca^{2+}]$) at 37 C. The excitation spectra, from 250 nm to 400 nm at a rate of 240 nm/min, were carried out at an emission wavelength of 490 nm. The maximum fluorescence was at 330 nm throughout the range of $[Ca^{2+}]$. The emission spectra, from 400 nm to 600 nm at a rate of 240 nm/min, were carried out at an excitation wavelength of 330 nm. The maximum fluorescence remained nearly constant at 490 nm throughout the range of $[Ca^{2+}]$. The maximal emission and excitation fluorescences were comparable to those reported by Tsien et al. (247) (Em: 492 nm; Ex: 339 nm).

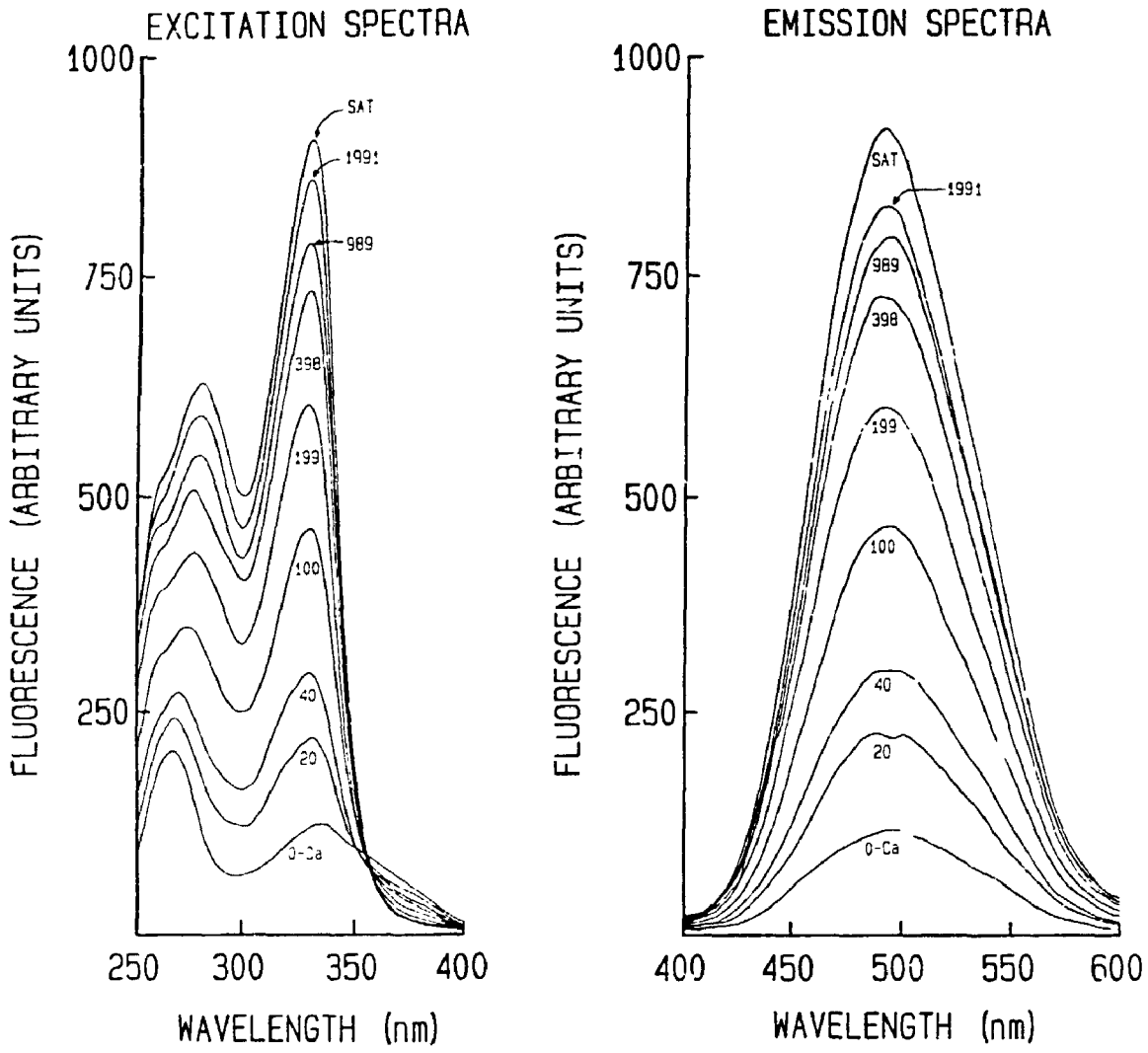

Figure 50. **Excitation and emission spectra of 20 μM quin2 with varying Ca^{2+} concentrations.** The excitation spectra were carried out at an emission wavelength of 490 nm, while the emission spectra were carried out at an excitation wavelength of 330 nm. Excitation and emission slit widths were 2.5 nm and 5 nm respectively. Ca^{2+} was raised stepwise to the level indicated for each individual spectrum by sequential additions of 87 mM K_2-Ca-EGTA to the cuvette. Concentration is indicated in nM, saturating [Ca^{2+}] (SAT) was 1.2 mM. The dye was dissolved in buffer containing 115 mM KCl, 20 mM NaCl, 1.252 mM $MgCl_2$, 2.223 mM K_2-EGTA, 10 mM MOPS at pH 7.05 and at 37 C.

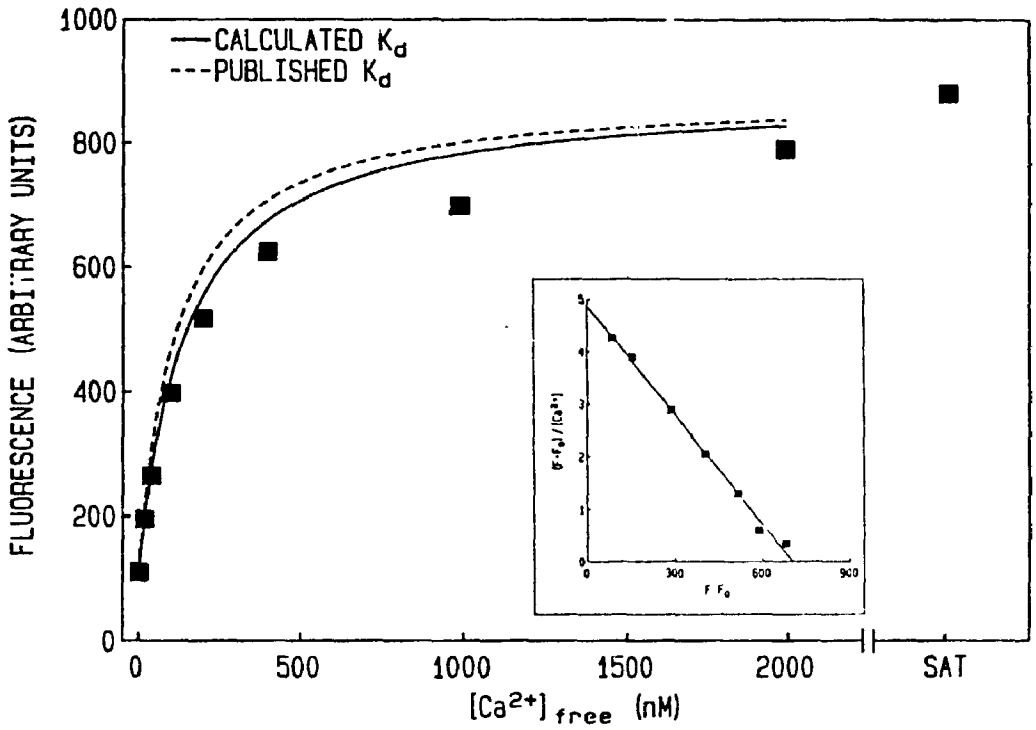

Figure 51. **A calibration curve for quin2 fluorescence vs free Ca^{2+} concentration ($[Ca^{2+}]_{free}$).** Fluorescence was measured with excitation and emission wavelengths of 330 and 490 respectively. The data was taken from the spectra shown in figure 50. Smooth lines were calculated using equation 4. Published K_d: 115 nM; calculated K_d: 139 nM (negative reciprocal of the slope of the Scatchard line). **Inset.** Scatchard plot for Ca^{2+}-dependent fluorescence of quin2. Solid line is the least-square fit to the data. F: quin2 fluorescence; F_o: quin2 fluorescence in the absence of Ca^{2+} (0-Ca)

The apparent K_d was estimated from the negative reciprocal slope of the "Scatchard like" plot of fluorescence. Plots of $(F-F_o)/[Ca^{2+}]$ vs $F-F_o$ were made by taking data from each set of emission spectra (Figure 51 inset). F is the fluorescence at 490 nm of quin2 excited at 330 nm in the presence of the calcium concentration $[Ca^{2+}]$. F_o is the fluorescence at 490 nm of quin2 excited at 330 nm in the absence of Ca^{2+} (0-Ca). A linear regression line was fitted to the data. The estimate of the slope for each of the 3 plots were compared by analysis of covariance and were found not to differ. The data from the three regressions were pooled and a common slope was calculated which gave apparent K_d of 139 $\pm$ 3 nM. The common slope was compared with the slope corresponding to the published value of K_d, 115 nM (247) and was found to be significantly different. Therefore the apparent K_d was 21% greater than the published K_d.

The following equation is used to predict dye fluorescence at a given $[Ca^{2+}]$ (247):

$$F = F_o + \frac{(F_{sat} - F_o) \times ([Ca^{2+}] / K_d)}{1 + ([Ca^{2+}] / K_d)} \qquad [4]$$

where F_o is the dye fluorescence in the absence of Ca^{2+} (0-Ca), F_{sat} is the dye fluorescence in the presence of a saturating concentration of Ca^{2+} and K_d is the dissociation constant for the dye-Ca complex. Figure 51 shows a plot of the fluorescence at 490 nm of quin2 excited at 330 nm, taken from one set of spectra, against free $[Ca^{2+}]$. The solid line shows the predicted dye fluorescence for the observed F_{sat}, F_o and apparent K_d (-1/slope of the Scatchard line). The dashed line shows the predicted dye fluorescence for the published K_d. These curves show that quin2 is most reliable for measuring Ca^{2+} concentrations ranging between 3 and 200 nM since observed quin2 fluorescence at higher $[Ca^{2+}]$ differs from predicted values. Large changes in $[Ca^{2+}]$ result in small changes in fluorescence at $[Ca^{2+}]$ between 200 nM and 2 uM. For this reason any measurement of $[Ca^{2+}]$ greater than 200 nM must be treated

with caution. Using the published K_d curve as opposed to the apparent K_d curve to convert quin2 fluorescence to $[Ca^{2+}]$ (see equation [1], a rearrangement of equation [4], in section 3.4.2) will give rise to small differences at $[Ca^{2+}]$ between 3 and 200 nM. At higher $[Ca^{2+}]$ the differences can be very large. Therefore quin2 is most reliable and least sensitive to the value of K_d used (apparent vs published) to convert fluorescence to $[Ca^{2+}]$ at low Ca^{2+} concentrations.

A.3.2 Fura-2

Figure 52 shows an excitation and emission spectra for fura-2 at different $[Ca^{2+}]$ at 37 C. The excitation spectra, from 250 nm to 400 nm at a rate of 240 nm/min, were carried out at an emission wavelength of 510 nm. The maximum fluorescence of the saturated dye was at 335 nm, whereas the maximum fluorescence of the uncomplexed dye (in the absence of Ca^{2+}) was at 355 nm. These maxima are comparable to those reported by Grynkiewicz et al. (250) (335 and 362 nm respectively). However the greatest difference between F_{sat} and F_0 was at 335 nm. Therefore all subsequent fluorescence measurements were carried out at an excitation wavelength of 335 nm. The emission spectra, from 400 nm to 600 nm at a rate of 240 nm/min, were carried out at an excitation wavelength of 335 nm. The maximum fluorescence remained nearly constant at 495 nm throughout the range of $[Ca^{2+}]$. The maximal excitation fluorescence was comparable to that reported by Grynkiewicz et al. (250) (510 nm).

The apparent K_d was estimated from the negative reciprocal slope of the "Scatchard like" plot of the fluorescence at 495 nm of fura-2 excited at 335 mm taken from the emission spectra (Figure 53 inset). A linear regression line was fitted to the data. The estimate of the slope of the regression line gave an apparent K_d of 143 $\pm$ 11 nM. The slope was compared with the sloped corresponding to the published value for K_d, 224 nM (250), and was found to be significantly different. Therefore the apparent K_d was 36% lower than the published K_d.

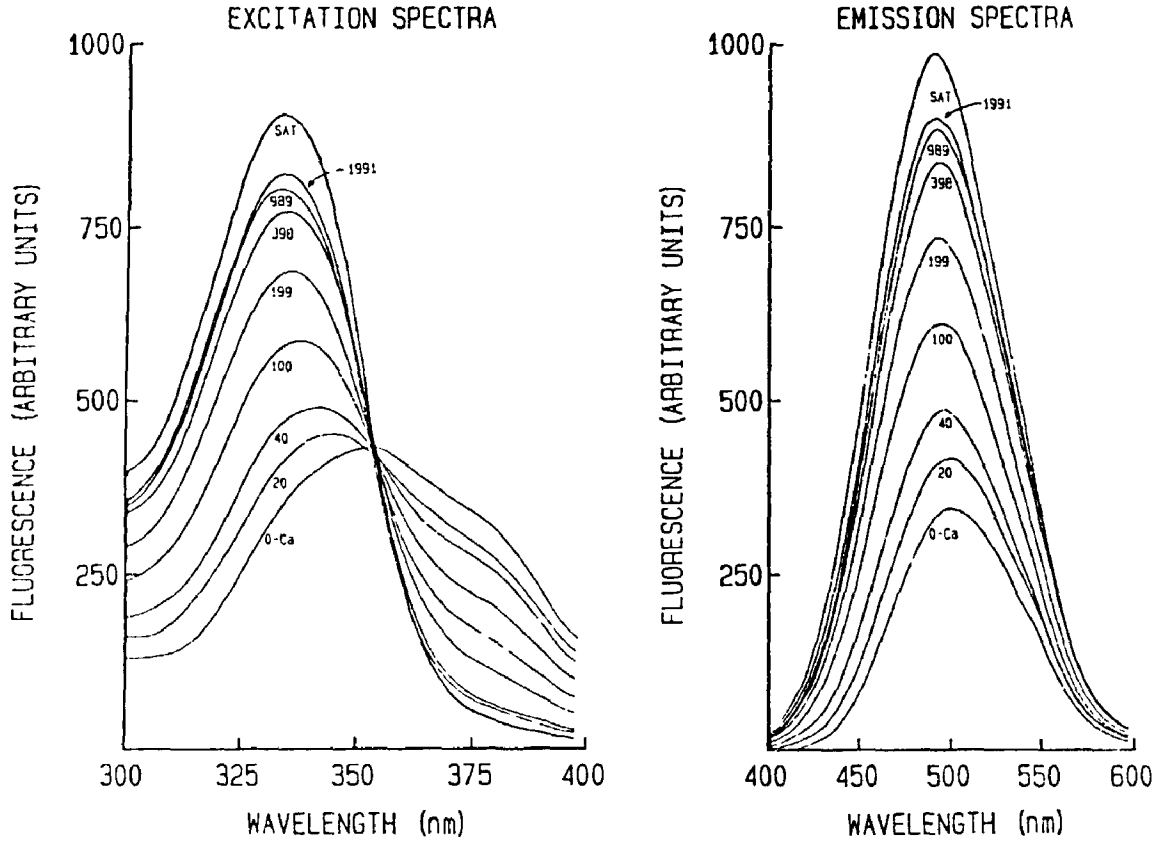

Figure 52. **Excitation and emission spectra of 2 μM fura-2 with varying Ca^{2+} concentrations.** The excitation spectra were carried out at an emission wavelength of 510 nm, while the emission spectra were carried out at an excitation wavelength of 335 nm. Excitation and emission slit widths were 2.5 nm and 5 nm respectively. Ca^{2+} was raised stepwise to the level indicated for each individual spectrum by sequential additions of 87 mM K_2-Ca-EGTA to the cuvette. Concentration is indicated in nM, saturating [Ca^{2+}] (SAT) was 1.2 mM. The dye was dissolved in buffer containing 115 mM KCl, 20 mM NaCl, 1.252 mM $MgCl_2$, 2.223 mM K_2-EGTA, 10 mM MOPS at pH 7.05 and at 37 C.

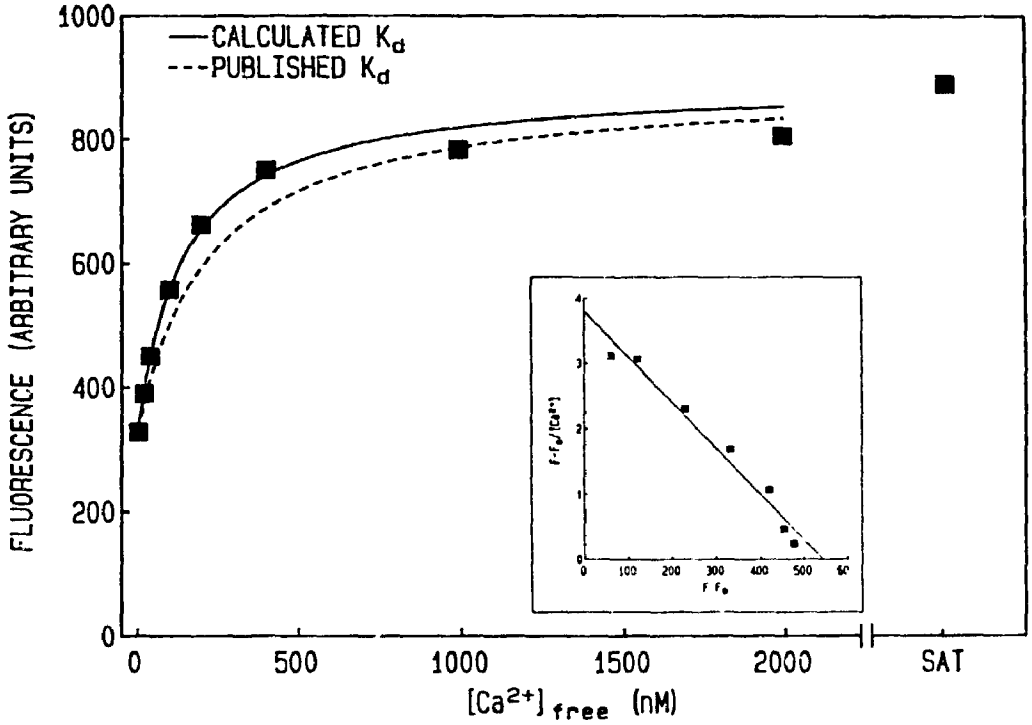

Figure 53. **A calibration curve for fura-2 fluorescence vs free Ca^{2+} concentration ($[Ca^{2+}]_{free}$).** Fluorescence was measured with excitation and emission wavelengths of 335 and 595 respectively. The data was taken from the spectra shown in figure 52. Smooth lines were calculated using equation 4. Published K_d: 224 nM; calculated K_d: 143 nM (negative reciprocal of the slope of the Scatchard line). **Inset.** Scatchard plot for Ca^{2+}-dependent fluorescence of fura2. Solid line is the least-square fit to the data. F: fura2 fluorescence; F_o: fura2 fluorescence in the absence of Ca^{2+} (0-Ca).

Figure 53 shows a plot of the fluorescence at 495 nm of fura-2 excited at 335 nm, taken from the spectra, against free $[Ca^{2+}]$. The solid and dashed line show the predicted dye fluorescence for the apparent K_d (-1/slope of the Scatchard line) and the published K_d respectively. These curves show that fura-2 is most reliable for measuring Ca^{2+} concentrations ranging from 3 nM and 400 nM when using the apparent K_d since observed fura-2 fluorescence at higher $[Ca^{2+}]$ differs from the predicted values. If the published K_d is used then fura-2 is most reliable at $[Ca^{2+}]$ greater than 1 uM. Large changes in $[Ca^{2+}]$ result in small changes in fluorescence at $[Ca^{2+}]$ between 200 nM and 2 uM. For this reason any measurement of $[Ca^{2+}]$ greater than 200 nM must be treated with caution. Using the published K_d curve as opposed to the apparent K_d curve to convert fura-2 fluorescence to $[Ca^{2+}]$ will give rise to small differences at $[Ca^{2+}]$ between 3 and 40 nM. At higher $[Ca^{2+}]$ the differences can be very large. Therefore fura-2 is sensitive to the value of K_d (apparent vs published) used to convert fluorescence to $[Ca^{2+}]$ for low Ca^{2+} concentration.

A.3.3 Indo-1

Figure 54 shows one of three sets of excitation and emission spectra for indo-1 at different $[Ca^{2+}]$ at 37 C. The excitation spectra, from 250 nm to 400 nm at a rate of 240 nm/min, were carried out at an emission wavelength of 405 nm. The maximum fluorescence remained nearly constant at 329 nm throughout the range of $[Ca^{2+}]$. The emission spectra, from 362 nm to 550 nm at a rate of 240 nm/min, were carried out at an excitation wavelength of 329 nm. The maximum fluorescence of the saturated dye was at 405 nm, whereas the maximum fluorescence of the uncomplexed dye (in the absence of Ca^{2+}) was at 468 nm. The maximum for the saturated dye is comparable to that reported by Grynkiewicz et al. (250) (410 nm) while the published wavelength for the maximum fluorescence of the uncomplexed dye is markedly longer at 482 nm. The greatest difference between F_{sat}

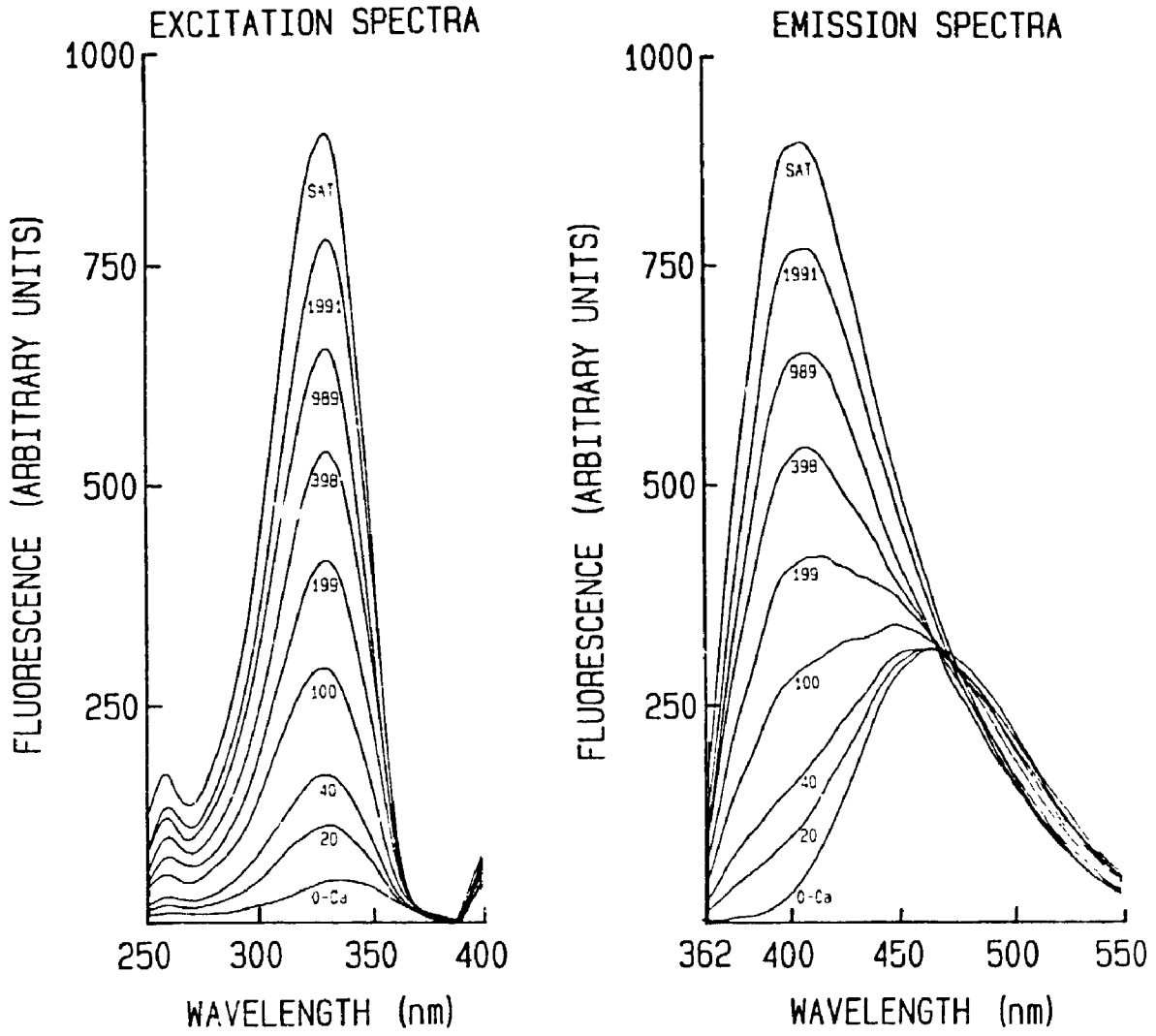

Figure 54. **Excitation and emission spectra of 2 μM Indo-1 with varying Ca^{2+} concentrations.** The excitation spectra were carried out at an emission wavelength of 405 nm, while the emission spectra were carried out at an excitation wavelength of 329 nm. Excitation and emission slit widths were 2.5 nm and 5 nm respectively. Ca^{2+} was raised stepwise to the level indicated for each individual spectrum by sequential additions of 87 mM K_2-Ca-EGTA to the cuvette. Concentration is indicated in nM, saturating [Ca^{2+}] (SAT) was 1.2 mM. The dye was dissolved in buffer containing 115 mM KCl, 20 mM NaCl, 1.252 mM $MgCl_2$, 2.223 mM K_2-EGTA, 10 mM MOPS at pH 7.05 and at 37 C.

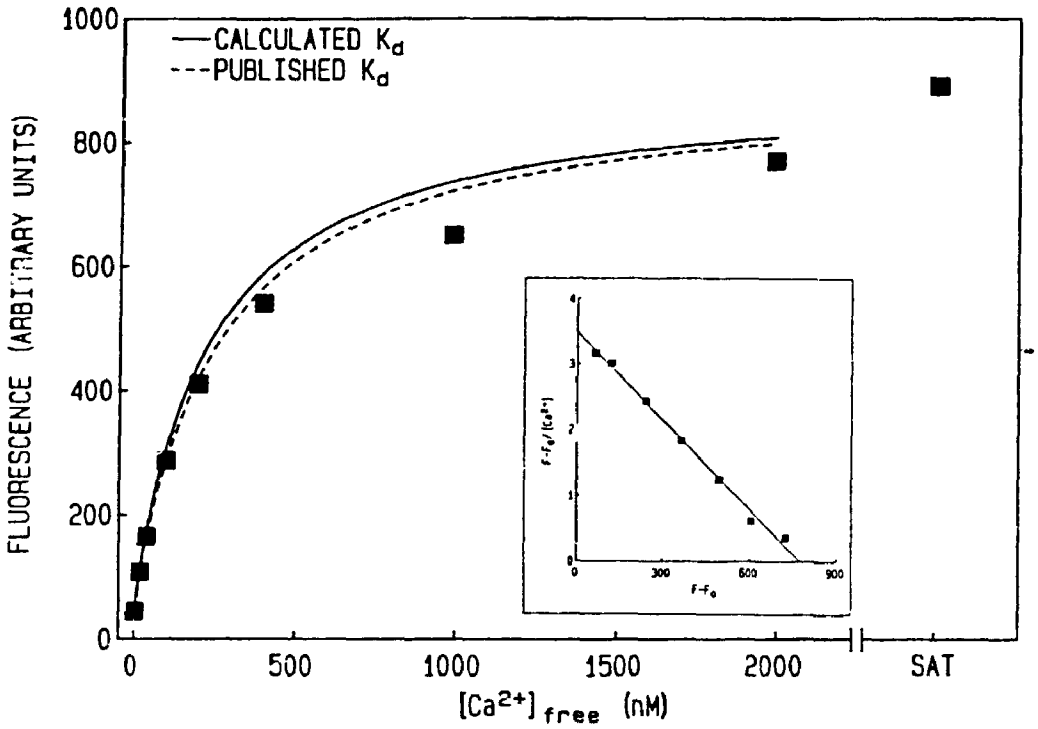

Figure 55. **A calibration curve for indo-1 fluorescence vs free Ca^{2+} concentration ($[Ca^{2+}]_{free}$).** Fluorescence was measured with excitation and emission wavelengths of 329 and 405 respectively. The data was taken from the spectra shown in figure 54. Smooth lines were calculated using equation 4. Published K_d: 250 nM; calculated K_d: 230 nM (negative reciprocal of the slope of the Scatchard line). **Inset.** Scatchard plot for Ca^{2+}-dependent fluorescence of indo-1. Solid line is the least-square fit to the data. F: indo-1 fluorescence; F_o: indo-1 fluorescence in the absence of Ca^{2+} (0-Ca).

and F_o was at 405 nm. Therefore all subsequent fluorescence measurements were carried out at an excitation wavelength of 329 nm and emission wavelength of 405nm.

The apparent K_d was estimated from the negative reciprocal slope of the "Scatchard like" plot of the fluorescence at 405 nm of indo-1 excited at 329 nm taken from each set of emission spectra (Figure 55 inset). A linear regression line was fitted to the data. The estimate of the slope for each of the 3 plots were compared by analysis of covariance and were found not to differ. The data from the three regressions were pooled and a common slope was calculated which gave apparent K_d of 230 $\pm$ 9 nM. The common slope was compared with the slope corresponding to the published value for K_d, 250 nM (250), and was found not to be significantly different.

Figure 55 shows a plot of the fluorescence at 405 nm of indo-1 excited at 329 nm, taken from one set of spectra, against free $[Ca^{2+}]$. The solid and dashed line show the predicted dye fluorescence for the apparent K_d (-1/slope of the Scatchard line) and the published K_d respectively. These curves show that indo-1 is most reliable for measuring Ca^{2+} concentrations ranging from 3 nM and 400 nM since observed indo-1 fluorescence at higher $[Ca^{2+}]$ differs from the predicted values. Large changes in $[Ca^{2+}]$ only results in a small change in fluorescence at $[Ca^{2+}]$ between 400 nM and 2 uM. For this reason any measurement of $[Ca^{2+}]$ greater than 400 nM must be treated with caution.

Indo-1 is the only dye, of the three studied, for which the published K_d is the same as its apparent K_d. As for quin2, it is reliable in predicting $[Ca^{2+}]$ between 3 and 400 nM.

A.3.4 Measurement of $[Ca^{2+}]_i$ in pituitary cells.

To determine which of the three dyes is most appropriate for measuring free intracellular Ca^{2+} concentration in rat pituitary cells, acutely dispersed rat pituitary cells were loaded with

the dyes. Loaded cells ($2.5x10^6$) were transferred to fluorimetric cuvettes, and fluorescence was recorded (Figure 56). Each trace was then analyzed for baseline stability, signal amplitude and signal to noise ratio. The signal amplitude was taken to be the difference between the baseline fluorescence and the maximum fluorescence resulting from the addition of 10^{-9} M rGRF to the cuvette. The signal to noise ratio was calculated by dividing the signal amplitude by the maximum noise amplitude. Baseline and maximum $[Ca^{2+}]_i$ were calculated using either the published or the apparent K_d.

Figure 56 panel A shows an example of a fluorescence recording of quin2 loaded pituitary cells. The baseline fluorescence is stable. The addition of the vehicle for GRF had no effect. GRF caused fluorescence to increase and to slowly reach a plateau. The signal amplitude was 4.25 arbitrary fluorescence units (aFU). The signal to noise ratio for this trace was 2.8. The baseline and maximum $[Ca^{2+}]_i$ were 195 nM and 287 nM respectively, when calculated using the published K_d (115 nM). When the apparent K_d (139 nM) was used, the baseline and maximum $[Ca^{2+}]_i$ were 236 nM and 347 nM respectively.

Panel B in Figure 56 shows an example of a fluorescence recording of fura-2 loaded pituitary cells. The baseline fluorescence, initially drifted upwards, however it stabilized about 1 min before vehicle addition. The addition of vehicle for GRF had no effect. GRF caused a rapid increase in fluorescence to a plateau level. The signal amplitude was 4.50 aFU. The signal to noise ratio for this trace was 2.6. The baseline and maximum $[Ca^{2+}]_i$ were 225 nM and 331 nM respectively, when calculated using the published K_d (224 nM). When the apparent K_d (143 nM) was used, the baseline and maximum $[Ca^{2+}]_i$ were 144 nM and 211 nM respectively.

Figure 56 panel C shows an example of a fluorescence recording of indo-1 loaded pituitary cells. The baseline fluorescence drifted upwards, suggesting that indo-1 was leaking

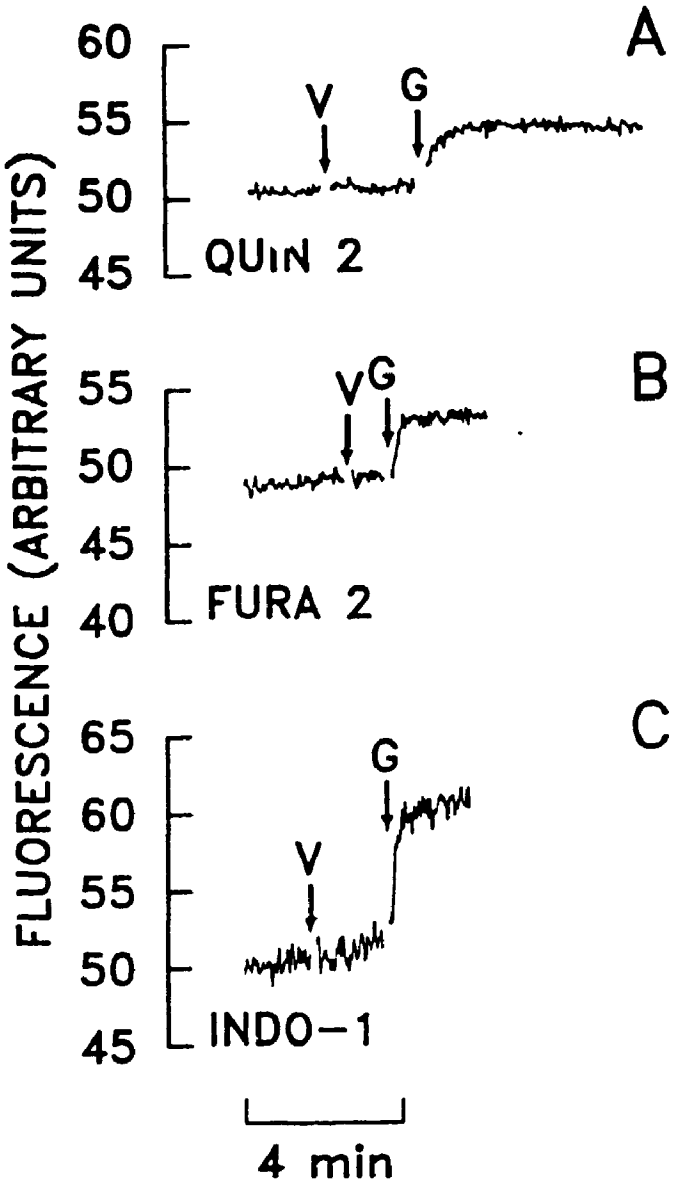

Figure 56. **The effect of GRF on quin2, fura2 and indo-1 Ca^{2+}-dependent fluorescence in rat pituitary cells.** Measurements were carried out with $2.5x10^6$ cells per cuvette in 1.2 mM $CaCl_2$ containing medium at 37 C and pH 7.35-7.4. **A.** Quin2 fluorescence was measured with excitation and emission wavelengths of 330 nm and 490 nm respectively. **B.** Fura2 fluorescence was measured with excitation and emission wavelengths of 335 nm and 495 nm respectively. **C.** Indo-1 fluorescence was measured with excitation and emission wavelengths of 329 nm and 405 nm respectively. Arrows indicate additions to the incubation medium. V: vehicle for GRF; G: 10^{-9} M rGRF.

out of the cells in to the Ca^{2+} containing medium. The addition of vehicle for GRF had no effect. GRF caused a rapid increase in fluorescence. Then fluorescence drifted upwards at the same rate as baseline. The signal amplitude was 8.25 aFU (corrected for drift). The signal to noise ratio for this trace was 3.3. The baseline and maximum $[Ca^{2+}]_i$ were 157 - 170 nM and 224 nM respectively, when calculated using the published K_d (250 nM). When the apparent K_d (230 nM) was used, the baseline and maximum $[Ca^{2+}]_i$ were 146 - 156 nM and 206 nM respectively.

The very different baseline $[Ca^{2+}]_i$'s may be attributed to cell preparations, since each dye was studied on different days using a different cell preparation, or to intrinsic differences of the dyes themselves (275). Though the absolute values may differ from cell type to cell type and from dye to dye, the range of $[Ca^{2+}]_i$ measured is well within the expected range of 100 to 400 nM for rat pituitary cells or rat adenoma cell lines (14,126,180,252,291,331).

Of the three dyes indo-1 had the highest signal amplitude and the largest signal to noise ratio. As already point out, the calculated value for the dissociation constant for the Ca-indo-1 complex (K_d) is the same as the published value. Indo-1 is also reliable in determining $[Ca^{2+}]$ between 3 and 400 nM. For these reasons it was decided to use indo-1 to measure $[Ca^{2+}]_i$ in purified somatotrophs and to use the published value of K_d to convert fluorescence to $[Ca^{2+}]_i$.

A.3.5 Indo-1 $[Ca^{2+}]_i$ measurements in purified somatotrophs.

Fluorescent measurements of indo-1 loaded purified rat somatotrophs were carried out to determine the most appropriate cell density for $[Ca^{2+}]_i$ determination. Different amounts of cells ($2x10^6$, 10^6, $5x10^5$ and $2.5x10^5$) were transferred to fluorometric cuvettes; baseline fluorescence and the response to 10^{-9} M rGRF were monitored (Figure 57).

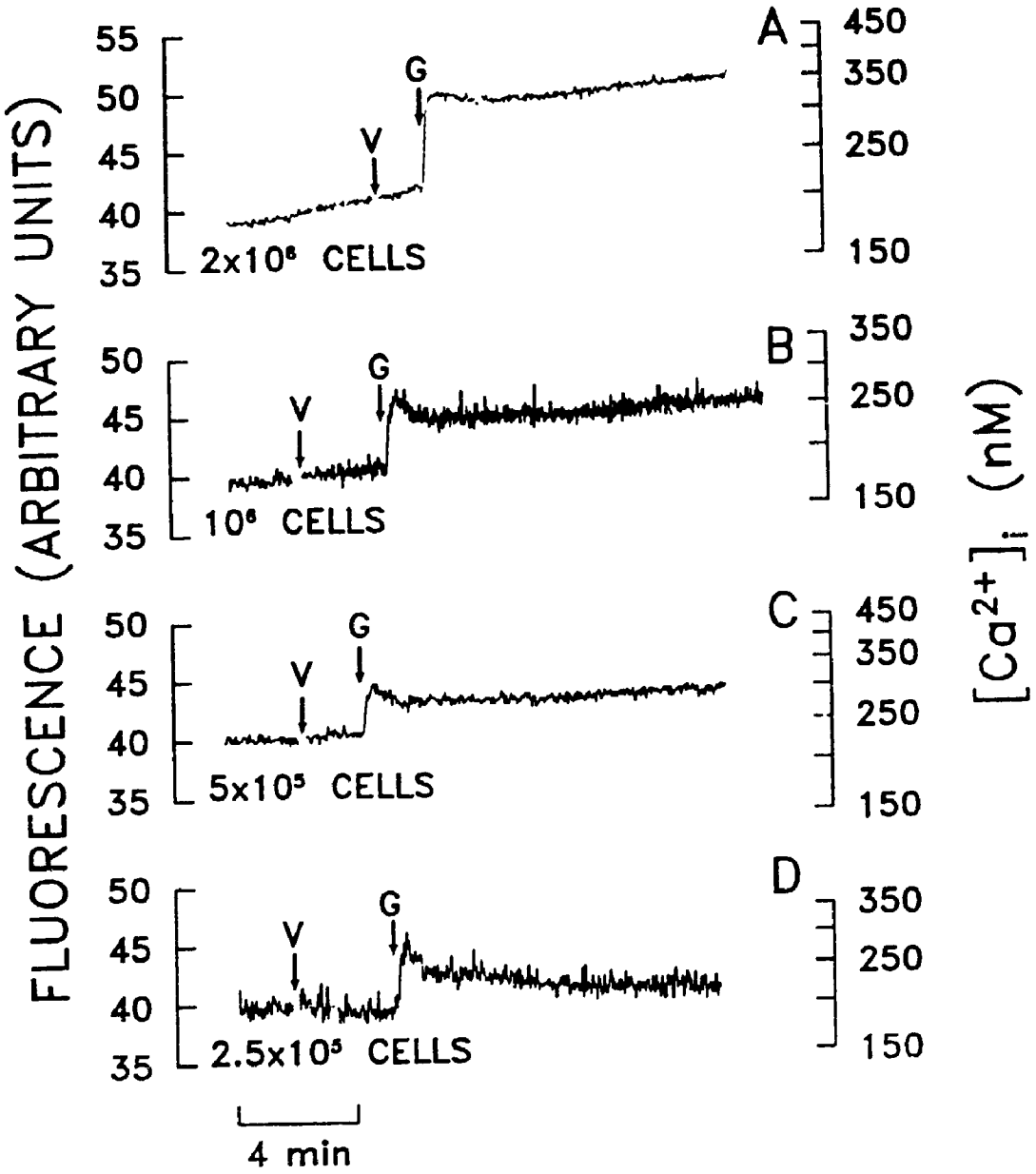

Figure 57. **Effect of cell density on Indo-1 measurements of GRF-induced changes in $[Ca^{2+}]_i$ in rat somatotrophs.** Measurements were carried out in 1.2 mM $CaCl_2$ containing medium at 37 C and pH 7.35-7.4 with excitation and emission wavelengths of 329 nm and 405 nm respectively. **A.** $2x10^6$ cells per cuvette. **B.** 10^6 cells per cuvette. **C.** $5x10^5$ cells per cuvette. **D.** $2.5x10^5$ cells per cuvette. Arrows indicate additions to the incubation medium. V: vehicle for GRF; G: 10^{-9} M rGRF.

At the highest density ($2x10^6$ cells per cuvette) baseline drifted upwards (Figure 57, panel A). As expected GRF caused fluorescence to increase; however the response was biphasic. The first phase consisted of a rapid increase followed by slow decrease to a nadir well above the baseline level. The second phase consisted of upward drift from the nadir at a lower rate than the baseline drift. As the cell density was reduced so was the upward baseline drift, such that at $5x10^5$ cells per cuvette the baseline was stable (Figure 57, panel C). The biphasic response was observed at all densities. When baseline was stable, the second phase of the GRF response was changed to an elevated and stable plateau between peak and baseline levels. Decreasing the number of cells per cuvette also resulted in a drop in the signal to noise ratio from as high as 11.3 at $2x10^6$ cell per cuvette to as low as 2.0 for $2.5x10^5$ cells per cuvette.

The upward drift of baseline fluorescence suggests that indo-1 is leaking out of the cell into the Ca^{2+} medium (leaked dye fluoresces maximally). With $2x10^6$ cells per cuvette, the amount of leaked indo-1 would result in a significant overall change in fluorescence with time. When the cell density is reduced, the amount of leaked indo-1 would result in an insignificant overall change in fluorescence, therefore the baseline would be stable. To determine the magnitude of indo-1 leakage, the intracellular indo-1 concentration was monitored over time (for about 300 min). Out of 39 experiments, totalling 278 measurements, only 4 showed a significant decrease in intracellular [indo-1]. The rate of loss of dye was between 0.19 uM/min and 0.049 uM/min. At the higher rate of loss, $2x10^6$ cells would increase the extracellular dye concentration at a rate of 320 pM/min, while $5x10^5$ cells would increase the concentration at a rate of 83 pM/min. The fluorescence due to 320 pM Ca-bound indo-1 is within the limits of detection of the spectrofluorometer, while that due to 83 pM Ca-bound indo-1 is not. Therefore dye leakage from $2x10^6$ cells would be detectable and that from $5x10^5$ would not.

The calculated $[Ca^{2+}]_i$ was not dependent on the cell density (Table III).

TABLE III. Calculated $[Ca^{2+}]_i$ for baseline and 10^{-9} M rGRF-induced peak and plateau indo-1 fluorescence for 2 measurements from dispersed pituitary cells at different densities.

Cell Density*	Calculated $[Ca^{2+}]_i$†		
	Baseline	Peak	Plateau‡
$2x10^6$	210, 270	314, 322	340, 353
10^6	199, 178	304, 250	286, 250
$5x10^5$	205, 236	321, 304	285, 300
$2.5x10^5$	216, 191	312, 278	305, 219

* Number of cells per fluorometric cuvette.
† K_d = 250 nM.
‡ $[Ca^{2+}]_i$ at the end of the observation period.

It was decided that $[Ca^{2+}]_i$ measurements would be carried out with $5x10^5$ cells per cuvette since, at this density, the baseline is stable, the biphasic response to GRF is present, the signal to noise ratio varies from 11.7 to 3.1, and a somatotroph preparation from 20 rats allows up to 16 determinations.

REFERENCES

1. Sheppard MS, Moss RL, Kraicer J (1984) Release of growth hormone (GH) from purified somatotrophs: interaction of GH releasing factor and somatostatin and role of adenosine 3',5' monophosphate. Endocrinology 115:2484-2491

2. Barinaga M, Bilezikjian LM, Vale WW, Rosenfeld MG, Evans RM (1984) Dual hypothalamic effects of growth hormone releasing factor on growth hormone release and gene transcription. Nature 314:279-281

3. Bilezikjian LM, Vale WW (1983) Stimulation of adenosine 3',5' monophosphate production by growth hormone releasing factor and its inhibition by somatostatin in rat pituitary cells in vitro. Endocrinology 113:1726-1731

4. Kraicer J, Spence JW (1981) Release of growth hormone from purified somatotrophs. I. Role of high K^+ and the ionophore A23187 to elucidate intracellular mechanisms of Ca^{++} stimulation. 3',5' monophosphate, and somatostatin. Endocrinology [illegible]

5. Sheppard MS, Kraicer [illegible] JW (1984) Mechanisms controlling the release of growth hormone from acutely [illegible] rat pituitary somatotrophs. In: Isaacs JA (ed) Perinatal Biochemical Endocrinology. Synthesis and Release of Adenohypophyseal Hormones. Plenum Press, New York, pp 405-424

6. Sheppard MS, Spence JW, Kraicer J (1983) Release of growth hormone from purified somatotrophs. Role of adenosine 3',5' monophosphate and [illegible] 3',5' monophosphate. Endocrinology 112:2011-2019

7. [illegible] (1985) A short review on the mechanism of somatotrophin release from rat pituitary cells. Endocrinology 117:1-6

8. [illegible] (1984) Release of growth hormone from purified somatotrophs: [illegible] and adenosine 3',5' monophosphate. Endocrinology 114:1954-1964

9. [illegible] (1984) Release of growth hormone from purified somatotrophs. [illegible] of [illegible] on stimulated concentrations of [illegible] 3',5' monophosphate and somatostatin. Endocrinology [illegible]

10. [illegible] (1984) [illegible] Endocrinology [illegible]

11. [illegible] (1984) [illegible] Endocrinology [illegible]

12. [illegible] (1984) [illegible] Endocrinology [illegible]

13. Koch BD, Dorflinger LJ, Schonbrunn A 1985 Pertussis toxin blocks both cyclic AMP-mediated and cyclic AMP-independent actions of somatostatin. J Biol Chem 260:13138-13145

14. Luini A, Lewis D, Guild S, Schofield G, Weight F 1986 Somatostatin, an inhibitor of ACTH secretion, decreases cytosolic free calcium and voltage-dependent calcium current in a pituitary cell line. J Neurosci 6:3128-3132

15. Thermos K, Reisine T 1988 Somatostatin receptor subtypes in the clonal anterior pituitary cell lines AtT-20 and GH_3. Mol Pharmacol 33:370-377

16. Knobil E 1966 The pituitary growth hormone: An adventure in physiology. Physiologist 9:25-44

17. Evans HM, Long JA 1921 The effect of the anterior lobe administered intraperitoneally upon growth, maturity, and oestrous cycles of the rat. Anat Rec 21:62-63

18. Popa G, Fielding U 1930 A portal circulation from the pituitary to the hypothalamic region. J Anat 65:88-91

19. Harris GW 1964 The development of ideas regarding hypothalamic-releasing factors. Metabolism 13:207-212

20. Franz J, Haselbach CH, Libert O 1962 Studies of the effect of hypothalamic extracts on somatotrophic pituitary function. Acta Endocrinol (Copenhagen) 41:336-350

21. Deuben RR, Meites J 1964 Stimulation of pituitary growth hormone release by a hypothalamic extract in vitro. Endocrinology 74:408-414

22. Pecile A, Müller E, Falconi G, Martini L 1965 Growth hormone-releasing activity of hypothalamic extracts at different ages. Endocrinology 77:241-246

23. Krulich L, Dhariwal APS, McCann SM 1965 Growth hormone-releasing activity of crude ovine hypothalamic extracts. Proc Soc Exp Biol Med 120:180-184

24. Machlin LJ, Horino M, Kipnis DM, Phillips SL, Gordon RS 1967 Stimulation of growth hormone secretion by median eminence extracts in the sheep. Endocrinology 80:205-207

25. Wilber JF, Porter JC 1970 Thyrotropin and growth hormone releasing activity in hypophysial portal blood. Endocrinology 87:807-811

26. Frohman LA, Maran JW, Dhariwal APS 1971 Plasma growth hormone responses to intrapituitary injections of growth hormone releasing factor (GRF) in the rat. Endocrinology 88:1483-1488

27. Reichlin S 1960 Growth and the hypothalamus. Endocrinology 67:760-773

28. Reichlin S 1961 Growth hormone content of the pituitaries from rats with hypothalamic lesions. Endocrinology 69:225-230

29. Frohman LA, Bernardis LL 1968 Growth hormone and insulin levels in weanling rats with ventromedial hypothalamic lesions. Endocrinology 82:1125-1132

30. Martin JB, Renaud LP, Brazeau P Jr 1974 Pulsatile growth hormone secretion: suppression by hypothalamic ventromedial lesions and by long-acting somatostatin. Science 186:538-540

31. Frohman LA, Bernardis LL, Kant KJ 1968 Hypothalamic stimulation of growth hormone secretion. Science 162:580-582

32. Martin JB 1972 Plasma growth hormone (GH) response to hypothalamic or extrahypothalamic electrical stimulation. Endocrinology 91:107-115

33. Krulich L, Dhariwal APS, McCann SM 1968 Stimulatory and inhibitory effects of purified hypothalamic extracts on growth hormone release from rat pituitary in vitro. Endocrinology 83:783-790

34. Rice RW, Critchlow V 1976 Extrahypothalamic control of stress-induced inhibition of growth hormone secretion in the rat. Endocrinology 99:970-976

35. Willoughby JO, Martin JB 1978 Pulsatile growth hormone secretion: inhibitory role of medial preoptic area. Brain Res 148:240-244

36. Martin JB 1976 Brain regulation of growth hormone secretion. In: Martini L, Ganong WF (eds) Frontiers in Neuroendocrinology, Vol. 4, Raven Press, New York, pp 129-168

37. Guillemin R, Brazeau P, Böhlen P, Esch F, Ling N, Wehrenberg WB 1982 Growth hormone-releasing factor from a human pancreatic tumor that caused acromegaly. Science 218:585-587

38. Rivier J, Spiess J, Thorner M, Vale W 1982 Characterization of a growth hormone-releasing factor from a human pancreatic islet tumour. Nature 300:276-278

39. Spiess J, Rivier J, Vale W 1983 Charactreization of rat hypothalamic growth hormone-releasing factor. Nature 303:532-535

40. Ling N, Esch F, Böhlen P, Brazeau P, Wehrenberg WB, Guillemin R 1984 Isolation, primary structure, and synthesis of human hypothalamic somatocrinin: Growth hormone-releasing factor. Proc Natl Acad Sci U S A 81:4302-4306

41. Brazeau P, Ling N, Böhlen P, Esch F, Ying S-Y, Guillemin R 1982 Growth hormone releasing factor, somatocrinin, releases pituitary growth hormone in vitro. Proc Natl Acad Sci U S A 79:7909-7913

42. Michel D, Lefèvre G, Labrie F 1983 Interactions between growth hormone-releasing factor, prostaglandin E_2 and somatostatin on cyclic AMP accumulation in rat adenohypophysial cells in culture. Molec Cell Endocrinol 33:255-264

43. Vale W, Vaughan J, Yamamoto G, Spiess J, Rivier J 1983 Effects of synthetic human pancreatic (tumor) GH releasing factor and somatostatin, triiodothyronine and dexamethasone on GH secretion in vitro. Endocrinology 112:1553-1555

44. Brazeau P, Ling N, Esch F, Böhlen P, Mougin C, Guillemin R 1982 Somatocrinin (growth hormone releasing factor) in vitro bioactivity; Ca^{++} involvement, cAMP mediated action and additivity of effect with PGE_2. Biochem Biophys Res Commun 109:588-594

45. Kraicer J, Sheppard MS, Luke J, Lussier B, Moor BC, Cowan JS 1988 Effect of withdrawal of somatostatin and growth hormone (GH)-releasing factor on GH release in vitro. Endocrinology 122:1810-1815

46. Kraicer J, Lussier B, Moor BC, Cowan JS 1988 Failure of growth hormone (GH) to feed back at the level of the pituitary to alter the response of the somatotrophs to GH-releasing factor. Endocrinology 122:1511-1514

47. Kato M, Suzuki M 1986 Time course and extracellular Ca^{2+} involvement of growth hormone (GH) releasing factor-induced GH secretion in perifused dispersed rat pituiray cells. Jpn J Physiol 36:1225-1239

48. French MB, Moor BC, Lussier BT, Kraicer J 1989 Protein kinase C is not essential for growth hormone (GH)-releasing factor-induced GH release from rat somatotrophs. Endocrinology 124:2235-2244

49. Lussier BT, Moor BC, French MB, Kraicer J 1988 Release of growth hormone from purified somatotrophs: effects of the calcium channel antagonists diltiazem and nifedipine on release induced by growth hormone-releasing factor. Can J Physiol Pharmacol 66:1373-1380

50. Holl RW, Thorner MO, Leong DA 1988 Intracellular calcium concentration and growth hormone secretion in individual somatotropes: effects of growth hormone-releasing factor and somatostatin. Endocrinology 122:2927-2932

51. Wehrenberg WB, Ling N, Brazeau P, Esch F, Böhlen P, Baird A, Ying S, Guillemin R 1982 Somtocrinin, growth hormone releasing factor, stimulates secretion of growth hormone in anesthetized rats. Biochem Biophys Res Commun 109:382-387

52. Tannenbaum GS, Ling N 1984 The interrelationship of growth hormone (GH)-releasing factor and somatostatin in generation of the ultradian rhythm of GH secretion. Endocrinology 115:1952-1957

53. Tannenbaum GS, Eikelboom R, Ling N 1983 Human pancreas GH-releasing factor analog restores high-amplitude GH pulses in CNS lesion-induced GH deficiency. Endocrinology 113:1173-1175

54. Bloch B, Gaillard RC, Brazeau P, Lin HD, Ling N 1984 Topographical and ontogeneic study of the neurons producing growth hormone-releasing factor in human hypothalamus. Regul Pept 8:21-31

55. Jacobowitz DM, Schulte H, Chrousos GP, Loriaux L 1983 Localization of GRF-like immunoreactive neurons in the rat brain. Peptides 4:521-524

56. Bloch B, Brazeau P, Bloom F, Ling N 1983 Topographical study of the neurons containing hpGRF immunoreactivity in monkey hypothalamus. Neurosci Lett 37:23-28

57. Bloch B, Brazeau P, Ling N, Bohlen P, Esch F, Wehrenberg WB, Benoit R, Bloom F, Guillemin R 1983 Immunohistochemical detection of growth hormone-releasing factor in brain. Nature 301:607-608

58. Miki N, Ono M, Shizume K 1984 Evidence that opiatergic and α-adernergic mechamisms stimulate rat growth hormone release via growth hormone-releasing factor (GRF). Endocrinology 114:1950-1952

59. Wehrenberg WB, Bloch B, Ling N 1985 Pituitary secretion of growth hormone in response to opioid peptides and opiates is mediated through growth hormone-releasing factor. Neuroendocrinology 41:13-16

60. Murakami Y, Kato Y, Kabayama Y, Tojo K, Inoue T, Imura H 1985 Involvement of growth hormone-releasing factor in growth hormone secretion induced by gamma-aminobutyric acid in conscious rats. Endocrinology 117:787-789

61. Frohman LA, Jansson J-O 1986 Growth hormone-releasing hormone. Endocr Rev 7:223-253

62. Arimura A, Culler MD 1985 Regulation of growth hormone secretion. In: Imura H (ed) The pituitary gland, Raven Press, New York, pp 221-259

63. Katakami H, Downs TR, Frohman LA 1987 Effect of hypophysectomy on hypothalamic growth hormone-releasing factor content and release in the rat. Endocrinology 120:1079-1082

64. Brazeau P, Vale W, Burgus R, Ling N, Butcher M, Rivier J, Guillemin R 1973 Hypothalamic polypeptide that inhibits the secretion of immunoreactive pituitary growth hormone. Science 179:77-79

65. Brazeau P, Rivier J, Vale W, Guillemin R 1974 Inhibition of growth hormone secretion in the rat by synthetic somatostatin. Endocrinology 94:184-187

66. Esch F, Böhlen P, Ling N, Benoit R, Brazeau P, Guillemin R 1980 Primary structure of ovine hypothalamic somatostatin-28 and somatostatin-25. Proc Natl Acad Sci U S A 77:6827-6831

67. Pradayrol L, Jörnvall H, Mutt V, Ribet A 1980 N-Terminally extended somatostatin: the primary structure of somatostatin-28. FEBS Lett 109:55-58

68. Schally AV, Huang W-Y, Chang RCC, Arimura A, Redding TW, Millar RP, Hunkapiller MW, Hood LE 1980 Isolation and structure of pro-somatostatin: A putative somatostatin precursor from pig hypothalamus. Proc Natl Acad Sci U S A 77:4489-4493

69. Meyers CA, Murphy WA, Redding TW, Coy DH, Schally AV 1980 Synthesis and biological actions of prosomatostatin. Proc Natl Acad Sci U S A 77:6171-6174

70. Brazeau P, Ling N, Esch F, Böhlen P, Benoit R, Guillemin R 1981 High biological activity of the synthetic repicaltes of somatostatin-28 and somatostatin-25. Regul Pept 1:255-264

71. Benoit R 1987 Peptides derived from mammalian prosomatostatin. In: Reichlin S (ed) Somatostatin: basic and clinical status, Plenum Press, New York, pp 33-50

72. Brazeau P 1986 Somatostatin: A peptide with unexpected physiologic activities. Am J Med 81(Suppl 6B):8-13

73. Owyang C, Wiley J 1987 Somatostatin inhibits intestinal motility via modulation of cyclic AMP-dependent cholinergic transmission. In: Reichlin S (ed) Somatostatin: basic and clinical status, Plenum Press, New York, pp 253-258

74. Dharmsathaphorn K 1987 Somatostatin in gastrointestinal function: Intestinal absorption and secretion. In: Reichlin S (ed) Somatostatin: basic and clinical status, Plenum Press, New York, pp 267-273

75. Pittenger GL, Vinik AI, Heldsinge AA, Seino S 1985 Regulation and actions of gastrointestinal somatostatin. In: Patel YC, Tannenbaum GS (eds) Somatostatin, Plenum Press, New York, pp 447-462

76. Dharmsathaphorn K 1985 Intestinal somatostatin function. In: Patel YC, Tannenbaum GS (eds) Somatostatin, Plenum Press, New York, pp 463-473

77. Solomon TE 1987 Effect of somatostatin on exocrine pancreas. In: Reichlin S (ed) Somatostatin: basic and clinical status, Plenum Press, New York, pp 275-283

78. Weir GC, Bonner-Weir S 1985 Pancreatic somatostatin. In: Patel YC, Tannenbaum GS (eds) Somatostatin, Plenum Press, New York, pp 403-423

79. Cowan JS, Moor B, Chow A, Kraicer J 1983 Characteristics of post-somatostatin reboun in growth hormone secretion from perifused somatotrophs. Endocrinology 113:1056-1061

80. Kraicer J, Cowan JS, Sheppard MS, Lussier B, Moor BC 1986 Effect of somatostatin withdrawl and growth hormone (GH)-releasing factor on GH release in vitro: amount available for release after disinhibition. Endocrinology 119:2047-2051

81. Gómez-Pan A, Rodriguez-Arnao MD 1983 Somatostatin and growth hormone releasing factor: synthesis, location, metabolism and function. Clin Endocrinol Metab 12:463-507

82. Vale W, Rivier C, Brown M 1977 Regulatory peptides of the hypothalamus. Annu Rev Physiol 39:473-527

83. Tannenbaum GS 1985 Physiological role of somatostatin in regulation of pulsatile growth hormone secretion. In: Patel YC, Tannenbaum GS (eds) Somatostatin, Plenum Press, New York, pp 229-259

84. Cowan JS, Layberry RA, Moor BC, Kraicer J 1985 Somatostatin can block the growth hormone releasing action of growth hormone-releasing factor in conscious dogs. Can J Physiol Pharmacol 63:Aix (Abstract)

85. Cowan JS, Gaul P, Moor BC, Kraicer J 1984 Secretory bursts of growth hormone secretion in the dog may be initiated by somatostatin withdrawal. Can J Physiol Pharmacol 62:199-207

86. Patel YC, Sirkant CB 1986 Somatostatin mediation of adenohypophysial secretion. Annu Rev Physiol 48:551-567

87. Alpert LC, Brawer JR, Patel YC, Reichlin S 1976 Somatostatinergic neurons in anterior hypothalamus: immunohistochemical localization. Endocrinology 98:255-258

88. Hökfelt T, Efendić S, Hellerström C, Johansson O, Luft R, Arimura A 1975 Cellular localization of somatostatin in endocrine-like cells and neurons of the rat with special references to A_1-cells of the pancreatic islets and to the hypoythalamus. Acta Endocrinol (Copenhagen) 80(Suppl. 200):5-41

89. Elde RP, Parsons JA 1975 Immunocytochemical localization of somatostatin in cell bodies of the rat hypothalamus. Am J Anat 144:541-548

90. Finley JCW, Maderdurt JL, Roger LJ, Petrusz P 1981 The immunocytochemical localization of somatostatin-containing neurons in the rat central nervous system. Neuroscience 6:2173-2192

91. Krisch B 1979 Immunohistochemical results on the distribution of somatostatin in the hypothalamus and in limbic structures of the rat. J Histochem Cytochem 27:1389-1390

92. Hökfelt T, Efendic S, Johansson O, Luft R, Arimura A 1974 Immunohistochemical localization of somatostatin (growth hormone release-inhibiting factor) in the guinea pig brain. Brain Res 80:165-169

93. Robins R 1987 Regulation of hypothalamic somatostatin secretion. In: Reichlin S (ed) Somatostatin: basic and clinical status, Plenum Press, New York, pp 149-156

94. Reichlin S 1983 Somatostatin. In: Krieger DT, Brownstein MJ, Martin JB (eds) Brain peptides, John Wiley and Sons, New York, pp 711-752

95. Arimura A, Fishback JB 1981 Somatostatin: regulation of secretion. Neuroendocrinology 33:246-256

96. Peterfrund RA, Vale W 1985 Somatostatin secretion from the hypothalamus. In: Patel YC, Tannenbaum GS (eds) Somatostatin, Plenum Press, New York, pp 183-200

97. Wakabayashi I, Demura R, Kanda M, Demura H, Shizume K 1976 Effect of hypophysectomy on hypothalamic somatostatin content in rats. Endocrinol Jpn 23:439-442

98. Hoffman DL, Baker BL 1977 Effect ot treatment with growth hormone on somatostatin in the median eminence of hypophysectomized rats. Proc Soc Exp Biol Med 156:265-271

99. Patel YC 1979 Growth hormone stimulates hypothalamic somatostatin. Life Sci 24:1589-1594

100. Sheppard MC, Kronheim S, Pimstone BL 1978 Stimulation by growth hormone of somatostatin release from the rat hypothalamus in vitro. Clin Endocrinol 9:583-586

101. Berelowitz M, Firestone SL, Frohman LA 1981 Effects of growth hormone excess and deficiency on hypothalamic somatostatin content and release and on tissue somatoststin distribution. Endocrinology 109:714-719

102. Chihara K, Minamitani N, Kaji H, Arimura A, Fujita T 1981 Intraventricularly injected growth hormone stimulates somatostatin release into rat hypophysial portal blood. Endocrinology 109:2279-2281

103. Ceda GP, Davis RG, Rosenfeld RG, Hoffman AR 1987 The growth hormone (GH)-releasing hormone (GHRH)-GH-somatomedin axis: evidence for rapid inhibition of GHRH-elicited GH release by insulin-like growth factors I and II. Endocrinology 120:1658-1662

104. Abe H, Molitch ME, Van Wyk JJ, Underwood LE 1983 Human growth hormone and somatomedin C suppress the spontaneous release of growth hormone in unaesthetized rats. Endocrinology 113:1319-1324

105. French MB, Vaitkus P, Cukerman E, Sirek A, Sirek OV 1987 Secretory pattern of canine growth hormone. Am J Physiol 252:E268-E272

106. Tannenbaum GS, Martin JB 1976 Evidence for an endogenous ultradian rhythm governing growth hormone secretion in the rat. Endocrinology 98:562-570

107. Takahashi Y, Ebihara S, Nakamura Y, Takahashi K 1981 A model of human sleep-related growth hormone secretion in dogs: effects of 3, 6, and 12 hours of forced wakfulness on plasma growth hormone, cortisol, and sleep stages. Endocrinology 109:262-272

108. Schalch DS, Reichlin S 1966 Plasma growth hormone concentration in the rat determined by radioimmunoassay: influence of sex, pregnancy, lactation, anesthesia, hypophysectomy and extrasellar pituitary transplants. Endocrinology 79:275-280

109. Plotsky PM, Vale W 1985 Patterns of growth hormone-releasing factor and somatostatin secretion into the hypophysial-portal circulation of the rat. Science 230:461-463

110. Struthers RS, Perrin MH, Vale W 1989 Nucleotide regulation of growth hormone-releasing factor binding to rat pituitary receptors. Endocrinology 124:24-29

111. Veliçelebi G, Patthi S, Provow S, Akong M 1986 Covalent cross-linking of growth-hormone releasing factor to pituitary receptors. Endocrinology 118:1278-1283

112. Zysk JR, Cronin MJ, Anderson JM, Thorner MO 1986 Cross-linking of a growth hormone releasing factor-binding protein in anterior pituitary cells. J Biol Chem 261:16781-16784

113. Seifert H, Perrin M, Rivier J, Vale W 1985 Growth hormone-releasing factor binding sites in rat anterior pituitary membrane homogenates: modulation by glucocorticoids. Endocrinology 117:424-426

114. Seifert H, Perrin M, Rivier J, Vale W 1985 Binding sites for growth hormone releasing factor on anterior pituitary cells. Nature 313:487-489

115. Veliçelebi G, Santacroce TM, Harpold MM 1985 Specific binding of synthetic human pancreatic growth hormone releasing factor (1-40-OH) to bovine anterior pituitaries. Biochem Biophys Res Commun 126:33-39

116. Wehrenberg WB, Seifert H, Bilezikjian LM, Vale W 1986 Down-regulation of growth hormone releasing factor receptors following continuous infusion of growth hormone releasing factor in vivo. Neuroendocrinology 43:266-268

117. Bilezikjian LM, Seifert H, Vale W 1986 Desensitization to growth hormone-releasing factor (GRF) is associated with down-regulation of GRF-binding sites. Endocrinology 118:2045-2052

118. Robison GA, Butcher RW, Sutherland EW 1971 Cyclic AMP, Academic Press, New York, pp 17-47

119. Reyl-Desmars F, Baird A, Zeytin FN 1985 GRF is a highly potent activator of adenylate cyclase in normal human, bovine and rat pituitary: interaction with somatostatin. Biochem Biophys Res Commun 127:977-985

120. Schettini G, Cronin MJ, Hewlett EL, Thorner MO, MacLeod RM 1984 Human pancreatic tumor growth hormone-releasing factor stimulates anterior pituitary adenylate cyclase activity, adenosine 3',5'-monophosphate accumulation, and growth hormone release in calmodulin-dependent manner. Endocrinology 115:1308-1314

121. Spada A, Vallar L, Giannattasio G 1984 Presence of an adenylate cyclase dually regulated by somatostatin and human pancreatic growth hormone (GH)-releasing factor in GH-secreting cells. Endocrinology 115:1203-1209

122. Labrie F, Gagné B, Lefèvre G 1983 Growth hormone-releasing factor stimulates adenylate cyclase activity in the anterior pituitary gland. Life Sci 33:2229-2233

123. Narayanan N, Lussier B, French M, Moor B, Kraicer J 1989 Growth hormone-releasing factor-sensitive adenylate cyclase system of purified somatotrophs: effects of guanine nucleotides, somatostatin, calcium, and magnesium. Endocrinology 124:484-495

124. Flockerzi V, Oeken H-J, Hofmann F, Pelzer D, Cavalié A, Trautwein W 1986 Purified dihydropyridine-binding site from skeletal muscle t-tubules is a functional calcium channel. Nature 323:66-68

125. Kato M, Suzuki M 1989 Growth hormone releasing factor depolarizes rat pituitary cells in Na^+-dependent mechanism. Brain Res 476:145-148

126. Schöfl C, Sandow J, Knepel W 1987 GRF elevates cytosolic free calcium concentration in rat anterior pituitary cells. Am J Physiol 253:E591-E594

127. Snyder GD, Yadagiri P, Flack JR 1989 Effect of epoxyeicosatrienoic acids on growth hormone release from somatotrophs. Am J Physiol 256:E221-E226

128. Koch BD, Blalock JB, Schonbrunn A 1988 Characterization of the cyclic AMP-independent action of somatostatin in GH cells. I. An increase in potassium conductance is responsible for both the hyperpolarization and the decrease in intracellular free calcium produced by somatostatin. J Biol Chem 263:216-225

129. Berridge MJ, Irvine RF 1989 Inositol phosphates and cell signalling. Nature 341:197-205

130. Berridge MJ 1987 Inositol trisphosphate and diacylglyceraol: two interacting second messemgers. Annu Rev Biochem 56:159-193

131. Irvine RF 1986 Calcium transients: Mobilization of intracellular Ca^{2+}. Br Med Bull 42:369-374

132. Rano RR 1988 Regulation of protein kinase C activity by lipids. FASEB J 2:2348-2355

133. Nishizuka Y 1986 Studies and perspectives of protein kinase C. Science 233:305-312

134. Rhee SG, Suh P-G, Ryu S-H, Lee SY 1989 Studies of inositol phospholipid-specific phospholipase C. Science 244:546-550

135. Chiu AS, Li PP, Warsh JJ 1988 G-protein involvement in central-nervous-system muscarinic-receptor-coupled polyphosphoinositide hydrolysis. Biochem J 256:995-999

136. Canonico PL, Cronin MJ, Thorner MO, MacLeod RM 1983 Human pancreatic GRF stimulates phosphatidylinositol labeling in cultured anterior pituitary cells. Am J Physiol 245:E587-E590

137. Escobar DC, Vicentini LM, Ghigo E, Ciccarelli E, Usellini L, Capella C, Cocchi D 1986 Growth hormone-releasing factor does not stimulate phosphoinositides breakdown in primary cultures of rat and human pituitary cells. Acta Endocrinol (Copenhagen) 112:345-350

138. Ohmura E, Okada M, Ohba Y, Onoda N, Sano T, Tsushima T, Shizume K 1988 Phorbol ester pretreatment attunuates the growth hormone (GH) response to GH-releasing factor in cultured rat pituitary cells. J Endocrinol 118:423-428

139. Sheppard MS, Eatock BA, Bala RM 1987 Characteristics of phorbol ester stimulated growth hormone release: inhibition by insulin-like growth factor I, somatostatin, and low calcium medium and comparison with growth hormone releasing factor. Can J Physiol Pharmacol 65:2302-2307

140. Ray KP, Hart GR, Wallis M 1986 Effects of dopamine and somatostatin on phorbol ester-stimulated prolactin and growth hormone secretion. Molec Cell Endocrinol 48:205-212

141. Negro-Vilar A, Lapetina EG 1985 1,2-Didecanoylglycerol and phorbol 12,13-dibutyrate enhance anterior pituitary hormone secretion in vitro. Endocrinology 117:1559-1564

142. Ohmura E, Friesen G 1985 12-O-Tetradecanoyl phorbol-13-acetate stimulates rat growth hormone (GH) release through different pathways from that of human pancreatic GH-releasing factor. Endocrinology 116:728-733

143. Ohmura E, Tsushima T, Murakami H, Wakai K, Shizume K 1984 Effect of phorbol esters on the release of growth hormone and prolactin from rat pituitary cell cultured in monolayer. Acta Endocrinol (Copenhagen) 107:185-191

144. Summers ST, Canonico PL, MacLeod RM, Rogol AD, Cronin MJ 1985 Phorbol esters affect pituitary growth hormone (GH) and prolactin release: the interaction with GH releasing factor, somatostatin and bromocriptine. Eur J Pharmacol 111:371-376

145. Smith MA, Vale WW 1980 Superfusion of rat pituitary cells attached to Cytodex beads: validation of a technique. Endocrinology 107:1425-1431

146. Kato M, Hattori M-A, Suzuki M 1988 Inhibition by extracellular Na^+ replacement of GRF-induced GH secretion from rat pituitary cells. Am J Physiol 254:E476-E481

147. Mason WT, Rawlings SR, Cobbett P, Sikdar SK, Zorec R, Akerman SN, Benham CD, Berridge MJ, Cheek T, Moreton RB 1988 Control of secretion in anterior pituitary cells - linking ion channels, messengers and exocytosis. J Exp Biol 139:287-316

148. Kato M, Suzuki M 1989 Effect of Li^+ substitution for extracellular Na^+ on GRF-induced GH secretion from rat pituitary cells. Am J Physiol 256:C712-C718

149. Srikant CB, Patel YC 1987 Somatostatin receptor: evidence for functional and structural heterogeneity. In: Reichlin S (ed) Somatostatin: basic and clinical status, Plenum Press, New York, pp 89-102

150. Srikant CB, Heisler S 1985 Relationship between receptor binding and biopotency of somatostatin-14 and somatostatin-28 in mouse pituitary tumor cells. Endocrinology 117:271-278

151. Richardson UI, Schonbrunn A 1981 Inhibition of adrenocorticotropin secretion by somatostatin in pituitary cells in culture. Endocrinology 108:281-290

152. Srikant CB, Patel YC 1982 Characterization of pituitary membrane receptors for somatostatin in the rat. Endocrinology 110:2138-2144

153. Reubi J-C, Perrin M, Rivier J, Vale W 1982 High affinity binding sites for somatostatin to rat pituitary. Biochem Biophys Res Commun 105:1538-1545

154. Enjalbert A, Tapia-Arancibia L, Rieutort M, Brazeau P, Kordon C, Epelbaum J 1982 Somatostatin receptors on rat anterior pituitary membranes. Endocrinology 110:1634-1640

155. Aguilera G, Parker DS 1982 Pituitary somatostatin receptors. Characterization by binding with a nondegradable peptide analogue. J Biol Chem 257:1134-1137

156. Lewis LD, Williams JA 1987 Structural characterization of the somatostatin receptor in rat anterior pituitary membranes. Endocrinology 121:486-492

157. Susini CH, Esteve JP, Vaysse N, Ribet A 1985 Calcium-dependence of somatostatin binding to receptors. Peptides 6:831-833

158. Srikant CB, Patel YC 1986 Somatostatin receptors on rat pancreatic acinar cells. Pharmacological and structural characterization and demonstration of down-regulation in streptozotocin diabetes. J Biol Chem 261:7690-7696

159. Reubi JC 1984 Evidence for two somatostatin-14 receptor types in rat brain cortex. Neurosci Lett 49:259-263

160. Tran VT, Beal MF, Martin JB 1985 Two types of somatostatin receptors differentiated by cyclic somatostatin analogs. Science 228:492-495

161. Srikant CB, Patel YC 1985 Somatostatin receptors. In: Patel YC, Tannenbaum GS (eds) Somatostatin, Plenum Press, New York, pp 291-304

162. Heisler S, Srikant CB 1985 Somatostatin-14 and somatostatin-28 pretreatment down-regulate somatostatin-14 receptors and have biphasic effects on forskolin-stimulated cyclic adenosine, 3',5'-monophosphate systhesis and adrenocorticotropin secretion in mouse anterior pituitary tumor cells. Endocrinology 117:217-225

163. Boyd RS, Ray KP, Wallis M 1988 Action of pertussis toxin on the inhibitory effects of dopamine and somatostatin on prolactin and growth hormone release from ovine anterior pituitary cells. J Mol Endocr 1:179-186

164. Litosch I 1987 Regulatory GTP-binding proteins: emerging concepts on their role in cell function. Life Sci 41:251-258

165. Reyl-Desmars F, Zeytin F 1985 Somatostatin inhibits growth hormone-releasing factor-stimulated adenylate cyclase activity in GH_3 cells. Biochem Biophys Res Commun 127:986-991

166. Harwood JP, Grew C, Aguilera G 1984 Action of growth hormone-releasing factor and somatostatin on adenylate cyclase and GH release in rat anterior pituitary. Molec Cell Endocrinol 37:277

167. Dorflinger LJ, Schonbrunn A 1983 Somatostatin inhibits vasoactive intestinal peptide-stimulated cyclic adenosine monophosphate accumulation in GH pituitary cells. Endocrinology 113:1541-1550

168. Belanger A, Labrie F, Borgeat P, Savary M, Cote J, Drouin J, Schally AV, Coy DH, Coy EJ, Immer H, Sestanj K, Nelson V, Gotz M 1974 Inhibition of growth hormone and thyrotropin release by growth hormone-release inhibiting hormone. Molec Cell Endocrinol 1:329-339

169. Carlson HE, Mariz IK, Daughaday WH 1974 Thyrotropin-releasing hormone stimulation and somatostatin inhibition of growth hormone secretion from perfused rat adenohypophyses. Endocrinology 94:1709-1713

170. Vale W, Brazeau P, Grant G, Nussey A, Burgus R, Rivier J, Ling N, Guillemin R 1972 Premières observation sur le mode d'action de la somatostatine, un facteur hypothalamique qui inhibe la sécrétion de l'hormone de croissance. C R Acad Sci [D] (Paris) 275:2913-2916

171. Israel J-M, Denef C, Vincent J-D 1983 Electrophysiological properties of normal somatotrophs in culture: An intracellular study. Neuroendocrinology 37:193-199

172 Koch BD, Schonbrunn A 1988 Characterization of the cyclic AMP-independent action of somatostatin in GH cells. II. An increas in potasium conductance initiates somatostatin-induced inhibition of prolactin secretion. J Biol Chem 263:226-234

173 Schlegel W, Wuarin F, Zbaren C, Wollheim CB, Zahud GR 1985 Pertussis toxin selectively abolishes hormone induced lowering of cytosolic calcium in GH_3 cells. FEBS Lett 189:27-32

174. Bean BP 1989 Neurotransmitter inhibition of neuronal calcium currents by changes in channel voltage dependence. Nature 340:153-156

175. Ikeda SR, Schofield GG, Weight FF 1987 Somatostatin blocks a calcium current in acutely isolated adult rat superior cervical ganglion neurons. Neurosci Lett 81:123-128

176. Tsunoo A, Yoshii M, Narahashi T 1986 Block of calcium channels by enkephalin and somatostatin in neuroblastoma-glioma hybrid NG108-15 cells. Proc Natl Acad Sci U S A 83:9832-9836

177. Lewis DL, Weight FF, Luini A 1986 A guanine nucleotide-binding protein mediates the inhibition of voltage-dependent calcium current by somatostatin in a pituitary cell line. Proc Natl Acad Sci U S A 83:9035-9039

178. Schlegel W, Wuarin F, Wollheim CB, Zahnd GR 1984 Somatostatin lowers the cytosolic free Ca^{2+} concentration in clonal rat pituitary cells (GH_3 cells). Cell Calcium 5:223-236

179. Holl RW, Thorner MO, Mandell GL, Sullivan JA, Sinha YN, Leong DA 1988 Spontaneous oscillations of intracellular calcium and growth hormone secretion. J Biol Chem 263:9682-9685

180. Pandiella A, Elahi FR, Vallar L, Spada A 1988 α_1-Adrenergic stimulation of in vivo growth hormone release and cytosolic free Ca^{2+} in rat somatotrophs. Endocrinology 122:1419-1425

181. Holl RW, Thorner MO, Zysk JR, Leong DA 1989 Ionophore bromo-A23187 reveals cellular calcium stores in single pituitary somatotropes. Molec Cell Endocrinol 64:105-110

182. Reisine T, Wang H-L, Guild S 1988 Somatostatin inhibits cAMP-dependent and cAMP-independent calcium influx in the clonal pituitary tumor cell line AtT-20 through the same receptor population. J Pharmacol Exp Ther 245:225-231

183. Douglas WW 1968 Stimulus-secretion coupling: The concept and clues from chromaffin and other cells. Br J Pharmacol 34:451-474

184. Douglas WW 1975 Stimulus-secretion coupling in mast cells: Regulation of exocytosis by cellular and extracellular calcium. In: Carafoli E, Clementi F, Drabikowski W, Margreth A (eds) Calcium Transport in Contraction and Secretion, North-Holland Publishing Company, Amsterdam, pp 167-174

185. Douglas WW 1974 Involvement of calcium in exocytosis and the exocytosis-vesiculation sequence. Biochem Soc Symp 39:1-28

186. Carafoli E 1987 Intracellular calcium homeostasis. Annu Rev Biochem 56:395-433

187. Carafoli E 1988 Intracellular calcium regulation, with special attention to the role of the plasma membrane calcium pump. J Cardiovasc Pharmacol 12 (Suppl. 3):S77-S84

188. Volpe P, Krause K-H, Hashimoto S, Zorzato F, Pozzan T, Meldolesi J, Lew DP 1988 "Calciosome," a cytoplasmic organelle: The inositol 1,4,5-trisphosphate-sensitive Ca^{2+} store of nonmuscle cells?. Proc Natl Acad Sci U S A 85:1091-1095

189. Nicholls DG 1986 Intracellular calcium homeostasis. Br Med Bull 42:353-358

190. Rasmussen H, Barrett PQ 1984 Calcium messenger system: An integrated View. Physiol Rev 64:938-984

191. Manery JF 1969 Calcium and membranes. In: Comar CL, Bronner F (eds) Mineral Metabolism An Advanced Treatise Volume III, Academic Press, New York, pp 405-452

192. Reuter H, Seitz N 1968 The dependence of calcium efflux from cardiac muscle on temperature and external ion composition. J Physiol (London) 195:451-470

193. Blaustein MP, Hodgkin AL 1968 The effect of cyanide on calcium efflux in squid axons. J Physiol (London) 198:46P-48P (Abstract)

194. Blaustein MP, Hodgkin AL 1969 The effect of cyanide on the efflux of calcium from squid axons. J Physiol (London) 200:497-527

195. Caroni P, Carafoli E 1983 The regulation of the Na^+-Ca^{2+} exchanger of heart sarcolemma. Eur J Biochem 132:451-460

196. Schatzmann HJ 1966 ATP-dependent Ca^{++}-extrusion from human red cells. Experientia 22:364-365

197. Niggli V, Adunyah ES, Penniston JT, Carafoli E 1981 Purified (Ca^{2+}-Mg^{2+})-ATPase of the erythrocyte membrane. Reconstitution and effect of calmodulin and phospholipids. J Biol Chem 256:395-401

198. Smallwood JI, Waisman DM, Lafrenière D, Rasmussen H 1983 Evidence that the erythrocyte calcium pump catalyzes a Ca^{2+}:nH^+ exchange. J Biol Chem 258:11092-11097

199. Niggli V, Sigel E, Carafoli E 1982 The purified Ca^{2+} pump of human erythrocyte membranes catalyzes an electroneutral Ca^{2+}-H^+ exchange in reconstituted liposomal systems. J Biol Chem 257:2350-2356

200. Dixon DA, Haynes DH 1989 Kinetic characterization of the Ca^{2+}-pumping ATPase of cardiac sarcolemma in four states of activation. J Biol Chem 264:13612-13622

201. Smallwood JI, Gügi B, Rasmussen H 1988 Regulation of erythrocyte Ca^{2+} pump activity by protein kinase C. J Biol Chem 263:2195-2202

202. Caroni P, Carafoli E 1981 Regulation of Ca^{2+}-pumping ATPase of heart sarolemma by a phosphorylation-dephosphorylation process. J Biol Chem 256:9371-9373

203. Furukawa K-I, Tawada Y, Shigekawa M 1989 Protein kinase C activation stimulates plasma membrane Ca^{2+} pump in cultured vascular smooth muscle cells. J Biol Chem 264:4844-4849

204. MacLennan DH 1970 Purification and properties of an adenosine triphosphatase from sarcoplasmic reticulum. J Biol Chem 245:4508-4518

205. Scharff O, Foder B, Skibsted U 1983 Hysteretic activation of the Ca^{2+} pump revealed by calcium transients in human red cells. Biochim Biophys Acta 730:295-305

206. Scharff O, Foder B 1982 Rate constants for calmodulin binding to Ca^{2+}-ATPase in erythrocyte membranes. Biochim Biophys Acta 691:133-143

207. Snowdowne KW, Borle AB 1984 Changes in cytosolic ionized calcium induced by activators of secretion in GH_3 cells. Am J Physiol 246:E198-E201

208. Stojilković SS, Izumi S, Catt KJ 1988 Participation of voltage-sensitive calcium channels in pituitary hormone release. J Biol Chem 263:13054-13061

209. Mayer ML, Westbrook GL 1987 The physiology of excitatory amino acids in the vertebrate central nervous system. Prog Neurobiol 28:197-276

210. Penner R, Matthews G, Neher E 1988 Regulation of calcium influx by second messengers in rat mast cells. Nature 334:499-504

211. Kuno M, Gardner P 1987 Ion channels activated by inositol 1,4,5-trisphosphate in plasma membrane of human T-Lymphocytes. Nature 326:301-304

212. Fox AP, Nowycky MC, Tsien RW 1987 Kinetic and pharmacological properties distinguishing three types of calcium currents in chick sensory neurones. J Physiol (London) 394:149-172

213. Fox AP, Nowycky MC, Tsien RW 1987 Single-channel recording of three types of calcium channels in chick sensory neurones. J Physiol (London) 394:173-200

214. Nowycky MC, Fox AP, Tsien RW 1985 Three types of neuronal calcium channel with different calcium agonist sensitivity. Nature 316:440-443

215. DeRiemer SA, Sakmann B 1986 Two calcium currents in normal rat anterior pituitary cells identified by a plaque assay. In: Heinemann U, Klee M, Neher E, Singer W (eds) Calcium electrogenesis and neuronal functioning. Experimental Brain Research, series 14, Springer-Verlag, Heidelberg, pp 139-154

216. McCleskey EW, Fox AP, Feldman D, Tsien RW 1986 Different types of calcium channels. J Exp Biol 124:177-190

217. Reuter H, Porzig H 1988 Calcium cahannels: diversity and complexity. Nature 336:113-114

218. Hofman F, Nastainczyk W, Röhrkasten A, Schneider T, Sieber M 1987 Regulation of the L-type calcium channel. TIPS 8:393-398

219. Armstrong CM, Matteson DR 1985 Two distinct populations of calcium channels in a clonal line of pituitary cells. Science 227:65-67

220. Tsien RW, Lipscombe D, Madison DV, Bley KR, Fox AP 1988 Multiple types of neuronal calcium channels and their selective modulation. TINS 11:431-437

221. Yatani A, Imoto Y, Codina J, Hamilton SL, Brown AM, Birnbaumer L 1988 The stimulatory G protein of adenylyl cyclase, G_s, also stimulates dihydropyridine-sensitive Ca^{2+} channels: evidence for direct regulation independent of phosphorylation by cAMP-dependent protein kinase or stimulation by a dihydropyridine agonist. J Biol Chem 263:9887-9895

222. Reuter H 1987 Modulation of ion channels by phosphorylation and second messengers. NIPS 2:168-171

223. Levitan IB 1985 Phosphorylation of ion channels. J Membr Biol 87:177-190

224. Reuter H 1983 Calcium channel modulation by neurotransmitters, enzymes and drugs. Nature 301:569-574

225. Reuter H, Scholz H 1977 The regulation of the calcium conductance of cardiac muscle by adrenaline. J Physiol (London) 264:49-62

226. Curtis BM, Catterall WA 1985 Phosphorylation of the calcium antagonist receptor of the voltage-sensitive calcium channel by cAMP-dependent protein kinase. Proc Natl Acad Sci U S A 82:2528-2532

227. Armstrong D, Eckert R 1987 Voltage-activated calcium channels that must be phosphorylated to respond to membrane depolarization. Proc Natl Acad Sci U S A 84:2518-2522

228. Hockberger P, Toselli M, Swandulla D, Lux HD 1989 A diacylglycerol analogue reduces neuronal calcium currents independently of protein kinase C activation. Nature 338:340-342

229. Levitan IB 1988 Modulation of ion channels in neurons and other cells. Annu Rev Neurosci 11:119-136

230. Lewis DL, Weight FF 1988 The protein kinase C activator 1-oleoyl-2-acetylglycerol inhibits voltage-dependent Ca^{2+} current in the pituitary cell line AtT-20. Neuroendocrinology 47:169-175

231. Marchetti C, Brown AM 1988 Protein kinase activator 1-oleoyl-2-acetyl-sn-glycerol inhibits two types of calcium currents in GH_3 cells. Am J Physiol 254:C206-C210

232. Streb H, Irvine RF, Berridge MJ, Schulz I 1983 Release of Ca^{2+} from a nonmitochondrial intracellular store in pancreatic acinar cells by inositol-1,4,5-trisphosphate. Nature 306:67-69

233. Supattapone S, Worley PF, Baraban JM, Snyder SH 1988 Solubilization, purification, and characterization of an inositol trisphosphate receptor. J Biol Chem 263:1530-1534

234. Ross CA, Meldolesi J, Milner TA, Satoh T, Supattapone S, Snyder SH 1989 Inositol 1,4,5-trisphosphate receptor localized to endoplasmic reticulum in cerebellar Purkinje neurons. Nature 339:468-470

235. Ehrlich BE, Watras J 1988 Inositol 1,4,5-trisphosphate activates a channel from smooth muscle sarcoplasmic reticulum. Nature 336:583-586

236. Meyer T, Holowka D, Stryer L 1988 Highly cooperative opening of calcium channels by inositol 1,4,5-trisphosphate. Science 240:653-656

237. Putney JW Jr 1986 A model for receptor-regulated calcium entry. Cell Calcium 7:1-12

238. Millar JA, Struthers AD 1984 Calcium antagonists and hormone release. Clin Sci 66:249-255

239. Borle AB 1981 Pitfalls of the ^{45}Ca uptake method. Cell Calcium 2:187-196

240. Borle AB 1975 Methods for assessing hormone effects on calcium fluxes in vitro. Methods Enzymol 37:513-573

241. Blinks JR, Prendergast FG, Allen DG 1976 Photoproteins as biological calcium indicators. Pharmacol Rev 28:1-93

242. Scarpa A, Brinley FJ, Tiffert T, Dubyak GR 1978 Metallochromic indicators of ionized calcium. Ann N Y Acad Sci 307:86-112

243. Tsien RY, Rink TJ 1980 Neutral carrier ion-selective microelectrodes for measurement of intracellular free calcium. Biochim Biophys Acta 599:623-638

244. Tsien RY 1980 New calcium indicators and buffers with high selectivity against magnesium and protons: design, synthesis, and properties of prototype structures. Biochemistry 19:2396-2404

245. Tsien RY, Pozzan T, Rink TJ 1982 T-cell mitogens cause early changes in cytoplasmic free Ca^{2+} and membrane potential in lymphocytes. Nature 295:68-71

246. Tsien RY 1981 A non-disruptive technique for loading calcium buffers and indicators into cells. Nature 290:527-528

247. Tsien RY, Pozzan T, Rink TJ 1982 Calcium homeostasis in intact lymphocytes: cytoplasmic free calcium monitored with a new, intracellularly trapped fluorescent indicator. J Cell Biol 94:325-334

248. Rink TJ, Pozzan T 1985 Using quin2 in cell suspensions. Cell Calcium 6:133-144

249. Tsien RY, Pozzan T, Rink TJ 1984 Measuring and manipulating cytosolic Ca^{2+} with trapped indicators. TIBS 9:263-266

250. Grynkiewicz G, Poenie M, Tsien RY 1985 A new generation of Ca^{2+} indicators with greatly improved fluorescence properties. J Biol Chem 260:3440-3450

251. Malgaroli A, Milani D, Meldolesi J, Pozzan T 1987 Fura-2 measurement of cytosolic free Ca^{2+} in monolayers and suspensions of various types of animal cells. J Cell Biol 105:2145-2155

252. Gershengorn MC, Thaw C 1985 Thyrotropin-releasing hormone (TRH) stimulates biphasic elevation of cytoplasmic free calcium in GH_3 cells. Further evidence that TRH mobilizes cellular and extracellular Ca^{2+}. Endocrinology 116:591-596

253. Schlegel W, Wollheim CB 1984 Thyrotropin-releasing hormone increases cytosolic free Ca^{2+} in clonal pituitary cells (GH_3 cells): direct evidence for mobilization of cellular calcium. J Cell Biol 99:83-87

254. Malgaroli A, Vallar L, Elahi FR, Pozzan T, Spada A, Meldolesi J 1987 Dopamine inhibits cytosolic Ca^{2+} increases in rat lactotroph cells: evidence of dual mechanism of action. J Biol Chem 262:13920-13927

255. Naor Z, Capponi AM, Rossier MF, Ayalon D, Limor R 1988 Gonadotropin-releasing hormone-induced rise in cytosolic free Ca^{2+} levels: mobilization of cellular and extracellular Ca^{2+} pools and relationship to gonadotropin secretion. Mol Endocrinol 2:512-520

256. Shangold GA, Murphy SN, Miller RJ 1988 Gonadotropin-releasing hormone-induced Ca^{2+} transients in single identified gonadotropes require both intracellular Ca^{2+} mobilization and Ca^{2+} influx. Proc Natl Acad Sci U S A 85:6566-6570

257. Limor R, Ayalon D, Capponi AM, Childs GV, Naor Z 1987 Cytosolic free calcium levels in cultured pituitary cells separated by centrifugal elutriation: effect of gonadotropin-releasing hormone. Endocrinology 120:497-503

258. Gershengorn M, Thaw C 1983 Calcium influx is not required for TRH to elevate free cytoplasmic calcium in GH_3 cells. Endocrinology 113:1522-1524

259. Morgan RO, Chang JP, Catt KJ 1987 Novel aspects of gonadotropin-releasing hormone action on inositol polyphosphate metabolism in cultured pituitary gonadotrophs. J Biol Chem 262:1166-1171

260. Naor Z, Azrad A, Limor R, Zakut H, Lotan M 1986 Gonadotropin-releasing hormone activates a rapid Ca^{2+}-independent phosphodiester hydrolysis of polyphosphoinositides in pituitary gonadotrophs. J Biol Chem 261:12506-12512

261. Raymond V, Leung PCK, Veilleux R, Lefèvre G, Labrie F 1984 LHRH rapidly stimulates phosphatidylinositol metabolism in enriched gonadotrophs. Molec Cell Endocrinol 36:157-164

262. Tashjian AH Jr, Heslop JP, Berridge MJ 1987 Subsecond and second changes in inositol polyphosphates in GH_4C_1 cells induced by thyrotropin-releasing hormone. Biochem J 243:305-308

263. Ramsdell JS, Tashjian AH Jr 1986 Thyrotropin-releasing hormone (TRH) elevation of inositol trisphosphate and cytosolic free calcium is dependent on receptor number: evidence for multiple rapid interactions between TRH and its receptor. J Biol Chem 261:5301-5306

264. Gershengorn MC 1986 Mechanism of thyrotropin releasing hormone stimuation of pituitary hormone secretion. Annu Rev Physiol 48:515-526

265. Knight DE, von Grafenstein H, Athayde CM 1989 Calcium-dependent and calcium-independent exocytosis. TINS 12:451-458

266. Baker PF, Knight DE 1986 Exocytosis: control by calcium and other factors. Br Med Bull 42:399-404

267. Zimmerberg J 1987 Molecular mechanisms of membrane fusion: steps during phospholipid and exocytotic membrane fusion. Biosci Rep 7:251-268

268. Maruyama Y 1989 Control of exocytosis in single cells. NIPS 4:53-56

269. Neher E 1988 The influence of intracellular calcium concentration on degranulation of dialysed mast cells from rat peritoneum. J Physiol (London) 395:193-214

270. Neher E, Marty A 1982 Discrete changes of cell membrane capacitance observed under conditions of enhanced secretion in bovine adrenal chromaffin cells. Proc Natl Acad Sci U S A 79:6712-6716

271. Burgoyne RD, Morgan A, O'Sullivan AJ 1988 A major role for protein kinase C in calcium-activated exocytosis in permeabilised adrenal chromaffin cells. FEBS Lett 238:151-155

272. Shortman K 1968 The separation of different cell classes from lymphoid organs. II. The purification and analysis of lymphocyte population by equilibrium density gradient centrifugation. Aust J Exp Biol Med Sci 46:375-396

273. Finkelstein MC, Adelberg EA 1977 Neutral amino acid transport in an established mouse lymphocytic cell line. J Biol Chem 252:7101-7108

274. Capponi AM, Lew PD, Schlegel W, Pozzan T 1986 Use of intracellular calcium and membrane potential fluorescent indicators in neuroendocrine cells. Methods Enzymol 124:116-135

275. Gelfand EW, Cheung RK, Grinstein S 1986 Mitogen-induced changes in Ca^{2+} permeability are not mediated by voltage-gated K^+ channels. J Biol Chem 261:11520-11523

276. Bliss CI 1952 The statistics of bioassay with special reference to the vitamins. Academic Press, New York, pp 445-628

277. Robberecht P, Coy DH, Waelbroeck M, Heiman ML, De Neef P, Camus J-C, Christophe J 1985 Structural requirements for the activation of rat anterior pituitary adenylate cyclase by growth hormone-releasing factor (GRF): discovery of (N-Ac-Tyr^1, D-Arg^2)-GRF(1-29)-NH_2 as a GRF antagonist on membranes. Endocrinology 117:1759-1764

278. Uchikawa T, Borle AB 1981 Solutions for the kinetic analysis of ^{45}calcium uptake curves. Cell Calcium 2:173-186

279. Sato M, Takahara J, Fujioka Y, Niimi M, Irino S 1988 Physiological role of growth hormone (GH)-releasing factor and somatostatin in the dynamics of GH secretion in the adult male rat. Endocrinology 123:1928-1933

280. Stolze H, Schulz I 1980 Effects of atropine, ouabain, antimycin A, and A23187 on "trigger Ca^{2+} pool" in exocrine pancreas. Am J Physiol 238:G338-G348

281. Winiger BP, Schlegel W 1988 Rapid transient elevations of cytosolic calcium triggered by thyrotropin releasing hormone in individual cells of the pituitary line GH_3B_6. Biochem J 255:161-167

282. Eto S, Wood JM, Hutchins M, Fleischer N 1974 Pituitary $^{45}Ca^{++}$ uptake and release of ACTH, GH, and TSH: effect of verapamil. Am J Physiol 226:1315-1320

283. Schofield JG, Bicknell RJ 1978 Effects of somatostatin and verapamil on growth hormone release and ^{45}Ca fluxes. Molec Cell Endocrinol 9:255-268

284. Saida K, Van Breemen C 1983 Mechanism of Ca^{++} antagonist-induced vasodilation: intracellular actions. Circ Res 52:137-142

285. Pang DC, Sperelakis N 1983 Nifedipine, diltiazem, bepridil and verapamil uptakes into cardiac and smooth muscles. Eur J Pharmacol 87:199-207

286. Enyeart JJ, Aizawa T, Hinkle PM 1985 Dihydropyridine Ca^{2+} antagonists: potent inhibitors of secretion from normal and transformed pituitary cells. Am J Physiol 248:C510-C519

287. Cauvin C, Loutzenhiser R, Van Breemen C 1983 Mechanisms of calcium antagonist-induced vasodilation. Annu Rev Pharmacol Toxicol 23:373-396

288. Triggle DJ, Swamy VC 1983 Calcium Antagonists: Some chemical-pharmacologic aspects. Circ Res 52(suppl. I):17-28

289. Matteson DR, Armstrong CM 1986 Properties of two types of calcium channels in clonal pituitary cells. J Gen Physiol 87:161-182

290. Cohen CJ, McCarthy RT 1987 Nimodipine block of calcium channels in rat anterior pituitary cells. J Physiol (London) 387:195-225

291. Albert PR, Wolfson G, Tashjian AH 1987 Diacylglycerol increases cytosolic free Ca^{2+} concentration in rat pituitary cells: relationship to thyrotropin-releasing hormone action. J Biol Chem 262:6577-6581

292. Albert PR, Tashjian AH 1985 Dual actions of phorbol esters on cytosolic free Ca^{2+} concentrations and reconstitution with ionomycin of acute thyrotropin-releasing hormone responses. J Biol Chem 260:8746-8759

293. Holl RW, Thorner MO, Leong DA 1989 Cytosolic free calcium in normal somatotropes: effects of forskolin and phorbol ester. Am J Physiol 256:E375-E379

294. Davidson JS, Wakefield IK, King JA, Mulligan GP, Millar RP 1988 Dual pathways of calcium entry in spike and plateau phases from chicken pituitary cells: sequential activation of receptor-operated and voltage sensitive calcium channels by gonadotropin-releasing hormone. Mol Endocrinol 2:382-390

295. Drummond IAS, Lee AS, Resendez E Jr, Steinhardt RA 1987 Depletion of intracellular calcium stores by calcium ionophore A23187 induces the genes for glucose-regulated protein in hamster fibroblasts. J Biol Chem 262:12801-12805

296. Maruyama T, Ishikawa H 1977 Somatostatin: its inhibiting effect on the release of hormone and IgG from clonal cells strains its Ca-influx dependence. Biochem Biophys Res Commun 74:1083-1088

297. Login IS, Judd AM 1986 Trophic effects of somatostatin on calcium flux: dynamic analysis and correlation with pituitary hormone release. Endocrinology 119:1703-1707

298. Login IS, Judd AM, MacLeod RM 1986 Association of $^{45}Ca^{2+}$ mobilization with stimulation of growth hormone (GH) release by GH-releasing factor in dispersed normal male rat pituitary cells. Endocrinology 118:239-243

299. Gershengorn MC, Thaw CN, Geras-Raaka E 1988 Benzodiazepines modulate voltage-sensitive calcium channels in GH_3 pituitary cells at sites distinct from thyrotropin-releasing hormone receptors. Endocrinology 123:541-544

300. Login IS, Judd AM, Cronin MJ, Spike K, Schettini G, Yasumoto T, MacLeod RM 1985 The effects of maitotoxin on $^{45}Ca^{2+}$ flux and hormone release in GH_3 rat pituitary cells. Endocrinology 116:622-627

301. Login IS, Judd AM, Cronin MJ, Yasumoto T, MacLeod RM 1985 Reserpine is a calcium channel antagonist in normal and GH_3 rat pituitary cells. Am J Physiol 248:E15-E19

302. Shangold GA, Kongsamut S, Miller RJ 1985 Characterization of voltage-sensitive calcium channels in a clonal pituitry cell line. Life Sci 36:2209-2215

303. Knepel W, Schöfl C, Götz DM 1988 Arachidonic acid elevates cytosolic free calcium concentration in anterior pituitary cells. Naunyn Schmiedebergs Arch Pharmacol 338:303-309

304. Makara GB, Rappay G, Garamvölgyi V, Nagy I, Dankó S, Bajusz S 1988 The tripeptide aldehyde, Boc-DPhe-Phe-Lysinal, is a novel Ca^{2+} channel inhibitor in pituitary cells. Eur J Pharmacol 151:147-149

305. Milligan JV, Kraicer J 1971 ^{45}Ca Uptake during the in vitro release of hormones from rat adenohypophysis. Endocrinology 89:766-773

306. Meier K, Knepel W, Schöfl C 1988 Potassium depolarization elevates cytosolic free calcium concentration in rat anterior pituitary cells through 1,4-dihydropyridine-sensitive, ω-conotoxin-insensitive calcium channels. Endocrinology 122:2764-2770

307. Sims SM, Kraicer J 1988 Hormonal control of membrane currents in somatotrophs. Society for Neuroscience Abstracts 14:141 (Abstract)

308. Ozawa S, Kimura N 1979 Membrane potential changes caused by thyrotropin-releasing hormone in clonal GH_3 cell and their relationship to secretion of pituitary hormone. Proc Natl Acad Sci U S A 76:6017-6020

309. Mason WT, Rawlings SR 1988 Whole cell recordings from cultured somatotrophs of the bovine adenohypophysis. J Physiol (London) 398:78P (Abstract)

310. Nussinovitch I 1988 Growth hormone releasing factor evokes rhythmic hyperpolarizing currents in rat anterior pituitary cells. J Physiol (London) 395:303-318

311. Miller JP, Beck AH, Simon LN, Meyer RB Jr 1975 Induction of hepatic tyrosine aminotransferase in vivo by derivatives of cyclic adenosine 3':5'-monophosphate. J Biol Chem 250:426-431

312. Costa MRC, Casnellie JE, Catterall WA 1982 Selective phosphorylation of the α subunit of the sodium channel by cAMP-dependent protein kinase. J Biol Chem 257:7918-7921

313. Costa MRC, Catterall WA 1984 Cyclic AMP-dependent phosphorylation of the α subunit of the sodium channel in synaptic nerve ending partcles. J Biol Chem 259:8210-8218

314. Swandulla D, Lux HD 1984 Changes in ionic conductances induced by cAMP in Helix neurons. Brain Res 305:115-122

315. Nakamura T, Gold GH 1987 A cyclic nuleotide-gated conductance in olfactory receptor cilia. Nature 325:442-444

316. Reisine T 1989 Phorbol esters and corticotropin releasing factor stimulate calcium influx in the anterior pituitary tumor cell line, AtT-20, through different intracellular sites of action. J Pharmacol Exp Ther 248:984-990

317. Reisine T, Guild S 1987 Activators of protein kinase C and cyclic AMP-dependent protein kinase regulate intracellular calcium levels through distinct mechanisms in mouse anterior pituitary tumor cells. Mol Pharmacol 32:488-496

318. Stojilkovic SS, Chang JP, Izumi I, Tasaka K, Catt KJ 1988 Mechanisms of secretory responses to gonadotropin-releasing hormone and phorbol esters in cultured pituitary cells: participation of protein kinase C and extracellular calcium mobilization. J Biol Chem 263:17301-17306

319. Williamson JR 1986 Role of inositol lipid breakdown in the generation of intracellular signals. State of the art lecture. Hypertension 8(Suppl II):II-140-II-156

320. Durst DS, Martin TFJ 1984 Thyrotropin-releasing hormone rapidly activates protein phosphorylation in GH_3 pituitary cells by a lipid-linked, protein kinase C-mediated pathway. J Biol Chem 259:14520-14530

321. Takai Y, Kishimoto A, Kikkawa U, Mori T, Nishizuka Y 1979 Unsaturated diacyglycerol as a possible messenger for the activation of calcium-activated, phospholipid-dependent protein kinase system. Biochem Biophys Res Commun 91:1218-1224

322. Schlegel W, Winiger BP, Mollard P, Vacher P, Wuarin F, Zahnd GR, Wollheim CB, Dufy B 1987 Oscillations of cytosolic Ca^{2+} in pituitary cells due to action potentials. Nature 329:719-721

323. Berridge MJ, Galic ıe A 1988 Cytosolic calcium oscillators. FASEB J 2:3074-3082

324. Kirsch GE, Yatani A, Codina J, Birnbaumer L. Brown AM 1988 α-Subunit of G_k activates atrial K^+ channels of chick, rat, and guinea $p_{ı}g$. Am J Physiol 254:H1200-H1205

325. Codina J, Grenet D, Yatani A, Birnbaumer L, Brown AM 1987 Hormonal regulation of pituitary GH_3 cell K^+ channels by G_k is mediated by its α-subunit. FEBS Lett 216:104-106

326. Codina J, Yatani A, Grenet D, Brown AM, Birnbaumer L 1987 The α-subunit of the GTP binding protein G_k opens atrial potassium channels. Science 236:442-445

327. Fabiato A 1988 Computer programs for calculating total from specified free or free from specified total ionic concentrations in aqueous solutions containing multiple metals and ligands. Methods Enzymol 157:378-417

328. Kruskal BA, Keith CH, Maxfield FR 1984 Thyrotropin-releasing hormone-induced changes in intracellular [Ca^{2+}] measured by microspectrofluorometry on individual quin2-loaded cells. J Cell Biol 99:1167-1172

329. Moisescu DG, Pusch H 1975 A pH-metric method for the determination of relative concentration of calcium to EGTA. Pflug Arch 355:R122 (Abstract)

330. Zar HJ 1984 Biostatistical analysis, ed 2. Prentice-Hall, Englewood Cliffs, NJ

331. Albert PR, Tashjian AH 1984 Thyrotropin-releasing hormone-induced spike and plateau in cytosolic free Ca^{2+} concentrations in pituitary cells. Relation to prolactin release. J Biol Chem 259:5827-5832